THE JOURNAL
OF
CHEMICAL PHYSICS

VOLUME 8 DECEMBER, 1940 NUMBER 12

Ozone in Silent Electric Discharge

WILLIAM H. OTTO AND WILLARD H. BENNETT
Electronic Research Corporation, Newark, Ohio

(Received August 12, 1940)

Ozone is produced in silent discharges in air by collisions intermediate between ionizing energies and attaching energies, due to the dissociation of oxygen molecules into atoms by electrons. A more detailed mechanism for the silent discharge is given.

THE rate of production of ozone has been measured for several forms of the silent electric discharge. The results of these measurements shed further light on the detailed processes of this form of discharge which has been receiving increased attention recently.[1]

The measurements of ozone generating rates were made using electrodes of either a straight wire form like that shown in Fig. 1(a) or in the form of segments of a wire arranged in a row as in Fig. 1(b), so that each segment discharged from an exposed end while the other end was attached firmly to a connecting wire bus. The discharge electrode was arranged to discharge towards the space between the two target electrodes whose cross sections were approximately air foil in shape, as shown in Fig. 2. This arrangement of electrodes was used in order that the electric wind produced by the discharge would produce air movement inside the enclosure where the discharge took place and thoroughly mix the ozone-laden air.

The enclosure used was constructed of galvanized iron and had a volume of 18 cubic feet. A formica disk six inches in diameter was fastened into a hole in the top of the tank, closing the hole. A copper tubing connection for high voltage extended through the disk into the tank for application of potential to the discharge device. Air at any desired humidity was admitted to that tank through a train which removed sulphur dioxide and dust, and the humidity was adjusted by passing the air through a suitable solution. For making a measurement, a 0.0369 cu. ft. sample of air was drawn off from the tank and bubbled slowly through potassium iodide solution. The solution was titrated with sodium arsenite.

Early in the investigation, it was found that paper and similar materials had a strong tendency to absorb ozone and that the rate of such absorption was proportional to the ozone concentration present. By removing all such materials from inside the tank, it was found that the rate of disappearance of ozone decreased greatly and also became proportional to the square of the ozone concentration present rather than proportional to concentration, indicating that ozone can disappear, at least at concentrations of 50 to 100 parts per million, by a bimolecular reaction at the galvanized surface. All the measurements here reported were made at much lower concentrations than those at which the

[1] A recent review appears in *Fundamental Processes of Electrical Discharge in Gases* by Loeb (John Wiley, 1939), pp. 514–536.

above supposed bimolecular reaction produces an appreciable effect. The procedure used was to operate the discharge under accurately controlled electrical conditions and to measure the ozone concentration hourly. About every 24 hours, the discharge was stopped, the air inside the tank was completely changed, and a new series of measurements begun in order to observe whether the discharge electrode had reached an

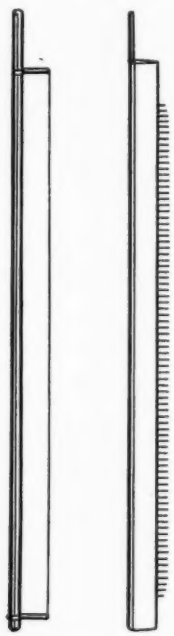

FIG. 1.

equilibrium condition. As will be observed later from the pictures, this is a significant precaution.

Three kinds of discharge electrodes were used. One electrode consisted of a straight 0.005-inch tungsten wire fastened to a $\frac{1}{4}$-inch brass rod support, as shown in Fig. 1(a). Another discharge electrode, of the kind shown in Fig. 1(b), used segments of 0.001-inch tungsten wire. A third electrode used segments of a 0.001-inch wire made by electroplating rhodium metal on 0.0009-inch nickel alloy wire. The a.c. used either for a.c. operation of the discharge or for supply to the rectifier circuit for the d.c. operations was drawn from a voltage regulator which remained steady to within less than $\frac{1}{2}$ percent. The current supplied to the discharge electrode was measured with a 150-volt electrostatic voltmeter connected across 1 megohm of resistance through which the discharge current passed, and the applied voltage in all cases was adjusted so that the discharge current was always just 0.120 milliampere. When the discharge was operated on a.c. a condenser with 0.1 microfarad capacity was put in series with the discharge circuit in order that any tendency of the discharge to pass a larger current with the discharge electrode negative than the current with the discharge electrode positive would be exactly compensated automatically by a d.c. bias accumulated on the interposed condenser. The discharge was passed until the rate of generation of ozone did not detectably increase between two successive days, in each instance.

OBSERVATIONS

In Table I are shown the rates of generation of ozone in milligrams per second per ampere. (See also Figs. 3(a), (b) and (c).) The pictures are representative of the respective discharge surfaces at equilibrium in each instance with the exception that the 5-mil straight wire appears to continue to etch indefinitely so that, after several months steady operation, the wire would etch through. The discharge from the 0.005-inch straight wire on negative d.c. and on a.c. is localized in spots so that the pictures are taken of these spots. There are four principal trends to be noticed in the data. (1) The smaller the radius of the curvature of the discharge surface,

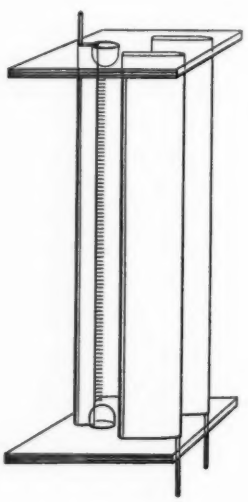

FIG. 2.

(*a*) 0.001" rhodium on nickel. (*b*) 0.001" tungsten. (*c*) 0.005" tungsten.

FIG. 3.

the smaller is the rate of generation of ozone. (2) The action of the rhodium coating is to reduce the formation of the oxide coat at the tip of the point and thereby to reduce the equilibrium radius of curvature. (3) The generation rate is greater on negative than on positive (the rate on a.c. is the average of the negative value and the positive value). (4) The excess for negative over positive is greater for the larger wire than for the smaller wire.

If each electron produced one molecule of ozone, the rate would be 48,000 mg per second amp. so that for the maximum rate shown, only about one electron in 16,500 produced a molecule of ozone.

If a sharp projection was deliberately put on a target electrode to induce the formation of streamers, the rate of generation of ozone could be increased to at least ten times the highest value shown in the table.

Discharge electrodes of several other metals were tried. Steel becomes covered with more of a growth of oxide than does tungsten, and the coating on steel is rust-colored. Platinum acquires a dense black coat at the region of the discharge. These coatings appear on either the negative or positive polarity. The greater the growth in every case, the greater was the rate of generation of ozone. It is quite possible that the oxide coats acted as insulating layers whose frequent breakdown resulted in local streamer formation, although any such effect was not particularly outstanding and, as seen later, could be explained on the basis of the increase of radius of curvature caused by the oxide coat.

TABLE I. *Generation rates of ozone in milligrams per second per ampere.*

DISCHARGE	0.001" RHODIUM ON NICKEL	0.001" TUNGSTEN	0.005" TUNGSTEN
d.c.+	1.05	1.20	1.95
a.c.	2.85	5.70	16.5
d.c.+	1.13	1.58	2.40
d.c.−	5.25	7.80	29.1
d.c.+	1.13	1.65	2.48

DISCUSSION

The explanation of the silent electric discharge in air when the discharge electrode is negative is as follows. The electric field near the emitting surface, due to the applied voltage, is distorted by the electrical charges produced by ionization near the point in general, and the discharge is pulsating in nature.[2] The pulsations are set off by a few electrons arising at or near the surface of the point. As these charges move away from the discharge point under the action of the field, they cause an avalanche-like accumulation of electronic charge. This cloud of electrons increases to a quantity of charge of about 10^{-10} coulomb. Most of this 10^{-10} coulomb is produced by ionization occurring in the last few free paths of the electrons so that most of the electrical charge in the pulse originates at a rather definite distance away from the tip of the point. This region of ionizing collisions will be referred to hereafter as the "ionizing sheath." As these electrons try to move on from the positive ions from which they have just been separated, they are retarded by these positive ions so that,

[2] A. F. Kip, Phys. Rev. **54**, 139 (1938); L. W. Trichel, Phys. Rev. **54**, 1078 (1938); Leonard B. Loeb and A. F. Kip, J. App. Phys. **10**, 142 (1939).

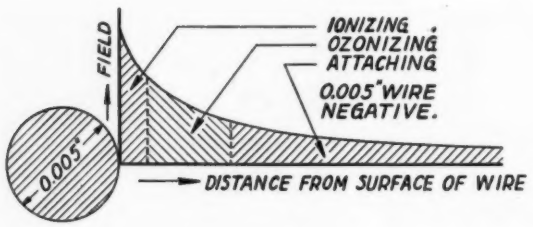

FIG. 4.

locally, the electric field is reduced below the field which would be there due to the applied voltage in the absence of such space charges. The magnitude of the pulse is limited by the ability of the positive ion charge to hold back on the electronic charges sufficiently to prevent the electrons from producing any more ionizations. Beyond the ionizing sheath, essentially all the electrons make collisions at energies less than the ionization potential 12.5 ev. The electrons can dissociate O_2 molecules to atoms resulting in the formation of ozone:

$$O+O_2 \rightarrow O_3$$

at energies down to 5.09 ev, and such ozone-producing collisions can occur in a sheath extending essentially from the ionizing sheath to a distance further from the tip of the point where the collisions occur at less than the dissociation potential. This will be referred to as the "ozoning sheath." Beyond the ozoning sheath, the electrons enter a region where their usual energy of collision is suitable for exciting molecular oxygen by collisions at a little more than 1.62 ev and in so doing, lose energy and attach to form stable negative molecular oxygen ions, after the method of Bradbury.[3] This last sheath will be referred to as the "attachment sheath." The negative ions tend to shield the region near the tip of the point and they must move away from the region near the tip of the point before the field can return to a sufficient intensity to support a new pulse.

The processes occurring when the discharge electrode is positive may be explained as follows. One or a few negative ions drift toward the region of intense field near the tip of the point. As soon as they make collisions at sufficient energy to liberate the attached electrons, the electrons initiate an avalanche-like accumulation of electronic charge. Most of the ionizations in this avalanche occur within a sheath around the tip of the point which is only a few ionization distances thick. The electrons go directly to the discharge point to be absorbed, and are not allowed much time in the gas for making the kind of collisions which result in dissociation of molecules into atoms. In this way, it is seen that much less ozone is produced when the discharge point is positive than when it is negative. Since the sheath in which ozone can be produced is so much thinner when the point is positive than when it is negative, it might be supposed that much less ozone should be generated on positive than that reported in the table of data above. There are two factors which can prevent such an extreme distinction from obtaining.

First, there is a persistent density of positive ions around the small positive discharge point under the relatively steady conditions of discharge at the value of current used here. This positive ion density partially shields the discharge point increasing the effective radius, and considerably reducing the proportion of collisions below that which would obtain in the absence of the positive ions. In this way, the positive ions increase the thickness of the sheath in which an electron can make its last few ionizations before arriving at the surface of the discharge point, and the distance in which an electron can dissociate molecules and produce ozone is correspondingly increased.

Second, excitation in excess of the dissociation energy can give rise to ultraviolet radiation

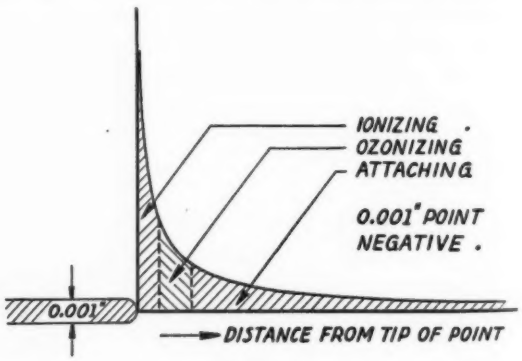

FIG. 5.

[3] N. E. Bradbury, Phys. Rev. **44**, 883 (1933). See also Loeb, reference 1, pp. 276–296.

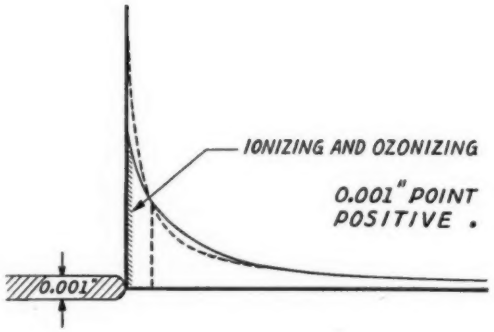

FIG. 6.

which in turn can dissociate molecules farther from the discharge point than the region of intense ionization.

The effect of the reduction of radius of curvature of the discharge electrode to reduce the rate of generation of ozone can be understood with Figs. 4–7. In Fig. 4 is represented the field as a function of distance from a straight 0.005-inch wire and the three sheaths are approximately located for the case when the discharge is negative. In Fig. 5 the field at the end of a 0.001-inch wire is shown assuming that the wire end is an approximation to a hyperboloid for regions near the tip.[4]

It is seen that the smaller radius of curvature causes a shorter range in which dissociating collisions are likely to occur. Figures 6 and 7 show the field around a 0.005-inch straight wire and a 0.001-inch wire end, respectively, on positive as the field is affected by the persistent

[4] Eyring, Mackeown and Millikan, Phys. Rev. **31**, 900 (1928).

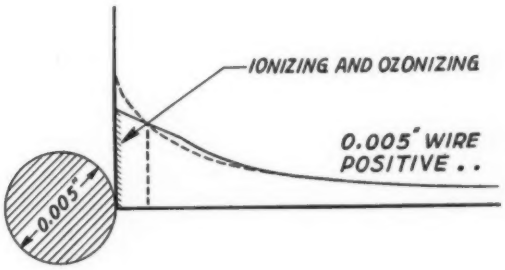

FIG. 7.

positive ion space charge. It is seen that the electric field next adjacent and electrode surface, where most of the electrons are, is much more intense for the 0.001-inch wire end than for the 0.005-inch straight wire so that the proportion of collisions which can dissociate molecules is less for the 0.001-inch than for the 0.005-inch electrode.

CONCLUSIONS

Ozone is produced in the silent electric discharge principally by collisions between electrons and oxygen molecules at energies suitable for molecular dissociation. When the discharge electrode is negative, collisions occur at dissociation energies principally in the region outside the ionizing sheath but well inside the sheath where the electrons excite the first critical potential in oxygen and attach to oxygen molecules. When the electrode is positive, collisions at dissociation energies occur in a thin sheath adjacent to the electrode surface, and dissociations also occur due to ultraviolet radiation of high energy.

The Further Concentration of S^{34} *

DAVID W. STEWART† AND KARL COHEN
Department of Chemistry, Columbia University, New York, New York

(Received September 17, 1940)

A further application has been made of the chemical exchange reaction between sulfur dioxide gas and a solution of sodium bisulfite to the problem of securing higher concentrations of sulfur of atomic weight 34. The exchange reaction was carried out in a series of countercurrent fractionation columns which previously had been used for the separation of the nitrogen and carbon isotopes. Using three fractionation units in cascade arrangement, we have secured sulfur containing 25 percent S^{34} at a rate of 3.2 grams per day, and have produced sufficient material for a large number of tracer experiments.

INTRODUCTION

THE concentration of S^{34} by a chemical exchange reaction has been described by Thode, Gorham and Urey,[1] and by Urey, Mills, Roberts, Thode, and Huffman.[2] The latter authors considered the systems:

SO_2 (gas) $-C_6H_5NO_2$ (liquid);
SO_2 (gas) $-CH_3OH$ (liquid);
SO_2 (gas) $-H_2O$ (liquid);
and H_2S (gas) $-$ NaHS (aqueous).

They found no change in the concentration of S^{34} in the first three systems, which depend upon the exchange with dissolved sulfur dioxide. In the solution of sodium hydrogen sulfide they found a slight exchange favoring the concentration of S^{34} in the gas phase. None of these systems were found to be as suitable as that suggested earlier by Thode, Gorham, and Urey. In this earlier work, exchange of S^{34} took place between a gas phase of SO_2 and a liquid phase consisting of a solution of sodium bisulfite in water, saturated with SO_2 at a pressure of 25 cm of Hg. As a result of this preliminary work, a more extensive series of fractionation columns has been used to carry out the reaction and considerable material with a maximum S^{34} concentration has now been produced.

The equilibrium may be represented by Eq. (1)

$$S^{34}O_2(g)+HS^{32}O_3^-(aq) \rightleftarrows S^{32}O_2(g)+HS^{34}O_3^-(aq). \quad (1)$$

The method of Urey and Greiff[3] has frequently been used to calculate the equilibrium constant for exchange reactions. This method involves the assumption that the ratio of the distribution functions for the ions in solution can be calculated by formulae applicable to the gaseous ions. Since the exact structure of the bisulfite ion in solution is not known, and since data as to its vibration frequencies are not available, such a calculation is not feasible.

The abundance of the stable isotopes of sulfur has been measured by Aston,[4] and more recently by Nier.[5] For reference, the relative abundance as determined by Nier may be given here: $S^{32}=100$; $S^{33}=0.78$; $S^{34}=4.4$; $S^{36}=0.016$. In the present work S^{33} was not concentrated appreciably and no effort was made to determine whether the extremely rare isotope, S^{36}, had been increased in concentration.

APPARATUS

The system of fractionation columns used in this work has been described by Thode and Urey.[6] It consists of three units in which the heaviest material produced by the first unit is used to feed the second unit, which, in turn,

* Publication assisted by the Ernest Kempton Adams Fund for Physical Research of Columbia University.

† Present address: Research Laboratories, Eastman Kodak Company, Rochester, New York.

[1] H. G. Thode, J. E. Gorham, and H. C. Urey, J. Chem. Phys. **6**, 296 (1938).

[2] Urey, Mills, Roberts, Thode and Huffman, J. Chem. Phys. **7**, 138 (1939).

[3] H. C. Urey and L. J. Greiff, J. Am. Chem. Soc. **57**, 321 (1935).

[4] F. W. Aston, *Mass Spectra and Isotopes* (London, 1933), p. 143.

[5] A. O. Nier, Phys. Rev. **53**, 282 (1938).

[6] H. G. Thode and H. C. Urey, J. Chem. Phys. **7**, 34 (1939).

supplies still heavier material to the final unit. Unit 1 consists of 24 meters of glass column with an inside diameter of 7 cm, packed with 6-mm Berl saddles. The second unit is 12 meters of glass column with an inside diameter of 2.2 cm, packed with 6-mm glass spirals of the Fenske type. The third unit consists of 7.5 meters of 1-cm glass column packed with 5-mm glass spirals. The columns are mounted side by side in 5-meter sections, and pumps are used to transport the liquid from the foot of one section to the top of the next. Figure 1 shows the arrangement of the apparatus as it was used for the concentration of S^{34}.

In operation, a saturated solution of sodium sulfite (1.6 *M*) was fed at the top of unit 1 by pump P_1. At the bottom of this unit sulfuric acid (2.8 *N*) in 15 percent excess was added by pump *P*, and the SO_2 was removed from the solution in a stripping column *S*. The SO_2 passed upward through the unit, converting the sodium sulfite solution to sodium bisulfite, and finally was removed from the system at *V* and carried to the drain by a stream of water passing through a separate stripping column.

Since S^{34} concentrates in the liquid phase, the material at the foot of unit 1 was heavier than normal. Unit 2 was, therefore, fed with material withdrawn at this point. At the foot of the second unit the refluxing process was repeated after a small fraction of the flow had again been removed to be fed to unit 3. At the bottom of the last unit all of the sulfur dioxide was refluxed by the addition of acid and sent upward through the whole apparatus. The pots in which the solutions were boiled at the foot of each unit were constructed entirely of copper with welded seams. These were heated by gas burners and boiled smoothly without bumping. Flasks made of glass were unsatisfactory on this account. In all essential respects the details of operation were the same as have been described by Thode and Urey for the separation of the nitrogen isotopes.

Operation

It was found in preliminary experiments that the most suitable pressure for operation with SO_2 was 25 cm of Hg.[7] This pressure was maintained by a vacuum pump which operated intermittently in order to remove inert gas from various sources which accumulated in the stripping column attached at *V*. The pump was operated by a pressure regulated relay so as to maintain a constant pressure at *V*. In the work with SO_2, the rate of gas flow through the apparatus was considerably less than in the work with ammonia. For this reason the pressure drop through the apparatus was much smaller than had been found previously, and so the entire apparatus operated at the optimum pressure without the need of a gas compressor between units.

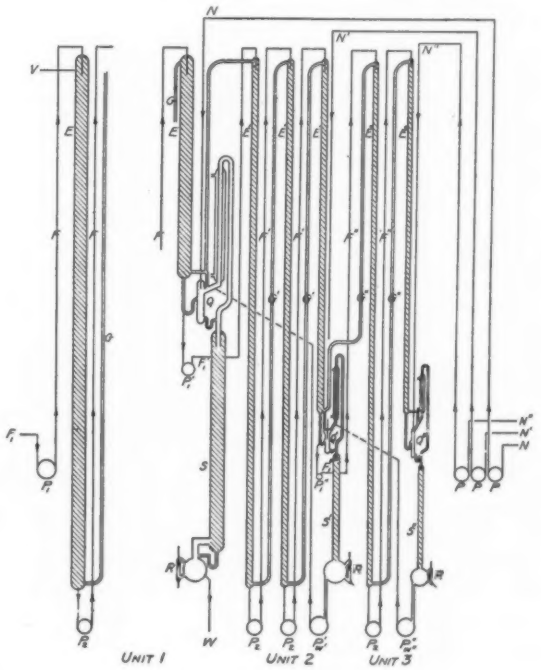

FIG. 1.

In an effort to improve the wetting characteristics of the packing, small amounts of various wetting agents were added to the sodium sulfite feed solution. Although none produced more than a very slight effect, the final experiments were made using sodium sulfite solution containing 0.05 cc of technical octyl alcohol per liter.

Although the three units had effected a 700-fold change in the isotope ratio in the ammonia-ammonium ion exchange, it was found that the efficiency was much lower in the concentration of S^{34}. At best, each unit produced only about a twofold change in the $S^{34} : S^{32}$ ratio. Since the

[7] Cf. K. Cohen, J. Chem. Phys. **8**, 588 (1940), Table II.

columns had been designed for liquid flows decreasing in the ratio of 100 to 10 to 1, they were not entirely suited to the present case since it was desired to maintain in each unit a flow inversely proportional to the working concentration of S^{34}. In the present work unit 1 was operated at a rate of flow well below its capacity and unit 3 carried slightly more than required for most efficient operation.

In the final experiment the apparatus was kept in constant operation for 27 days. During most of this time unit 1 was fed sodium sulfite solution at the rate of 26 cc per minute, unit 2 was fed bisulfite at the rate of 10.5 cc per minute and unit 3 was fed at about 2.6 cc per minute. Governor-controlled motors were used to drive the pumps feeding sulfite and acid to the three units. These pumps, as well as those used elsewhere in the apparatus, were of the rubber-tube type previously described.[6]

After several days of operation it was noted that the solution flowing through unit 2 and unit 3 was colored a light yellow, and small amounts of a precipitate which appeared to be free sulfur appeared at the points where sulfuric acid was added to the bisulfite solution. A qualitative examination of the starting material, which was technical $Na_2SO_3 \cdot 7H_2O$, showed the presence of moderate amounts of sulfate and traces of complex sulfur acids (probably thiosulfates) which liberated colloidal sulfur upon prolonged boiling with acid.

The efficiency with which SO_2 was stripped from the acidified solution at the foot of each unit was checked during the final run by examining the waste liquor pumped from each of the pots. By titration of this liquid, the correct proportion of sulfuric acid to sodium bisulfite was determined.

Results

The concentration of S^{34} at the foot of unit 3 was determined frequently by withdrawing samples of SO_2 and analyzing directly on a mass spectrometer, of the type previously described.[6]

During the first 14 days of operation, several upsets occurred which probably delayed the attainment of equilibrium by at least 3 days. The maximum concentration, corresponding to 27 percent S^{34}, was attained 21 days after the start of the experiment. At this time the concentration of S^{34} was about 8 percent at the foot of unit 1 and about 15 percent at the foot of unit 2.

By experiment, it was found that heavy material could be withdrawn at the foot of unit 3 at a rate of 30 cc of solution per day without decreasing the concentration below 25 percent S^{34}. This rate corresponds to a production of 3.2 grams of sulfur per day, or 0.8 gram of S^{34} (in 25 percent concentration). Production was maintained at this rate for 6 days, after which the experiment was stopped and the columns drained and rinsed.

By titrating small portions of the combined drainings and rinsings with alkali to the pH of a solution of sodium sulfite, the hold-up was determined for unit 1. This was found to be equivalent to 23 moles of sulfur. As in previous experiments, the hold-up in unit 2 was 3.0 moles and in unit 3, 0.35 mole. Since S^{34} was distributed exponentially in the columns it was possible to find by integration the total moles of S^{34} which had been accumulated in the columns when equilibrium was attained. The rate of accumulation of S^{34} indicated by this calculation was 1.1 grams per day. This is in reasonably good agreement with the value of 0.8 gram per day when it is remembered that the latter amount was withdrawn entirely at the foot of unit 3, whereas the over-all production will include an additional amount transported by unit 2 and not fully utilized because of the limited feed possible to unit 3.

Huffman and Urey[8] have shown that T, the rate of transport of the heavy material, is given by the expression

$$T = wN(\alpha - 1), \qquad (2)$$

where w is the total flow in the column, N is the mole fraction of S^{34} in the original material and α is the simple process fractionation factor under the conditions of production.* Using this equation and assuming a transport of 0.03 mole of S^{34} per day, an experimental value for α is found

[8] J. R. Huffman and H. C. Urey, J. Ind. Eng. Chem. **29**, 531 (1937).

* According to K. Cohen (reference 7), $T = wN(\alpha' - 1)$, where α' varies continuously from α, the simple process factor (at zero time), to 1 (at equilibrium time). Equation (2) should be interpreted, strictly, as $\langle T \rangle_{Av} = wN(\langle \alpha' \rangle_{Av} - 1)$. The actual productive transport will be close to $\langle T \rangle_{Av}$, and this is what gives value to the calculation of α'_{Av}.

to be 1.012. This value is identical with that found experimentally in the concentration of C^{13} by means of the HCN − NaCN exchange.[9]

The concentration of S^{34} obtained in this experiment is sufficient for most applications where the isotope is to be used as a tracer. The increase in concentration was very much less, however, than had been obtained in experiments with $N^{15}H_3 - N^{14}H_3$ using the same apparatus. This can be attributed, aside from a difference in the simple process factor, to a lower plate efficiency and to side reactions resulting in a loss of heavy material. A decreased plate efficiency is to be expected since the heavier SO_2 molecules diffuse less rapidly than do molecules of NH_3. Several factors could easily cause a loss of heavy material in this experiment. Oxygen dissolved in the solutions might oxidize bisulfite to sulfate, and it has been shown by Voge,[10] using radioactive sulfur as an indicator, that no exchange takes place between SO_3^{--} and SO_4^{--} in either acid or alkaline solutions. Such an oxidation would, therefore, constitute a forward flow, and the heavy material lost in this way might be a considerable part of the transport of the column. Another serious difficulty in the process seems to be in the possible auto-oxidation of $NaHSO_3$. This process has been extensively studied by Foerster and his co-workers and by Bassett and Durrant.[11] While the two groups of workers do not agree entirely on the mechanism of the reaction, their results show conclusively that bisulfite solutions are transformed with time into solutions containing only sulfate, thiosulfate, polythionates, and free sulfur. Foerster and Haufe[12] point out that the decomposition takes place in two steps. In the first of these, sulfate, thiosulfate, and polythionates are formed. In the second step, the thiosulfate and polythionates are converted to sulfate and free sulfur, with the regeneration of a small amount of sulfite. They have shown that the first step is catalyzed by selenium, and have measured the reaction velocity at various temperatures in the presence of different amounts of catalyst, and in solutions containing excesses of both Na_2SO_3 and H_2SO_3. The decomposition is accelerated by increased acidity, and is essentially complete in seven hours at 80°C in the presence of 0.06 molar H_2SO_3 and 1.2 mg SeO_2 per cc of 5.7 *M* $NaHSO_3$. While the auto-oxidation in our fractionation columns at room temperature is undoubtedly much slower than this, a loss of even 0.01 percent of the total flow by this process would result in greatly decreased efficiency.

In an attempt to detect a loss of heavy sulfur through oxidation by the air or through the auto-oxidation process, sulfur present as sulfate in the waste liquor at the foot of each unit was examined in the mass spectrometer, after reduction to sulfide by means of carbon or powdered iron and subsequent combustion of H_2S to produce SO_2. The isotopic composition was found to be the same as for ordinary sulfur, within the limits of accuracy of the analytical method, which is about 0.01 percent of S^{34}. Failure to find increased amounts of S^{34} at this point is not surprising, since any material lost by oxidation would be greatly diluted by ordinary sulfate, added as sulfuric acid. No experiments were made to analyze for S^{34} in the sulfate present in the bisulfite solution before the sulfuric acid was added.

In all, 55 grams of Na_2SO_3, containing 25 atom percent of S^{34}, were obtained. In addition, the total hold-up of the columns, amounting to approximately 3 kg of Na_2SO_3, was obtained with concentrations of S^{34} ranging downward from 20 percent to the normal concentration of 4.2 percent. This material is now available for use in tracer experiments, particularly those in biological work requiring prolonged feeding of sulfur-containing compounds where the well-known radioactive sulfur is not entirely suitable.

Our thanks are due to Professor H. C. Urey for his interest and support in this investigation. Dr. C. A. Hutchison and Dr. I. Roberts were associated with the early experiments using the present apparatus. Mr. Charles E. Miller shared in the operation of the apparatus during the final experiment, as did also Mr. B. Weinstock.

[9] C. A. Hutchison, D. W. Stewart and H. C. Urey, J. Chem. Phys. **8**, 532 (1940).
[10] H. H. Voge, J. Am. Chem. Soc. **61**, 1032 (1939).
[11] H. Bassett and R. G. Durrant, J. Chem. Soc. 1401–68 (1927).
[12] F. Foerster and E. Haufe, Zeits. f. anorg. allgem. Chemie **177**, 17 (1929).

The Absorption Spectra of Europium Ion in Some Hydrated Salts

F. H. SPEDDING, C. C. MOSS* AND R. C. WALLER
Chemical Laboratory, Iowa State College, Ames, Iowa
(Received August 5, 1940)

The absorption spectra of crystalline $EuCl_3 \cdot 6H_2O$, $EuBr_3 \cdot 6H_2O$, and $Eu_2(SO_4)_3 \cdot 8H_2O$ were photographed at various temperatures in the visible and ultraviolet region of the spectra. The salts were found to have low-lying excited levels at about 300 cm^{-1}, 390 cm^{-1}, 938 cm^{-1}, 970 cm^{-1} and, perhaps, 430 cm^{-1}, which arose from excited electronic, crystal and vibrational frequencies. These levels are discussed in relation to existing theories of specific heat, magnetic susceptibility, etc., of europium.

THE theory of line spectra arising from atoms and molecules in the gaseous phase seems to be in a fairly satisfactory state. Condon and Shortley in their introduction to *The Theory of Atomic Spectra*[1] state:

> "All known features of atomic spectra are now at least semiquantitatively explained in terms of quantum-mechanical treatment of the nuclear atom model."

Simple molecular spectra of gases are also rapidly yielding to attack. Theoretical chemists and physicists are now turning their attention to the energy states of solids. Unfortunately for exact quantitative agreement, most solids and solutions give broad, diffuse bands at room temperatures. However, compounds of the rare earths produce spectra which are fairly sharp at room temperatures and which are extremely sharp at low temperatures, the line widths comparing very favorably with the absorption spectra of gases. The rare earths, therefore, offer an excellent testing ground upon which to check theoretical considerations about energy states of atoms when they are in the condensed phase.

The sharp absorption spectra of the rare earths arise from transitions within the incomplete $4f$ shell; that is to say, the absorption lines originate from transitions between terms arising from rearrangements of the $4f^n$ configuration. These electrons are shielded to some extent from the fields of the neighboring atoms by the completed $5s5p$ shells. However, the spectra in their fine structure reflect the nature of the fields surrounding the rare earth ion and, accordingly, such spectra should prove to be a powerful tool for the study of the fields existing in solids and solutions. Unfortunately, sufficient precise experimental data are not available to give reliable confirmation of the many theoretical suggestions which have been made in the literature. In this paper we have investigated the absorption spectra of three salts of Eu at various temperatures, and we are presenting the data so that they may be used to check present theories and to furnish material for further extension of them.

EXPERIMENTAL

1. Materials

The europium salts used in this investigation were prepared from some exceptionally pure europium sulphate which was very kindly given to us by Dr. H. N. McCoy. He had prepared it according to the methods outlined in his papers on europium.[2]

$EuCl_3 \cdot 6H_2O$ salts were prepared from $Eu_2(SO_4)_3 \cdot 8H_2O$ by dissolving the salt in conductivity water and precipitating the europium as the oxalate by means of oxalic acid. The europium oxalate was filtered out on ashless filter paper and ignited to the oxide in a platinum crucible. The oxide was dissolved in redistilled dilute C.P. HCl. The resulting solution was evaporated until $EuCl_3 \cdot 6H_2O$ crystals came down. These crystals were twice recrystallized at room temperature from conductivity water containing a few drops of dilute HCl.[3]

It is extremely important to *recrystallize* the salts at *room* temperatures as the solutions of the oxide in the various acids were always slightly yellow. This yellow color was due to very small impurities of iron. These, we believe, were introduced into the oxide when it was ignited in platinum, since most laboratory platinum

* Exchange Scholar from the Queen's University of Belfast, Northern Ireland. This author is also indebted to the Ministry of Education of His Majesty's Government in Northern Ireland for the award of a Research Grant.

[1] E. U. Condon and G. H. Shortley, *The Theory of Atomic Spectra* (Cambridge Press, 1935).

[2] H. N. McCoy, J. Am. Chem. Soc. **57**, 1758 (1935); 58, 1577, 2279 (1936).

[3] It is necessary to recrystalline with a small amount of acid present to prevent any tendency to hydrolyze.

retains some reduced iron from previous use which is not removed by ordinary cleaning of platinum ware. The ignition of the basic rare earth oxides takes up some of this iron and if it is not removed by recrystallization, it tends to make the crystals almost opaque to ultraviolet light. While, usually, only one hydrate is reported for each salt, more may exist, for most of the rare earth salts have not been extensively investigated. It is known that the cerium salts and the corresponding trivalent iron salts have several hydrates, the one obtained depending on the conditions such as temperature, acidity, etc., under which it was formed. Analyses were made to make certain that the salts were the hydrate named. For example europium in $EuCl_3 \cdot 6H_2O$ was found to be 41.48 percent, while the theoretical value was 41.7 percent. The chloride was found to be 29.03 percent, while the theoretical value was 29.01 percent. Therefore, the salt was the hydrate assumed. For these reasons the methods of preparing the salts and an analysis of the crystals should always be given when reporting on spectra, magnetic susceptibilities or other properties of rare earth crystals. This has not been done in most papers dealing with magnetic susceptibilities of the rare earths, and may account for the wide discrepancies between the results of various investigators.

$EuBr_3 \cdot 6H_2O$ crystals were prepared in exactly the same manner as the $EuCl_3 \cdot 6H_2O$ except that redistilled C.P. HBr was used instead of HCl. Analysis showed the crystals to be the six hydrate.

$Eu_2(SO_4)_3 \cdot 8H_2O$ crystals were prepared from the original salt by twice recrystallizing from conductivity water containing one or two drops of dilute sulphuric acid. The recrystallization was done at room temperatures in a vacuum desiccator according to the procedure described in a previous paper.[4]

Liquid nitrogen was used for the cooling medium instead of liquid air because it is free from the broad oxygen bands which tend to obscure part of the spectrum.

2. Absorption cells

These varied with the type of sample in use and also with the region which was being investigated. Three types of sample were employed (a) single crystals, 2–3 mm thick (b) thin conglomerates, 1–2 mm thick (c) thick conglomerates, 6–10 mm thick. In case (a) the crystal chosen, usually about 5 mm across, was simply attached to a piece of stout cardboard with a suitable hole cut out through which light could be passed. This type of sample could be used at room temperature and at the temperature of liquid nitrogen, both in the visible and ultraviolet region.

In case (b) the crystals of the salt were gently broken in an agate mortar until all were of a small and roughly uniform size.[5] This "conglomerate" of crystals was then packed into a tiny cell consisting essentially of two plane, parallel, quartz plates, each having dimensions 15×5×1 mm. The plates were kept apart by a frame of cardboard cut out in the center. The completed cell was held intact by adhesive tape. This type of cell could be used at all temperatures and for all regions of the spectra.

In case (c) the conglomerate was put in small glass flasks having plane-parallel sides. These were made by blowing out tubing of suitable diameter in carbon moulding blocks. These cells could not be used in the far ultraviolet, since the glass does not transmit there. Also, in such thick conglomerates very little ultraviolet light can be transmitted, since most of it is lost through scattering from the surface of the crystals before it gets through.

3. Apparatus

The source of light was a 500-watt tungsten bulb in the visible, and a hydrogen arc of the Urey type in the ultraviolet. The cooling Dewars, general apparatus, and procedure used were the same as described in previous papers.[6] The spectrograph used was a Hilger E-1 Littrow type quartz instrument. Exposure times varied from half a minute to 17 hours.

Results

Table I gives the results obtained. All lines were observed and measured on at least two separate plates. It has been shown elsewhere[7] that the positions of the lines in the conglomerate spectra are the same as those in the single crystal. In the conglomerate, however, the intensities of the weaker lines are greatly enhanced. Therefore, only the positions of the conglomerate lines are given when all were observed. Where complete absorption occurred for the thick conglomerate, the positions of the lines in a thin conglomerate (marked with an asterisk) or the single crystal (marked with a prime) are listed. When brackets are shown, the edges and intensity center are given. The wavelengths are listed only for the low temperature results, except in the cases where no low temperature lines are observed. The letter *H* denotes a line which is markedly intensified at high temperatures, and may not be picked up at all at low temperatures. Similarly *L* denotes a low temperature line; that is to say, a line believed to be electronic in nature and originating from the basic state. The columns headed *I* give the intensities of the lines as estimated visually with respect to other *neighboring* lines on a scale extending from 0 to 10. A line marked 0 was so

[4] Spedding, Nutting and Hamlin, J. Chem. Phys. **5**, 191 (1937).

[5] If the conglomerate is too fine a powder, extremely thin, conglomerates have to be used to get any light through. Then a considerable proportion of the light gets through by reflection instead of transmission, and the absorption is faint or entirely masked.

[6] Various papers by F. H. Spedding.

[7] F. H. Spedding and R. S. Bear, Phys. Rev. **39**, 946 (1932); **42**, 58–76 (1932).

TABLE I. *Absorption lines of europium salts.*

$EuCl_3 \cdot 6H_2O$					$EuBr_3 \cdot 6H_2O$					$Eu_2(SO_4)_3 \cdot 8H_2O$				
	80°K		300°K			80°K		300°K			80°K		300°K	
A	cm^{-1}	I	cm^{-1}	I	A	cm^{-1}	I	cm^{-1}	I	A	cm^{-1}	I	cm^{-1}	I
			16289*H*	1*d*	6135.9			16293*H*	0*d*	6142.7	16275	0*s*	16276	
6129.1			16311							6138.9	16285[e]		16281	0*d*
6126.1			16319H	2*d*	6125.0			16322					16287	
6123.5			16326		6122.7			16328*H*	2*s*				16319	
5963.9	16763*L*	1*d*			6120.1			16335		6124.6	16323	0*s*	16327	0*d*
					5967.8	16752*L*	0*d*			6120.8	16333[e]		16336	
					5943.6			16820		5944.0			16819	
5939.8			16831		5940.5			16829	2*d*	5940.4			16829	2*d*
5937.0			16839*H*	4*d*	5937.6			16837		5936.9			16839	
5934.1			16847											
5931.7			16854											
5928.2			16864*H*	4*d*										
5924.6			16874		5924.6			16874		5926.0	16870		16872	
5921.8	16882	?			5921.5			16883*H*	2*d*	5924.6	16874	3*s*	16880*H*	8*d*
					5918.3			16892		5921.8	16882		16889	
					5898.8	16948							16946	
5900.2			16944		5897.4	16952	1*d*	16952		5896.3	16955		16956*H*	8*d*
5897.0	16953	1*s*	16956*H*	5*d*	5896.0	16956		16961	3*d*	5895.6	16957	6*s*	16966	
5892.2			16967		5891.1			16970		5894.8	16959			
					5855.6	17073								
					5853.5	17079	2*d*							
5854.5	17076	2			5851.5	17085		17087	1*d*					
5848.4	17094													
5847.0	17098*L*	4*d*	17097*L*	0*d*										
5845.3	17103													
5835.1	17133	1			5834.4	17135								
					5833.0	17139	4*s*							
					5831.7	17143								
5827.9	17154				5828.3			17153	1*d*					
5826.2	17159*L*	8*s*												
5824.5	17164		17163*L*	1*s*										
					5806.6	17217								
					5805.3	17221*L*	3*s*							
5803.2	17227				5803.9	17225								
5800.9	17234	4*d*												
5798.9	17240													
5796.8	17246				5795.5	17250								
5794.5	17253	3*s*			5794.2	17254	3*s*			5794.5	17253			
5793.1	17257		17257		5793.1	17257				5793.8	17255	1*vs*		
5792.1			17260	3*s*	5791.5			17262		5792.8	17258		17262	
5791.1			17263		5790.1			17266	5*s*	5790.8			17264	1*vs*
					5788.8			17270		5790.1			17266	
5773.7	17315													
5770.7	17324	1*d*	17323	0*d*	5770.7			17324*H*	0*d*					
5767.7	17333													
5756.8	17366	0			5753.1			17377*H*	0*d*					
5740.6	17415	0												
					5726.8	17457	2*d*							
5723.5	17467													
5721.2	17474	5*d*	17469	1*d*	5720.9			17475	0*d*					
5718.9	17481													
5573.8			17936*H*	0*d*				17949*H*	1*d*	5569.4			17950	0*vd*
										5557.1			17990	
										5548.4			18018	0*vd*
5543.2			18035	1*s*	5542.3			18038*H*	1*d*	5542.9			18036	
5534.0			18065	0*d*	5531.6			18073*H*	0*d*	5534.3			18064	0*vd*
5526.7			18089	0*d*	5524.5			18096*H*	1*d*	5520.2			18100	
5380.9			18579*		5385.0			18565						
5378.3			18588*	3*d*	5378.6			18587*H*	4*d*					
5376.3			18595*		5273.3			18609						
5375.7	18604*H*	0	18597*							5371.6	18611			
5373.7			18608*H	6*s*						5370.5	18615	0*s*	18619	
5369.4			18619*		5371.4	18612	1*d*	18615		5369.0	18620			
					5368.2			18623	8*s*					
5368.2			18623*		5365.9			18631		5366.0	18630		18633*H*	8*d*
5365.0			18634*	3*d*	5364.5			18636		5365.0	18634	0*s*		
5362.7			18642*		5360.7			18649	4*d*	5363.7	18638		18646	
					5358.4	18657	0*d*	18662						
										5347.0	18697			
										5345.5	18702	0*s*		
										5344.1	18707		18705	
5343.0	18711		18711*		5342.4	18713		18712		5341.8	18715		18718*H*	8*d*
5342.1	18714*H*	6*s*	18721*H	8*d*	5341.5	18716	4*s*	18728	8*d*	5340.3	18720	2*s*	18730	
5341.0	18718		18734*		5340.4	18720		18744		5338.9	18725			
					5338.4	18727	?			5337.8	18729			
5281.1	18930									5336.9	18732	0*s*		
5279.5	18936*L*	2*d*			5279.8	18935*L*	?			5335.8	18736			
5277.8	18942													
5271.4	18965	1*d*			5269.7	18971*L*	?							
5264.2	18991													
5263.4	18994	5*s*												
5262.5	18997		18997*		5263.1	18995				5262.5	18997			
5261.1			19002*	6*s*	5262.0	18999	5*s*			5261.6	19000	8*vs*		
5260.0			19006*		5260.9	19003		19002		5260.8	19003		19004	
					5259.5			19008	7*s*	5257.8	19014		19008	9*s*
5258.4	19012				5257.8	19014		19013		5257.0	19017	8*vs*	19012	
5257.3	19016	8*d*			5257.0	19017	5*s*							
5255.9	19021		19020*		5256.2	19020		19022		5256.4	19019		19020	
5254.5	19026		19026*	6*s*	5254.8	19025				5254.2	19027		19024	9*s*
5253.1	19031	6*s*	19031*		5253.7	19029	5*s*	19031	7*s*	5253.4	19030	8*vs*	19027	
5251.8	19036				5252.8	19032				5252.8	19032		19033	
					5250.6			19040					19037	9*s*
										5245.9	19057	0*s*	19040	
										5242.1	19071			

TABLE I.—*Continued.*

$EuCl_3 \cdot 6H_2O$					$EuBr_3 \cdot 6H_2O$					$Eu_2(SO_4)_3 \cdot 8H_2O$				
	80°K		300°K			80°K		300°K			80°K		300°K	
A	cm^{-1}	I	cm^{-1}	I	A	cm^{-1}	I	cm^{-1}	I	A	cm^{-1}	I	cm^{-1}	I
5235.5	19095	0			5235.0	19095*L*	1*d*							
5223.2	19140				5223.2	19140*L*	1*d*							
5222.1	19144L	3*d*								5219.1	19155	0*s*		
5221.0	19148									5214.7	19171			
5121.0	19522	0												
5119.4	19528	0												
4892.8			20433*	0*d*	4891.7			20437*H*	0*d*	4878.1			20494	0*d*
4871.0			20524*	1*d*	4873.1			20515*H*	1*d*	4871.7			20521	
4865.8			20546*	?	4863.9			20554*H*	0*d*	4866.2			20544	
					4855.1			20591*H*	0*d*	4864.3			20552	1*d*
										4861.7			20563	
					4845.3	20633								
					4844.3	20637*L*	2*s*							
					4843.6	20640								
4841.7	20648				4842.4	20646								
4840.8	20652*L*	4*s*			4841.5	20649*L*	2*s*							
4839.9	20656				4840.8	20652								
4838.9	20660													
4838.0	20664*L*	4*s*												
4837.0	20668													
										4827.7	20708	0*vs*		
										4825.3	20718			
4772.2	20949	0			4772.2	20949*L*	?							
4754.7	21026	0			4755.4			21023*H*	2*d*					
4753.3			21032*	2*d*						4754.2			21028	0*d*
4743.0	21078	1*s*								4740.0			21091	
4740.7			21088*	0	4735.8			21110*H*	1*d*					
4732.4	21125	1*s*	21129*	2*d*										
4720.6	21178				4725.0	21158*L*	0*d*							
4720.1	21180	2			4723.2	21166*L*	0*d*							
4719.7	21182													
4719.2			21184*	0						4710.1	21225	0*vs*	21184	0*d*
4717.9	21190									4707.6	21236		21239	
4717.2	21193	2												
4716.6	21196													
4711.0			21221*	0	4711.9	21217	0*d*	21216						
					4711.2			21220	2*d*					
					4710.1			21225						
4703.0	21257	0			4703.5	21255*L*	0*d*							
4686.1			21334*	2*d*	4684.1			21343*H*	0*d*	4690.2			21315	0*d*
4676.6			21377*	0	4677.3	21374	0*d*			4671.5			21400	
					4674.9			21385	0*d*					
					4670.9	21403	0*d*			4667.4				
4668.1			21416*	0	4668.5			21414	1*d*	4663.9			21419	0*s*
4662.2	21443												21435	
4661.6	21446	5*s*												
4660.9	21449				4660.7	21450				4660.9	21449			
4660.3			21452*		4660.1	21453	3*s*			4660.2	21452	10*s*		
4659.4			21456*	3*s*	4659.6	21455				4659.6	21455			
4658.5			21460*		4658.5			21460		4658.7			21459	
					4657.4			21465	3*s*	4657.8			21463	9*s*
					4656.6			21469		4657.2			21466	
										4654.8	21477			
4655.3	21475									4654.4	21479	7*vs*		
4654.4	21479	7*s*								4653.7	21482		21485	
4653.5	21483		21483*		4654.0	21481							21489	8*s*
4652.2			21489*	6*s*	4653.1	21485	6*s*						21492	
4650.9			21495*		4652.0	21490		21490		4651.8	21491			
					4650.9			21495	7*s*	4651.1	21494	7*s*		
					4649.6			21501		4650.5	21497			
													21499	
4649.2	21503				4648.6	21506				4649.4	21502		21502	7*s*
4646.8	21514*L*	10*d*	21511*		4646.2	21517	8*d*	21514		4648.7	21505	10*s*	21504	
4644.5	21525		21523**L*	10*d*	4643.8	21528		21528	10*d*	4648.1	21508		21510	
4642.3			21535*					21542		4644.9	21523		21514	10*s*
										4644.0	21527	10*s*	21519	
										4643.4	21530		21530	
													21534	9*s*
													21538	
4637.3	21558	1*d*	21562*	0	4636.5	21562				4637.1	21559	0*s*	21554	
4636.5					4635.0	21569	3*d*	21568		4633.7	21575			
4632.6	21580				4633.3	21577		21576	2*d*	4632.0	21583	0*s*		0*d*
4630.9	21588	2*d*						21582		4629.1	21596			
4629.2	21596		21592*	2*d*	4629.2	21596								
4624.3	21619				4627.9	21602	3*d*	21602						
4622.3	21628	3*d*	21629*	2*d*	4626.4	21609		21608	1*d*				21608	
4620.4	21637				4625.3			21614		4625.5	21613	1*d*	21614	1*d*
					4620.6	21636				4619.5	21641		21651	
					4619.6	21641	3*d*	21640						
					4618.5	21646		21645	1*d*					
					4617.9			21649						
					4616.2	21657*L*	0*d*							
4615.5	21660													
4613.8	21668	2*d*	21671*	2*d*						4615.3	21661	1*d*	21665	1*d*
4612.1	21676				4611.7	21678	0*d*			4613.4	21700		21697	
4610.6	21683	1*d*			4610.4			21684	0*d*					
					4609.3	21689								
					4608.5	21693	1*s*							
					4607.4	21698								

TABLE I.—*Continued.*

$EuCl_3 \cdot 6H_2O$					$EuBr_3 \cdot 6H_2O$					$Eu_2(SO_4)_3 \cdot 8H_2O$				
	80°K		300°K			80°K		300°K			80°K		300°K	
A	cm^{-1}	I	cm^{-1}	I	A	cm^{-1}	I	cm^{-1}	I	A	cm^{-1}	I	cm^{-1}	I
4607.0	21700	1*d*			4605.1	21709				4601.5	21726	0*d*	21718	0*d*
4603.0	21719	1*d*			4604.0	21714	1*s*	21715	?	4595.1	21756		21760	
					4603.0	21719								
4590.1	21780				4599.6	21735*L*	0*d*			4591.1	21775			
4588.6	21787	2*d*			4594.7	21758*L*	0*d*							
4587.1	21794				4589.0	21785						0*d*		
4585.9			21800*	0	4588.0	21790	2*d*	21792	0*d*					
					4586.9	21795				4585.0	21804			
4580.6	21825	1*d*			4582.1	21818*L*	0*d*			4582.1	21818	0*s*		
										4580.2	21827			
					4576.8	21843*L*	0*d*			4576.4	21845	0*s*		
										4574.1	21856			
4568.9	21881	1*d*			4569.1	21880	2*d*			4571.8	21867	0*s*		
					4568.3			21884	0*d*	4570.3	21874			
4474.4	22343				4474.8	22341(O_2)	0*d*							
4472.4	22353	(O_2—band)								4453.5	22448	0*s*		
4470.6	22362									4451.1	22460			
4449.9	22466	0								4448.1	22475	0*s*		
										4446.3	22484			
4439.6	22518	0								4440.0	22516			
										4438.3	22525	1*s*	22525	
										4436.7	22533		22535	0*d*
													22545	
										4430.6	22564	0*d*		
										4426.1	22587			
										4423.1	22602	1*d*	22602	0*d*
										4415.1	22643		22643	
										4308.0			23206	0*d*
4302.6			23235*	0	4301.5			23241*H*	0*d*	4301.5			23241	
4293.8	23283	1*s*			4294.3	23280	1*s*							
4292.5			23290*	0*d*	4291.6			23295	0*d*	4292.8			23288	0*d*
										4283.3			23340	
					4274.9			23386*H*	0	4279.0			23364	0*d*
										4272.8			23397	
					4262.8			23452*H*	0	4268.6			23420	0*d*
			23915*	4*d*						4262.8			23452	
			23966*		4182.4			23903						
					4179.6			23919*H*	5*d*					
					4176.8			23935						
										4172.4	23960		23970	
					4179.3			23978*H*	2*d*	4171.4	23966	4*s*	23984*H*	9*d*
										4170.2	23973		23998	
										4164.6	24005	0*s*		
										4162.7	24016			
										4161.0	24026	0*s*		
4159.1	24037	1*s*								4159.3	24036			
4156.8	24050	1*s*	24047*	4*d*	4156.3	24053	0*d*			4156.3	24053		24053	
4153.4	24070	2*d*	24088*		4153.6	24069	1*d*	24069		4155.2	24059	5*d*		
					4151.1	24083	0*d*	24084	5*d*	4154.0	24066		24067*H*	8*d*
								24099					24081	
4147.2			24106*	1*s*						4145.9	24113		24103	
					4145.3			24117	?	4145.4	24116	1*s*	*H*	3*d*
					4106.5	24345	1*s*			4144.6	24121		24125	
4104.3	24358	0			4104.9	24354	1*s*			4105.8	24349			
4103.4			24363*	1*s*				24363	1*s*	4103.9	24360	6*s*	24365	
4101.7	24373	0			4102.3	24370	1*s*			4102.3	24370		24370	6*s*
4100.7			24379*	1*s*	4100.4	24381	1*s*	24383	1*d*	4101.4	24375	0*s*	24375	
4095.0	24413	1*d*	24416*	0	4095.5	24410	2*s*			4100.6	24380		24381	
										4098.5	24392		24384	0*s*
										4097.3	24399		24388	
										4094.8	24414	0*s*	24402	0*s*
										4093.8	24420		24418	
					4093.7			24421	1*s*	4093.6			24421	0*s*
										4093.2			24424	
			24562*							4070.2			24562	
			24610*	1*d*						4067.1			24580	0*d*
										4051.1	24617	0*d*	24598	
			24700*							4059.3	24628		24620	
			24733*	1*d*						4058.1	24635	0*d*	24635	2*d*
										4055.6	24650		24650	
										4046.6			24705	
										4044.7			24717	0*d*
										4042.2			24732	
					4027.5	24822*L*	0*d*							
					4023.7	24846*L*	0*d*			4022.4	24854	0*d*		
					4018.0	24881*L*	0*d*			4021.2	24861			
4008.0			24943*	?										
4002.7	24976*													
4001.8	24982*	1*d*												
4001.0	24987*													
					4000.2	24992*								
					3999.8	24994*L	2*s*							
					3999.4	24997*				3998.7	25000			
										3998.2	25004	3*s*		
										3997.3	25010			
3996.0	25018*				3995.5	25021*				3995.7	25020		25020	
3995.4	25022*	1*d*			3994.9	25025*L	2*s*			3995.0	25024	3*s*	25050	3*d*
3995.0	25024*				3994.4	25028*				3994.2	25029		25080	
3990.9	25050*				3990.4	25053*								
3990.3	25054*	1*d*	25055′		3990.1	25055*	1*d*							
3989.6	25058*		25065′	1*d*	3989.6	25058*								
3986.9			25075′		3988.7			25064*	1*d*					

TABLE I.—*Continued.*

$EuCl_3 \cdot 6H_2O$					$EuBr_3 \cdot 6H_2O$					$Eu_2(SO_4)_3 \cdot 8H_2O$				
	80°K		300°K			80°K		300°K			80°K		300°K	
A	cm^{-1}	I	cm^{-1}	I	A	cm^{-1}	I	cm^{-1}	I	A	cm^{-1}	I	cm^{-1}	I
										3986.1	25080			
										3985.3	25085	5s		
					3984.4	25091*				3984.4	25091			
3983.7	25095*	1d			3983.7	25095*L	2s							
					3983.1	25099*								
										3983.1	25099			
3980.6	25115′	1d								3982.3	25104	5s		
					3980.6	25115*				3981.4	25110			
					3979.9	25119*	3d							
					3979.3	25123*		25125*	1d	3979.5			25122	3d
3976.9	25138′	0			3971.8	25170*				3975.0	25150		25140	
					3971.2	25174*L	1d			3974.2	25155	4d		
					3970.8	25177*				3973.4	25160			
3968.4	25192′	0			3969.3	25186*				3969.7	25184			
					3967.9	25195*	4d			3967.3	25199	4d	25200	
3966.0	25207′	0			3966.2	25206*		25201*	2d	3965.7	25209			
3964.5			25217′	0	3964.1	25219*				3963.5	25223			
					3963.5	25223*	2d							3d
					3963.0	25226*								
3962.7	25228′	0d			3962.6	25229*				3961.9	25233	4d		
					3961.9	25233*	2s							
					3961.3	25237*		25235*	2d	3960.8	25240		25245	
3957.2	25263′	1d			3958.6	25254*	1d							
					3954.3	25282*L	1d			3953.3	25288			
3952.1	25296′	2			3952.1	25296*				3948.2			25321	
					3951.6	25299*	3s							
					3951.0	25303*								
					3950.5	25306*				3943.7	25350	5d		
					3949.7	25311*	3s			3940.9			25368	5d
3949.0	25316′	5d	25315′		3949.0	25316*								
3945.8	25336′		25355′	2d	3948.2	25321*								
			25392′		3947.4	25326*	3s							
					3946.6	25331*				3934.3	25410		25418	
					3947.4			25326*						
					3946.1			25334*	4d					
					3944.9	25342*		25342*						
3943.8	25349′				3943.0			25354*						
		5d			3941.5	25364*	8d	25367*	5d					
3939.8	25375′				3939.0			25380*						
3936.7	25395′	0d			3938.2	25385*								
					3933.0	25419*								
					3932.3	25423*L	1d							
3931.4	25429′	1d			3931.7	25427*								
3929.4	25442′	2d			3929.6	25441*								
					3928.9	25445*L	1d							
					3928.3	25449*								
3924.8	25472*	?												
3898.9	25641*	1d												
3895.4	25664*	?												
3857.5	25916*	1d	25919′		3860.2			25898*						
3854.7			25935′	4d	3853.2			25945*H	0d					
3852.2			25952′		3846.4			25991*						
3851.4			25957′											
3848.8			25975′	2d										
3846.4			25991′											
3845.8			25995′											
3844.8	26002*	0	26009′	2d										
3843.1			26013′											
					3835.3	26066*				3836.2	26060	1s		
					3835.0	26068*L	1s			3835.0	26068			
3834.6	26071*	1s	26074′	0	3834.7	26070*								
					3834.3	26073*				3833.9	26076	1s		
					3834.0	26075*L	1s			3833.0	26082			
					3833.6	26078*								
										3828.3	26114	1s		
										3827.4	26120			
										3826.2	26128	1s		
										3825.3	26134			
3822.6			26153′	0										
3818.0			26184′	0										
3815.0	26205*	0			3814.5	26208*L	0d							
					3813.4	26216*L	1d			3812.8	26220			
3811.5	26229*	0	26224′							3811.6	26228	2s		
3809.9			26240′	1d						3810.6	26235			
3807.6			26256′		3807.6	26255*	1d	26259*	0d					
3806.6	26263*	2d	26285′		3804.5	26277*	0d			3805.5	26270			
3802.6	26290*	0	26294′	1d	3801.6	26297*L	1d			3804.1	26280	0d		
3800.8	26303′	2d	26302′							3799.0	26315			
					3798.0	26322*	0d			3797.6	26325	0d		
3794.0	26350*	0	26357′	0	3794.7	26345*	1d	26344*	0d					
3792.6	26360*	0d			3792.4	26361*	1d							
3783.8	26421*	1d			3783.1	26426*L	0d							
3778.4	26459′	?			3777.8	26463*L	0d							

TABLE I.—*Continued.*

$EuCl_3 \cdot 6H_2O$					$EuBr_3 \cdot 6H_2O$					$Eu_2(SO_4)_3 \cdot 8H_2O$				
	80°K		300°K			80°K		300°K			80°K		300°K	
A	cm^{-1}	*I*	cm^{-1}	*I*	A	cm^{-1}	*I*	cm^{-1}	*I*	A	cm^{-1}	*I*	cm^{-1}	*I*
3771.9	26504*	1*d*			3772.8	26498**L*	1*d*							
					3767.8	26533*								
					3767.4	26536*	2*s*							
					3767.0	26539*				3767.1	26538			
					3765.8	26547*								
					3765.3	26551*	2*s*							
					3764.7	26555*		26558*	1*d*					
3763.9	26561*	1*d*	26561′		3763.1	26566*								
3762.4			26571′	1*d*	3762.7	26569*	2*s*			3762.6	26570	4*d*		
3761.3	26579′	0	26580′		3762.1	26573*				3762.0			26574	
					3760.7	26583*								
					3760.3	26586**L*	1*s*							
					3760.0	26588*				3759.7			26590	4*d*
					3758.2	26601*				3758.3	26600			
					3757.6	26605**L*	2*s*							
3755.8	26618*	0			3757.1	26609*				3757.6			26605	
					3754.2	26629*	0*d*							
3751.7	26647′				3752.4	26642*				3754.7	26626			
		3*d*	26655′		3751.8	26646*	3*s*			3752.7	26640	2*d*	26637	
3749.5	26663′				3751.3	26650*		26658*	1*d*	3751.0	26652		26652	0*d*
			26664′	2*d*	3749.6	26662*								
					3749.0	26666*	3*s*			3748.9			26667	
			26672′		3748.6	26669*								
3742.6	26712′	3*d*	26716	1*d*	3742.7	26711**L*	1*d*			3743.4	26706			
3741.2	26722′									3741.7	26718	2*d*	26710	
										3740.0	26730		26729	0*d*
3731.8	26789*	0			3732.1	26787**L*	1*d*			3732.8	26782		26748	
3730.3			26800′	1*d*						3730.2	26800	2*d*	26791	
										3728.1	26816		26810	0*d*
										3688.9	27101		26829	
										3687.9	27108	0*d*	27111	
										3686.9	27115		27124	0*d*
										3682.2	27150		27136	
										3680.2	27165	0*d*	27167	
										3678.1	27180		27182	0*d*
3676.0	27196*	0			3676.0	27196**L*	0*d*			3675.3	27201		27187	
3674.1			27210′	0*d*						3672.6	27221	0*d*	27218	
										3669.9	27241		27233	1*d*
										3668.8			27249	
3663.4			27289′	0*d*	3663.8	27286**L*	0*d*			3662.8	27294		27299	
					3660.5	27311**L*	0*d*			3661.2	27306	0*d*	27312	2*d*
3659.5			27318′	0*d*						3659.5	27318		27326	
3623.6	27587*				3624.1	27585*				3622.9	27594		27602	
3623.1	27593*	2*s*					4*s*			3621.2	27607	5*s*	27619	5*d*
3622.3	27599*				3623.3	27591*				3619.6	27619		27634	
3622.0			27601′		3622.7	27596*				3618.4	27629		27640	
3621.2			27607′	1*d*	3622.2	27600*	4*d*			3618.0	27632	1*s*	27643	1*d*
3620.4			27613′		3621.5	27605*				3617.4	27636		27647	
					3621.1	27608*				3615.6	27650		27662	
3620.4	27613*				3620.4	27613*	4*d*			3615.1	27654	1*s*	27665	1*d*
3619.9	27617*	2*s*			3619.8	27618*				3614.6	27658		27668	
3619.3	27622*		27619′		3619.4			27621*	2*s*	3605.2	27730		27738	
3618.7			27626′	1*d*						3604.5	27735	3*s*	27747	2*s*
3617.8			27633′							3603.9	27740		27754	
					3618.2	27630*				3599.0	27777		27782	
					3617.7	27634**L*	3*s*			3598.4	27782	0*s*	27790	0*d*
					3617.2	27638*				3597.9	27786		27798	
					3615.3	27652*				3592.5	27828		27834	
					3614.8	27656**L*	3*s*			3592.0	27832	0*s*	27842	0*d*
3614.3	27660*	1*s*			3614.3	27660*				3591.4	27836		27850	
					3608.7	27703**L*	0*d*			3546.9			28186	
3585.3	27884*	1*d*			3585.7	27881*				3546.2			28191	0*d*
					3585.1	27885**L*	1*d*			3545.6			28196	
					3584.5	27890*				3278.8			30490	
										3277.4			30503	0*d*
										3276.0			30516	
3275.3			30523′							3272.2			30552	
3271.1			30562′	0*d*						3270.7			30566	2*d*
										3269.2			30580	
3265.1			30618′	0						3246.0	30798		30624	
										3245.5	30803	0*s*	30639	2*d*
3260.5			30661′	0						3245.1	30807		30652	
3245.3	30805*	0	30954′							3232.7	30925		30940	
				1*d*						3232.2	30930	1*s*	30984	0*d*
3224.6			31003′							3231.7	30935		31029	
3220.3	31044*	0								3220.3	31044			
										3219.2	31055	1*d*		
3215.7			31088′	0*d*						3218.0	31066			
										3214.0	31105			
										3213.4	31111	1*d*		
										3212.7	31117			
										3210.2	31142			
										3209.6	31148	0*d*		
										3208.9	31154			
3206.1	31182*	2*d*	31196′							3205.3	31189		31198	
3204.0	31202*		31203′	2*d*						3203.6	31206	5*d*	31215	4*d*
			31209′							3201.9	31222		31229	
										3200.1	31240			
										3199.7	31244	1*d*		
										3199.1	31250			
										3196.0	31280		31280	
										3195.4	31286	1*d*	31293	
										3194.5	31295		31305	

TABLE I.—*Continued.*

$EuCl_3 \cdot 6H_2O$					$EuBr_3 \cdot 6H_2O$					$Eu_2(SO_4)_3 \cdot 8H_2O$				
	80°K		300°K			80°K		300°K			80°K		300°K	
A	cm^{-1}	I	cm^{-1}	I	A	cm^{-1}	I	cm^{-1}	I	A	cm^{-1}	I	cm^{-1}	I
										3191.9	31320		31320	
										3191.3	31326	2d	31333	0d
										3190.6	31333		31345	
3186.9	31369*		31392′							3186.8	31370		31377	
3186.1	31377*	1d	31405′	3d						3181.8	31420	5d	31430	5d
3185.3	31385*		31415′							3177.9	31458		31480	
3181.3			31425′							3176.7	31470			
3179.9			31438′	5d						3176.2	31475	0s		
3179.0	31447*	0	31451′							3175.7	31480			
3176.7	31470*	0	31488′	1d						3174.8	31489			
										3174.2	31495	2s		
										3173.6	31501			
										3172.8	31509			
										3172.2	31515	1s		
										3171.8	31519			
										3170.4	31530			
										3170.1	31535	1s		
										3159.7	31540			
3164.5			31591′	0						3165.6	31580		31596	
										3163.9	31597	5d	31624	3d
										3162.7	31609		31650	
										3162.1	31615		32635	
										3161.1	31625	5d	32648	0d
										3160.1	31635		32658	
										3047.3			32699	
										3056.1			32712	0d
										3054.9			32725	
										3050.7			32770	
										3049.3			32785	0d
										3047.9			32800	
										3038.2			32904	
										3038.0			32907	0s
										3037.7			32910	
3032.6	32965*	1d	32974′							3031.3	32979		32986	
3031.3			32979′H	3s						3030.9	32984	2s	32992	2s
3030.7	32986*	1s	32984′							3030.5	32988		32998	
										3029.5	32999		33009	
										3029.2	33002	2s	33015	2s
										3028.9	33006		33021	
3022.6	33074*	0d								3022.3	33078			
										3022.0	33081	1s		
										3021.7	33084			
										3020.9	33093		33091	
3018.8	33116*	0d								3020.2	33100	1s	33102	2d
										3019.5	33108		33112	
3016.1	33146*	0d								3017.4	33132		33134	
										3016.1	33146	3d	33148	2d
2995.9	33369*	1d								3014.8	33160		33162	
										2994.8	33381		33391	
										2994.0	33390	2s	33401	1d
										2993.1	33400		33410	
2987.2	33466*	2d	33490′							2985.5	33485		33497	
2982.8	33516*		33515′	4d						2984.0	33502	4d	33513	4d
2981.0			33536′							2982.5	33519		33530	
										2981.6	33529		33542	
2978.6	33563*	1d								2980.6	33540	4d	33550	4d
										2979.8	33550		33558	
										2978.1	33569		33573	
										2977.7	33573	2s	33579	1d
										2977.3	33578		33585	
										2972.7			33630	
										2971.2			33647	0d
										2969.6			33665	
2945.2	33944*	0								2943.1	33968		33714	
										2942.7	33972	2s	33729	0d
										2942.4	33976		33743	
2940.7	33995*	1								2939.3	34012		33981	
2940.1			34002′	1d						2938.8	34018	4s	33985	2d
2938.9	34016*	0								2938.2	34024		33990	
										2937.5	34033		34021	
										2937.2	34036	0s	34027	4d
2936.3			34047′	0						2936.9	34039		34033	
										2936.8			34031	
										2936.6			34043	0d
										2936.3			34046	
2935.1	34061*									2935.0	34062		34069	
		1d								2934.6	34066L	3s	34074	0d
2932.5	34090*		34089′	0						2934.2	34071		34079	
										2931.7	34100		34105	
										2931.2	34106	5s	34109	4d
										2930.7	34112		34112	
										2927.1			34153	
										2925.8			34169	0d
										2924.4			34185	
2914.5	34301*	0								2912.1	34329		34344	
										2911.9	34332	2s	34344	1d
2910.2	34352*	0								2911.6	34335		34349	
2903.2	34435*	1								2901.2	34459		34464	
										2900.8	34463	0d	34469	0d
										2900.5	34467		34473	

TABLE II. *Level at about 300 cm^{-1}.*

$EuCl_3 \cdot 6H_2O$	$EuBr_3 \cdot 6H_2O$	$Eu_2(SO_4)_3 \cdot 8H_2O$
17,260 − 16,956 = 304	17,266 − 16,961 = 305	17,264 − 16,956 = 308
19,026 − 18,721 = 305	19,031 − 18,728 = 303	19,024 − 18,718 = 306
21,523 − 21,221 = 302	21,414 − 21,110 = 304	21,514 − 21,212 = 302
26,240 − 25,935 = 305	21,528 − 21,220 = 308	24,370 − 24,067 = 303
26,664 − 26,357 = 307	21,645 − 21,343 = 302	24,421 − 24,114 = 307
27,626 − 27,318 = 308	21,715 − 21,414 = 301	31,293 − 30,984 = 309
	24,421 − 24,117 = 304	33,015 − 32,712 = 303
Mean Interval: = 305 at 300°K	25,367 − 25,064 = 303	33,401 − 33,102 = 299
301 at 78°K	Mean Interval: = 304 at 300°K	Mean Interval: = 306 at 300°K
	301 at 78°K	298 at 78°K

faint as to be invisible under the magnification of the comparator microscope while a line marked 1 was just barely discernible. These lines were observed through a jeweler's eyeglass and were scratched on the gelatine of the plate by means of a sharp fine needle. Measurements were then made from the scratches. A line marked 5 was completely absorbed in the conglomerate but not in the single crystal, while one marked 10 was completely absorbed in the thinnest single crystals. The letter *d* signifies that the edges of the lines were not clearly defined, *s* that the edges were clean and sharp, ? that the line was observed only on one plate. The sharp lines at low temperatures are probably accurate to one wave number, the accuracy being somewhat greater in the ultraviolet than in the red. The edges of some broad diffuse bands at room temperatures may be in error by as much as 10 wave numbers. However, in general, most lines and edges at 78°K can be depended on to at least 2 wave numbers, scratched lines to about 5 cm^{-1}. At 298°K, the errors may be 5 cm^{-1}.

DISCUSSION OF RESULTS

Tables II, III, IV and V give evidence for the existence of low-lying, excited levels in the Eu spectra. The existence of these levels was established in two entirely independent ways. First: Absorption lines arising from these low-lying excited levels should show marked intensity changes with temperature. At very low temperatures where the population in these levels should be practically nil due to the Boltzmann distribution, the lines arising from these levels should be absent in the spectra. As the temperature is increased, the population in these states should increase and a corresponding increase in the intensity of the absorption lines from these levels should be noted. From the temperature range in which the lines increase markedly in intensity, it is possible by making use of the Boltzmann relation to fix, approximately, the interval in inverse centimeters between the basic state and the low-lying excited state. Second: Lines arising from the basic state and the low excited states and terminating in common upper levels should be separated from each other by the intervals between the low-lying states. Thus constant frequency intervals should be observed throughout the spectra. In every case the low frequency component should show marked temperature dependence, since it arises from one of the low-lying excited levels. In the examples given these conditions have been fulfilled. Further, the existence of these levels can be followed from salt to salt by observing the corresponding lines in the various salts. This could not be done if the constant frequency intervals were just due to chance in a given salt. Only clear-cut examples were chosen for the tables. We feel that the evidence for the 300 and the 385, 938 and 970 levels is conclusive. We also feel that there is very strong evidence for a level at about 435 cm^{-1}.

In general, the lines shift about 10 wave numbers to longer wave-lengths as the temperature is decreased from 298°K to 78°K. As the crystal cools, it contracts and changes the effective fields on the electrons. Since the excited levels are, in general, more sensitive to electric and magnetic fields than the $^7F_0$ state, they are influenced more by the increased fields due to contraction. This results in a red shift of the lines.

In addition to the constant interval frequencies reported above there are a number of others. Most of these have intervals lying between 20 cm^{-1} and 150 cm^{-1}. Accordingly, if the number of times a given interval occurs in the spectra is plotted against the frequency interval, certain

TABLE III. *Level at about 390 cm^{-1}.*

$EuCl_3 \cdot 6H_2O$	$EuBr_3 \cdot 6H_2O$	$Eu_2(SO_4)_3 \cdot 8H_2O$
17,260 − 16,864 = 396	17,266 − 16,883 = 383	17,255 − 16,874 = 381
19,002 − 18,608 = 394	19,008 − 18,623 = 385	18,999 − 18,615 = 384
19,026 − 18,634 = 392	19,031 − 18,649 = 382	19,017 − 18,634 = 383
21,523 − 21,129 = 394	24,363 − 23,978 = 385	Mean Interval: = 383
Mean Interval: = 394	Mean Interval: = 384	

intervals such as 20 cm^{-1}, 38 cm^{-1}, etc., stand out as peaks. This is particularly true of the frequency intervals about 80 cm^{-1} and 130 cm^{-1} for the sulfate, 90 cm^{-1} and 120 cm^{-1} for the chloride, etc. (These frequencies would be slightly different at liquid-air temperatures because of the shift.) The red components are always present at the lowest temperatures investigated and do not show temperature dependence in contrast with the lines mentioned earlier in the paper. Therefore, the constant interval cannot be associated with the common basic state from which all of the lines originate at low temperatures. Thus it must be concluded that each of the excited levels has associated with it another level separated from it by about the same distance. At first glance this may not seem probable, but closer examination shows that it is just what should be expected if vibrational frequencies are associated with electronic levels. These vibratory frequencies are functions of the masses of the atoms involved and the force constants between the atoms. Since they are associated with various electronic states of the same atoms the mass factors do not change. Also, as a first approximation, the force constants do not change either, since the excited electrons ($4f$) do not take part directly in the bond and lie rather deep within the atom. As a second approximation, however, they should affect the bond and give rise to slight differences in the frequencies. This is what is observed, for the frequency intervals are not exact but are grouped about certain frequencies.

As a rule the intense lines can be traced from salt to salt, and in salts of similar crystal symmetry they occur in practically the same places. This fact, combined with other evidence presented in earlier papers,[8] leads to the conclusion that this type of line arises from pure electronic transitions within the atoms which are subjected to strong crystalline fields. The weaker associated lines usually occur on the violet side of the main lines. They are observed only in very thick crystals or conglomerates, and the number observed continues to increase as the thickness of the conglomerate is increased. They are extremely sensitive to changes in the crystal structure and the mass of the surrounding atoms and they do not show a line to line correspondence between various salts. We attribute these weak lines to vibrational and oscillational frequencies superimposed upon the electronic frequencies. Occasionally one of these associated lines, because of particularly favorable selection rules or resonance, may be very intense, *so that great care should be taken in interpreting the nature of fields in solids from the number and positions of the intense lines.* The excited levels at about 385 and 420 show all the characteristics of the vibrational type except for their strong intensities. Because of the fact that similar intervals are found on other excited levels, we feel that these levels are really vibrational levels of about 85 and 120 cm^{-1} superimposed on the first excited electronic level at 305 cm^{-1}. Amelia Frank and Van Vleck,[9] assuming Russell-Saunders coupling of the (f) electrons, have developed a theory correlating magnetic susceptibility data on europium salts with energy levels, and from Selwood's[10] data have predicted where the levels should occur. Since the lowest two levels are the only ones important in the calculations up to room temperatures, and since the separation parameter is fixed from the experimental data, their

TABLE IV. *Level at about 430 cm^{-1}.*

$EuCl_3 \cdot 6H_2O$	$EuBr_3 \cdot 6H_2O$	$Eu_2(SO_4)_3 \cdot 8H_2O$
17,260 − 16,839 = 421	17,266 − 16,829 = 437	17,264 − 16,829 = 435
19,026 − 18,608 = 418		21,514 − {21,029 = 435
21,456 − 21,032 = 424	21,464 − 21,023 = 441	21,501 − {21,029 = 435
21,800 − 21,377 = 423		21,489 − {21,091
24,363 − 23,940 = 423	24,421 − 23,978 = 443	24,421 − 23,984 = 437
Mean Interval: = 422	Mean Interval: = 440	Mean Interval: = 435

TABLE V.

$EuCl_3 \cdot 6H_2O$	$EuBr_3 \cdot 6H_2O$	$Eu_2(SO_4)_3 \cdot 8H_2O$
17,260 − 16,289 = 971	17,266 − 16,293 = 973	17,264 − 16,281 = 983
− 16,319 = 941	− 16,328 = 938	− 16,327 = 937
19,002 − 18,033 = 967	19,008 − 18,038 = 970	19,008 − 18,027 = 981
− 18,065 = 937	− 18,073 = 935	− 18,082 = 926
21,489 − 20,524 = 965		21,489 − 20,507 = 982
− 20,546 = 943		− 20,552 = 937
31,591 − 30,618 = 973		31,624 − 30,639 = 985
− 30,661 = 930		
938	937	937
Mean Intervals:	Mean Intervals:	Mean Intervals:
970	971	983

[8] Previous publications of F. H. Spedding.

[9] J. H. Van Vleck and A. Frank, Phys. Rev. **34**, 1494, 1625 (1929). Also Frank, Phys. Rev. **39**, 119 (1932); **48**, 765 (1935).

[10] H. A. Bethe and F. H. Spedding, Phys. Rev. **52**, 454 (1937). F. H. Spedding, *ibid.* **58**, 255 (1940).

TABLE VI. μ (*eff.*).

T	SELWOOD'S EXPER.	CALC. 300 CM^{-1}	CALC. (300, 385, 420 CM^{-1})
83°K	2.06	2.13	1.94
153°K	2.73	2.81	2.59
223°K	3.14	3.16	2.97
293°K	3.41	3.39	3.22
343°K	3.58	3.53	3.34

approximation gives a very fair fit with our results if we assume that the field is cubic and that the 385 cm^{-1}, 420 cm^{-1} levels are of a vibratory nature. If we assume that the three levels are of electronic nature split apart by a rhombic field, the agreement is very poor in their approximation, as can be seen from Table VI.

Since there are fourteen levels with $J=0$, eighteen levels with $J=1$, etc., arising from the (f^6) configuration, one would not expect Russell-Saunders coupling to be obeyed as some of these levels would be greatly perturbed. This has been shown in the analogous cases of Tm and Pr.[10] Now that the levels have been experimentally observed, Frank and Van Vleck's calculations should be repeated, taking into account these perturbations. Lange[11] and Gobrecht[12] state that the fields in europium salts are far from cubic since more than one level is found around 300 cm^{-1}. Such conclusions are unfounded until the nature of these levels has been established. Also, any calculation of the screening constant σ using the Goudsmit formula is valueless until the amount of perturbation of the levels has been taken into account.

It would be desirable that the specific heat of $Eu_2(SO_4)_3 \cdot 8H_2O$ be determined over the temperature range from liquid-air to room temperatures, for, by comparing it with the published specific heats of $Gd_2(SO_4)_3 \cdot 8H_2O$,[13] the nature of the two levels around 400 cm^{-1} could be definitely established. If they are due to vibration, the same vibrations should be present in the Gd salt and they should make no contribution to the difference in the specific heats between the salts. If they are electronic in origin their contribution would be considerable. At present we feel that the evidence rather supports the contention that the crystalline field about europium in the hydrated halogen and sulphate crystals is predominantly cubic. This is in agreement with similar evidence from Er and Nd. It cannot, of course, be completely cubic, since the gross structures of the crystals are monoclinic, and since it is known that the intensity of absorption varies in different directions in the crystals. However, it seems to us that the rhombic part of the field is small compared with the cubic contributions. Further research will be necessary before this point can be settled.

From a study of the double salts of neodymium nitrate Ewald[14] concluded that superimposed upon the main energy levels of the neodymium ion were certain "Raman frequencies" due to the negative radical of the salt. He found that with the double nitrates the multiplets were repeated on the short wave-length side at distances comparable with the Raman frequencies of the NO_3 group. Only in one place did we find a difference between the halides and sulfate of europium at a Raman interval and there the patterns did not recur. Since there were numerous places where the spectra did not agree, we concluded that the agreement of this one interval was due to chance, and that at least in the case of the sulphate of europium the sulphate frequencies did not occur superimposed upon the electronic frequencies.

We wish to thank Dr. H. N. McCoy for his generous gift of the europium used in this investigation and the Ministry of Education of His Majesty's Government in Northern Ireland for the research grant to Mr. Moss.

[11] Lange, Ann. d. Physik **31**, 609 (1938).
[12] Gobrecht, Ann. d. Physik **31**, 600 (1938).
[13] Ahlberg and Clark, J. Am. Chem. Soc. **57**, 437 (1935).
[14] H. Ewald, Zeits. f. Physik **110**, 428 (1938).

The Normal Vibrations of Molecules of the Tetramethylmethane Type

SAMUEL SILVER*
Department of Physics, Massachusetts Institute of Technology, Cambridge, Massachusetts
(Received September 24, 1940)

The normal modes of a tetrahedral $A(CH_3)_4$ molecule have been investigated. For fixed orientations of the methyl groups, there are two configurations in which the molecule as a whole possesses the symmetry group T^d. The group theory analysis has been applied to one of these configurations, referred to as the eclipsed form, and on the basis of Redlich's theorem a set of symmetry coordinates has been derived for each set of equivalent points. Every symmetry coordinate is associated with an irreducible representation of the group, and, as a consequence, the secular determinant is factored to the maximum extent possible on symmetry considerations alone. Using a simple valence potential, the secular equations for the totally symmetric and doubly degenerate modes have been developed. Calculations have been made for tetramethylmethane, $C(CH_3)_4$, tetramethylsilane, $Si(CH_3)_4$, and the tetramethylammonium ion, $N^+(CH_3)_4$, assuming in every case that the force constants associated with the methyl groups are the same as in ethane. The results are in reasonable agreement with frequencies observed in the Raman spectra and a tentative assignment of the latter is suggested.

INTRODUCTION

THERE has been very little published in the way of an analysis of the normal modes of $A(CH_3)_4$ molecules. These molecules are of interest in relation to a number of problems and it was thought worth while to undertake a detailed investigation. The present paper reports the first stage in the analysis and it is the hope of the author that more experimental data will be forthcoming which will make a complete study possible.

In its application to specific cases this paper concerns itself with the tetramethylmethane and tetramethylsilane molecules and the tetramethylammonium ion. Various observers[1–3] of the Raman spectra of these molecules have interpreted the region below 1000 cm^{-1} in terms of the AB_4 model on the assumption that, in certain modes, the so-called skeletal modes, the methyl groups may be regarded as particles of mass 15. The spectra are suggestive of such an interpretation since, in the region mentioned above, they are closely analogous to the CCl_4 spectrum both in the number of lines and their characteristics. On the other hand, it was found that on the AB_4 model these lines cannot be accounted for by a simple force system and it is necessary to introduce forces which have a dubious interpretation in terms of the molecule as a whole. Thus, Kohlrausch and Köppl[1] and Edsall[3] applied a Urey-Bradley treatment to tetramethylmethane and tetramethylammonium, respectively, assuming a $1/r^n$ repulsion between the methyl groups, whereas Howard's[4] work on ethane shows that reasonable results are to be expected on a simple valence force system alone. The author[5] attempted to take into account the effect of the motions of the hydrogen atoms in these modes and used a simple valence potential plus a valence type of cross term. Although the numerical results were satisfactory, the treatment suffered from the defects that the analysis of the hydrogen motions can properly be applied only to the totally symmetric vibration and that the cross term introduced into the potential plays a more important role than the primary valence forces. Recently the writer examined the AB_4 treatment in detail,[6] using a large number of force models, and concluded that the assumption that the lowest observed lines correspond to the skeletal modes is unsatisfactory. In this

* Present address: Mendenhall Laboratory, Ohio State University, Columbus, Ohio.

[1] Tetramethylmethane: Kohlrausch and Barnes, Anal. Soc. Espan. Fis. Quim. **30**, 733 (1932); D. H. Rank: J. Chem. Phys. **1**, 572 (1933); Kohlrausch and Köppl, Zeits. f. physik. Chemie **B26**, 209 (1934).

[2] Tetramethylsilane: Rank and Bordner, J. Chem. Phys. **3**, 248 (1935).

[3] Tetramethylammonium: J. T. Edsall, J. Chem. Phys. **5**, 225 (1937).

[4] J. B. Howard, J. Chem. Phys. **5**, 442 (1937).

[5] S. Silver, J. Chem. Phys. **7**, 1113 (1939).

[6] S. Silver, Ph.D. Thesis, Massachusetts Institute of Technology (June, 1940).

connection the calculations of Wall and Eddy[7] are of interest. They found that four lines in the spectrum of tetramethylmethane can be treated as skeletal modes under a simple valence potential, but of these only three lie in the region below 1000 cm^{-1}, and the fourth, corresponding to the upper triply degenerate mode of the equivalent AB_4 system, lies in the neighborhood of 1250 cm^{-1}. This agrees with the results obtained by the more complete analysis reported here, and the two methods taken together are able to account for a considerable portion of the spectrum.

It would be desirable to develop the theory, along lines similar to Howard's treatment of ethane,[4] for arbitrary orientations of the methyl groups relative to the AC_4 skeleton. However, certain difficulties arise in developing the normal coordinates and this first report is limited to the model in which the methyl groups are prevented from rotating freely by potential barriers. Pitzer[8] has studied the specific heat data of tetramethylmethane, obtained by Aston and Messerly,[9] and concluded that in this molecule the barriers have a magnitude of about 4200 cal./mole. With barriers of such height, the methyl groups will be confined to torsional oscillations about their axes even at ordinary temperatures, and the model of fixed methyl groups is, therefore, a plausible one. The molecule as a whole then possesses a unique equilibrium configuration and it is possible to apply group theory to the problem.

Mathematical Procedure

In treating the normal vibrations of molecules involving a large number of degrees of freedom, it is convenient to use Wigner's[10] method. The molecule, composed of n atoms, is considered in one of its equilibrium configurations, at rest in space. A set of Cartesian axes is chosen to coincide with the principal axes of this configuration; the origin is at the center of gravity. Let x_k^0, y_k^0, z_k^0 be the coordinates of the equilibrium position of the kth atom; x_k, y_k, z_k the components of its displacement from that position. The only restriction imposed on the displacements is that they be small compared to the dimensions of the molecule. Infinitesmal rigid rotations and translations are included as modes of zero frequency. The secular determinant for the frequencies is, therefore, of order $3n$ and possesses six roots equal to zero.

A direct solution of the determinantal equation is generally impossible. It is necessary to find beforehand a set of new coordinates in terms of which the kinetic and potential energies are separable into parts, there being no cross terms between coordinates constituting one part and those of another. This effectively factors the determinant and reduces the problem to solving determinants of lower order. The factorability depends largely on the symmetry of the molecule and it is possible to find a desired set of coordinates on the basis of symmetry considerations alone, independent of the force model used. In this connection group theory proves helpful and its application for this purpose is well known from the work of Wigner[10] and Wilson.[11] The same mathematical methods are used here and we shall simply refer to their papers for the necessary details. However, the symmetry coordinates derived in this paper differ somewhat from those employed by Wilson and we wish to discuss their general features in this section.

Suppose the molecule under consideration to possess a group G of proper and improper rotations which express its symmetry. Under any operation of the group the equilibrium configuration transforms into itself with every atom k occupying the position held previously by an atom l of the same species. Atoms which transform into each other under the operations of the group are said to be *equivalent*. It was shown by Redlich[12] that for each set of equivalent points there exists a transformation matrix, independent of the masses of the atoms and the force constants, which transforms the displacement coordinates into a set of symmetry coordinates, such that every symmetry coordinate belongs to an irreducible representation of the group G.

[7] F. T. Wall and C. R. Eddy, J. Chem. Phys. **6**, 107 (1938).
[8] K. Pitzer, J. Chem. Phys. **5**, 473 (1938).
[9] Aston and Messerly, J. Am. Chem. Soc. **58**, 2354 (1936).
[10] E. Wigner, Göttingen Nachrichten (1930), p. 133.
[11] E. B. Wilson, Jr., Phys. Rev. **45**, 706 (1934).
[12] O. Redlich, Zeits. f. physik. Chemie **B28**, 371 (1935).

The simplification introduced by this theorem is obvious, and the coordinates derived in this paper are a set of Redlich coordinates. We may, of course, also require that the transformation matrices be orthonormal.

In order to find the number of coordinates belonging to a given irreducible representation $\Gamma^{(i)}$, we regard each set of equivalent points as an individual sub-molecule possessing the symmetry group G, and apply to it the theory developed by Wigner for the entire molecule. The displacement coordinates of a given sub-molecule, τ, are conceived as forming a configuration space, and the symmetry coordinates are associated with a new set of orthogonal axes, having the property that under every operation of the group, axes belonging to a given irreducible representation transform into each other according to that representation. It must be noted that the symmetry coordinates of every sub-molecule include its infinitesimal rigid rotations and translations. Consider the irreducible representation $\Gamma^{(i)}$. If it is l_i dimensional, the coordinates belonging to that representation are degenerate and can be divided into a_i^τ sets of l_i each, such that under every operation R, the l_i coordinates of a given set transform among themselves according to $\Gamma^{(i)}$. There are, therefore, $a_i^\tau l_i$ coordinates in the space, τ, belonging to $\Gamma^{(i)}$. The problem is then to determine a_i^τ. Consider a general vector in the configuration space of the sub-molecule and the representation $\Gamma^\tau(R)$ which it generates under the operation R. Since the vector can be resolved along the new axes, the representation Γ^τ can be written as a sum of the irreducible representations of those axes,

$$\Gamma^\tau(R)=\sum_i a_i^\tau \Gamma^i(R). \tag{1}$$

In terms of the characters (1) can be written as

$$\chi^\tau(R)=\sum_i a_i^\tau \chi^i(R) \tag{2}$$

and the a_i^τ can be determined with the help of the orthogonality properties of the characters:

$$a_i^\tau=\frac{1}{h}\sum_R \chi^i(R)^*\chi(R)^\tau, \tag{3}$$

where $\chi^i(R)^*$ is the complex conjugate of $\chi^i(R)$, and h is the number of elements of the group. The characters of the irreducible representations have been tabulated by Wigner[10] for all the symmetry groups and the complete character can be found by the procedure described in the papers of Wigner and Wilson referred to above. The normal coordinates belonging to the irreducible representation $\Gamma^{(i)}$ are linear combinations of the symmetry coordinates of all subspaces belonging to that representation, the coefficients being functions of the masses of the atoms and the force constants of the molecule. The number of normal coordinates of that representation is

$$\sum_\tau a_i^\tau l_i$$

falling into sets of l_i each; the number of independent frequencies of type $\Gamma^{(i)}$ is

$$n_i=\sum_\tau a_i^\tau.$$

There is a further element to be taken into consideration in determining the symmetry coordinates. An irreducible representation of a given type is not unique. Rather there exists an infinity of such representations, but all of these can be transformed into each other by similarity transformations.[13] That is, the n_i sets of coordinates of type $\Gamma^{(i)}$ generate irreducible representations under the operations of the group, but these are not necessarily the same. If they are different, they can be transformed into each other by similarity transformations and, therefore, they all possess the same character. It is desirable to choose the n_i sets so that they generate identical representations. Every coordinate may then be associated with a row of the representation matrix[13] and maximum factorization of the secular determinant is obtained. The factorization follows from the condition that the potential energy be invariant under the operations of the group and the results[14] are: (1) There are no cross terms between coordinates of different irreducible representations, and (2) there can be no cross terms between coordinates belonging to a degenerate representation if those coordinates transform according to different rows of the

[13] See E. Wigner, *Grüppentheorie* (Vieweg, Braunschweig, 1931), particularly Chap. X–XIII.

[14] A proof is given by J. Rosenthal and G. Murphy, Rev. Mod. Phys. **8**, 317 (1936).

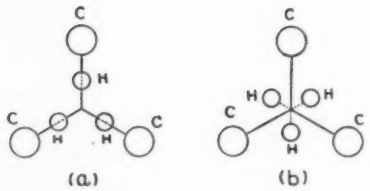

FIG. 1. The orientation of the methyl groups in the configurations possessing complete T^d symmetry. A methyl group is shown in projection onto the plane of the carbon atoms of the other three methyl groups. (a) Eclipsed configuration, (b) staggered configuration.

same matrices. Hence, if a representation is l_i dimensional and occurs n_i times in the complete representation of the molecule as a whole, there will be l_i factors in the potential energy with identical coefficients (except, perhaps, for algebraic sign) involving n_i coordinates each. The secular determinant will thus possess among its factors an n_ith order determinant repeated l_i times.

Lastly, we point out a relation between the coefficients of the transformation matrix of a subspace which is helpful in finding the matrix. The derivation is based on symmetry considerations alone and is identical with that given by Wigner[15] for the normal coordinates. We shall simply quote the result. Let S^μ be a symmetry coordinate in the subspace τ, belonging to one of the a_s^τ sets of the irreducible representation $\Gamma^{(s)}$. The dimension of the representation is l_s. Let $x_{l\alpha}$ be the α-component ($\alpha=x$, y, or z) of the displacement of the lth atom in the set of equivalent points. Then

$$S^\mu=\sum_{\alpha=x}^{z}\sum_{l}\overset{\mu}{S}_{l\alpha}x_{l\alpha}.$$

The amplitudes $\overset{\mu}{S}_{l\alpha}$ satisfy the following relation:

$$\frac{h}{l_s}\delta_{ss'}\overset{\mu}{S}_{l\alpha}=\sum_{R}\sum_{\beta}\chi^{s'}(R)R_{\alpha\beta}\overset{\mu}{S}_{R^{-1}(l),\beta}, \qquad (4)$$

where h is the number of elements in the group, $R^{-1}(l)$ is the atom into which the lth atom is transformed by the operation inverse to R, and $((R_{\alpha\beta}))$ is the matrix representing the transformation of the equivalent points into each other under the operation R. That is, if the kth atom is transformed into the lth atom by the operation R, we have

$$\overset{0}{x}_{l\alpha}=\sum_{\beta}R_{\alpha\beta}\overset{0}{x}_{k\beta}. \qquad (5)$$

In simple cases, Eq. (4) is sufficient for the determination of the coefficients $\overset{\mu}{S}_{l\alpha}$. In more complex cases, the amplitude relations are useful in checking whether or not a trial coordinate belongs to a given representation.

DERIVATION OF THE SYMMETRY COORDINATES OF AN $A(CH_3)_4$ TYPE MOLECULE

It has already been pointed out in the introduction that the treatment in this paper assumes that the methyl groups are prevented from rotating freely by internal potential barriers and that the molecule as a whole possesses a unique equilibrium configuration. For a tetrahedral arrangement of the methyl groups about the central A atom there are two orientations of the hydrogens in which the molecule possesses the complete symmetry of the tetrahedral group T^d. Consider the hydrogen atoms of a given methyl group and their projections onto the plane of the other methyl carbon atoms (see Fig. 1). In one configuration, the eclipsed form, the hydrogens project onto the A−C diagonals; in the second, the staggered configuration, the projections of the C−H bonds bisect the angles between the adjacent A−C bonds. There is no conclusive evidence at present as to which is the stable

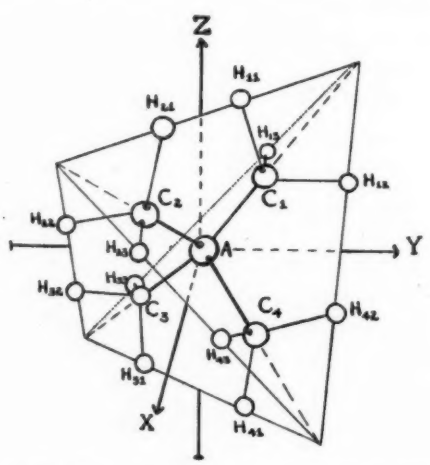

FIG. 2. The eclipsed configuration of tetrahedral $A(CH_3)_4$ molecules. In the scheme of numbering, the central atom, A, is number 5.

[15] See reference 10, Section 3, Eq. (18).

configuration of the molecule. Only the eclipsed form is considered here, but with the aid of a model and the descriptions of the coordinates given below, the coordinates of the staggered configuration may likewise be derived. For the types of frequencies treated numerically in the succeeding section, using a simple valence potential, the same results are obtained for both configurations. This can easily be seen physically and has also been verified by carrying through the calculations. The present treatment accordingly sheds no light on the question of which is the stable configuration.

The tetrahedral group T^d possesses twenty-four elements which may be described in terms of the tetrahedral $A-C_4$ structure. There are four threefold axes (C_3) formed by the A−C diagonals, possessing two elements each, the rotations $2\pi/3$ and $-2\pi/3$; three twofold axes (C_2) joining the midpoints of opposite edges of the tetrahedrons, possessing one element each, a rotation through π; six reflection planes (σ_d) formed by the six pairs of adjacent C_3 axes; three twofold rotary-reflection axes (S_4) of two elements each, $+\pi/2$ and $-\pi/2$, coinciding with the three C_2 axes; the identity operation (E) possessing one element. The twofold rotation axes are mutually orthogonal and intersect at the center of gravity of the tetrahedron. They are principal axes of the system and may be chosen as the system of coordinates for the problem. The complete configuration is shown in Fig. 2, together with the scheme of numbering the atoms. To complete the description of the system the equilibrium positions are given in Tables I and II. R_0 is the equilibrium length of the A−C bond, r_0 the length of the C−H bond.

TABLE I. *Equilibrium positions of the apical carbon atoms.*

C_1	$-\frac{R_0}{\sqrt{3}}$,	$\frac{R_0}{\sqrt{3}}$,	$\frac{R_0}{\sqrt{3}}$
C_2	$\frac{R_0}{\sqrt{3}}$,	$-\frac{R_0}{\sqrt{3}}$,	$\frac{R_0}{\sqrt{3}}$
C_3	$-\frac{R_0}{\sqrt{3}}$,	$-\frac{R_0}{\sqrt{3}}$,	$-\frac{R_0}{\sqrt{3}}$
C_4	$\frac{R_0}{\sqrt{3}}$,	$\frac{R_0}{\sqrt{3}}$,	$-\frac{R_0}{\sqrt{3}}$

TABLE II. *Equilibrium positions of the hydrogen atoms.*

$H_{11}: -a, a, b$ $H_{21}: a, -a, b$ $H_{31}: -a, -a, -b$ $H_{41}: a, a, -b$

$H_{12}: -a, b, a$ $H_{22}: a, -b, a$ $H_{32}: -a, -b, -a$ $H_{42}: a, b, -a$

$H_{13}: -b, a, a$ $H_{23}: b, -a, a$ $H_{33}: -b, -a, -a$ $H_{43}: b, a, -a$

$$a=\frac{R_0}{\sqrt{3}}-\frac{r_0}{3\sqrt{3}};\quad b=\frac{R_0}{\sqrt{3}}+\frac{5r_0}{3\sqrt{3}}$$

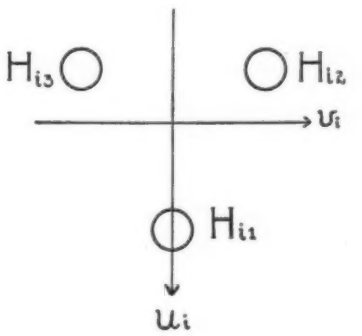

FIG. 3. The auxiliary u_i, v_i, w_i axes. The w_i axis points outward from the plane of the paper.

It is helpful to define an auxiliary set of right-handed axes u_i, v_i, w_i for each methyl group. The w_i axis lies along the $A\rightarrow C_i$ diagonal. The u_i axes are such that they transform into each other under the twofold rotations. The equilibrium position of the H_{i1} atom lies on the positive u_i axis. The origins of the auxiliary systems are most conveniently taken at the equilibrium positions of the centers of gravity of the hydrogen atoms. The scheme according to which the hydrogen atoms are labeled relative to their respective u, v, w axes is shown in Fig. 3. It is evident that the H_{ik} atom transforms into the H_{jk} atom under the twofold rotation carrying C_i into C_j. The direction cosines of the u, v, w systems in the X, Y, Z axes can easily be obtained from the description above.

The configuration space of the displacements from the equilibrium configuration of the entire molecule has fifty-one dimensions and can be resolved into the following subspaces of equivalent points: τ_1, the twelve-dimensional space of the apical carbon atoms; τ_2, the thirty-six-dimensional space of the hydrogen atoms; τ_3, the three-dimensional space of the central A atom. We now proceed to classify the frequencies and the symmetry coordinates by the method outlined in the preceding section. In Table III we have the characters of the irreducible representa-

tions for every class of elements, $\chi(R)$, the character of the complete representation for the entire molecule, and $\chi^{\tau_i}(R)$, the characters of the complete representations of the subspaces. Placzek's notation for the irreducible representations is also given: A_1, A_2, nondegenerate representations; E, doubly degenerate; F_1, F_2, triply degenerate representations. The selection rules are also given according to Placzek's tables.[16]

Applying Eq. (3), we get

$$\Gamma(R)=3\Gamma^{(1)}+\Gamma^{(2)}+4\Gamma^{(3)}+5\Gamma^{(4)}+8\Gamma^{(5)},$$

$$\Gamma^{\tau_1}(R)=\Gamma^{(1)}+\Gamma^{(3)}+\Gamma^{(4)}+2\Gamma^{(5)},$$

$$\Gamma^{\tau_2}(R)=2\Gamma^{(1)}+\Gamma^{(2)}+3\Gamma^{(3)}+4\Gamma^{(4)}+5\Gamma^{(5)},$$

$$\Gamma^{\tau_3}(R)=\Gamma^{(5)},$$

that is, the molecule has three nondegenerate modes of class $\Gamma^{(1)}$, one nondegenerate mode of class $\Gamma^{(2)}$, four doubly degenerate modes, five triply degenerate modes of class $\Gamma^{(4)}$ and eight triply degenerate modes of class $\Gamma^{(5)}$. The secular determinant can be factored on symmetry considerations alone into one third-order determinant, one first-order determinant, two identical fourth-order determinants and a fifth- and eighth-order determinant, both repeated three times. It is easily verified that the rotations and translations belong to $\Gamma^{(4)}$ and $\Gamma^{(5)}$, respectively, and, therefore, the latter two determinants will possess a zero root. The resolution of the representations of the subspaces shows that we must find one totally symmetric coordinate in the displacements of the apical carbon atoms, two totally symmetric coordinates in the hydrogen subspace; one coordinate in the hydrogen subspace which is totally symmetric to the proper rotations E, C_2, and C_3 and antisymmetric to the improper rotations σ_d and S_4. The latter coordinate, $\Gamma^{(2)}$, gives rise to the linear factor of the secular determinant and is therefore the normal coordinate of that class regardless of the nature of the forces between the atoms. In class $\Gamma^{(3)}$ we must find a set of doubly degenerate coordinates in the apical carbon atoms and three sets in the hydrogen subspace. The coordinates of class $\Gamma^{(4)}$ are divided into one set of triply degenerate coordinates in the methyl group carbon atoms and four sets of triply degenerate coordinates in the hydrogen displacements. Class $\Gamma^{(5)}$ has one set of triply degenerate coordinates for the central A atom, two sets in the methyl group carbon atoms, and five sets in the hydrogen atoms. In the analytical description of these coordinates, $\Gamma^{(1)}$ coordinates are labeled P, $\Gamma^{(2)}$ is labeled S, $\Gamma^{(3)}$ are denoted by T, and $\Gamma^{(4)}$ and $\Gamma^{(5)}$ by U and V, respectively. We shall describe these briefly.

TABLE III.

	E	$8C_3$	$3C_2$	$6\sigma_d$	$6S_4$	Selection Rules for the Fundamental Frequencies: Raman Effect	Infra-Red
$\Gamma^{(1)}A_1$	1	1	1	1	1	active (P)	inactive
$\Gamma^{(2)}A_2$	1	1	1	−1	−1	inactive	inactive
$\Gamma^{(3)}E$	2	−1	2	0	0	active (D)	inactive
$\Gamma^{(4)}F_1$	3	0	−1	−1	1	inactive	inactive
$\Gamma^{(5)}F_2$	3	0	−1	1	−1	active (D)	active
$\chi(R)$	51	0	−1	5	−1		
$\chi^{\tau_1}(R)$	12	0	0	2	0		
$\chi^{\tau_2}(R)$	36	0	0	2	0		
$\chi^{\tau_3}(R)$	3	0	−1	1	−1		

(a) Class $\Gamma^{(1)}$, P coordinates: For the apical carbon atoms there is one coordinate of this class, and it is unique. It is the totally symmetric mode of a tetrahedral $A-C_4$ molecule in which the carbon atoms all move in phase along the diagonals. The hydrogen coordinates may be chosen in an infinite number of ways, but a suitable pair suggested by the valence model are: P_2, all hydrogen atoms move in phase along the C−H bonds and P_3, all hydrogen atoms move in phase perpendicularily to the C−H bonds giving a totally symmetric distortion of the A−C−H angles.

(b) Class $\Gamma^{(2)}$; S coordinate: This coordinate may be obtained by compounding the rotations of the H_3 groups about the w_i axes. By choosing the rotations of all four groups in the same sense about their respective axes we get a coordinate having the proper symmetry. As was pointed out above, there is only one coordinate of this class for the molecule as a whole and it gives rise to the linear factor of the secular determinant. The symmetry coordinate described here is, therefore, also the normal coordinate of the molecule belonging to this class.

[16] G. Placzek, *Handbuch der Radiologie*, Vol. VI, Part II, p. 205.

(c) Class $\Gamma^{(3)}$, T coordinates: For the apical carbon atoms we use the doubly degenerate modes of an AB_4 molecule.[17] The combination of these modes results in an elliptical motion of each C atom in the plane perpendicular to the A−C diagonal. With proper choice of phases these may be resolved into two modes at right angles to each other. The coordinate T_5 is the component of this motion in the σ_d planes intersecting in the Z axis, T_6 is the component perpendicular to T_5. The displacements in T_6 are parallel to the XY plane and are shown in Fig. 4 in projection onto that plane. To obtain the hydrogen coordinates we compound the doubly degenerate modes which would be possessed by an equilateral H_3 molecule. These are conveniently described in terms of the u, v, w axes of the H_3 group. T_7 and T_8 are compounded out of the translational modes in the uv plane. A suitable pair are the mutually orthogonal translations in the positive u_i and v_i directions. The coordinates T_9 and T_{10} are built up from the rotations about the u_i and v_i axes, respectively. We have then

$$T_9: \quad u_{ij}=v_{ij}=0; \quad w_{i1}=0; \quad w_{i2}=-w_{i3},$$

$$T_{10}: \quad u_{ij}=v_{ij}=0; \quad w_{i1}=-2w_{i2}=-2w_{i3}.$$

From the direction cosines of the u_i, v_i, w_i axes the displacements in terms of x_{ij}, y_{ij}, z_{ij} are easily obtained. T_{11} and T_{12} are formed from the doubly degenerate vibrations in the H_3 plane which conserve angular momentum about the w_i axis and leave the center of gravity of the H_3 group stationary. The latter are shown in the figures below. That the compounding of these motions does give the proper symmetry coordinates is verified by studying the representations generated in the transformations under the group operations and by means of the amplitude relations of Eq. (4).

(d) Class $\Gamma^{(4)}$, U coordinates: The single set of coordinates of this class in the apical carbon subspace is given by the three orthogonal rotations of the C_4 skeleton about the X, Y, and Z axes. This, again, is easily verified by studying

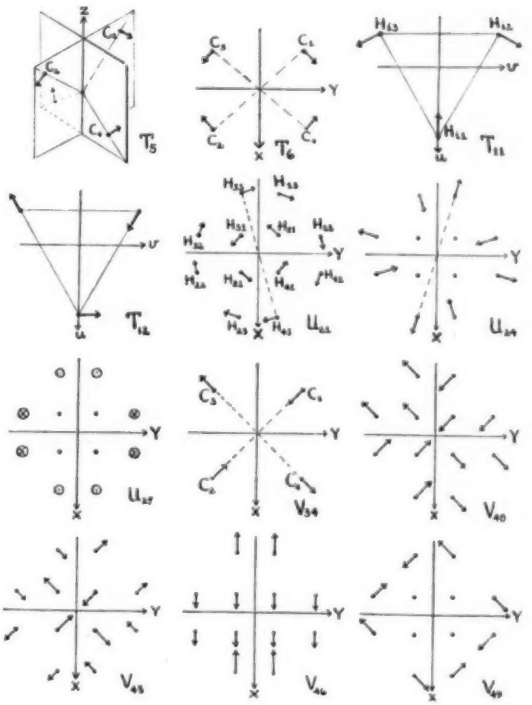

FIG. 4. Diagrams of the symmetry coordinates. Only those coordinates which are not completely evident from the descriptions in the text are shown. Of a set of triply degenerate coordinates only one member is illustrated. The other two members of the set can be obtained by setting up corresponding diagrams in the XZ and YZ planes. ⊙ and ⊗ represent displacements out from, and into, the plane of the paper, respectively.

the symmetry properties of the displacements under the operations of the group. We thus obtain U_{13}, U_{14}, and U_{15}. This immediately suggests one of the sets in the hydrogen subspace: the rigid rotations of the H skeleton about the coordinate axes, giving $U_{16}, \cdots, U_{18}$. The remaining hydrogen coordinates are obtained by trial and error methods. Here we are guided by the character table and the amplitude relations. In the figures the displacements are shown in projection onto the coordinate planes.

(e) Class $\Gamma^{(5)}$; V coordinates: There is a single set of these coordinates in the central atom A. The three displacements of the A atom along the coordinate axes are the symmetry coordinates. For continuity of numbering they are labeled $x_5=V_{28}$, $y_5=V_{29}$, $z_5=V_{30}$. The normal coordinates of the tetrahedral C_4 molecule give the proper coordinates of the apical carbon atoms. First there is the set of translations

[17] M. Born has given an analytical and graphical description of the normal modes of the AB_4 molecule in his *Optik* (J. Springer, Berlin, 1933), Chap. VIII, pp. 553–560. The coordinates developed here differ from those only in the choice of the axes of reference.

parallel to the coordinate axes: V_{31}, V_{32}, V_{33}. The second set are the normal modes in which the C_4 skeleton has no angular momentum and leaves the center of gravity stationary. The carbon atoms move along the edges of the tetrahedron, one pair approaching each other along an edge, the other pair moving apart along the opposite edge. The displacements are parallel to the coordinate planes and are accordingly shown in projection in the diagrams. The carbon coordinates suggest directly two sets of hydrogen coordinates. One is the set of translations of the H skeleton parallel to the coordinate axes. The second set is formed by displacements of each H_3 group as a rigid system in such a manner that the centers of gravity of the H_3 groups execute motions identical with the displacements of the apical carbons described above. The remaining three sets of hydrogen coordinates are again determined by trial and error methods.

In determining the coordinates there are three elements which are considered. First, each set of coordinates must generate representations in accord with the character table. Second, the coefficients are checked by use of the amplitude relations of Eq. (4). Third, within a given class of coordinates every succeeding set which is found is checked for orthogonality with the sets of that class already obtained. If a set is found which possesses the correct symmetry properties of the class but is not orthogonal to the other members of the class, it may be orthogonalized by Schmidt's orthogonalization process. The complete set of coordinates is given below both in analytical form and graphically. All the coordinates have been normalized to unity.

$$P_1=\frac{1}{(12)^{\frac{1}{2}}}[x_1-x_2+x_3-x_4-y_1+y_2+y_3-y_4-z_1-z_2+z_3+z_4]$$

$$P_2=\frac{1}{(324)^{\frac{1}{2}}}\begin{bmatrix} x_{11}+x_{12}-5x_{13}-x_{21}-x_{22}+5x_{23}+x_{31}+x_{32}-5x_{33}-x_{41}-x_{42}+5x_{43} \\ -y_{11}+5y_{12}-y_{13}+y_{21}-5y_{22}+y_{23}+y_{31}-5y_{32}+y_{33}-y_{41}+5y_{42}-y_{43} \\ +5z_{11}-z_{12}-z_{13}+5z_{21}-z_{22}-z_{23}-5z_{31}+z_{32}+z_{33}-5z_{41}+z_{42}+z_{43} \end{bmatrix}$$

$$P_3=\frac{1}{(648)^{\frac{1}{2}}}\begin{bmatrix} 5x_{11}+5x_{12}+2x_{13}-5x_{21}-5x_{22}-2x_{23}+5x_{31}+5x_{32}+2x_{33}-5x_{41}-5x_{42}-2x_{43} \\ -5y_{11}-2y_{12}-5y_{13}+5y_{21}+2y_{22}+5y_{23}+5y_{31}+2y_{32}+5y_{33}-5y_{41}-2y_{42}-5y_{43} \\ -2z_{11}-5z_{12}-5z_{13}-2z_{21}-5z_{22}-5z_{23}+2z_{31}+5z_{32}+5z_{33}+2z_{41}+5z_{42}+5z_{43} \end{bmatrix}$$

$$S_4=\frac{1}{(24)^{\frac{1}{2}}}\begin{bmatrix} x_{11}-x_{12}-x_{21}+x_{22}+x_{31}-x_{32}-x_{41}+x_{42}+y_{11}-y_{13}-y_{21}+y_{23}-y_{31}+y_{33}+y_{41}-y_{43} \\ -z_{12}+z_{13}-z_{22}+z_{23}+z_{32}-z_{33}+z_{42}-z_{43} \end{bmatrix}$$

$$\begin{cases} T_5=\dfrac{1}{(24)^{\frac{1}{2}}}[x_1-x_2+x_3-x_4-y_1+y_2+y_3-y_4+2(z_1+z_2-z_3-z_4)] \\ T_6=\dfrac{1}{\sqrt{8}}[x_1-x_2+x_3-x_4+y_1-y_2-y_3+y_4] \end{cases}$$

$$\begin{cases} T_7=\dfrac{1}{(72)^{\frac{1}{2}}}\begin{bmatrix} x_{11}+x_{12}+x_{13}-x_{21}-x_{22}-x_{23}+x_{31}+x_{32}+x_{33}-x_{41}-x_{42}-x_{43} \\ -y_{11}-y_{12}-y_{13}+y_{21}+y_{22}+y_{23}+y_{31}+y_{32}+y_{33}-y_{41}-y_{42}-y_{43} \\ +2(z_{11}+z_{12}+z_{13}+z_{21}+z_{22}+z_{23}-z_{31}-z_{32}-z_{33}-z_{41}-z_{42}-z_{43}) \end{bmatrix} \\ T_8=\dfrac{1}{(24)^{\frac{1}{2}}}\begin{bmatrix} x_{11}+x_{12}+x_{13}-x_{21}-x_{22}-x_{23}+x_{31}+x_{32}+x_{33}-x_{41}-x_{42}-x_{43} \\ +y_{11}+y_{12}+y_{13}-y_{21}-y_{22}-y_{23}-y_{31}-y_{32}-y_{33}+y_{41}+y_{42}+y_{43} \end{bmatrix} \end{cases}$$

$$T_9=\frac{1}{(24)^{\frac{1}{2}}}\begin{bmatrix}x_{12}-x_{13}-x_{22}+x_{23}+x_{32}-x_{33}-x_{42}+x_{43}-y_{12}+y_{13}+y_{22}-y_{23}+y_{32}-y_{33}-y_{42}+y_{43}\\-z_{12}+z_{13}-z_{22}+z_{23}+z_{32}-z_{33}+z_{42}-z_{43}\end{bmatrix}$$

$$T_{10}=\frac{1}{(72)^{\frac{1}{2}}}\begin{bmatrix}2x_{11}-x_{12}-x_{13}-2x_{21}+x_{22}+x_{23}+2x_{31}-x_{32}-x_{33}-2x_{41}+x_{42}+x_{43}\\-2y_{11}+y_{12}+y_{13}+2y_{21}-y_{22}-y_{23}+2y_{31}-y_{32}-y_{33}-2y_{41}+y_{42}+y_{43}\\-2z_{11}+z_{12}+z_{13}-2z_{21}+z_{22}+z_{23}+2z_{31}-z_{32}-z_{33}+2z_{41}-z_{42}-z_{43}\end{bmatrix}$$

$$T_{11}=\frac{1}{(72)^{\frac{1}{2}}}\begin{bmatrix}x_{11}-2x_{12}+x_{13}-x_{21}+2x_{22}-x_{23}+x_{31}-2x_{32}+x_{33}-x_{41}+2x_{42}-x_{43}\\-y_{11}-y_{12}+2y_{13}+y_{21}+y_{22}-2y_{23}+y_{31}+y_{32}-2y_{33}-y_{41}-y_{42}+2y_{43}\\+2z_{11}-z_{12}-z_{13}+2z_{21}-z_{22}-z_{23}-2z_{31}+z_{32}+z_{33}-2z_{41}+z_{42}+z_{43}\end{bmatrix}$$

$$T_{12}=\frac{1}{(24)^{\frac{1}{2}}}\begin{bmatrix}x_{11}-x_{13}-x_{21}+x_{23}+x_{31}-x_{33}-x_{41}+x_{43}+y_{11}-y_{12}-y_{21}+y_{22}-y_{31}+y_{32}+y_{41}-y_{42}\\+z_{12}-z_{13}+z_{22}-z_{23}-z_{32}+z_{33}-z_{42}+z_{43}\end{bmatrix}$$

$$U_{13}=\frac{1}{\sqrt{8}}(y_1+y_2-y_3-y_4-z_1+z_2+z_3-z_4)$$

$$U_{14}=\frac{1}{\sqrt{8}}(x_1+x_2-x_3-x_4+z_1-z_2+z_3-z_4)$$

$$U_{15}=\frac{1}{\sqrt{8}}(x_1-x_2-x_3+x_4+y_1-y_2+y_3-y_4)$$

$$U_{16}=\frac{1}{[8(b^2+2a^2)]^{\frac{1}{2}}}\begin{bmatrix}by_{11}+ay_{12}+ay_{13}+by_{21}+ay_{22}+ay_{23}-by_{31}-ay_{32}-ay_{33}-by_{41}-ay_{42}-ay_{43}\\-az_{11}-bz_{12}-az_{13}+az_{21}+bz_{22}+az_{23}+az_{31}+bz_{32}+az_{33}-az_{41}-bz_{42}-az_{43}\end{bmatrix}$$

$$U_{17}=\frac{1}{[8(b^2+2a^2)]^{\frac{1}{2}}}\begin{bmatrix}bx_{11}+ax_{12}+ax_{13}+bx_{21}+ax_{22}+ax_{23}-bx_{31}-ax_{32}-ax_{33}-bx_{41}-ax_{42}-ax_{43}\\+az_{11}+az_{12}+bz_{13}-az_{21}-az_{22}-bz_{23}+az_{31}+az_{32}+bz_{33}-az_{41}-az_{42}-bz_{43}\end{bmatrix}$$

$$U_{18}=\frac{1}{[8(b^2+2a^2)]^{\frac{1}{2}}}\begin{bmatrix}ax_{11}+bx_{12}+ax_{13}-ax_{21}-bx_{22}-ax_{23}-ax_{31}-bx_{32}-ax_{33}+ax_{41}+bx_{42}+ax_{43}\\+ay_{11}+ay_{12}+by_{13}-ay_{21}-ay_{22}-by_{23}+ay_{31}+ay_{32}+by_{33}-ay_{41}-ay_{42}-by_{43}\end{bmatrix}$$

$$U_{19}=\frac{1}{[8(a^2+b^2)(b^2+2a^2)]^{\frac{1}{2}}}\begin{bmatrix}aby_{11}+a^2y_{12}-(a^2+b^2)y_{13}+aby_{21}+a^2y_{22}-(a^2+b^2)y_{23}\\-aby_{31}-a^2y_{32}+(a^2+b^2)y_{33}-aby_{41}-a^2y_{42}+(a^2+b^2)y_{43}\\-a^2z_{11}-abz_{12}+(a^2+b^2)z_{13}+a^2z_{21}+abz_{22}-(a^2+b^2)z_{23}\\+a^2z_{31}+abz_{32}-(a^2+b^2)z_{33}-a^2z_{41}-abz_{42}+(a^2+b^2)z_{43}\end{bmatrix}$$

$$U_{20}=\frac{1}{[8(a^2+b^2)(b^2+2a^2)]^{\frac{1}{2}}}\begin{bmatrix}abx_{11}-(a^2+b^2)x_{12}+a^2x_{13}+abx_{21}-(a^2+b^2)x_{22}+a^2x_{23}-abx_{31}\\+(a^2+b^2)x_{32}-a^2x_{33}-abx_{41}+(a^2+b^2)x_{42}-a^2x_{43}\\+a^2z_{11}-(a^2+b^2)z_{12}+abz_{13}-a^2z_{21}+(a^2+b^2)z_{22}-abz_{23}+a^2z_{31}\\-(a^2+b^2)z_{32}+abz_{33}-a^2z_{41}+(a^2+b^2)z_{42}-abz_{43}\end{bmatrix}$$

$$U_{21}=\frac{1}{[8(a^2+b^2)(b^2+2a^2)]^{\frac{1}{2}}}\begin{bmatrix}(a^2+b^2)x_{11}-abx_{12}-a^2x_{13}-(a^2+b^2)x_{21}+abx_{22}+a^2x_{23}\\-(a^2+b^2)x_{31}+abx_{32}+a^2x_{33}+(a^2+b^2)x_{41}-abx_{42}-a^2x_{43}\\+(a^2+b^2)y_{11}-a^2y_{12}-aby_{13}-(a^2+b^2)y_{21}+a^2y_{22}+aby_{23}\\+(a^2+b^2)y_{31}-a^2y_{32}-aby_{33}-(a^2+b^2)y_{41}+a^2y_{42}+aby_{43}\end{bmatrix}$$

$$\begin{cases} U_{22}=\dfrac{1}{[8(a^2+b^2)]^{\frac{1}{2}}}(ax_{11}-bx_{13}+ax_{21}-bx_{23}-ax_{31}+bx_{33}-ax_{41}+bx_{43}-bz_{11} \\ \qquad +az_{13}+bz_{21}-az_{23}-bz_{31}+az_{33}+bz_{41}-az_{43}) \\ U_{23}=\dfrac{1}{[8(a^2+b^2)]^{\frac{1}{2}}}(ay_{11}-by_{12}+ay_{21}-by_{22}-ay_{31}+by_{32}-ay_{41}+by_{42}+bz_{11} \\ \qquad -az_{12}-bz_{21}+az_{22}-bz_{31}+az_{32}+bz_{41}-az_{42}) \\ U_{24}=\dfrac{1}{[8(a^2+b^2)]^{\frac{1}{2}}}(ax_{12}-bx_{13}-ax_{22}+bx_{23}-ax_{32}+bx_{33}+ax_{42}-bx_{43}-by_{12} \\ \qquad +ay_{13}+by_{22}-ay_{23}-by_{32}+ay_{33}+by_{42}-ay_{43}) \end{cases}$$

$$\left(a=\frac{R_0}{\sqrt{3}}-\frac{r_0}{3\sqrt{3}};\quad b=\frac{R_0}{\sqrt{3}}+\frac{5r_0}{3\sqrt{3}}\right)$$

$$\begin{cases} U_{25}=\dfrac{1}{\sqrt{8}}(x_{11}-x_{12}+x_{21}-x_{22}+x_{31}-x_{32}+x_{41}-x_{42}) \\ U_{26}=\dfrac{1}{\sqrt{8}}(y_{11}-y_{13}+y_{21}-y_{23}+y_{31}-y_{33}+y_{41}-y_{43}) \\ U_{27}=\dfrac{1}{\sqrt{8}}(z_{12}-z_{13}+z_{22}-z_{23}+z_{32}-z_{33}+z_{42}-z_{43}) \end{cases}$$

$$\begin{cases} V_{28}=x_5 \\ V_{29}=y_5 \\ V_{30}=z_5 \end{cases} \qquad \begin{cases} V_{31}=\frac{1}{2}(x_1+x_2+x_3+x_4) \\ V_{32}=\frac{1}{2}(y_1+y_2+y_3+y_4) \\ V_{33}=\frac{1}{2}(z_1+z_2+z_3+z_4) \end{cases} \qquad \begin{cases} V_{34}=\dfrac{1}{\sqrt{8}}(x_1-x_2-x_3+x_4-y_1+y_2-y_3+y_4) \\ V_{35}=\dfrac{1}{\sqrt{8}}(x_1+x_2-x_3-x_4-z_1+z_2-z_3+z_4) \\ V_{36}=\dfrac{1}{\sqrt{8}}(y_1+y_2-y_3-y_4+z_1-z_2-z_3+z_4) \end{cases}$$

$$\begin{cases} V_{37}=\dfrac{1}{(12)^{\frac{1}{2}}}(x_{11}+x_{12}+x_{13}+x_{21}+x_{22}+x_{23}+x_{31}+x_{32}+x_{33}+x_{41}+x_{42}+x_{43}) \\ V_{38}=\dfrac{1}{(12)^{\frac{1}{2}}}(y_{11}+y_{12}+y_{13}+y_{21}+y_{22}+y_{23}+y_{31}+y_{32}+y_{33}+y_{41}+y_{42}+y_{43}) \\ V_{39}=\dfrac{1}{(12)^{\frac{1}{2}}}(z_{11}+z_{12}+z_{13}+z_{21}+z_{22}+z_{23}+z_{31}+z_{32}+z_{33}+z_{41}+z_{42}+z_{43}) \end{cases}$$

$$\begin{cases} V_{40}=\dfrac{1}{(24)^{\frac{1}{2}}}\begin{bmatrix} x_{11}+x_{12}+x_{13}-x_{21}-x_{22}-x_{23}-x_{31}-x_{32}-x_{33}+x_{41}+x_{42}+x_{43} \\ -y_{11}-y_{12}-y_{13}+y_{21}+y_{22}+y_{23}-y_{31}-y_{32}-y_{33}+y_{41}+y_{42}+y_{43} \end{bmatrix} \\ V_{41}=\dfrac{1}{(24)^{\frac{1}{2}}}\begin{bmatrix} x_{11}+x_{12}+x_{13}+x_{21}+x_{22}+x_{23}-x_{31}-x_{32}-x_{33}-x_{41}-x_{42}-x_{43} \\ -z_{11}-z_{12}-z_{13}+z_{21}+z_{22}+z_{23}-z_{31}-z_{32}-z_{33}+z_{41}+z_{42}+z_{43} \end{bmatrix} \\ V_{42}=\dfrac{1}{(24)^{\frac{1}{2}}}\begin{bmatrix} y_{11}+y_{12}+y_{13}+y_{21}+y_{22}+y_{23}-y_{31}-y_{32}-y_{33}-y_{41}-y_{42}-y_{43} \\ +z_{11}+z_{12}+z_{13}-z_{21}-z_{22}-z_{23}-z_{31}-z_{32}-z_{33}+z_{41}+z_{42}+z_{43} \end{bmatrix} \end{cases}$$

$$\begin{cases} V_{43}=\dfrac{1}{(48)^{\frac{1}{2}}}\Big[\begin{matrix} 2x_{11}-x_{12}-x_{13}-2x_{21}+x_{22}+x_{23}-2x_{31}+x_{32}+x_{33}+2x_{41}-x_{42}-x_{43} \\ -2y_{11}+y_{12}+y_{13}+2y_{21}-y_{22}-y_{23}-2y_{31}+y_{32}+y_{33}+2y_{41}-y_{42}-y_{43}\end{matrix}\Big] \\ V_{44}=\dfrac{1}{(48)^{\frac{1}{2}}}\Big[\begin{matrix} x_{11}-2x_{12}+x_{13}+x_{21}-2x_{22}+x_{23}-x_{31}+2x_{32}-x_{33}-x_{41}+2x_{42}-x_{43} \\ -z_{11}+2z_{12}-z_{13}+z_{21}-2z_{22}+z_{23}-z_{31}+2z_{32}-z_{33}+z_{41}-2z_{42}+z_{43}\end{matrix}\Big] \\ V_{45}=\dfrac{1}{(48)^{\frac{1}{2}}}\Big[\begin{matrix} y_{11}+y_{12}-2y_{13}+y_{21}+y_{22}-2y_{23}-y_{31}-y_{32}+2y_{33}-y_{41}-y_{42}+2y_{43} \\ +z_{11}+z_{12}-2z_{13}-z_{21}-z_{22}+2z_{23}-z_{31}-z_{32}+2z_{33}+z_{41}+z_{42}-2z_{43}\end{matrix}\Big] \end{cases}$$

$$\begin{cases} V_{46}=\dfrac{1}{(24)^{\frac{1}{2}}}(x_{11}+x_{12}-2x_{13}+x_{21}+x_{22}-2x_{23}+x_{31}+x_{32}-2x_{33}+x_{41}+x_{42}-2x_{43}) \\ V_{47}=\dfrac{1}{(24)^{\frac{1}{2}}}(y_{11}-2y_{12}+y_{13}+y_{21}-2y_{22}+y_{23}+y_{31}-2y_{32}+y_{33}+y_{41}-2y_{42}+y_{43}) \\ V_{48}=\dfrac{1}{(24)^{\frac{1}{2}}}(2z_{11}-z_{12}-z_{13}+2z_{21}-z_{22}-z_{23}+2z_{31}-z_{32}-z_{33}+2z_{41}-z_{42}-z_{43}) \end{cases}$$

$$\begin{cases} V_{49}=\tfrac{1}{4}(x_{12}-x_{13}-x_{22}+x_{23}-x_{32}+x_{33}+x_{42}-x_{43}+y_{12}-y_{13}-y_{22}+y_{23}+y_{32}-y_{33}-y_{42}+y_{43}) \\ V_{50}=\tfrac{1}{4}(x_{11}-x_{13}+x_{21}-x_{23}-x_{31}+x_{33}-x_{41}+x_{43}+z_{11}-z_{13}-z_{21}+z_{23}+z_{31}-z_{33}-z_{41}+z_{43}) \\ V_{51}=\tfrac{1}{4}(y_{11}-y_{12}+y_{21}-y_{22}-y_{31}+y_{32}-y_{41}+y_{42}-z_{11}+z_{12}+z_{21}-z_{22}+z_{31}-z_{32}-z_{41}+z_{42}). \end{cases}$$

The Secular Equations for the A_1 and E Type Frequencies, Using a Simple Valence Potential

In Section 2, it was pointed out that if the symmetry coordinates are chosen properly, the potential energy separates into parts, each composed of coordinates belonging to only one irreducible representation. Since the transformation matrices of every subspace are orthogonal, the kinetic energy will contain no cross terms at all, and, therefore, it is likewise separable into parts according to the irreducible representations. Every class of frequencies can be treated separately, therefore, and the secular equations may be set up independently. For the present treatment it was assumed that the potential energy function may be divided into a simple valence potential involving the distortions in the valence bonds and angles and the potential barriers hindering the rotation of the methyl groups about the $A-C_i$ axes. The nature of the forces giving rise to the barriers is unknown but it is reasonably safe to assume that they are of minor importance in those modes in which there is no relative rotation between the various parts of the molecule. An examination of the A_1 and E type coordinates reveals that such is the case in these modes and for them the barrier potentials may be disregarded to the first approximation. The potential function then reduces to

$$2V=K_{AC}\sum_{i=1}^{4}\delta R_i^2+K_\Omega\sum_{\text{pairs } i,j}(R_0\delta\Omega_{ij})^2+K_H\sum_{i=1}^{4}\sum_{j=1}^{3}\delta r_{ij}^2+K_\beta\sum_{i=1}^{4}\sum_{j=1}^{3}(r_0\delta\beta_{ij})^2+K_\gamma\sum_{i=1}^{4}\sum_{\text{pairs } j,k}(r_0\delta\gamma_{jk}^i)^2,$$

where δR_i = the change in length of the $A-C_i$ bond, $\delta\Omega_{ij}$ = the distortion in the C_i-A-C_j valence angle, δr_{ij} = the change in length of the C_i-H_{ij} bond, $\delta\beta_{ij}$ = the distortion in the $A-C_i-H_{ij}$ valence angle, and $\delta\gamma_{jk}^i$ = the distortion in the $H_{ij}-C_i-H_{ik}$ angle. The most direct method of expressing V in terms of the symmetry coordinates is to express $\delta R_i, \cdots, \delta\gamma_{jk}^i$ in terms of the displacement coordinates, and then to substitute the expressions of the latter in terms of the symmetry coordinates. The inverse transformation is easily obtained, since the matrices are orthogonal,

by interchanging rows and columns. If we let M be the mass of the methyl group carbon atoms and m be the mass of the hydrogen atoms, we obtain:

(a) P coordinates,

$$2T_P = M\dot{P}_1^2 + m(\dot{P}_2^2 + \dot{P}_3^2),$$

$$2V_P = \left[K_{AC} + \frac{K}{3} + \frac{8}{3}(K_\beta + K_\gamma)\right]P_1^2 + K_H P_2^2 + (K_\beta + K_\gamma)P_3^2 + 2(K_H/\sqrt{3})P_1P_2 - 2[\sqrt{8/3}(K_\beta + K_\gamma)]P_1P_3.$$

The secular equation is

$$\Delta_P = \begin{vmatrix} \alpha - M\lambda_P & K_H/\sqrt{3} & -\sqrt{8/3}(K_\beta + K_\gamma) \\ K_H/\sqrt{3} & K_H - m\lambda_P & 0 \\ -\sqrt{8/3}(K_\beta + K_\gamma) & 0 & (K_\beta + K_\gamma) - m\lambda_P \end{vmatrix} = 0,$$

where $\alpha = K_{AC} + K_H/3 + 8/3(K_\beta + K_\gamma)$ and $\lambda_P = \omega_P^2 = 4\pi^2\nu_P^2$.

(b) T coordinates,

$$2T_T = M\dot{T}_5^2 + m(\dot{T}_7^2 + \dot{T}_{10}^2 + \dot{T}_{11}^2),$$

$$2V_T = aT_5^2 + bT_7^2 + cT_{10}^2 + dT_{11}^2 + 2eT_5T_7 + 2fT_5T_{10} + 2gT_5T_{11} + 2hT_7T_{10} + 2jT_7T_{11} + 2kT_{10}T_{11}$$

and identical expressions in the coordinates T_6, T_8, T_9, and T_{12}, respectively. These give two identical fourth-order determinantal equations corresponding to the twofold degeneracy of these modes. The secular equation is

$$\Delta_T = \begin{vmatrix} a - M\lambda_T & e & f & g \\ e & b - m\lambda_T & h & j \\ f & h & c - m\lambda_T & k \\ g & j & k & d - m\lambda_T \end{vmatrix} = 0$$

with

$$a = 3K_\Omega + \frac{4}{3}K_H + 6K_\beta\left(\frac{1}{6} + \frac{r_0}{2R_0}\right)^2 + \frac{8}{3}K_\gamma,$$

$$b = \frac{4}{9}K_H + \frac{K_\beta}{18} + \frac{8}{9}K_\gamma,$$

$$c = \frac{K_H}{9} + \frac{8}{9}K_\beta + \frac{2}{9}K_\gamma,$$

$$d = \frac{4}{9}K_H + \frac{K_\beta}{18} + \frac{25}{18}K_\gamma,$$

$$e = -\frac{4}{3\sqrt{3}}K_H - \frac{K_\beta}{\sqrt{3}}\left(\frac{1}{6} + \frac{r_0}{2R_0}\right) - \frac{8}{3\sqrt{3}}K_\gamma,$$

$$f = \frac{2}{3\sqrt{3}}K_H - \frac{4K_\beta}{\sqrt{3}}\left(\frac{1}{6} + \frac{r_0}{2R_0}\right) + \frac{4}{3\sqrt{3}}K_\gamma,$$

$$g = -\frac{4}{3\sqrt{3}}K_H - \frac{K_\beta}{\sqrt{3}}\left(\frac{1}{6} + \frac{r_0}{2R_0}\right) + \frac{10}{3\sqrt{3}}K_\gamma,$$

$$h = -\frac{2}{9}K_H + \frac{2}{9}K_\beta - \frac{4}{9}K_\gamma,$$

$$j = \frac{4}{9}K_H + \frac{K_\beta}{18} - \frac{10}{9}K_\gamma,$$

$$k = -\frac{2}{9}K_H + \frac{2}{9}K_\beta + \frac{5}{9}K_\gamma.$$

In solving these equations for any particular case it is best to substitute the numerical values of any known constants into the determinants and then to expand into the corresponding algebraic equations. The cubic may then be solved by trigonometric methods while for the quartic the method of the reducing cubic was found convenient.

Application to Tetramethylmethane, $C(CH_3)_4$, Tetramethylsilane, $Si(CH_3)_4$, and Tetramethylammonium, $N^+(CH_3)_4$

From the table of selection rules it is seen that both the A_1 and E frequencies are Raman active, the first giving rise to totally polarized lines, the second to depolarized lines. The Raman spectrum of tetramethylmethane has been measured by Kohlrausch and his co-workers and by Rank;[1] the tetramethylsilane spectrum was observed by Rank and Bordner;[2] the tetramethylammonium spectrum was obtained by Edsall[3] by using a solution of tetramethylammonium chloride. Rank's data for tetramethylmethane has been used in these calculations. Polarization data are available only for tetramethylammonium but a comparison of the spectra together with the numerical results makes it possible to extend the interpretation to the other two molecules. The observed spectra are reproduced in Table IV for convenient reference.

The polarization data indicate that some of the observed lines are not fundamentals, since the selection rules allow only three polarized lines. We may be reasonably sure, however, that the 752 cm^{-1} line of $N^+(CH_3)_4$ is a fundamental and is the lowest mode of class $\Gamma^{(1)}$. Edsall reports that this line is very sharp and intense. Similar properties of the 734 cm^{-1} and 596 cm^{-1} lines of $C(CH_3)_4$ and $Si(CH_3)_4$ have been reported by Rank and Bordner, and for the present calculations these have been assigned to the lowest $\Gamma^{(1)}$ modes of these molecules. Referring to the secular determinant for these frequencies

Table IV. *Observed Raman frequencies (cm^{-1}). Numbers in parentheses are the estimates of the relative intensities. P = polarized ($\rho < 6/7$), D = depolarized ($\rho = 6/7$).*

$C(CH_3)_4$	$Si(CH_3)_4$	$N^+(CH_3)_4$
335 (10)	202 (20)	372 (*D*)
415 (3)	239 (15)	455 (*D*)
734 (20)	598 (20)	752 (*P*)
925 (15)	696 (15)	955 (*D*)
1263 (20)	863 (10)	1455 (*D*)
1455 (15)	1264 (10)	2930 (*P*)
2713 (5)	1427 (15)	2967 (*P*)
2746 (3)	2905 (10)	2991 (*P*)
2794 (3)	2963 (10)	3037 (*D*)
2865 (7)		and weak
2893 (5)		lines at
2913 (10)		1047
2938 (3)		1173
2957 (7)		1289

Table V. *Comparison of the calculated and observed frequencies (cm^{-1}).*

Tetramethyl-methane		Tetramethyl-silane		Tetramethyl-ammonium	
Calc.	Obs.	Calc.	Obs.	Calc.	Obs.
335 (2)	(335)	202 (2)	(202)	372 (2)	(372)
734 (1)	(734)	597 (1)	(598)	752 (1)	(752)
929 (2)	925	901 (2)	863	939 (2)	955
1448 (1)	1455	1422 (1)	1427	1454 (1)	
1484 (2)		1484 (2)		1484 (2)	1455
2895 (1)	2893	2893 (1)	2905	2896 (1)	2930
3013 (2)	2913 2957	3010 (2)	2963	3013 (2)	3037

( ) give the assigned degeneracies. $K_H = 4.79 \times 10^5$ dynes/cm; $K_\beta = K_\gamma = 0.468 \times 10^5$ dynes/cm; $K_{CC} = 5.20 \times 10^5$, $K_{Si-C} = 3.31 \times 10^5$, and $K_{N-C} = 5.51 \times 10^5$ dynes/cm; $K_\Omega = 0.399 \times 10^5$, 0.137×10^5, 0.501×10^5 dynes/cm in the respective molecules.

we see that there are four constants K_{AC}, K_H, K_β, K_γ. The latter three constants are taken from Howard's work on ethane[4] and following his procedure we assume $K_\beta = K_\gamma$. This leaves K_{AC} unknown. Using the above assignments of the lowest nondegenerate modes, the latter constant is determined, and the other two frequencies may be calculated in each case.

For the doubly degenerate modes we have two additional constants, K_Ω and r_0/R_0. Pauling and Brockway[18] have measured the distances in the tetramethylmethane molecule by electron diffraction methods. The values adopted here are $r_0 = 1.10$A and $R_0 = 1.55$A. The C−H distance, r_0, is assumed to be the same in all three molecules. Since the C−C distance in tetramethylmethane is the same as in diamond, we assume that the Si−C distance in tetramethylsilane is the same as in the cubic form of silicon carbide in which every silicon atom is tetrahedrally surrounded by four carbon atoms. We thus obtain $R_0 = 1.89$A. The N−C distance was calculated from the tetrahedral radii of the N and C atoms, taken from tables given by Rice.[19] These are 0.70 and 0.77, respectively, giving $R_0 = 1.47$A. There remains, then, only one unknown constant, K_Ω. There is really no conclusive evidence for the assignment of the lowest doubly degenerate mode. However, the lowest lines observed in all three spectra are very intense and in $N^+(CH_3)_4$,

[18] Pauling and Brockway, J. Am. Chem. Soc. 59, 1224 (1937).

[19] Rice, *Electronic Structure and Chemical Binding* (McGraw Hill Co., 1940), Chap. 16, p. 319.

at least, the lowest line is known to be depolarized. It is probably a fundamental. Furthermore, the Wall and Eddy calculation referred to in the introduction indicates that these lines are probably doubly degenerate. Such was assumed, and from the expanded form of the secular equation, the constant K_α was determined in every case. The other three frequencies of this class could then be calculated. The results are shown in Table V; frequencies in parentheses were used to determine constants.

Note that in every case two frequencies are obtained in the neighborhood of 1450 cm^{-1}, whereas only one is observed in the spectra. In tetramethylammonium, the polarization data enable us to assign this line with a high degree of certainty, that is, the observed 1455 cm^{-1} is due to a doubly degenerate mode and corresponds to the calculated 1484 cm^{-1} E type frequency. The agreement is quite good, being within 2 percent. In the other two molecules, we can make no definite assignments although there is excellent agreement between the observed 1455 and calculated 1448 in tetramethylmethane and between the observed 1427 and calculated 1422 in tetramethylsilane. The calculated lines represent the totally symmetric bending motions within the methyl groups and should correspond to totally polarized Raman lines. However, this line is absent from the tetramethylammonium spectrum and similar anomalous intensities have been observed in other molecules.[20] It is, therefore, uncertain whether the 1455 cm^{-1} and 1427 cm^{-1} lines referred to above are to be associated with the nondegenerate or doubly degenerate modes. The agreement is satisfactory in either case, considering the simple force system which has been used. Further experimental data is necessary, however, before any conclusion can be reached.

There is also doubt concerning the 2895 cm^{-1} mode of tetramethylmethane. It is inviting to associate it with the observed 2893 cm^{-1} line. However, the next higher line, 2913 cm^{-1}, is only 0.7 percent different from the calculated value and is more intense than the lower observed line. The 2913 line may, therefore, be the proper choice of the upper nondegenerate mode, but again without further experimental data no definite statements can be made.

In the tables we have aligned the calculated 3010 cm^{-1} frequencies with the highest lines observed in the spectra. With the help of the polarization data we can make a fairly certain assignment of the 3037 line of tetramethylammonium, associating it with the highest calculated doubly degenerate mode. The agreement in this case is then 0.8 percent. Nothing conclusive can be said for the other molecules.

In the region of the spectra below 1000 cm^{-1} we have obtained satisfactory results for tetramethylmethane and tetramethylammonium. The polarization data of the latter again is in agreement with the predicted depolarized line at 939 cm^{-1}. The difference between this and the observed 955 cm^{-1} is about 2 percent. The 955 cm^{-1} line of $N^+(CH_3)_4$ and the 925 cm^{-1} line of $C(CH_3)_4$ can thus be assigned to doubly degenerate modes. The tetramethylsilane spectrum is more complicated. In the region below 1000 cm^{-1} there are five intense lines compared to only four in the other molecules. We cannot tell at present whether or not they are all fundamentals. The difference between the observed 863 cm^{-1} and the calculated 901 cm^{-1} is only 4 percent but this is too large for any definite assignment.

The results are generally satisfactory. It is apparent from the preceding discussion why the four lowest lines could not be treated in terms of an AB_4 molecule with the use of a simple force system. The present treatment also substantiates the calculations of Wall and Eddy on tetramethylmethane. It is interesting to note that the deformation constant, K_α, determined by their approximate method compares favorably with the value found here. However, it must also be pointed out that no complete analysis can be made on the basis of the Raman spectra and the accompanying polarization data. Depolarized lines may be due to triply degenerate modes as well as doubly degenerate modes. There is a decided need for a re-examination of the Raman spectra and for studies of the infra-red spectra of these molecules. Aside from their application to the molecules discussed here, the calculations

[20] F. Stitt, J. Chem. Phys. **7**, 297 (1939). See the discussion on page 304.

yield another interesting result. It will be noted that the three highest calculated lines are practically identical in the three cases, and it is also to be noted that the same force constants have been used for the methyl groups in every case. These frequencies are almost totally insensitive to the forces operating in the AC_4 skeleton. The interpretation is directly evident. The skeleton is involved to a very small extent in these modes, and, therefore, they may rightly be considered as vibrations within the methyl groups.

ACKNOWLEDGMENTS

It is with pleasure that the author takes this opportunity to express his appreciation to Professor J. C. Slater and Professor L. Harris for their supervision and encouragement during the course of this work. Thanks are due to Professor Slater for helpful discussions and criticisms on the preparation of the paper. The author is also indebted to the Massachusetts Institute of Technology for the award of an Institute Fellowship which made it possible for him to pursue this research.

DECEMBER, 1940 JOURNAL OF CHEMICAL PHYSICS VOLUME 8

The Entropy of Dilution of Strong Electrolytes in Aqueous Solutions

H. S. FRANK,* *Department of Chemistry, Lingnan University, Hongkong, China*

AND

A. L. ROBINSON, *Department of Chemistry, University of Pittsburgh, Pittsburgh, Pennsylvania*

(Received June 1, 1940)

The relative partial molal entropy of water, $\bar{S}_1 - S_1^0$, in aqueous electrolyte solutions is calculated from existing data. An attempt is made to correlate these values with changes in the structure of water in the solutions. It is found that cations of small radii and ions capable of forming hydrogen bonds with the water, such as H_3O^+, OH^- and NH^+_4, help to stabilize the water structure, while large ions and ions of nonspherical and nontetrahedral shapes have an effect in the opposite direction. In dilute solutions the entropy of dilution depends largely on the ionic strength. In all cases deviations from the Debye-Hückel limiting law are positive.

THE present status of thermodynamic electrolyte theory has been well summarized by Scatchard[1] who shows how the main experimental results can be explained on the basis of plausible physical assumptions. For very dilute solutions it seems unlikely that the limiting law of Debye and Hückel[2] will need substantial modification. For some time the experimental evidence from heats of dilution and heat capacities seemed not to give full support to the Debye-Hückel limiting law, but the recent calculations of Young[3,4] leave little doubt that here also the predictions of the limiting law are quantitatively fulfilled, at least for electrolytes of 1–1 and 2–1 valence types.

So far as we know, no attempt has been made to interpret the thermodynamic properties of electrolyte solutions in a way involving the detailed structure of the solution. Since there is experimental evidence that the structure of electrolyte solutions changes with concentration[5–7] we considered it desirable to calculate from existing data the differential entropy of dilution, that is, the relative partial molal entropy of water, $\bar{S}_1 - S_1^0$, in such solutions. Since entropy is related to structural complexity it seemed that the influence of structure would

* Visiting Professor in the Department of Chemistry of the University of Pittsburgh, September, 1939 to March, 1940.

[1] G. Scatchard, Chem. Rev. **19**, 309 (1936).

[2] P. Debye and E. Hückel, Physik. Zeits. **24**, 193 (1923).

[3] T. F. Young and W. L. Groenier, J. Am. Chem. Soc. **58**, 187 (1936).

[4] T. F. Young and P. Seligmann, J. Am. Chem. Soc. **60**, 2379 (1938).

[5] R. Suhrmann and H. Breyer, Zeits. f. physik. Chemie **B20**, 17 (1932); **B23**, 193 (1933).

[6] G. W. Stewart, J. Chem. Phys. **7**, 869 (1939).

[7] H. E. Wirth, J. Am. Chem. Soc. **62**, 1128 (1940).

reveal itself more directly in the entropy values than in the heats of dilution and activity data from which they are derived. $\bar{S}_1$, $\bar{S}_2$ and S are simply related by thermodynamic equations so that any one may be chosen for discussion, but $\bar{S}_1$ values should reflect more directly changes in the water structure with addition of solute. Moreover, the $\bar{S}_1$ curves are more convenient for plotting and bring out more distinctly the individualities of different solutes.‡

The $\bar{S}_1-S_1^0$ values of Table I were calculated by use of the equation

$$\bar{S}_1-S_1^0=(\bar{L}_1-RT\ln(a_1/N_1))/T.$$

$\bar{L}_1$ is the relative partial molal heat content of the water $(\bar{H}_1-H_1^0)$ and a_1 is its activity, referred to pure water as the standard state. N_1, the mole fraction of water in the solute, computed from $N_1=55.51/55.51+\nu m$ takes account of the entropy of mixing, so that the values of Table I represent the non-ideal part of the entropy. For this reason $\bar{S}_2$ values obtained by use of the equation $N_1d\bar{S}_1+N_2d\bar{S}_2=0$ do not go to infinity at infinite dilution, but to zero. For the dilute region the equation used was $\bar{S}_1-S_1^0=(\bar{L}_1-jRT\ln N_1)/T$, where j is the freezing point deviation function of Lewis and Randall.[8] In this region, for which data are not tabulated but are represented graphically in Fig. 3, we have used the freezing point data of Scatchard.[9] For concentrations of $0.1m$ and above we have used the vapor pressure data of R. A. Robinson[10] as

TABLE I. *Differential entropy of dilution, $\bar{S}_1-S_1^\circ$, in aqueous solutions at 25°. (All entropy values are in calorie-degree^{-1}-mole^{-1}.)**

$m=$	0.1	0.5	1.0	2.0	3.0	4.0
HCl	−0.082	−0.0051	−0.0104	−0.0182	−0.0057	−0.0154
NH_4Cl	−0.078	−0.0056	−0.0117	−0.0203	−0.0097	0.0081
LiCl	−0.077	−0.0039	−0.0075	−0.0052	0.0017	0.0028
NaCl	−0.057	−0.064	0.0074	0.0378	0.0803	0.134
KCl	−0.058	−0.083	−0.0044	0.0264	0.0603	0.0955
CsCl	−0.052	0.0013	0.0045	0.0418		
HBr	−0.066	−0.0033	−0.0070	−0.0145	−0.0258	
LiBr	−0.065	−0.0038	−0.0055	0.0034	0.0241	0.0685
NaBr	−0.055	0.047	0.0093	0.0478	0.103	0.179
KBr	−0.054	0.028	0.0067	0.0367	0.089	0.148
NaI	−0.026	0.0017	0.0190	0.0621	0.138	0.241
KI	−0.031	0.0012	0.0110	0.0597	0.129	0.204
$LiNO_3$	−0.071	−0.0025	−0.0034	0.0082	0.034	0.082
$NaNO_3$	−0.044	0.0028	0.015	0.055	0.101	0.160
KNO_3	−0.023	0.0049	0.018	0.084	(1.09)?	
LiOH	−0.089	−0.0099	−0.020	−0.046		
NaOH	−0.072	−0.0019	0.077	0.014	0.0204	−0.0016
KOH	−0.086	−0.0036	−0.0040	0.0091	0.0124	0.0158
KF	−0.054	−0.0025	−0.0039			
$MgCl_2$	−0.0021	−0.0125	−0.0239			
$CaCl_2$	−0.0021	−0.0107	−0.0110			
$SrCl_2$	−0.0023	−0.0062	−0.0072			
$BaCl_2$	−0.0024	−0.0088	−0.0045			
$Sr(NO_3)_2$	−0.043	0.0065	0.0365			
Na_2SO_4	−0.0019	0.0065	0.044			
$MgSO_4$	−0.0034	−0.029	−0.052	−0.139	−0.26	
$CuSO_4$	−0.0043	−0.023	−0.048			
$ZnSO_4$	−0.0039	−0.022	−0.045			
$CdSO_4$	−0.0043	−0.026	−0.060	−0.216	−0.285	(−1.94)?

* The values of Table I are given with unwarranted precision to facilitate the drawing of smooth curves. A general estimate of the accuracy of these values is difficult since they are derived from several sources but no gross deviations from the smoothed curves were observed. For purposes of our discussion relative values are of more interest and these should be more reliable.

‡ It is perhaps worth while to emphasize that any correct statement about entropy must have reference, explicitly or by implication, to the whole system, whether the quantity immediately under discussion is $\bar{S}_1$, $\bar{S}_2$ or S.

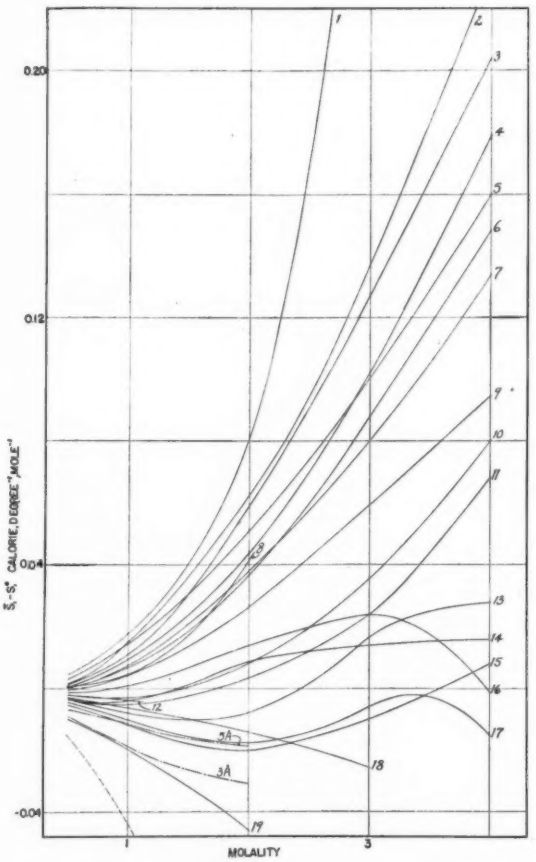

FIG. 1. Relative partial molal entropy of water, $\bar{S}_1-S_1^0$ in 1−1 solutions. 1, KNO_3; 2, NaI; 3, KI; 4, NaBr; 5, $NaNO_3$; 6, KBr; 7, NaCl; 8, CsCl; 9, KCl; 10, $LiNO_3$; 11, LiBr; 12, KF; 13, LiCl; 14, KOH; 15, NH_4Cl; 16, NaOH; 17, HCl; 18, HBr; 19, LiOH; – – –, Debye-Hückel limiting law; –·–·–· calculated for $a=3$ and 5A from extended Debye-Hückel theory.

[8] G. N. Lewis and M. Randall, *Thermodynamics* (McGraw-Hill, New York, 1923), p. 342.

[9] G. Scatchard and S. S. Prentiss, J. Am. Chem. Soc. **54**, 2696 (1932); *ibid.* **55**, 4355 (1933).

[10] R. A. Robinson and D. A. Sinclair, J. Am. Chem. Soc. **56**, 1830 (1934); R. A. Robinson, *ibid.* **57**, 1161 (1935); **57**, 1165 (1935); R. A. Robinson and R. S. Jones, *ibid.* **58**, 959 (1936).

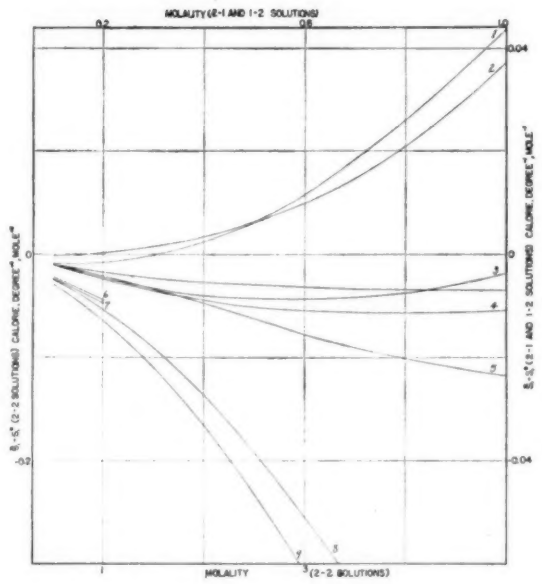

FIG. 2. Relative partial molal entropy of water, $\bar{S}_1-S_1^0$, in 2−1, 1−2 and 2−2 solutions. 1, Na_2SO_4; 2, $Sr(NO_3)_2$; 3, $BaCl_2$; 4, $CaCl_2$; 5, $MgCl_2$; 6, $ZnSO_4$; 7, $CuSO_4$; 8, $MgSO_4$; 9, $CdSO_4$.

far as possible for obtaining a_1 values. In other cases the values given in Landolt-Börnstein,[11] corrected where necessary to 25°, were used. The heat content data, where available, were from E. Lange and A. L. Robinson, and in other cases were taken from Bichowsky and Rossini[12] (where the data are given at 18°) corrected to 25° by the heat capacities of Rossini.[13]

The curves of Figs. 1 and 2, which are smoothed plots of the data of Table I, follow a general course. $\bar{S}_1-S_1^0$ initially decreases with increasing concentration, the curves typically passing through an inflection and a minimum followed in some cases by a sharp rise to high positive values and in other cases by a leveling off or even a maximum. The initial fall of $\bar{S}_1-S_1^0$, shown better in Fig. 3 where several salts are represented in the range of high dilution, is to be interpreted in terms of the Debye-Hückel theory. The limiting law gives

$$\bar{S}_1-S_1^0=\frac{\pi^{\frac{1}{2}}}{6(55.51)(1000)}\cdot\frac{N^{\frac{1}{2}}\epsilon^{\frac{1}{2}}}{k^{\frac{1}{2}}(DT)^{\frac{1}{2}}}\cdot\left(1+\frac{3T}{D}\frac{dD}{dT}\right)(\Sigma\nu_i z_i^2)^{\frac{1}{2}}m^{\frac{1}{2}};$$

at 25° in aqueous solutions

$$\bar{S}_1-S_1^0=-0.0155(\Sigma\nu_i z_i^2)^{\frac{1}{2}}m^{\frac{1}{2}}\text{ cal. degree}^{-1}\text{ mole}^{-1}.$$

The inflections of Figs. 1 and 2 are caused by the proportionality of $\bar{S}_1-S_1^0$ with $m^{\frac{1}{2}}$ demanded by the limiting law. In terms of this theory, which considers the medium as a continuous dielectric, the initial fall of $\bar{S}_1$ is to be attributed to the polarizing effect of the increasing average electric field strength in the solution. Alternatively the effect might be interpreted as due to the change in electrostriction pressure.[14] The ion cloud of Debye-Hückel theory also connotes a certain degree of organization which will make a small negative contribution to $\bar{S}_2$ and add a positive term to $\bar{S}_1$. This contribution is contained implicitly in the equations of the theory.

Since $\bar{S}_2-\bar{S}_2^0$ is positive and has values for uni-univalent solvents of approximately 0.5 e.u. at

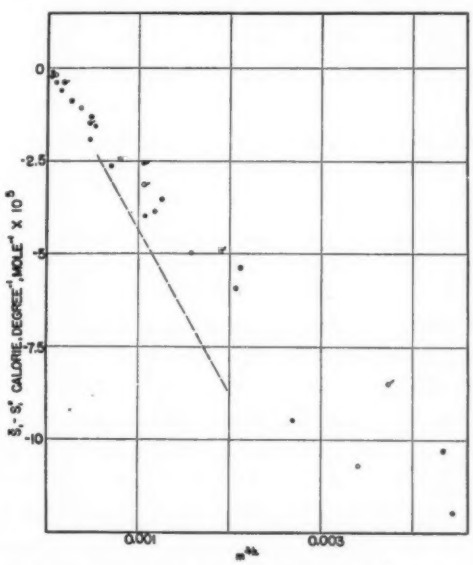

FIG. 3. Relative partial molal entropy of water, $\bar{S}_1-S_1^0$, in dilute solutions. ○ NaCl, ♂ NaBr, ⊕ KCl, ⊖ KBr, ● NH_4Cl, – – – – limiting law.

[11] Landolt-Börnstein *Physikalisch-chemische Tabellen*, fifth edition and supplementary volumes (Springer, Berlin).

[12] F. R. Bichowsky and F. D. Rossini, *The Thermochemistry of the Chemical Substances* (Reinhold Publishing Corp., New York, 1936).

[13] M. Randall and F. D. Rossini, J. Am. Chem. Soc. **51**, 323 (1929); F. D. Rossini, Bur. Stand. J. Research **7**, 47 (1931).

[14] W. M. Latimer and C. Kasper, J. Am. Chem. Soc. **51**, 2293 (1929).

0.01m there must also be a considerable structural disorganizing effect occurring as an infinitely dilute salt solution is gradually concentrated. We suggest interpreting this by assuming that the influence of the ion cloud on the envelope water is different from the average influence on the water as a whole. At infinite dilution the envelope water, the layer of water molecules immediately surrounding an ion, is, except for thermal agitation and the orienting effect of the structure of the water itself, completely under the influence of its central ion. By contrast the water as a whole is, practically, pure water. As the concentration increases and an ion cloud is produced, this will compete with the influence of the central ion on the envelope water, since its charge is of opposite sign. This competition will increase the entropy of the envelope water. On the other hand "average" water will no longer be infinitely distant from the ion centers and will therefore be subjected to orientation polarization and reduction in entropy. S contains both $\bar{S}_1$ and $\bar{S}_2$ but, as in the case of the heat contents, the contribution of the solute is predominant, so that $S-S^0$ is positive over the whole concentration range.

Since the Debye-Hückel theory is adequate for the very dilute region it should be immaterial whether we discuss the water as a continuous medium or consider its molecular structure. However, there exists an anomaly in the case of NH_4Cl which it seems plausible to ascribe to a structural effect. Scatchard and Prentiss[9] have shown that all of the ammonium halides give anomalous freezing point effects, and, since the heat of dilution curve for NH_4Cl[15] is not markedly abnormal in dilute solution, it seems likely that if the heat content data were available for the other ammonium halides their entropies would show the same peculiarity exhibited by NH_4Cl in Fig. 3. Scatchard's representation of the freezing point data makes it appear that there is a departure from the square root law in the case of these salts. However his unsmoothed data combined with $\bar{L}_1$ values give an $\bar{S}_1-S_1^0$ curve which seems to be linear with $m^{3/2}$ with as good accuracy as the curves for the other salts represented in Fig. 3, but with a larger slope. It should be remarked that the limiting slopes obtained from Fig. 3 by inspection for the alkali halides are too small by perhaps 20 percent. This is presumably another instance of the difficulty of obtaining good limiting slopes by inspection, a difficulty which was overcome by Young[3,4] in the case of heat of dilution data by an analytical method. We do not believe that this difficulty completely accounts for the difference in limiting slope between NaCl and NH_4Cl. This difference is in the direction to be expected if the NH^+_4 exerts an additional stabilizing influence on the water structure by virtue of its tetrahedral shape and its ability to form hydrogen bonds.

In attempting to discuss the course of the $\bar{S}_1-S_1^0$ curves in more concentrated solutions the use of a detailed structural picture enables certain regularities to be discerned. We assume that the upturn of the $\bar{S}_1-S_1^0$ curves is caused by a breaking down of the water structure by the presence of an increasing number of foreign centers, in this case ions. We will then expect that the greater the disturbance of structure produced by one of these centers the earlier and the more pronounced will be the rise in $\bar{S}_1-S_1^0$. Conversely, the more readily an ion can fit into the water structure the higher the concentration will be at which the minimum in $\bar{S}_1-S_1^0$ occurs. These expectations are confirmed as shown in Table I and Figs. 1 and 2. For the uni-univalent electrolytes the maximum disturbing effect is shown by KNO_3. This might be attributed to the plane triangle structure of the nitrate ion and its inability to fit smoothly into the four coordinated structure of water. In general the $\bar{S}_1-S_1^0$ values are more positive for iodides than for bromides and the bromide values are greater than those for chlorides. The effect of the cations is $Li^+<K^+<Na^+$ for chlorides, bromides, iodides and hydroxides up to $3m$; it is interesting that this order of cation effect is the same as that of the Despretz constants.[16] It should be noted that the order for the alkali metal hydroxides is the same as for the halides whereas the order of the activity coefficients for the hydroxides and

[15] H. Streeck, Zeits. f. physik. Chemie **A169**, 103 (1934).

[16] The Despretz constant is the equivalent lowering of the temperature of the density maximum in the solution. Values for the alkali and ammonium halides are given by Wright, J. Chem. Soc. **115**, 119 (1919).

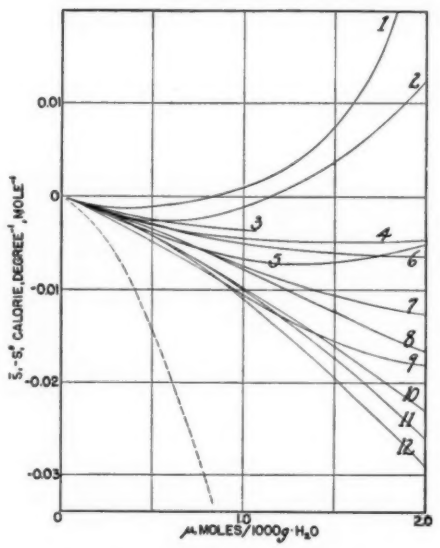

FIG. 4. Relative partial molal entropy of water, $\bar{S}_1 - S_1^0$, against ionic strength. 1, NaCl; 2, Na_2SO_4; 3, KF; 4, $BaCl_2$; 5, LiCl; 6, $SrCl_2$; 7, $CaCl_2$; 8, $MgCl_2$; 9, HCl; 10, $CuSO_4$; 11, $CdSO_4$; 12, $MgSO_4$; – – – –, limiting law.

fluorides[17] is opposite to that found for the other halides. The minimum disturbance of the water structure, most negative values of $\bar{S}_1 - S_1^0$, is shown by small ions and by ions capable of fitting into the water structure by hydrogen bridging, H_3O^+, OH^-, NH^+_4 and F^-.

As shown in Fig. 1 the curve representing the Debye-Hückel limiting law lies below all of the experimental curves. Figure 1 also shows $\bar{S}_1 - S_1^0$ values calculated according to the extended Debye-Hückel theory[18] for a (distance of closest approach) values of 3 and 5A. It seems that even below $0.5m$ the deviations from the limiting law cannot be attributed in any important degree to ion size since the few experimental curves which fall close to the calculations of the extended theory belong to just those electrolytes that are expected to exert a strong stabilizing influence on the water structure. For all substances the deviations from the limiting law are monotonically increasing functions of m within the range studied. These deviations represent largely, in terms of our picture, the effect of the ions in destroying the water structure. The corresponding deviations of $\bar{S}_2$ from the limiting law values are all negative and are to be interpreted largely as due to an extra orienting effect which an ion can have on its water envelope by virtue of the progressive disappearance of one of the factors which was opposing it. The concentration at which the breakdown effect of a small addition just counterbalances its electrostatic orienting effect will be marked by a minimum in $\bar{S}_1$ and a maximum in $\bar{S}_2$.

For purposes of testing this theory it is unfortunate that activity data for tetramethyl ammonium chloride are not available to higher concentrations and that among the alkyl ammonium halides heat of dilution data are at hand only for the methyl ammonium chlorides. Qualitatively, however, it is easy to see from the data that exist that $\bar{S}_1 - S_1^0$ turns up rapidly and reaches very high values in the case of $(CH_3)_4NCl$. This follows from the fact that the j values for a variety of tetraalkyl ammonium halides studied by J. Lange[19] show no great diversity of trend nor great differences from the values for the alkali halides, whereas the $\bar{L}_1$ values for the 0, 1, 2, 3 and 4 methyl ammonium chlorides[15] show an increasing tendency in the order named to turn up sharply to very high positive values, $(CH_3)_4NCl$ approximating the behavior of KNO_3 and $NaNO_3$ in this regard. Thus $\bar{L}_1 - jRT \ln N_1$ must follow the same trend, and we have the progressive replacement of the hydrogens in NH^+_4 by methyl groups producing an increasing tendency for the ion to interfere with water structure. More data on similar substances with larger alkyl groups would be desirable. It would be particularly interesting to study the possibilities regarding a limit to the amount of disorganization an ion can produce in water.

Since $\bar{S}_1 - S_1^0$ according to the Debye-Hückel theory is proportional to $(\Sigma \nu_i z_i^2)^{\frac{1}{2}} m^{\frac{1}{2}}$ we shall expect the curves for salts of different valence types to fall together in the dilute range when a plot is made against the ionic strength. Such a plot is shown in Fig. 4. All the salts studied show a reasonable relationship to each other particularly below $\mu = 0.5$. This seems to suggest that the effect of an ion in breaking up the

[17] K. Fajans and G. Karagunis, Zeits. f. angew. Chemie **43**, 1046 (1930); H. S. Harned and G. Akerlöf, Physik. Zeits. **27**, 430 (1926).

[18] T. H. Gronwall, V. K. LaMer and K. Sandved, Physik. Zeits. **29**, 358 (1928).

[19] L. Ebert and J. Lange, Zeits. f. physik. Chemie **A139**, 584 (1928); J. Lange, *ibid.* **A169**, 147 (1934).

structure of water is proportional to the square of its charge, so that, for instance, one magnesium ion has practically the same effect as four lithium ions. At high dilutions the deviation $\bar{S}_1-\bar{S}_{1\text{im law}}$ is of the approximate form $\Delta_1=am^2$, which gives for the corresponding deviation in S_2, $\Delta_2=-2(55.51)am$. The coefficient of m here is related to the coefficient of the linear term of the mean activity coefficient in such a way that the temperature independent numerical factors carry through from one to the other. There is here at least a suggestion that the concept of ionic strength may be important in the higher activity coefficient terms.

Accepting the validity of the use of the ionic strength to bring the $\bar{S}_1$ values for electrolytes of different valence types into relationship to each other, the relative values for NaCl and Na_2SO_4 as well as for $MgCl_2$ and $MgSO_4$ indicate that the sulphate ion has a smaller specific disruptive influence on the water structure than the chloride ion. It would be reasonable to associate this with the tetrahedral form of sulphate ion and the fact that its size is smaller than that of a tetrahedron consisting of four water molecules.

Another tentative conclusion that can be drawn from the data at hand is that the influence of size in the cases of the doubly charged cations is less important than with the singly charged cations. The differences between rare gas ions and those with *d* electrons seem also to be small.

The suggestions we are making for the interpretation of the entropy data fall closely in line with the picture given by Suhrmann and Breyer[5] on the basis of optical studies. In comparing the two sets of results one of the interesting points that emerge is that the substances for which we find a turning down of the $\bar{S}_1-S_1^0$ curves at high concentration are just those for which they find evidence of "chemical interaction" between the ions and water, namely, solutes containing H_3O^+, OH^- or bivalent cations. It seems possible that the "chemical interaction" in the case of the bivalent cations is related to the higher coordination number which Bernal and Fowler[20] and Eley and Evans[21] attribute to water near these ions. In the case of H_3O^+ and OH^- the nature of the interaction must be different but it is not surprising that an effect exists which shows up in the optical and in the entropy data.

The maxima and leveling off of some of the curves of Fig. 1 suggest interpretation in terms of an approach to a more or less constant structure of the solutions at high concentrations. Perhaps experimental indications of a superlattice structure in certain aqueous solutions[22] are consistent with this suggestion.

It remains to discuss the possibility that association is at least partially responsible for the trend of some of the curves of Figs. 1 and 2 at higher concentrations. This is difficult since the effect on $\bar{S}_1-S_1^0$ of a fractional value for the degree of dissociation will be the resultant of a number of factors. The contribution to the entropy of mixing can be calculated and an estimate made of the effect on the Debye-Hückel term by the reduction in true ionic strength. The relative structure disturbing effects of a pair of ions and their parent molecule is, however, very uncertain. Furthermore, a term which may easily overshadow all of these is the entropy change due to the release of some envelope water when a pair of ions unites. How much of the water of hydration is released in this process and how much entropy it returns to the average water molecule are quantities which will presumably differ in a specific way from solute to solute. Examining the data for evidence of association we recall that the nitrates and bivalent sulphates have been suspected of a tendency in this direction.[23] Comparison of the $\bar{S}_1-S_1^0$ curves of the alkali nitrates with those for the chlorides, bromides and iodides, and of the curves for sodium and magnesium sulphates with the corresponding chloride curves gives, however, no support to this suspicion. It appears that the effect of association on the entropy of dilution will make itself evident, if at all, only when the discussion of the subject has reached a more advanced stage.

[20] J. D. Bernal and R. H. Fowler, J. Chem. Phys. **1**, 515 (1933).

[21] D. D. Eley and M. G. Evans, Trans. Faraday Soc. **34**, 1093 (1938).

[22] S. Freed, J. Chem. Phys. **6**, 297, 654, 655 (1938); J. A. Prins, *ibid.* **3**, 72 (1935); Trans. Faraday Soc. **33**, 110 (1937).

[23] C. W. Davies, *The Conductivity of Solutions*, second edition (Wiley, New York, 1933).

Diamagnetic Anisotropy and Electronic Structure of Aromatic Molecules

HARVEY BROOKS
Harvard University, Cambridge, Massachusetts

(Received October 9, 1940)

Previous theories of the diamagnetic anisotropy of aromatic molecules, based on the method of molecular orbitals, neglect the correlation effects between electrons. In the present theory the anisotropy is treated from the standpoint of the Heitler-London-Pauling-Slater approximation by the inclusion of ionic terms in the secular equation. By means of an approximate treatment it is shown that correlation effects tend to reduce the diamagnetic susceptibility, the effect being relatively greater in complex molecules than in benzene. The contribution of higher order permutation integrals is also discussed and found to be negligible. The correct approximation lies intermediate between the pure H-L-S-P and pure molecular orbital approximations, but in order to explain the high value of the anisotropy, one is forced to assume that the true situation lies much closer to the molecular orbital viewpoint. The variation of the anisotropy of benzene through all intermediate stages of approximation is discussed by means of a more exact model. All calculations were carried out by treating the permutational degeneracy by means of the Dirac vector model.

INTRODUCTION

MEASUREMENTS on the diamagnetic susceptibility of single crystals of aromatic substances reveal a surprising degree of anisotropy.[1] For benzene it has been found that the molecular susceptibility is twice as large in a direction perpendicular to the plane of the molecule as in any direction in this plane. The effect is usually ascribed to electronic orbits which include several nuclei.[2] Such orbits are confined to a definite plane and hence can respond only to a component of the external magnetic field which is perpendicular to this plane, thus giving rise to anisotropy. In benzene and related aromatic molecules the electrons responsible are the six $2p\pi$ electrons, which are not involved in the hybridized coplanar single bonds. The free migration of these electrons in the plane of the benzene ring gives rise to the diamagnetic current which is responsible for the abnormally high susceptibility along the perpendicular axis.[3] Quantitative theories of the effect have been worked out by Pauling[4] and by F. London,[5] who calculated the ratio of the anisotropy of various condensed ring compounds to that of benzene, obtaining good agreement with experiment. In Pauling's theory the molecule is treated as a superconducting electrical circuit, the ideas involved being essentially classical. London uses a quantum-mechanical approach, based on Hueckel's theory of the various aromatic molecules.[6] The method is equivalent to the approximation of tight binding in the Bloch theory of metals.[7] The fact that both theories are in such good agreement with experiment, in spite of the many approximations involved, is evidence that the ratios of the anisotropies reduce to purely geometrical quantities, which have a significance beyond that of the particular model adopted for specific calculations.[8]

The weakness of both theories, based as they are on the molecular-orbital or Hund-Mulliken[9] viewpoint, is that they neglect the electrostatic interaction of the electrons except insofar as it can be represented by a Hartree field. No account

[1] K. Lonsdale, Reports on Progress in Physics **4**, 368 (1937). Cf. this review for experimental methods and further references to the literature.

[2] C. V. Raman and K. S. Krishnan, Proc. Roy. Soc. **A113**, 511 (1927); P. Ehrenfest, Physica **5**, 388 (1925); Zeits. f. Physik **58**, 719 (1929); K. Lonsdale, Proc. Roy. Soc. **A159**, 149 (1937); J. Chem. Soc. **1**, 364 (1938).

[3] The same phenomenon arises in the ions CO_3^- and NO_3^- having resonating π-bonds. The mechanism in this case is still somewhat obscure and has never received a quantitative explanation. Cf., for example, K. Lonsdale, Proc. Roy. Soc. **A171**, 541 (1939).

[4] L. Pauling, J. Chem. Phys. **6**, 676 (1936).

[5] F. London, J. de phys. et rad. **8**, 397 (1937).

[6] E. Hueckel, Zeits. f. Physik **70**, 204 (1931); **72**, 310 (1931); **76**, 628 (1932); **83**, 632 (1933).

[7] Cf., for example, N. F. Mott and H. Jones, *Properties of Metals and Alloys* (Oxford, 1936), p. 65.

[8] I am indebted to Professor F. London for this observation.

[9] Cf., for example, R. S. Mulliken, J. Chem. Phys. **1**, 492 (1933); J. H. Van Vleck and A. Sherman, Rev. Mod. Phys. **7**, 167 (1935), Chapter V.

is taken of the considerable energy necessary to get two electrons on the same atom, with the result that the so-called ionic configurations occur with much too large a probability in the wave function for the molecule as a whole. The indications are that the energy involved in putting two electrons on the same atom is of the order of 15 ev, whereas the resonance energy arising from the interatomic transfer of electrons is of the same order. By sacrificing part of the resonance energy it would be possible to eliminate part of the ionic terms and still obtain a higher total binding energy because of the decrease in Coulomb repulsion. The opposite extreme, in which no ionic terms occur at all, is the Heitler-London approximation,[10] in which two electrons are never found on the same atom. In this approximation, however, the diamagnetic current becomes very small as will be shown. Such diamagnetism as is present must be ascribed wholly to the nonorthogonality of the wave functions on adjacent atoms, an effect which will also be shown quite negligible.

The present paper is an effort to treat diamagnetic anisotropy from the standpoint of the H-L theory by inclusion of ionic terms in the secular equation. Naturally, the inclusion of such terms is in principle all that is necessary for a rigorous solution of the problem, regardless of the starting approximation, but in practice the best that can be done is to treat the ionic terms as a perturbation, applying ordinary Schrödinger perturbation theory with the solution of the H-L secular equation as the zeroth approximation. In the first section this is done for benzene and naphthalene. In the second section an attempt at a more accurate treatment of benzene is made, in order to show how the anisotropy varies between the two approximations. Finally a short discussion is given of the effect of nonorthogonality.

These calculations provide a good illustration of the usefulness of the Dirac vector model[11] in molecular calculations, especially in problems where approximately orthogonal wave functions are desirable.

Benzene and Naphthalene

1. Secular equations for benzene

The Hamiltonian for the benzene molecule may be written:

$$H=\sum_i T_i+\sum_i H_0(i)+\sum_{i<j} e^2/r_{ij}, \qquad (1)$$

where $T=(h^2/8\pi^2m)(i\nabla-\alpha)^2$ and $\alpha=(2\pi e/hc)\,\mathbf{A}(\mathbf{r})$ in the notation of F. London,[5] $\mathbf{A}$ being the vector potential. Also $H_0(i)=\Sigma_k H_k(i)$, where $H_k(i)$ is the potential due to a single ion in the position k in the benzene ring. The effect of the hydrogens is omitted altogether, inasmuch as we are interested only in the π-electrons which are not involved in the hydrogen bonds. In the H-L method the basic eigenfunctions are determinants of atomic functions, each lying on a different atom. In addition we must have determinants in which two atomic eigenfunctions, with opposite spin, lie on the same atom. It is convenient to multiply each atomic function $K(i)$ by a gauge factor $\exp(i\alpha_k\cdot\mathbf{r}_i)$, in order to shift the origin of the vector potential to atom k.[12]

The scheme used for setting up the secular equation is the Serber extension of the Dirac vector model to interconfigurational perturbations.[13] A configuration is specified by a certain set of atomic orbitals, while substates of a given configuration arise from the various ways of assigning spins to the orbitals. The fundamental formula is Serber's Eq. (13):

$$(H-W)^{R_iR_j} = \sqrt{2}^{r_i-r_j}\sum_P{}'(H_P{}^{R_iR_j}-\Delta_P{}^{R_iR_j}W)\mathbf{P}^{R_iR_j}. \qquad (2)$$

Here R_i, R_j label two configurations; r_i, r_j are the number of doubly occupied orbits in R_i and R_j, respectively. $H_P{}^{R_iR_j}$ and $\Delta_P{}^{R_iR_j}$ are energy and nonorthogonality integrals; $\mathbf{P}^{R_iR_j}$ is a permutation matrix with certain rows and columns omitted owing to the exclusion principle. As is well known, benzene may be treated as a six-electron problem. The permutation matrices for

[10] Cf., for example, J. H. Van Vleck and A. Sherman, Rev. Mod. Phys. **7**, 167 (1935), Chapter III. The method is hereinafter designated as H–L.

[11] P. A. M. Dirac, *Quantum Mechanics*, second edition (Oxford, 1935), Chap. X; J. H. Van Vleck, Phys. Rev. **45**, 405 (1934); R. Serber, *ibid.* **45**, 461 (1934).

[12] For a detailed explanation of this procedure see F. London, reference 5, or R. Peierls, Zeits. f. Physik **80**, 763 (1933).

[13] R. Serber, Phys. Rev. **45**, 461 (1934).

the simple transpositions in this case have been given by Serber[14] and from them all other permutations may be obtained by matrix multiplication. The summation in (2) is taken over all permutations of the six orbitals, but permutations which exchange identical orbits are considered equivalent and only counted once.

The complete energy matrix, according to Eq. (2), will split up into squares and rectangles, each corresponding to the intersection of two configurations. Down the principal diagonal are ranged squares which represent the interaction of each configuration with itself. One of these squares is, of course, just the ordinary H-L secular equation. Neglecting all permutation integrals except those corresponding to simple transpositions, the only integrals which occur in the H-L square are the direct integral and the simple exchange integral[15]

$$\int\cdots\int \mathrm{I}(1)\exp(-i\boldsymbol{\alpha}_1\cdot\mathbf{r}_1)\mathrm{II}(2)\exp(-i\boldsymbol{\alpha}_2\cdot\mathbf{r}_2)$$
$$\times\mathrm{III}(3)\exp(-i\boldsymbol{\alpha}_3\cdot\mathbf{r}_3)\mathrm{IV}(4)\exp(-i\boldsymbol{\alpha}_4\cdot\mathbf{r}_4)$$
$$\times\mathrm{V}(5)\exp(-i\boldsymbol{\alpha}_5\cdot\mathbf{r}_5)\mathrm{VI}(6)\exp(-i\boldsymbol{\alpha}_6\cdot\mathbf{r}_6)$$
$$\times H\mathrm{I}(2)\exp(i\boldsymbol{\alpha}_1\cdot\mathbf{r}_2)\mathrm{II}(1)\exp(i\boldsymbol{\alpha}_2\cdot\mathbf{r}_1)$$
$$\times\mathrm{III}(3)\exp(i\boldsymbol{\alpha}_3\cdot\mathbf{r}_3)\mathrm{IV}(4)\exp(i\boldsymbol{\alpha}_4\cdot\mathbf{r}_4)$$
$$\times\mathrm{V}(5)\exp(i\boldsymbol{\alpha}_5\cdot\mathbf{r}_5)$$
$$\times\mathrm{VI}(6)\exp(i\boldsymbol{\alpha}_6\cdot\mathbf{r}_6)d\tau_1\cdots d\tau_6. \quad (3)$$

Neither the Coulomb nor the exchange integral can give rise to diamagnetic anisotropy. Physically this is evident from the fact that in an electron exchange there is no net transport of charge; the two electrons involved merely change places. Thus there is no mechanism for a diamagnetic current. Mathematically this can be seen by collecting the phase factors in the integral (3). Assuming that the maximum contribution to the integral occurs when $\mathbf{r}_2\sim\mathbf{r}_1$, the product of the phase factors is approximately unity so that the matrix element is independent of the presence of the field.[16] Thus the solution of the ordinary H-L secular equation is independent of the field, and we obtain no diamagnetic anisotropy.[17]

To explain the anisotropy one must include the off-diagonal rectangles in the secular equation, thus taking into account the ionic configurations. If the Coulomb repulsion in these configurations is not too great, they may mix with the ground state to a considerable extent. The matrix elements between certain ionic configurations and the ground state, and between different ionic configurations, are proportional to a "hopping" integral, which is the analog of the resonance integral in the Bloch theory of metals[7] and which, in the presence of a magnetic field, contains a phase factor $\exp(2\pi if/6)$, where $f=(eS/hc)H$, S being the area of the benzene ring.[12] Roughly it corresponds to the jump of a single electron across the potential barrier between neighboring atoms, induced by the electric field of the ions and the "time-exposure" charge of the remaining electrons. As an example, consider matrix elements between the ground state and an excited configuration represented by (1, 2), a notation which means that atom 1 is doubly occupied while atom 2 is unoccupied.[18] All matrix elements are proportional to an integral

$$\int\cdots\int \mathrm{I}(1)\exp(-i\boldsymbol{\alpha}_1\cdot\mathbf{r}_1)$$
$$\times\mathrm{II}(2)\exp(-i\boldsymbol{\alpha}_2\cdot\mathbf{r}_2)\cdots\mathrm{VI}(6)\exp(-i\boldsymbol{\alpha}_6\cdot\mathbf{r}_6)$$
$$\times H\mathrm{I}(1)\exp(i\boldsymbol{\alpha}_1\cdot\mathbf{r}_1)\mathrm{I}(2)\exp(i\boldsymbol{\alpha}_1\cdot\mathbf{r}_2)\cdots$$
$$\times\mathrm{V}(6)\exp(i\boldsymbol{\alpha}_6\cdot\mathbf{r}_6)d\tau_1\cdots d\tau_6. \quad (4)$$

In this example each pair of phase factors multiplies to unity except that attached to electron 2. Replacing $\mathbf{r}_2$ by its mean value $\frac{1}{2}(\mathbf{R}_1+\mathbf{R}_2)$, one obtains the phase factor $\exp(2\pi if/6)$ outside the integral. Here $\mathbf{R}_1$ and $\mathbf{R}_2$ represent the position vectors of the correspondingly numbered nuclei.

In practice the interaction integral (4) would have a different value for each pair of configurations, but for simplicity we shall disregard this

[14] R. Serber, J. Chem. Phys. **2**, 697 (1934).

[15] The notation is that used by A. L. Sklar and M. Goeppert-Mayer, J. Chem. Phys. **6**, 645 (1938).

[16] This is not rigorously true, but it is readily shown, by expanding the exponential in power series, that the alteration in the exchange integral is quite negligible.

[17] There is, however, some contribution from the higher order permutation integrals, which we have neglected. See concluding section of this paper.

[18] Hereafter we shall designate the doubly occupied orbit as the negative ion and the unoccupied orbit as the positive ion or hole. Configurations having one doubly occupied orbit (and hence one unoccupied) will be called singly ionized; two doubly occupied orbits, doubly ionized, etc.

complication and assume the same value for all the hopping integrals, $W_1 \exp(2\pi if/6)$.[19]

2. Perturbation theory

The solution of the complete secular equation is approximated by means of perturbation theory. In order to explain the diamagnetic anisotropy it is necessary to go to the sixth order. The only configurations which interact to a first approximation are such as can be formed from each other by the transfer of one electron to a neighboring atom. Thus the ground configuration can only have matrix elements to singly ionized configurations in which the positive and negative ions are on adjacent positions in the ring. Singly ionized configurations only interact with each other if they differ by one place in the position of one of the ions. Thus (1, 2) interacts with (1, 3) or (6, 2) but not with (1, 4), (6, 3), or (2, 1).

Fortunately, in the perturbation theory, only those terms are of interest which depend explicitly on the magnetic field. In other words only terms corresponding to a series of transitions which carry an electron completely around the ring can give rise to a diamagnetic contribution. Only for such a chain of transitions will the phase factors on successive matrix elements fail to multiply to unity. Thus the second-order energy is given by

$$E^{(2)}=\sum_{m,\, n\,(m\neq n)}\frac{(0|H|(m,n))((m,n)|H|0)}{E_0-E_{(m,\,n)}},$$

$$=\sum_m\frac{W_1\exp(2\pi if/6)W_1\exp(-2\pi if/6)}{E_0-E_{(m,\,m+1)}}. \quad (5)$$

and the phase factors always cancel giving a correction to the energy which is independent of the magnetic field. The relevant sixth-order terms are all included in the formula

$$\sum_{\lambda,\,\mu,\,\nu,\,\pi,\,\sigma}^{\neq 0}\frac{(0|H|\lambda)(\lambda|H|\mu)(\mu|H|\nu)(\nu|H|\pi)(\pi|H|\sigma)(\sigma|H|0)}{(E_0-E_\lambda)(E_0-E_\mu)(E_0-E_\nu)(E_0-E_\pi)(E_0-E_\sigma)}, \quad (6)$$

where each index stands for an ionic configuration. A possible numerator would be

$$(0|H|1,2)(1,2|H|1,3)(1,3|H|6,3)$$
$$\times(6,3|H|5,3)(5,3|H|5,4)(5,4|H|0)$$
$$=W_1^6\exp(2\pi if), \quad (6')$$

which depends explicitly on the magnetic field through the phase factor.

Calculations based on these general principles have been carried out for benzene and naphthalene. In order to make the problem manageable the following simplifications were introduced:

(a) In the frequency denominators E_0-E_λ, the energies of all configurations of the same degree of ionization were taken as the same. This is a sort of "center of gravity" assumption, which enables us to carry through the calculation without diagonalizing the excited states, as matrix products are invariant of the representation.

(b) The energy of a singly ionized configuration is taken as J_0 above the ground state, of doubly ionized $2J_0$, etc.

The application of formula (6) gives an expression for the energy in the form

$$E=E_0+CW_1^6J_0^{-5}\cos 2\pi f. \quad (7)$$

The numerical constant C is always negative because the ground state, being lowest, is repelled downward by all the other states. From Eq. (7) one obtains immediately an expression for the extra susceptibility in the direction perpendicular to the plane of the molecule:

$$\Delta\chi=\chi_\perp-\chi_{||}=C\frac{W_1^6}{J_0^5}\left(\frac{2\pi eS}{hc}\right)^2. \quad (8)$$

Since C is negative, this always leads to diamagnetism.

Evaluation of the constant C is rather complicated, because one must take account not only of all possible ionic configurations (140 in number for benzene), but also of the exchange degeneracy among the six electrons. It was necessary first to diagonalize the H-L matrix for the ground configuration of the molecule. An approximate form

[19] Explicit calculations suggest that this assumption is very badly fulfilled, and that the hopping integrals may even have different signs. Such calculations must not be taken too seriously, however. See discussion in the concluding remarks of this paper.

of the eigenfunction was used, for benzene the symmetrical linear combination of the two Kekule structures.[20]

$\psi_{\mathrm{I}}=$ 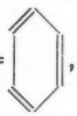 , $\psi_{\mathrm{II}}=$. (9)

The Pauling-Slater bond eigenfunctions,[21] ψ_{I} and ψ_{II}, are readily expressed in terms of the eigenfunctions of the vector model. For benzene it was found that use of the exact eigenfunction increased the coefficient C by about 5 percent over the value obtained with the approximate function. For comparison with naphthalene, however, the inexact eigenfunction was used, since the ground state of naphthalene could not be determined exactly in terms of Dirac eigenfunctions without an undue amount of labor.[22]

3. Naphthalene

In the case of naphthalene there is an exchange degeneracy among ten electrons, and the permutation matrices have not been calculated. However, it is possible to arrange the orbits in such a symmetrical fashion that the necessary permutation matrices are obtainable directly from those of the six-electron problem. An expression has been given for the wave function of the lowest state in terms of three bond eigenfunctions by Pauling and Wheland.[20] The corresponding structures are:

$\psi_{\mathrm{I}}=$, $\psi_{\mathrm{II}}=$ 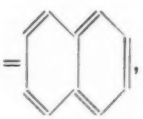 , (10a)

$\psi_{\mathrm{III}}=$ 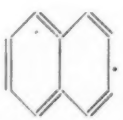 .

The ground state is expressed approximately by

$$\psi_0=\psi_{\mathrm{I}}+0.6\psi_{\mathrm{II}}+0.6\psi_{\mathrm{III}}. \qquad (10b)$$

As in benzene the diamagnetism first makes its appearance in the sixth approximation of perturbation theory, corresponding to the migration of an electron about one of the benzene rings.

4. Numerical results

The constant C takes on the following values for various cases.

(1) Benzene, taking into account only singly ionized configurations:

$$C=-259.2, \qquad (11a)$$

taking into account all ionic configurations

$$C=-936.0. \qquad (11b)$$

(2) Naphthalene, taking into account only singly ionized configurations

$$C=-402.2, \qquad (11c)$$

taking into account all ionized configurations up to triply ionized

$$C=-1515.0. \qquad (11d)$$

With these values of C Eq. (8) is valid provided the Coulomb energy is very large compared to the hopping energy. Although this assumption cannot be well-fulfilled at actual values of the internuclear distance, the formula may still be used to obtain the limiting value of the ratio $\Delta\chi_{\mathrm{naph}}/\Delta\chi_{\mathrm{benz}}$ in the limit of large separation. This ratio approaches a constant, 1.62, which is much lower than the ratio 2.19 calculated by London, and also than the observed ratio. The discrepancy indicates that the correlation of the electrons is relatively more effective in naphthalene than in benzene in cutting down the susceptibility. The physical interpretation of this result is not very clear. In the calculations it arises from the fact that, whereas in benzene all the bonds are equivalent and take on an equal amount of double-bond character, in naphthalene they are not equivalent, owing to the lower symmetry of the molecule, and take on alternately $\frac{1}{3}$ and $\frac{2}{3}$ double-bond character.[23] It turns out that the bonds having $\frac{1}{3}$ double-bond character are much less readily polarized ionically than those of $\frac{2}{3}$

[20] L. Pauling and G. W. Wheland, J. Chem. Phys. **1**, 362 (1933).

[21] J. C. Slater, Phys. Rev. **32**, 349 (1928); L. Pauling, J. Chem. Phys. **1**, 280 (1933). Other references, see Van Vleck and Sherman, reference 9.

[22] A rigorous solution of the naphthalene problem has been given by J. Sherman, J. Chem. Phys. **2**, 488 (1934) in terms of bond eigenfunctions. The approximate solutions give total energies in error by about 8 percent for benzene and 16 percent for naphthalene, but the general form of the wave functions is not seriously affected. By analogy with benzene we should not expect the use of the exact solutions for naphthalene to increase the calculated anisotropy by more than 10 or 12 percent, which would not alter any of our general conclusions.

[23] L. Pauling, *Nature of the Chemical Bond* (Cornell, 1939), p. 134.

double-bond character, with the result that the single bonds form a sort of barrier to the free passage of ions about the ring. The "reduction" of the anisotropy due to correlation effects is, of course, not nearly so great as indicated by the extreme form of the theory. Nevertheless there is some evidence for such a reduction in the fact that in almost all the cases cited by London[5] the observed anisotropy ratio is less than the calculated value. Furthermore, the best agreement is obtained using the lowest of all the measured values of $\Delta\chi_{\text{benz}}$, originally due to Krishnan,[24] which is 54×10^{-6} ergs per gauss per mole. Use of the much higher value, 62×10^{-6}, due to Lonsdale[25] would reduce the "observed" ratios by 13 percent, and necessitate the assumption of a considerable correlation effect to explain the discrepancy. Against this viewpoint one may argue the nice internal consistency among the other ratios, which agree very closely with experiment among each other. On the other hand, the effect of the correlation is chiefly a function of symmetry, and so we should expect it to have about the same relative effect on naphthalene, anthracene, diphenyl, etc., which have the same symmetry.

The extreme form of the H-L calculation allows only for diamagnetic currents which traverse one of the benzene rings in naphthalene. These currents will make the maximum contribution because currents which traverse the entire molecule involve the excitation of many more ionic terms, and so do not appear before the tenth order of perturbation theory. A rigorous treatment of these currents by perturbation theory would be impossible, but we have succeeded in making a rough estimate, based essentially on a count of the number of terms which enter into the perturbation formula. In this way we find:

$$\Delta\chi_{\text{naph}}/\Delta\chi_{\text{benz}}=1.62[1+612(W_1/J_0)^4]. \quad (12)$$

Thus in taking account of the currents which circumnavigate the whole molecule, we tend to improve the ratio $\Delta\chi_{\text{naph}}/\Delta\chi_{\text{benz}}$ towards better agreement with experiment, although the improvement is somewhat exaggerated by Eq. (12), because the derivation of (12) omits certain terms which would tend to cancel out some of the contribution to the second term of (12).

TABLE I. *Comparison between perturbation theory and rigorous solution of simplified problem with $S=\frac{1}{2}$.*

q	x'	C	
		EXACT	PERTURBATION
0.0	−4.0	−0.111	
0.53	−4.1	−0.109	
1.86	−4.5	−0.084	
2.91	−5.0	−0.052	−0.612
3.88	−5.6	−0.029	−0.145
4.44	−6.0	−0.020	−0.074
5.36	−6.7	−0.011	−0.029
5.73	−7.0	−0.009	−0.021
6.92	−8.0	−0.0044	−0.0081

[24] K. S. Krishnan, B. C. Gusha and S. Banerjee, Phil. Trans. **A231**, 235 (1933).
[25] K. Lonsdale, Proc. Roy. Soc. **A159**, 197 (1937). Indirect calculation based on the measurements of B. Cabrera and U. H. Fahlenbrach, Zeits. f. Physik **89**, 682 (1934).

A RIGOROUS SOLUTION: INTERPOLATION BETWEEN THE TWO APPROXIMATIONS

In discussing the relative anisotropies of molecules one can always assume with some plausibility that the higher order terms in the perturbation development contribute in the same ratio as the leading terms for different molecules, but when we come to discuss the order of magnitude of the anisotropies themselves, the perturbation theory is not very suitable. For example, with $J_0/|W_1|=8.2$, the resonance energy (total) in the molecular orbital theory and the Coulomb excitation energy in the H-L theory are of the same order of magnitude, so that the perturbation expansion is meaningless. In fact it is impossible to find values of the integrals which will explain the large anisotropy and still leave the H-L theory a good approximation. The true state of affairs probably lies intermediate between the two approximations. Although an exact solution is impossible in the general case, it is possible to set up a simplified problem for benzene which can be solved exactly and which gives considerable information about the intermediate approximations. One must assume that: (1) Only singly ionized configurations need be considered, and (2) the variation in Coulomb energy between the various excited configurations is small compared to the hopping energy.

Condition (1) is automatically satisfied by a secular problem in which the total spin of the

molecule is assumed to be 2 instead of 0 as it is in reality. Once the two electrons with opposite spins are placed on the same atom to form a singly ionized configuration, the remaining electrons all have parallel spins and so must stay on separate atoms. Thus all but singly ionized configurations are automatically excluded.

The sixfold non-ionic H-L configuration may be diagonalized by means of Bloch spin waves[26]

$$\phi_l^0=(1/\sqrt{6})\sum_m \exp(2\pi ilm/6)\ \psi(m), \quad (13)$$

where $\psi(m)$ symbolizes the Slater determinant in which the antiparallel spin lies on atom m of the benzene ring. One also takes linear combinations of the ionic states in the form

$$\phi_l^\lambda=(1/\sqrt{6})\sum_m \exp(2\pi ilm/6)\ (m, m+\lambda),$$
$$l=-2,\ -1,\ 0,\ 1,\ 2,\ 3, \quad \lambda=1,\ 2,\ 3,\ 4,\ 5, \quad (14)$$

where the configuration symbol $(m, m+\lambda)$ has the usual significance.[27] Because of the cyclic symmetry of benzene the secular equation factors according to l. We shall be interested only in the state $l=0$, since this has the same symmetry as the true ground state of the molecule. The secular equation to be solved is of sixth degree, having five ionic states and one non-ionic. We first diagonalize the five ionic states which are assumed to have the same Coulomb energy and then, adjoining the non-ionic state, solve the resultant equation by the method of perturbations caused by a single state.[28] The secular equation for the ionic states alone is then

$$2|W_1|\exp(2\pi if/6)\ b(\lambda+1)+2|W_1|\exp(-2\pi if/6)\ b(\lambda-1)=|W_1|\epsilon\, b(\lambda), \quad (15)$$

where $b(\lambda)$ is the coefficient of ϕ_0^λ in the wave function which diagonalizes the ionic part of the energy matrix; ϵ is the energy in units of $|W_1|$. Setting $b(\lambda)=a(\lambda)\exp(-2\pi if\lambda/6)$ we have

$$a(\lambda+1)+a(\lambda-1)=\tfrac{1}{2}\epsilon a(\lambda);\ a(6)=a(0)=0. \quad (15')$$

With the given boundary conditions the solutions are

$$a(\lambda)=(1/\sqrt{3})\sin(\pi s\lambda/6),\ s=1,\ 2,\ 3,\ 4,\ 5$$
$$\epsilon=4\cos(\pi s/6). \quad (16)$$

One now calculates the new matrix elements to the ground state by means of the transformation coefficients $b(\lambda)$, obtaining for the complete secular equation

$$\sum_s \frac{(8/3)[1-(-1)^s\cos 2\pi f]}{x-4\cos(\pi s/6)}-x=q;$$
$$q=J_0/|W_1|, \quad (17)$$

where x is the energy measured in units of $|W_1|$ from the mean energy of the ionic states as origin. Setting $f=0$ in (17) we obtain

$$(8/3)x/(x^2-12)+(16/3)/x-x=q, \quad (18)$$

which is the secular equation in the absence of the field. Let the solution of (17) be written in the form

$$x=x'+x''(2\pi f)^2,$$

where x' is the solution of (18) corresponding to the lowest state of this symmetry. Setting this back into (17) and expanding the whole equation in terms of $(2\pi f)$, we find from the coefficient of $(2\pi f)^2$

$$\Delta\chi=-\frac{\tfrac{3}{2}(x'+q)-12x'(x'^2-4)^{-1}}{3+8(x'^2+12)(x'^2-12)^{-2}+16x'^{-2}}\times|W_1|\left(\frac{2\pi eS}{hc}\right)^2. \quad (19)$$

The corresponding formula, using the H-L ap-

TABLE II. *Values of resonance integral $|W_1|$ necessary to give correct anisotropy for various amounts of Coulomb energy J_0.*

J_0	$\lvert W_1\rvert$	q
0.0 ev	4.4 ev	0.0
2.2	4.5	0.5
3.4	4.6	0.75
4.75	4.75	1.0
6.2	5.0	1.25
8.0	5.3	1.5
9.9	5.7	1.75
12.2	6.1	2.0
18.8	7.5	2.5
30.5	10.2	3.0

[26] F. Bloch, Zeits. f. Physik **61**, 206 (1930). Applied to benzene by E. Hueckel, Zeits. f. Physik **70**, 204 (1931).

[27] That is, negative ion on m, positive at $m+\lambda$.

[28] E. U. Condon and G. Shortley, *Theory of Atomic Spectra* (Cambridge, 1935), p. 37; L. Brillouin, J. de phys. et rad. **3**, 379 (1932).

proximation with perturbation theory is,

$$\Delta\chi = -128\,|W_1|^6 J_0^{-5}(2\pi eS/hc)^2. \quad (20)$$

Values of x', q, and $\Delta\chi$ for both exact and perturbation theory are shown in Table I. As we should expect, formula (20) becomes identical with London's result for $q=0$, i.e., Coulomb energy neglected. In the neighborhood of $q=0$, $\Delta\chi$ falls off as $-q^2$, and for large values of q as q^{-5}. Perturbation theory is a poor approximation over the range of values of q which would probably obtain in practice. If for $q=0$, we take $W_1=-4.4$ ev, the value found by London,[5] then as q increases it is necessary to assume larger values of $|W_1|$ in order to obtain the same value for the anisotropy. In Table II are shown values of $|W_1|$ and J_0 which must be assumed to give the same susceptibility as for $q=0$. It is evident that for $q>2.5$, $|W_1|$ and J_0 must be unreasonably large.

For the case of spin zero the results are probably qualitatively similar to the above. A more direct comparison may be obtained as follows. We can apply a perturbation procedure starting from the molecular orbital approximation, and treating the Coulomb energy as a perturbation between different configurations of molecular orbitals. The susceptibility is unaffected in the first approximation, and in the second falls off as $-q^2$. The coefficient of q^2 can be found by application of second-order perturbation theory. The correction to the susceptibility arises entirely from the change in spacing of the energy levels, and consequently of the frequency denominators, owing to the presence of the field. On the other hand, one finds by examination of Eq. (19) that the susceptibility is remarkably well represented by a cosine function

$$\Delta\chi = -(1/9)\,|W_1|\cos(0.383q)\ (2\pi eS/hc)^2 \quad (21)$$

up to about $q=3.0$. By expanding the cosine in powers of q one may compare the coefficient of q in the argument of the cosine with that obtained by perturbation theory, and the two agree within 17 percent. It may be assumed that an analogous situation obtains with the solution for $S=0$. By perturbation theory, starting from the molecular orbital approximation we find

$$\Delta\chi_{\text{benz}} = -(2/9-0.0058q^2)\,|W_1|\,(2\pi eS/hc)^2. \quad (22)$$

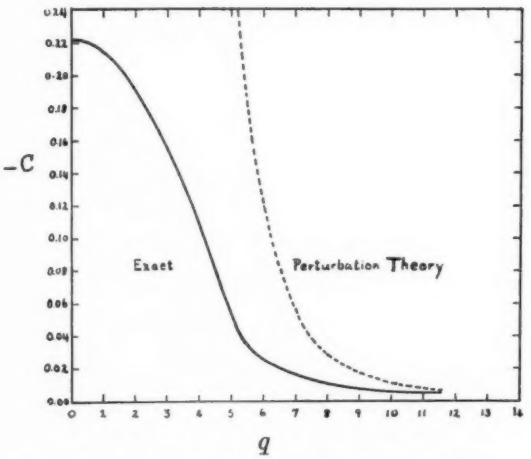

FIG. 1. Comparison of perturbation theory and approximated rigorous theory for spin 0 as explained in text. Shows coefficient C of $W_1(2\pi eS/hc)^2$ in Eq. (7) for various values of $q=J_0/W_1$, ratio of Coulomb to hopping energy.

Assuming $\Delta\chi=-(2/9)\,|W_1|\cos aq\ (2\pi eS/hc)^2$, then for very small q the cosine can be expanded, and comparing the two results we have

$$(2/9)(1-\tfrac{1}{2}a^2q^2)=2/9-0.0058q^2.$$

In this way one finds $a=0.228$. If this value is increased by 17 percent in analogy with the solution for $S=2$, one deduces finally:

$$\Delta\chi_{\text{benz}} = -(2/9)\,|W_1|\cos(0.266q)\ (2\pi eS/hc)^2, \quad (23)$$

which is probably valid down to $q=4$ or $q=5$, since the rate of falling off is somewhat less than in the case of spin 2.

The trend of the anisotropy as a function of the Coulomb ratio q is represented in Fig. 1. For values of q up to about 4.5, the curve is approximated by formula (23). The remainder of the curve, where the cosine representation breaks down, was determined in the following way. The secular problem for spin zero was set up and all but singly ionized configurations omitted. The resulting secular equation could be solved rigorously by a procedure almost identical with that used in deducing Eq. (19). The formula for the anisotropy thus obtained was multiplied by a numerical factor in order to make it agree asymptotically with the original H-L perturbation theory formula (8) with $C=-983$, the value obtained with the exact expression for the ground state. The resulting curve was found to join in

very nicely with the cosine function at about $q=5$.[29]

We have taken 15 ev as an upper limit on J_0, which is a rough estimate of the energy of formation of a negative carbon ion in the benzene ring.[30] With this estimate and Lonsdale's experimental value of $\Delta\chi_{benz}$ substituted into Eq. (23), we may solve for q, obtaining $q=2.4$, whence we find

$$|W_1|=6.25 \text{ ev},$$

which is not unreasonable. In one respect these results are encouraging in that they indicate that the departure from London's[5] approximation is not serious even for comparatively large values of the Coulomb interaction. On the other hand, they suggest that any effort to explain the anisotropy and still retain the essential features of the H-L approximation is almost certainly foredoomed to failure.

As an illustration of this we return to the spin 2 example and consider the wave functions for the case $q=1.86$, which corresponds to about the same degree of reduction of the anisotropy as $q=2.4$ in the spin 0 case. We find that the wave function is 40 percent non-ionic and 60 percent ionic. In the H-L theory it would, of course, be 100 percent non-ionic, whereas in the molecular orbital approximation it would be 17 percent non-ionic and 83 percent ionic. Thus, in order to explain the anisotropy we must assume that the double bonds are about equally of ionic and covalent character, corresponding much more closely to the molecular orbital theory.

Nonorthogonality

There still remains to be investigated the possibility that the nonorthogonality of the atomic wave functions rather than the perturbation due to ionic states can be used to account for the large magnetic anisotropy even with the H-L model. Although, as we have shown, the simple exchange integrals are nearly independent of the magnetic field, this is not true of integrals arising from higher order permutations, such as may occur if the atomic wave functions are not strictly orthogonal. In fact the departure from orthogonality may be very considerable. Goeppert-Mayer and Sklar[30] give a value of $\frac{1}{4}$ for the overlap of adjacent wave functions, and if one were to follow the more correct procedure in assuming screened ionic fields instead of Coulomb fields in setting up the atomic functions, probably the overlap would be appreciably larger.[31] The only higher order exchange integrals which are left with a phase factor are those arising from permutations which contain as factors one or more cycles of order three or greater. Actually the only permutations which make an appreciable contribution are the simple cycles (123), (1234), (123456) and their equivalents with respect to the symmetry of the benzene ring. It is readily verified that such integrals have the phase factors $\exp(2\pi if/6)$, $\exp(6\pi if/6)$, $\exp(2\pi if)$, respectively. We have obtained numerical values for the permutation integrals[32] in terms of the one- and two-electron integrals evaluated by Sklar and Lyddane.[33] It is also a simple matter to find the mean value of the corresponding permutations with respect to the ground state. In this way one obtains finally

$$\Delta\chi_{benz}=0.0066\,(2\pi eS/hc)^2. \qquad (24)$$

The numerical coefficient is to be compared with the experimental value of -1.0, and is wrong both in sign and in magnitude. Even with considerably larger values of the overlap, it is difficult to see how the anisotropy from this cause could be made more than a few percent of the observed.

It may seem at first surprising that the diamagnetic current arising from nonorthogonality should be so small, when it is well known that the nonorthogonality has a far from negligible effect in most molecular calculations.[10] The explanation lies in the fact that the largest higher-order permutation integrals, which are also the most numerous, are those corresponding to per-

[29] The reason that this solution cannot be used all the way to $q=0$ is that it does not have the proper behavior for small q, that is, it does not approach the molecular orbital solution parabolically.

[30] Estimated from calculations by M. Goeppert-Mayer and A. L. Sklar, J. Chem. Phys. **6**, 645 (1938). The lowest ionic level is given as 8 volts above ground, but probably the average of all singly ionized levels is considerably higher.

[31] J. Bardeen and J. H. Van Vleck, Proc. Nat. Acad. **25**, 82 (1939); L. Brillouin, J. de phys. et rad. **4**, 334 (1933).

[32] Actually what is evaluated is not simply the permutation integral H_P, but the expression $(H_P-W\Delta_P)$, where W is the mean energy of the ground states.

[33] A. L. Sklar and R. H. Lyddane, J. Chem. Phys. **7**, 374 (1939).

mutations which are factorable into simple transpositions.[34] Permutation integrals of this type, however, have no phase factor depending on the magnetic field for the same reason that the simple exchange integrals are independent of the field.

It remains to discuss how the nonorthogonality of the atomic functions will influence the other calculations of this paper. Evidently it is much more serious in its effects when ionic terms are included in the calculation, since the nonorthogonality integral between different configurations may contain the atomic overlap only to the first power, whereas the nonorthogonality between different functions of the same configuration always contains the atomic overlap at least squared. The principal effect of the nonorthogonality, however, may be taken care of by setting the energy parameter W in the off-diagonal elements of the secular equation equal to W_0, the mean energy of the non-ionic configuration. The quantity $W_1-\delta W_0$ then enters all the equations formally exactly like W_1, and none of the conclusions are changed if W_1 is evaluated empirically. Provided only interactions between nearest neighbors are considered, it is possible to carry out an exact solution of the secular problem leading to Eq. (19), including nonorthogonality. The result is:

$$\Delta\chi=\frac{2(W_1-\delta W_0)}{1+\delta y'+\delta\beta' D^{-1}}\quad\frac{y''}{1+\delta(y'+\beta')}\left(\frac{2\pi eS}{hc}\right)^2 \tag{25a}$$

with

$$D=1+(8/3)(y'^2+12)(y'^2-12)^{-2}+(16/3)y'^{-2}, \tag{25b}$$

$$2y''D=\tfrac{1}{2}(y'+\beta')-4y'(y'^2-4)^{-1}, \tag{25c}$$

$$\beta'=\frac{1+\delta y'}{W_1-\delta(W_0+J_0)}J_0. \tag{25d}$$

Here W_0 is the mean energy of the non-ionic configuration. The values of y' and β' can be lifted directly from Table I, where y' is equivalent to x' and β' is equivalent to q. For sufficiently large values of β' it is seen that y' approaches $-\beta'$ and hence β' approaches $J_0/(W_1-W_0)$. Thus β' approaches q, and so for sufficiently large values of q Eq. (25a) becomes identical with Eq. (19). This means that the H-L perturbation theory is not affected by the nonorthogonality provided we stop with the lowest order which gives rise to anisotropy. On the other hand, when $J_0=0$, i.e., molecular orbital viewpoint adopted, an assumed overlap of $\frac{1}{4}$ reduces the calculated value of the anisotropy by $\frac{1}{4}$, owing to the renormalization of the wave functions. In the case of spin zero, however, a similar calculation shows that the formula for the anisotropy is practically unaffected by the nonorthogonality, due to cancellation of various terms. Thus we may assume that even with a considerable overlap of the atomic functions, the curve of Fig. 1 is still a good representation of the anisotropy formula for all values of q.

[34] J. H. Van Vleck, Phys. Rev. **49**, 232 (1936).

Discussion

The discussion of diamagnetic anisotropy provides a much more exacting test of the approximations used in calculating molecular wave functions than the calculation of resonance and binding energies, since the degree of the anisotropy is very sensitive to the exact form of wave function used. The calculations in this paper, therefore, may be taken as fairly certain indication of the superiority of the Hund-Mulliken type of approximation over the Heitler-London type for aromatic and probably other unsaturated molecules. This means that in order to account for the anisotropy we must assume that the resonating double bond has a partial ionic character, which is nearly as important as its covalent character. This conclusion is in opposition to what is usually believed about the two approximations. On the other hand, in the case of aromatic molecules we have reason to suspect that the Hund-Mulliken model would be better than for most molecules, since we are dealing with $2p\pi$ wave functions whose nodes lie in the plane of the ring, so that the charge cloud tends to stay away from between the nuclei and hence is considerably more mobile than it would be in other molecules.

It is true that the present method of including the ionic terms is very crude in that it assumes all the "hopping" integrals to be the same, which is actually far from the case. On the other hand, it does appear that any other assumption would be even less favorable for explaining a large mag-

netic anisotropy, so that in adopting a standard W_1 we have allowed the H-L model to put its best foot forward, so to speak. Attempts at calculating the anisotropy with explicitly evaluated "hopping" integrals result in far too small values, though naturally not much reliance can be put in the hopping integrals so calculated. One may conclude, perhaps, that neither approximation is very satisfactory for describing the magnetic properties of the molecules. The situation is somewhat analogous to that which obtains in atomic theory, where we find that wave functions which give very satisfactory values for the energy levels are useless for calculating the diamagnetism, since the wave functions do not possess the minimizing property with respect to the diamagnetism. A really satisfactory account of the magnetic anisotropy of large molecules must await the development of approximation methods which are far more accurate than those at present available.

In conclusion it is a pleasure to acknowledge my indebtedness to Professor Van Vleck for suggesting this problem and for many valuable discussions, and also to Professor F. London of Duke University for helpful correspondence.

DECEMBER, 1940 JOURNAL OF CHEMICAL PHYSICS VOLUME 8

Separation by Thermal Diffusion of Mixtures of Gases Having the Same Molecular Weight*

F. T. WALL AND C. E. HOLLEY, JR.
Noyes Chemical Laboratory, University of Illinois, Urbana, Illinois

(Received September 16, 1940)

Separations by means of thermal diffusion of mixtures of gases having the same molecular weight have been investigated experimentally and theoretically. Six pairs of gases were considered, namely: $CO_2-C_3H_8$, CO_2-N_2O, $N_2O-C_3H_8$, $CO-C_2H_4$, $CO-N_2$, and $N_2-C_2H_4$. The experiments were carried out in a thermal diffusion column 274 cm long. Assuming the molecules to behave as rigid elastic spheres, theoretical calculations were made for the various combinations and the results compared with the experiments. Except for the pair CO_2-N_2O, the theory and experiment agree as to order of magnitude and direction of separation.

WHEN a mixture of gases is introduced into an apparatus for which the temperature is not uniform, it is found that the composition of the gases will vary in the different parts of the apparatus. This effect which results from thermal diffusion was predicted theoretically by Enskog[1] in 1911 and by Chapman[2] in 1917. The effect was also verified experimentally by Chapman and Dootson[3] and it was suggested by Chapman[4] that the method could be used for the separation of isotopes and of different gases having the same molecular weight.

It was not, however, until Clusius and Dickel[5] developed apparatus making the thermal diffusion cumulative that the method became useful for actual separations. Clusius and Dickel's apparatus (subsequently modified by Brewer and Bramley[6]) consisted essentially of a long vertical tube with a hot wire down the center. When a mixture of gases is introduced into such a system, it is found that, after a steady state is reached, the compositions at the top and bottom are different.

Most of the recent thermal diffusion work has been directed toward the separation of isotopes. Since isotopes or isotopic compounds differ only in their masses, the theory of thermal diffusion is considerably simplified for mixtures of that type. The theory can also be simplified in another

* A preliminary note on this subject by the same authors appeared earlier; J. Chem. Phys. **8**, 348 (1940).
[1] Enskog, Physik. Zeits. **12**, 56, 533 (1911).
[2] Chapman, Phil. Trans. **A217**, 115 (1917).
[3] Chapman and Dootson, Phil. Mag. **33**, 248 (1917).
[4] Chapman, Phil. Mag. **34**, 146 (1917); **38**, 182 (1919).
[5] Clusius and Dickel, Naturwiss. **26**, 546 (1938); **27**, 148, 487 (1939); Zeits. f. physik. Chemie **44**, 397, 473 (1939).
[6] Brewer and Bramley, J. Chem. Phys. **7**, 553, 972 (1939); Science **90**, 165 (1939).

manner; namely, by eliminating the mass effect and considering pairs of chemically different gases of the same molecular weight. This suggests that it would be desirable to investigate experimentally the separation by thermal diffusion of different gases of the same molecular weight in order to provide a further check on the theory. In this paper there will be reported the results of such experimental studies, and those results will be compared with the theory.

Theoretical

In discussing the phenomenon of thermal diffusion, it is convenient to consider a quantity k_T defined as the quotient D_T/D_{12}, where D_T is the coefficient of thermal diffusion and D_{12} is the coefficient of ordinary diffusion for a mixture of the two gases. According to Enskog's and Chapman's theory, the first approximation to k_T is given by[7]

$$k_T=\frac{-5(C-1)x_1x_2(s_1x_1-s_2x_2)}{Q_1x_1^2+Q_{12}x_1x_2+Q_2x_2^2}, \tag{1}$$

where x_1 and x_2 are the mole fractions of gases 1 and 2, and where C, s_1, s_2, Q_1, Q_{12} and Q_2 depend upon the nature of the molecules. In case the molecules have the same mass and, in addition, behave as rigid elastic spheres, these quantities take on relatively simple forms, *viz.:*

$$\begin{aligned}
C&=\tfrac{6}{5},\\
s_1&=\tfrac{2}{5}\{(\sigma_1/\sigma_{12})^2-1\},\\
s_2&=\tfrac{2}{5}\{(\sigma_2/\sigma_{12})^2-1\},\\
Q_1&=5\tfrac{9}{25}(\sigma_1/\sigma_{12})^2,\\
Q_{12}&=8\tfrac{6}{25}+3\tfrac{2}{25}(\sigma_1\sigma_2/\sigma_{12}^2)^2,\\
Q_2&=5\tfrac{9}{25}(\sigma_2/\sigma_{12})^2.
\end{aligned} \tag{2}$$

In these expressions, σ_1 and σ_2 are the diameters of the molecules and

$$\sigma_{12}=(\sigma_1+\sigma_2)/2. \tag{3}$$

The diameters σ_1 and σ_2 are related to the viscosities η_1 and η_2 by means of equations of the type

$$\eta_1=\frac{5}{16\sigma_1^2}\left(\frac{kTm_1}{\pi}\right)^{\frac{1}{2}}, \tag{4}$$

m_1 being the mass of a molecule.

If we further define a quantity ϵ as follows,

$$\epsilon=(\sigma_1-\sigma_2)/(\sigma_1+\sigma_2), \tag{5}$$

then

$$\begin{aligned}
s_1&=\tfrac{2}{5}(2\epsilon+\epsilon^2),\\
s_2&=\tfrac{2}{5}(-2\epsilon+\epsilon^2),\\
Q_1&=5\tfrac{9}{25}(1+\epsilon)^2,\\
Q_{12}&=8\tfrac{6}{25}+3\tfrac{2}{25}(1-\epsilon^2)^2,\\
Q_2&=5\tfrac{9}{25}(1-\epsilon)^2.
\end{aligned} \tag{6}$$

Substitution of Eqs. (6) into Eq. (1) will give

$$k_T=\frac{-10x_1x_2[2\epsilon+(x_1-x_2)\epsilon^2]}{59+118(x_1-x_2)\epsilon+(59-182x_1x_2)\epsilon^2+32x_1x_2\epsilon^4}. \tag{7}$$

For rigid elastic spheres, k_T is independent of the temperature, but it is clear from (7) that it depends greatly on the composition. If ϵ is small, however, k_T/x_1x_2 will be nearly independent of the composition, so, following Furry, Jones and Onsager[8] we introduce another quantity α where

$$\alpha=k_T/x_1x_2. \tag{8}$$

Then

$$\alpha=\frac{-20\epsilon-10\epsilon^2(x_1-x_2)}{59+118(x_1-x_2)\epsilon+(59-182x_1x_2)\epsilon^2+32x_1x_2\epsilon^4} \tag{9}$$

which for small values of ϵ gives

$$\alpha=-20\epsilon/59. \tag{10}$$

Since

$$\epsilon=(\sigma_1-\sigma_2)/(\sigma_1+\sigma_2) \tag{5}$$

it follows from (4) that

$$\epsilon=(\sqrt{\eta_2}-\sqrt{\eta_1})/(\sqrt{\eta_2}+\sqrt{\eta_1}). \tag{11}$$

Thus from a knowledge of the viscosities of a

[7] The fundamental equations which appear here were taken from Chapman and Cowling, *The Mathematical Theory of Non-Uniform Gases* (Cambridge, 1939), where the results of the theory are conveniently summarized.

[8] Furry, Jones and Onsager, Phys. Rev. **55**, 1083 (1939).

pair of gases one can calculate α for the pair by means of Eq. (9).

If one desires the actual coefficient of thermal diffusion D_T instead of k_T or α, it is necessary to multiply k_T by D_{12}. According to Enskog's and Chapman's theory, the first approximation to D_{12} for rigid, elastic spherical molecules of equal mass is

$$D_{12}=6(1-\epsilon^2)(\eta_1\eta_2)^{\frac{1}{2}}/5\rho, \tag{12}$$

where ρ is the density and the other quantities are as previously defined. It is seen that D_{12} depends upon the temperature, so that D_T will depend upon both the temperature and composition.

To compare theoretical values of α, k_T or D_T (calculated from viscosity data) with experimental measurements obtained by the use of a thermal diffusion column, it is necessary to bring in the theory of such a column. The column will be assumed to consist of two vertical concentric cylinders, the inner one heated to a temperature T_2 and the outer one cooled to a temperature T_1. The thickness of the annular space will be denoted by $2w$ and the length of the column by $2l$. According to Furry, Jones and Onsager,[8] α is related to measurable quantities as follows:

$$\alpha=\frac{4A\rho gw^4}{63\eta D_{12}f(\Delta T/T)}. \tag{13}$$

In this equation g is the acceleration of gravity and ρ, η and D_{12} are previously defined quantities evaluated for the mixture at the average temperature, $T=(T_1+T_2)/2$. Taking $\Delta T=T_2-T_1$, then $f(\Delta T/T)$ is a function depending upon the nature of the interactions between the molecules. It so happens that $f(\Delta T/T)$ does not deviate greatly from unity as long as $\Delta T/T$ is small, so it will be omitted from (13) when that equation is used for numerical calculations.

The only remaining quantity A can be determined from the equilibrium separation factor which is

$$\frac{x_1(+l)x_2(-l)}{x_2(+l)x_1(-l)}=e^{4Al}, \tag{14}$$

where x_1 and x_2 are the equilibrium mole fractions, $+l$ denoting the top of the column and $-l$ the bottom. The value of A obtained from (14) would have to be modified somewhat before introducing it into (13) if the remixing in the column due to longitudinal diffusion were not small compared to the remixing due to convection,[8] but, for the applications here considered, it turns out that such a modification is unnecessary.

In case one desires D_T instead of α from the experimental measurements, one needs only use the relation

$$\begin{aligned} D_T&=x_1x_2\alpha D_{12}\\ &=4x_1x_2A\rho gw^4/63\eta, \end{aligned} \tag{15}$$

from which $f(\Delta T/T)$ has been omitted for the reason mentioned previously. It will be observed that a knowledge of the coefficient of ordinary diffusion D_{12} is unnecessary when calculating D_T from the results of thermal diffusion in a column.

Experimental

The thermal diffusion column was made of three concentric brass tubes 274 cm long. The inner tube was heated by means of No. 22 Chromel wire and the outer jacket cooled by means of tap water. The intermediate chamber of the column into which the gas mixtures were introduced had an inner radius of 1.0 cm and an outer radius of 1.76 cm. A thermocouple was fitted closely to the hot side of the diffusion space in order to determine the temperature of the hot side during the experiments. The cold side temperature was measured by means of thermometers in the inlet and outlet water of the outer jacket. Since the flow of water was rapid, little increase in temperature was observed, so a mean of the two readings was taken as the temperature of the cold side.

The gas mixtures investigated were introduced into the previously evacuated inner chamber through suitable inlet tubes. It was found by trial that thirty minutes was ample time for steady states to be reached from fresh mixtures in the column. After a steady state had been attained, several 20-ml samples were removed alternately from the bottom and top at fifteen-minute intervals. Since the samples were small compared to the total amount of gas present,

TABLE I.

Combination	Composition in Mole Percent Before Diffusion	After Diffusion Top	Bottom	Difference ±0.4
1. CO_2 and C_3H_8	34.4% CO_2	36.5	33.6	2.9
	53.6	55.9	52.9	3.0
	69.1	70.2	67.9	2.3
2. CO_2 and N_2O	36.1% CO_2	37.1	35.2	1.9
	42.5	43.3	41.4	1.9
	54.5	55.0	53.4	1.6
	70.1	70.4	69.0	1.4
3. N_2O and C_3H_8	33.9% N_2O	34.9	33.7	1.2
	48.0	48.2	46.7	1.5
	66.5	67.4	65.5	1.9
4. CO and C_2H_4	33.8% CO	35.5	29.7	5.8
	46.7	48.8	41.4	7.4
	58.8	61.2	55.1	6.1
	73.4	77.2	72.8	4.4
5. CO and N_2	26.8% CO	26.7	26.8	−0.1
	38.0	37.6	37.9	−0.3
6. N_2 and C_2H_4	34.8% N_2	38.2	31.6	6.6
	48.3	53.0	45.1	7.9
	69.3	72.8	66.1	6.7

their analyses could be averaged and referred to the original mixture without appreciable error.

The gas mixtures were made up of compounds having molecular weights of 28 or 44, to the nearest whole mass unit. Three gases of each molecular weight were mixed in pairs; nitrogen, carbon monoxide and ethylene ($M=28$), and nitrous oxide, carbon dioxide and propane ($M=44$).

For all mixtures introduced into the column, analyses were carried out both before and after thermal diffusion. Except for the mixtures of nitrous oxide and propane, the analyses were carried out by means of absorption pipettes using the common reagents prescribed in gas analysis procedures. Since no suitable absorbing agents could be found for either nitrous oxide or propane, their mixtures were analyzed by means of a Zeiss portable interferometer of the Rayleigh type. Pure propane was introduced into one gas chamber of the interferometer and various known mixtures into the other side. Dial readings corresponding to matching of the interference lines were then plotted against composition; the graph thus obtained was used for analysis purposes.

The results of the experimental studies are summarized in Table I. In each case the temperature on the hot side was about 235°C and that on the cold side near 21°C. The total gas pressures were about 800 mm Hg. The percentage compositions after thermal diffusion are the averages of at least four measurements. By least-squares methods the probable errors in the concentrations are found to be about ±0.4 percent.

DISCUSSION

It will be observed from the results in Table I that the separations are quite substantial except in the case of nitrogen and carbon monoxide. These separations cannot be attributed to the very small mass differences which exist, but must be associated with differences in structure. To check this hypothesis we have calculated values of α and D_T by means of the equations previously set forth.

For making the theoretical calculations, Eqs. (9) and (12) were used. ϵ was evaluated by taking viscosities at the mean temperature, 401°K. Although ϵ would be independent of the temperature for the model assumed (rigid elastic spheres), it will have a slight dependence on temperature if Sutherland's[9] formula for viscosity is employed. Values of the viscosity coefficients were obtained from the *International Critical Tables*, from tables in Chapman and Cowling's book[8] and in the case of propane from the results of Trautz and Kurz.[10] The viscosities used in the calculations together with values of ϵ are given in Table II.

For the determination of α and D_T from experimental data, recourse was made to Eqs. (13) and (15). Unfortunately, experimental values of D_{12} were found in the *International Critical Tables* only for the pairs $CO-N_2$, $CO-C_2H_4$, and CO_2-N_2O. Accordingly, experimental values of α were calculated only for those combinations. D_T was computed for all combinations, however, since a knowledge of D_{12} is not necessary for that calculation.

TABLE II.

A. Viscosities at 401°K Gas	$\eta\times10^6$ poises	B. ϵ at 401°K Gas Pair	ϵ
CO_2	195.7	$CO_2-C_3H_8$	−0.149
N_2O	194.2	CO_2-N_2O	−0.00192
C_3H_8	107.2	$N_2O-C_3H_8$	−0.147
CO	221.9	$CO-C_2H_4$	−0.124
N_2	221.5	$CO-N_2$	−0.00045
C_2H_4	134.6	$N_2-C_2H_4$	−0.124

[9] Sutherland, Phil. Mag. **36**, 507 (1893); **17**, 320 (1909).
[10] Trautz and Kurz, Ann. d. Physik **9**, 981 (1931).

Comparisons of the experimental and theoretical values of α and D_T appear in Table III. In each case x_1 refers to the mole fraction of the first named compound of the mixture.

TABLE III

Except for orders of magnitude, the theoretical and experimental values summarized in Table III do not agree very well. The differences can be attributed mainly to the approximations involved in the derivations of the equations used. In all cases save that of CO_2-N_2O, the theoretical values of α and D_T are larger than the experimental values. This would be expected because the rigid elastic sphere model which was assumed would give rise to a larger separation than other models. Theoretically CO and N_2 have very small values of α and D_T, which is in agreement with the fact that no separation was observed within the experimental error. Moreover, the separations which were observed all took place in the right direction; that is, the large molecules went to the bottom of the column and the small ones to the top in accordance with the theory.

Of the six combinations here considered, only the results for CO_2-N_2O are badly out of line in that the observed separations are much greater than would be predicted. The fact that the viscosities of N_2O and CO_2 are so near each other means that small errors in those viscosities could have a large effect on ϵ. It might be supposed that a large temperature coefficient of ϵ is responsible for the discrepancy, but the work of Trautz and Kurz[10] shows that N_2O and CO_2 have nearly equal viscosities over a wide range of temperatures. Accordingly, the deviations cannot be attributed entirely to errors in viscosities. The experimental measurements can be off, or some factor not considered in the theory might be responsible.

TABLE III.

	A. $CO_2-C_3H_8$			
x_1	0.344	0.536	0.691	
D_T (exp.)	0.00074	0.00069	0.00048	
D_T (theor.)	0.0013	0.0015	0.0014	
	B. CO_2-N_2O			
x_1	0.361	0.425	0.545	0.701
α (exp.)	0.0071	0.0067	0.0056	0.0057
α (theor.)	0.00065	0.00065	0.00065	0.00065
D_T (exp.)	0.00033	0.00033	0.00027	0.00024
D_T (theor.)	0.000025	0.000026	0.000027	0.000023
	C. $N_2O-C_3H_8$			
x_1	0.339	0.480	0.665	
D_T (exp.)	0.00031	0.00036	0.00041	
D_T (theor.)	0.0013	0.0015	0.0014	
	D. $CO-C_2H_4$			
x_1	0.338	0.467	0.588	0.734
α (exp.)	0.016	0.017	0.014	0.012
α (theor.)	0.040	0.042	0.043	0.046
D_T (exp.)	0.00080	0.00094	0.00072	0.00051
D_T (theor.)	0.0020	0.0024	0.0024	0.0021
	E. $CO-N_2$			
x_1	0.268	0.380		
α (exp.)	0	0		
α (theor.)	0.00015	0.00015		
D_T (exp.)	0	0		
D_T (theor.)	0.0000089	0.000011		
	F. $N_2-C_2H_4$			
x_1	0.348	0.483	0.693	
D_T (exp.)	0.00089	0.00099	0.00076	
D_T (theor.)	0.0021	0.0024	0.0022	

The authors are indebted to Professor H. M. Mott-Smith of the Physics Department of the University of Illinois for helpful discussions and suggestions in connection with the theory. They are also indebted to Dr. M. J. Copley, now at the Eastern Regional Research Laboratory, with whom the early part of the work was carried out, and to Professor W. H. Rodebush for his encouragement and suggestions.

The Thermodynamics of Films: Energy and Entropy of Extension and Spreading of Insoluble Monolayers

WILLIAM D. HARKINS, T. FRASER YOUNG AND EDWARD BOYD
George Herbert Jones Chemical Laboratory, University of Chicago, Chicago, Illinois

(Received April 3, 1940)

The thermodynamic relations of insoluble monolayers on a mobile subphase are given, and equations are presented for their (a) increase of entropy, (b) heat absorbed, (c) increase of heat content, and (d) increase of internal energy, during expansion. Two different methods of expansion are considered: in *spreading* the decrease of area of the subphase is equal to the increase of area of the monolayer; in *extension* the monolayer expands but the area of the clean surface of the subphase remains constant. The two-dimensional phases are classified as: I. gas; II. liquid (L_1) expanded; III. intermediate or transition; IV. liquid (L_2) condensed; and V. solid. The extreme limits of molecular area for the intermediate liquid phase are for pentadecylic acid about 22 and 44A², while those for the liquid phases IV, III, and II, are from about 20.5 to 52A² which indicates that, beginning with a two-dimensional liquid in its most condensed condition, the mean molecular distances may be increased by as much as 60 percent without a destruction of the liquid state. This is very different from what is found in three dimensions. The heat absorbed in the melting of the two-dimensional solid is zero, so this is phase change of the second order. The quantity, $h_s=(\partial H_s/\partial\sigma)_{p,T}$, which is the increase in heat content when the monolayer spreads over unit area, has a value of several hundred ergs cm^{-2} for a solid film. The increase of heat content for the other two-dimensional phases may be illustrated by the approximate values for pentadecylic acid: it is zero for (L_2), or the liquid condensed phase; rises in the intermediate phase very gradually to a nearly constant magnitude of 300 ergs cm^{-2} as the area is increased and decreases to about 50 erg cm^{-2} in the liquid expanded phase (L_1). For any two-dimensional phase spread on water or on mercury the value of h for extension is greater than that for spreading by h_s the total surface energy of the three-dimensional liquid, which is about 116 erg cm^{-2} for water, and 540 for mercury. The increase of heat content ΔH_m during the spreading of a mole of pentadecylic acid has been calculated for the case in which the film spreads from the lowest to the highest area at which the phase exists. For the solid phase this energy is of the order of about a fifth of a kcal. mole^{-1} at 18°C, while ΔH_m for the intermediate phase is 8.3 kcal. mole^{-1}, and for the liquid expanded (L_2) phase is very small. At 25°C the value for the intermediate phase has fallen to 4.6, and that for the liquid expanded phase (L_2) has increased to 1.0 kcal. mole^{-1}.

1. INTRODUCTION

A RECENT paper from this laboratory[1] gives values for the energy of transformation of certain three-dimensional solids into monolayers on water but the general energy relations of the films themselves, except those for free energy alone, have been unknown. It is shown in the present paper that quite remarkable characteristics, associated with the expansion of such layers, appear when thermodynamic calculations are made from data which exhibit the variation of the film pressure π with the temperature at a constant area per molecule σ in the film.

The work of Harkins and Nutting shows that the latent heat of surface solution of crystals of myristic and pentadecylic acid depends very little upon the state in which the film exists, and very greatly upon the molecular area to which it spreads. The energies of extension and of spreading of monolayers are, in contrast, highly dependent upon the type of film involved, though the dependence on area does not disappear. It is necessary, therefore, to consider the types of phases which may exist, and the transformations between them.

As a specific example of a polar-nonpolar (amphipathic) substance we may choose pentadecylic acid, and, in order to avoid the effects of salt formation, due to the interaction of this acid and the metallic ions inevitably present in the water, suppose this to be spread on water at a pH of 2 or 3. At extremely high molecular areas the film is a perfect gas, which becomes imperfect as the area is decreased along an isothermal. At an area represented by some point A (Fig. 1) islands of a two-dimensional liquid begin to form, so an isothermal line between A and a point B represents a two-phase system. At 14.5°C the area[2] at A is 2350A², while at 22.5°C it is about 800A². In Fig. 1 the curves which

[1] W. D. Harkins and G. C. Nutting, J. Am. Chem. Soc. **61**, 1702 (1939).

[2] Adam and Jessop, Proc. Roy. Soc. **A112**, 362 (1926).

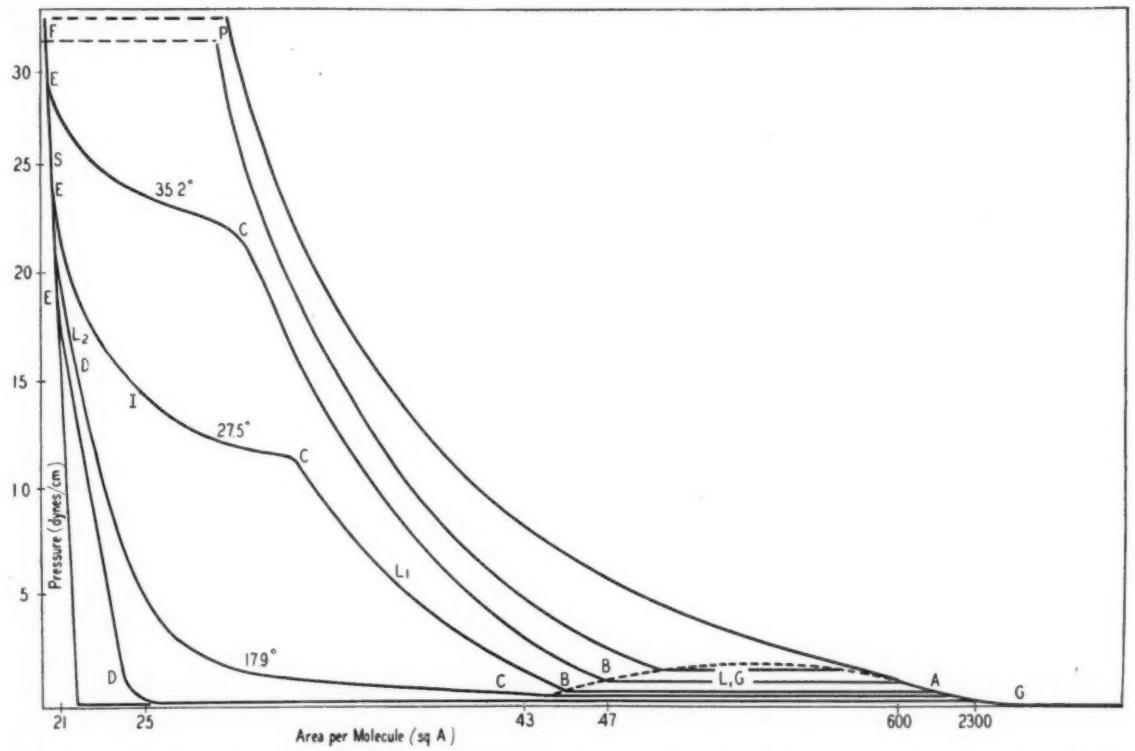

FIG. 1. Pressure-area diagram for two-dimensional phases. Phases: FE = solid; ED = liquid condensed (L_2); DC = intermediate; CB = liquid expanded (L_1); BA = heterogeneous, gas with islands of L_1 or region L_1G; G = gas. At areas below 43A² molecule^{-1} the curves give the relations for pentadecylic acid; at higher areas the pressures plotted are too high and the area axis is much compressed.

represent the pressure-area relations at areas below 43A² are those determined experimentally for pentadecylic acid, but above 43A² the diagram is very much compressed along the area axis, and considerably expanded in the direction of the pressure. The region L_1G below the dotted line represents the area in which mixtures of gaseous film with islands of the liquid L_1 may exist. The critical point is the highest point on the dotted curve. A point B which at 27.5° lies at 46A, represents complete condensation of the vapor to the liquid phase L_1, designated by Adam as "liquid expanded." If this isotherm is followed, the pressure π is found to rise rapidly as the area σ is decreased and the curve exhibits almost exactly the form of an equilateral hyperbola, until at C, where the molecular area is 32A² a phase transformation occurs to the *intermediate* film. The term by which this phase is designated signifies that on a π, σ diagram this phase is intermediate between C and the tactic which forms at D (see for example the isotherm at 17.9°). The change from liquid L_1, to intermediate phase resembles that for a first-order change, except (1) that the transition on either a π, σ or a π, T diagram is not entirely abrupt, and (2) as the area is decreased isothermally below that of the transition, the pressure does not remain constant, as in an ordinary first-order change, but rises very slowly, and then more and more rapidly until, without apparent discontinuity the curve becomes linear with a high negative slope, that is, the compressibility of the film is now small. Thus the *intermediate* or transition phase has a compressibility which is extremely great at areas just above those at C. It decreases at first very slowly, and then more and more rapidly until it becomes that of the region linear in π, σ, which at 27.5° is too short to be distinguished in Fig. 1. However, at 17.9° the transformation to the linear region (L_2) designated by Adam as "liquid condensed," occurs at D at an area of 22.6A² per molecule. The intermediate phase exhibits the character-

istics of a liquid, but its properties are very different from those of L_2. For example, there is considerable hysteresis with time in the former but not in the latter.

At E the liquid film solidifies by a transformation of the second order. This results in a large decrease in compressibility, and a large increase in the viscosity, which changes from Newtonian, that is, independent of the rate of shear, to non-Newtonian, and also obeys quite different laws otherwise. Thus the viscosity of the liquid condensed film L_2 follows the relation, $\log \eta = \log \eta_0 + k\pi$, an equation which is not true for the solid. The phases may be classified in their order along an isothermal as the molecular area is decreased:

PHASES AND ORDER OF CHANGE BETWEEN THEM

I. Gas, G.
First order
II. Liquid expanded, $L_1 = BC$
Diffuse first order (possibly second)
III. Intermediate (or transition), $I = CD$
Third order (possibly second)
IV. Liquid condensed, $L_2 = DE$
Second order
V. Solid, $S = EF$.

Since the existence of a third-order change is difficult to prove experimentally, the intermediate and liquid condensed films may be considered as subdivisions of a single phase, but, as will be seen later, the properties of the two are very different.

2. THERMODYNAMICS OF EXTENSION AND OF SPREADING OF A MONOLAYER

The maximum work (dW) done by a system when its area (σ) is increased or decreased is

$$dW = -\gamma d\sigma + pdv, \tag{1}$$

where γ is the surface tension. The zeta-function of Gibbs is defined by him as

$$F = E - ST + pv, \tag{2}$$

where the symbols are those of Lewis and Randall.

The Helmholtz free energy is defined as

$$A = E - ST, \tag{3}$$

so

$$F = A + pv. \tag{4}$$

If a process is reversible and isothermal, $T\Delta S = Q$ is the heat absorbed, and

$$dA = -dW,$$

$$dF = -dW + pdv + vdp. \tag{6}$$

From (1) and (6)

$$dF = \gamma d\sigma + vdp, \tag{7}$$

so if p is constant

$$(\partial F/\partial \sigma)_{p,T} = \gamma \tag{8}$$

and

$$(\partial F/\partial \sigma)_{p,T} d\sigma = \gamma d\sigma. \tag{9}$$

For a saturated surface $\gamma = f(p, T)$ only, so

$$\Delta F = \gamma \Delta \sigma. \tag{10}$$

The heat content (H) is defined by

$$H = E + pv \tag{11}$$

or

$$dH = dE + pdv + vdp, \tag{12}$$

and from 2

$$H = F + ST \tag{13}$$

or

$$dH = dF + TdS + SdT. \tag{14}$$

In the treatment which follows, energy values designated by small letters refer to the change of energy for unit area. Thus in

$$h = (\partial H/\partial \sigma)_T,$$

the h designates the increase of heat content of a film of very large area for unit increment of area.

Let us consider a trough filled with a body of water with a plane surface partly covered with a monolayer. The area of the film together with that of the subphase may be increased by one sq. cm by the use of some mechanical device while the area of the water surface is kept constant. Thus a ring of suitable dimensions, already lying in the surface, may be pulled upward until there is a unit increase of area of the film. If the film area is thus increased by $d\sigma_f$, instead of unity, the equation for the process which may be designated as *extension* (e), may be written

$$dF_e = (\partial F/\partial \sigma_f)_{T,\sigma_w} d\sigma_f = \gamma d\sigma_f \tag{15a}$$

or

$$\Delta F(\Delta\sigma = 1 \text{ cm}^2) = (\partial F/\partial \sigma_f)_{T,\sigma_w} = f_e, \tag{15b}$$

which gives the *free energy of extension* of the

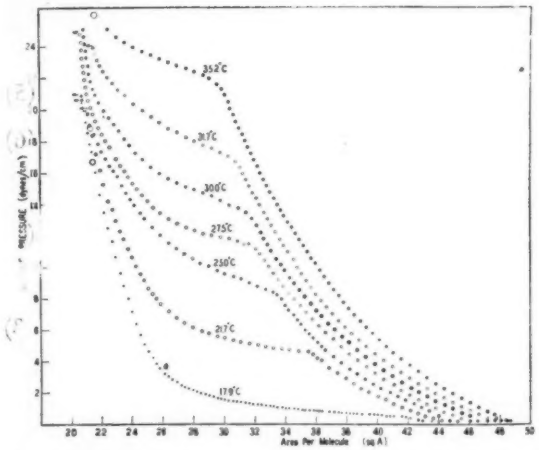

FIG. 2. Pressure-area diagram of pentadecylic (C_{15}) acid films.

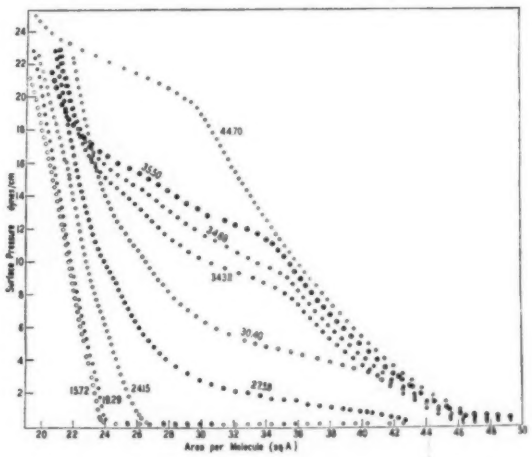

FIG. 3. Pressure-area diagram of palmitic (C_{16}) acid films. At low pressures the expansion of the film with increase of temperature is very small up to 19°, and very rapid from 24° to 28°. The films were compressed slowly in order to obtain accuracy at the lower pressures, but this makes the curves unreliable at pressures above about 13 dyne cm^{-1}, since in a part of this region the film is unstable with respect to the formation of a three-dimensional system (collapse).

film. The entropy of extension is

$$s_e=(\partial S/\partial\sigma_f)_{T,\sigma_w}=-(\partial\gamma_f/\partial T)\sigma_f. \quad (16)$$

The increment of heat content is given by

$$h_e=(\partial H/\partial\sigma_f)_{T,\sigma_w}=\left[\frac{\partial(\gamma_f/T)}{\partial(1/T)}\right]_{\sigma_f} \quad (17)$$

and the heat absorbed (q) by

$$q_e=T(\partial S/\partial\sigma_f)_{T,\sigma_w}=-T(\partial\gamma_f/\partial T)_{\sigma_f}=Ts_e. \quad (18)$$

Similar equations may be written for the energy of *spreading* of a film. This process (s) may be assumed to occur as follows: The surface of the water in the trough is separated into two parts by a movable barrier. On one side of the barrier the surface is covered by the film, on the other side the water surface is clean. Let the barrier be moved in such a way that the area of the film is increased by 1 sq. cm, and that of the water decreased by this amount.

The equations for *spreading* are:

$$dF_s=(\partial F/\partial\sigma_f)_{T,\Sigma}d\sigma_f-(\partial F/\partial\sigma_w)_{T,\Sigma}d\sigma_w$$
$$=-(\gamma_w-\gamma_f)d\sigma_f=-\pi d\sigma_f, \quad (19)$$

where $\Sigma=\sigma_w+\sigma_f$.

The increase of entropy which accompanies the spreading of the film over the water is from (16)

$$s_s=(\partial S/\partial\sigma_f)_{T,\Sigma}=-(\partial^2F/\partial T\partial\sigma_f)_\Sigma$$
$$=-(\partial\pi/\partial T)_{\sigma_f,\Sigma}. \quad (20a)$$

The heat absorbed is

$$q_s=Ts_s \quad (20b)$$

and the increase in heat content

$$h_s=(\partial H/\partial\sigma_f)_{T,\Sigma}=-\left[\frac{\partial(\pi/T)}{\partial(1/T)}\right]_{\sigma_f,\Sigma}. \quad (21)$$

Equations (15) to (18) which give the energy and entropy of *extension* for the films are also applicable to pure liquids.

Thus using Eq. (17) Harkins calculated the increase of the heat content when the surface area of water is increased, as $h=116$ ergs per cm^{-2} at 20°.

In Eq. (19) π is defined as

$$\pi=\gamma_w-\gamma_f, \quad (22a)$$

and it can be shown that in Eq. (16),

$$s_e=s_s-s_w \quad (22b)$$

and in Eq. (17),

$$h_e=h_s-h_w. \quad (22c)$$

} (22)

The energy changes of the greatest interest are those associated with the isothermal expansion (or compression) of a film between any molal area σ_1, and any other molal area σ_2. The heat content and heat absorbed may be calculated for either the spreading or the extension

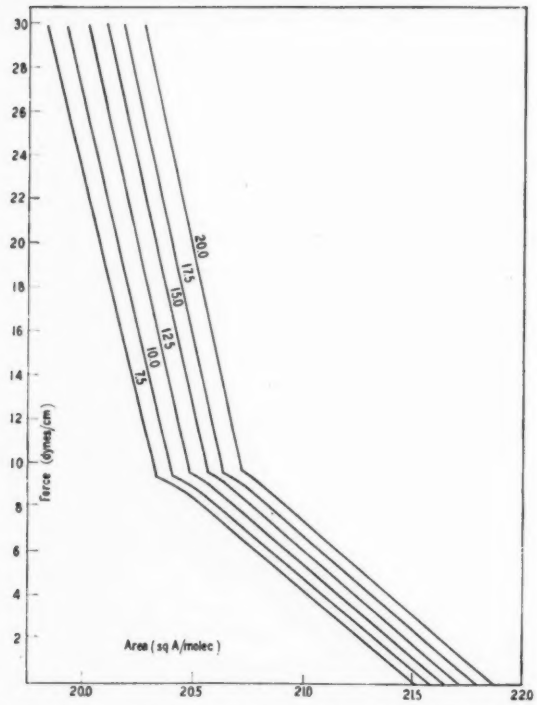

FIG. 4. Pressure-area diagram of hexadecyl (C_{16}) alcohol. Exhibits only the solid and liquid phases (with the vapor phase at low pressures) between 7.5 and 20°C. The values at 20°C were obtained by direct measurement, and at the other temperatures were calculated using the temperature coefficients.

of the film. For one mole of material the increase of heat content is

$$\Delta H_m = \int_{\sigma_1}^{\sigma_2} (\partial H/\partial\sigma)_T d\sigma_m = \int_{\sigma_1}^{\sigma_2} h d\sigma_m, \quad (23)$$

and the heat absorbed:

$$Q_m = T\int_{\sigma_1}^{\sigma_2} (\partial S/\partial\sigma)_T d\sigma_m = T\int_{\sigma_1}^{\sigma_2} s d\sigma_m, \quad (24)$$

where ΔH_m and h of Eq. (23) and Q_m and s of Eq. (24) stand for $(\Delta H_m)_e$, h_e, $(Q_m)_e$, and s_e when the process is one of extension, and for $(\Delta H_m)_s$, $(Q_m)_s$, and s_s when the process is one of spreading.

The heat absorbed may readily be calculated from ΔH and ΔF of any process. For *spreading:*

$$(Q_m)_s = (\Delta H_m)_s - (\Delta F_m)_s = (\Delta H_m)_s + \int_{\sigma_1}^{\sigma_2} \pi d\sigma_m. \quad (25)$$

For extension:

$$(Q_m)_e = (\Delta H_m)_e - (\Delta F_m)_e = (\Delta H_m)_e - \int_{\sigma_1}^{\sigma_2} \gamma d\sigma_m. \quad (26)$$

3. Apparatus and Materials

Pressure-area and pressure-temperature measurements were made with the film balance described by Nutting and Harkins.[3] Subsolutions were placed in a shallow trough of stainless steel equipped with a hollow bottom through which water was circulated from a 260-l thermostat. Because of the heavy insulation placed about the thermostat and the circulating system it was possible to maintain the water at a known temperature, constant to within ±0.001°C in the range 0 to 50°C. To measure the temperature of the surface region thermocouples were installed just above and just below the film. The thermal e.m.f.'s were measured by means of a White double potentiometer in conjunction with a type HS galvanometer of high voltage sensitivity. The constant temperature junctions of the thermocouples were placed in an ice-bath prepared according to Roper.[4] As in previous work from these laboratories, when the air and subsolution temperatures become equal it is assumed that with the air saturated with moisture, the film is also at the same temperature. Film temperatures were read to ±0.01°C.

In all of the experiments films were spread on either 0.01N sulfuric, or hydrochloric acid prepared from water redistilled from alkaline permanganate and condensed in tin.

The preparation of the substances used in the film has been described by Reid and Meyer.[5]

Additional purification was effected by vaporization and condensation in a high vacuum according to the method of Harkins and Mulliken,[6] at a temperature just above the melting points. Quantitative spreading of the films was accomplished by the use of a precision pipet described by Harkins and Anderson.[7]

4. Pressure-Temperature-Area Relations of Monolayers

The data needed for this work are those which give the pressure-temperature relations at con-

[3] G. C. Nutting and W. D. Harkins, J. Am. Chem. Soc. **61**, 1180 (1939).
[4] E. E. Roper, J. Am. Chem. Soc. **60**, 866 (1938).
[5] E. E. Reid and J. D. Meyer, J. Am. Chem. Soc. **55**, 1574 (1933).
[6] W. D. Harkins, Science **54**, 359 (1921); R. S. Mulliken, J. Am. Chem. Soc. **44**, 37 (1922).
[7] W. D. Harkins and T. F. Anderson, J. Am. Chem. Soc. **59**, 2189 (1937).

stant area of the films, but in order to gain a proper view of the effect of the various surface phases upon the magnitudes involved it is very helpful to have in addition the pressure-area diagrams, so that a three-dimensional model of each system may be kept in mind. The pressure-area isotherms at various temperatures for pentadecylic acid, palmitic acid, and hexadecyl alcohol are given in Figs. 2 and 3 and 4.

If the π, σ curves were sufficiently accurate and numerous it would be possible to obtain the pressure-temperature (π, T) relations from these figures, but since this is not the case the pressure-temperature relations were determined by a direct method. The film was first spread on a large area of the subphase and then compressed to the desired molecular area at a relatively low temperature. The temperature was then increased slowly and the pressures of the film at constant area were recorded with intervals of from a seventh to about half a degree. Curves thus obtained for palmitic and pentadecylic acids and hexadecyl alcohol are exhibited in Figs. 5 (a and b) and 6. The data of Nutting and Harkins[8] were also used in the calculations. The original numerical data, about twice as numerous as those recorded in their paper were utilized.

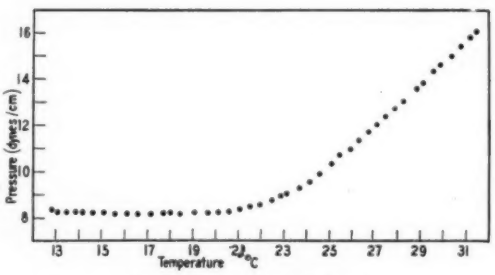

(a) Molecular area = 21A².

5. Energy of Extension and Spreading of the Monolayers

The processes of extension and of spreading of a monolayer have been defined and described in Section 2, and equations are given for the calculation of the energy and entropy involved. In the calculation of the slopes of the π, T curves the chord method[9] was used. This utilized the initial data and does not involve the graphical method for the determination of tangents, which was employed almost always as an independent method of obtaining the values.

The results obtained from the calculations are exhibited in Table I which represents a case chosen for illustrative purposes. This gives the energy and entropy for a monolayer of pentadecylic acid at 20°C and an area of 34.3A² mole^{-1}. Row A gives the free surface energy of water ($f = 72.75$ ergs cm^{-2}) and the values calculated by the use of Eqs. (16), (17) and (18). The increase in the heat content h is 116 ergs cm^{-2},

[8] G. C. Nutting and W. D. Harkins, J. Am. Chem. Soc. **61**, 2044 (1939).

[9] T. R. Running, *Graphical Mathematics* (John Wiley & Sons, New York, 1927), p. 65; T. F. Young and O. G. Vogel, J. Am. Chem. Soc. **54**, 3030 (1932).

FIG. 5. Pressure-temperature diagram of (a) pentadecylic acid and (b) palmitic acid.

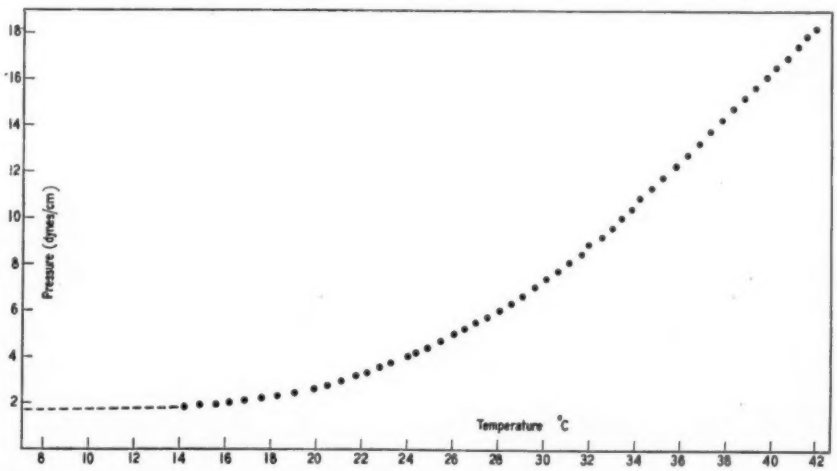

(b) Molecular area = 24A².

the entropy s is 0.14_8 erg cm^{-2} deg.$^{-1}$, and q the heat absorbed in the expansion or formation of the water surface is $43._3$ ergs cm^{-2}.

The same equations are used in calculating (row B) the energy involved in the extension of the film, together with that of the area of the subphase upon which it rests. The free energy increase is less than for the clean water surface. ($f=69.7_5$) but it is seen that the increase in the heat content of the film is surprisingly high; $h=394$, so the heat absorbed in the extension of the film and the entropy are both extremely large: $q=324$, and $s=1.10_5$.

In a similar way (row C), $f=-3.0$ corresponds to an experimental value for the film pressure, and the other results are calculated from the data by the use of Eqs. (20), (21) and (20b). The values obtained are $h=278$, $q=281$, and $s=0.959$, which are all very high, but not so high as those for the extension of the film.

It may be determined by inspection that the values in C are those in B minus those in A; this is exactly what they must be, since

$$\text{Process } C=\text{Process } B-\text{Process } A.$$

The values for the intermediate film of pentadecylic acid at a much higher molecular area, 38A^2, are also given in Table I. The values of h, q, and s for either extension or spreading, are lowered by 6 to 10 percent by the increase of area from 34 to 38A^2.

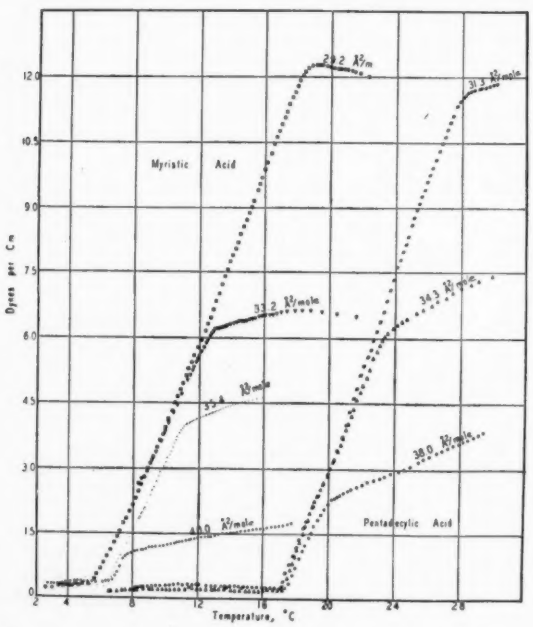

FIG. 6. Pressure-temperature diagram of pentadecylic and myristic acids.

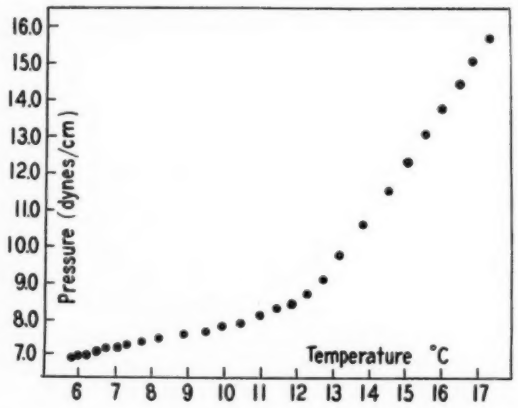

FIG. 7. Pressure-temperature diagram of hexadecyl alcohol at $\sigma=20$A^2.

Values are also given for the expanded film at the same area. It is apparent that both the energy of extension and of spreading are very much less for this phase than for the transition or intermediate film. Thus h for spreading is 252 ergs cm^{-2} for the intermediate, and only 45 ergs cm^{-2} for the expanded film.

The values for both the liquid and the solid film of hexadecyl alcohol at a molecular area of 20 sq. A are given in Table II. These show that h, s, and q for the condensed liquid film are almost the same as those for the expanded film of pentadecylic acid, while those for the solid film rise as high as 508 ergs cm^{-2}, which is the energy h for extension of the film.

6. Discussion

The energy of extension and that of spreading of a film have been shown to have extremely high values for the *intermediate* or *transition* phase, and a low or even a zero value for the energy of spreading in its condensed liquid (L_2) phase. The energy of extension of a film is to be distinguished from its energy of spreading over water, from which it differs by the value of the appropriate energy, i.e., h_e or q, for a clean water surface.

The question arises: Should the transition and the liquid condensed regions, with their extreme

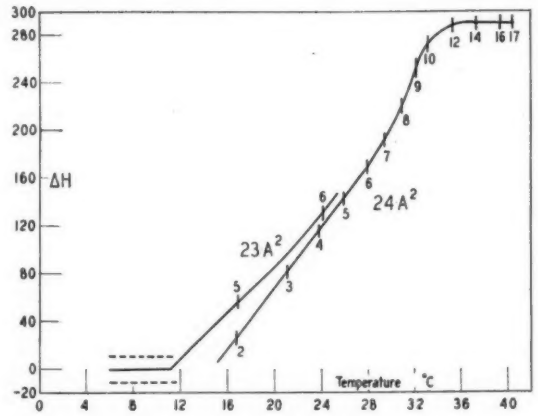

FIG. 8. Increase of the heat content ($h_s = (\partial H_s/\partial\sigma)_{p,T}$ in erg cm^{-2}, of a palmitic acid film as a function of temperature and pressure. The numbered lines along the curves give the film pressure (π) in dyne cm^{-1}.

difference of properties, be considered as constituting a single phase, or as two different phases? The answer that this work gives is that the relations of the energy of extension and of spreading seem to indicate that they belong to two phases with a transition of the third order between them. Thus (1) The value of the heat function (h) for the spreading of palmitic acid over one sq. cm of water is zero for the condensed liquid film at an area of 23A² per molecule up to a temperature of about 15°C. Above this temperature the value of the heat function increases rapidly and continuously along a smooth curve up to a temperature of about 33°C, after which it exhibits no break or kink but reaches a value of 290 ergs/cm² at 36 to 40°C (Fig. 8).

According to the classification used in Table III each of the three liquid surface phases differs greatly in its properties from the other two. Since the assumed transition between the L_2 and the I phase is of the third order, which is very difficult to prove or disprove, an equally satisfactory classification, though one which is less simple, assumes that the L_2 and I films constitute a single phase. If this is adopted it may be said that both the heat absorbed on spreading and the compressibility are small in the phase while it is in its more condensed state, but that both increase rapidly after the rapid expansion of the phase begins. This latter region of the phase may be designated as the transition region.

That the L_2 film is a liquid is indicated by the fact that its viscosity is Newtonian, and by the relation between viscosity and film pressure as expressed in the table. The equation which expresses the data is that developed theoretically by Moore and Eyring[10] for the viscosity of liquid monolayers, and the experimental and theoretical values of the constant k are of the same order of magnitude.

The values of the heat of spreading given in Table III are those for a monolayer of pentadecylic acid, and those for the compressibility are characteristic of the n-long chain paraffin acids.

The effects of change of temperature and of molecular area upon the value of the heat function for spreading (h_s) are illustrated by Tables IV to VI.

TABLE I. *Energy (erg cm^{-2}) of extension and spreading of pentadecylic acid.*

	f	h	$q=Ts$	s
Intermediate film at 20°C and $\sigma=34.3A^2$				
A. Clean water	72.75	116	43.25	0.148
B. Film (extension)	69.75	394	324	1.106
$C=B-A$ (spreading)	−3.0	278	281	0.959
Intermediate film at 18° and $\sigma=38A^2$				
A. Clean water	73.05	115.5	42.49	0.146
B. Film (extension)	72.32	367	295	1.014
$C=B-A$ (spreading)	−0.73	252	253	0.869
Expanded film at 22°C and $\sigma=38A^2$				
A. Clean water	72.46	116_4	44.00	0.14_9
B. Film (extension)	69.80	161	91.6	0.31
$C=B-A$ (spreading)	−2.64	45	47.6	0.16

7. ENERGY ABSORBED IN THE SEPARATION OF THE MOLECULES OF A FILM

Equations (23) to (26) may be used to determine the heat absorbed or the increase of the

TABLE II. *Energy of extension and spreading of a liquid and a solid film of hexadecyl alcohol at $\sigma=20.0A^2$.*

	f	h	$q=Ts$	s
Condensed liquid film at 9°C $\pi=7.7$ dyne/cm				
A. Clean water	74.37	115.5	41.17	0.14_6
B. Film (extension)	66.7	166	99.6	0.35_3
$C=B-A$ (spreading)	−7.7	$50._7$	58.4	0.20_7
Solid film at 16°C $\pi=13.8$ dyne/cm				
A. Clean water	73.34	116.1	42.77	0.148
B. Film (extension)	59.5	508	449	1.55
$C=B-A$ (spreading)	−13.8	392	406	1.40_4

[10] W. J. Moore and H. Eyring, J. Chem. Phys. **6**, 391 (1938).

heat content when a film is changed from any area σ_1 to any other area σ_2, provided enough values of h are known. At present the only film substance for which enough data are known to determine the heat relations over a wide range of area at different temperatures, is pentadecylic acid. From Table V, however, which gives the maximum values for h_s in the intermediate or transition phase (DC), it may be concluded that less heat is absorbed by myristic than by pentadecylic acid when the area is increased.

Let us consider the spreading of a pentadecylic acid film, beginning with a solid monolayer at $\sigma = 20A^2$ molecule^{-1}. While h_s for the solid film is high, $\Delta\sigma$ is only about $0.5A^2$, since the solid melts at about $20.5A^2$, the exact area being dependent upon the temperature. Thus the heat absorbed cannot be expected to be greater than 200 cal. mole^{-1}. The value of h has not been determined for pentadecylic acid, since the solid film is metastable with respect to a change to the three-dimensional acid. However, h for the spreading of a solid film of hexadecyl alcohol at 16°C is 400 erg cm^{-2}, which would give Q_m for an increase of area of $0.5A^2$ as 290 cal., and the value for pentadecylic acid should be considerably less than this.

On further increase of area the solid melts, but without the absorption of heat; that is the melting of such a solid film is a true change of the *second order*.

Increase of area in the liquid condensed ($L_2 = ED$) region, is accompanied by only a very small increase in the heat content (ΔH_m) of the film, since h_s is very small, and $\Delta\sigma$ is in general less than $1.5A^2$. Q_m is slightly larger since it includes the

$$\int_{\sigma_1}^{\sigma_2} \pi d\sigma$$

term. The magnitude of this quantity depends upon the temperature, and at 18°C is about 25 cal. mole^{-1}.

While both ΔH_m and Q_m for spreading are thus very small from F to D (Fig. 1), the high values of h_s for the *transition* or *intermediate* phase, indicate that both quantities will be large from D to C, and this is shown in Table VII. The value $h_s = 0$ in the upper left-hand corner of Table VI indicates that the film is in the liquid condensed (L_2) state, and the low values (57 to 68) of this quantity in the lower right-hand corner signify the expanded liquid (L_1) state.

In Table VII these values are converted into

TABLE III. *Comparison of some properties of the liquid condensed (L_2), intermediate I, and liquid expanded (L_1) states of monolayers. (Values illustrate the general order of magnitude only.)*

	L_2*	I	L_1
Heat absorbed on spreading, q_s	0	0 to const. at 300	60
Compressibility	0.008	0.3	0.03
Hysteresis	Small	Large	Small
Relation of viscosity to film pressure	$\log \eta = \log \eta_0 + k\pi$	Unknown	Unknown

* The viscosity relation given above for the liquid condensed film (L_2) is that developed theoretically on the basis of the assumption that the film is a true liquid. The experimental values of the viscosity show that not only is the logarithm of the viscosity (η) a truly linear function of the pressure (π) as the theory demands, but also the value of k is in agreement in order of magnitude with the value calculated by Eyring on the basis of his theory of liquids.

TABLE IV. *Increase of the heat function (h_s) for the spreading of palmitic acid over water (energy in erg cm^{-2}) as the film is changed from condensed liquid in the direction toward the expanded liquid.*

Type of Film	Molecular Area 24A²				Molecular Area 23A²			
	t°	Film pressure π	h_s	q	t°	Film pressure π	h_s	q
Liquid Condensed	5–11	4	0±20	0±20	15.0	1	0±20	0±20
	17	5	60	65	16.8	2	26	28
	24	6	130	136	21.2	3	88	91
					23.8	4	120	124
					26.0	5	144	149
					28.0	6	170	176
					29.6	7	195	202
					31.0	8	223	231
					32.2	9	250	259
					33.2	10	274	286
					34.5	11	285	296
					35.4	12	288	300
					36.4	13	290	30

TABLE V. *Maximum values of the heat content (h_s) of a transition film at each specified molecular area σ in A².*

Myristic Acid σ	Myristic Acid h_s	Pentadecylic Acid σ	Pentadecylic Acid h_s
29.2	285	31.3	340
33.2	245	34.3	280
35.4	230	38.0	265
40.0	200		

TABLE VI. *Effect of temperature and molecular area (σ) upon the increase of heat content (h_s) of a pentadecylic acid film over an aqueous acidic subphase (energy in erg cm^{-2}, area in A² molecule^{-1}.)*

t	Area σ = 21	22	26	31.3	34.3	38	43
18	0	172	310		310	265	
21.7	76	228	334	335	280	57	60
25	248	260	290	330	68	57	
27.5	263	292	317	240	63	57	

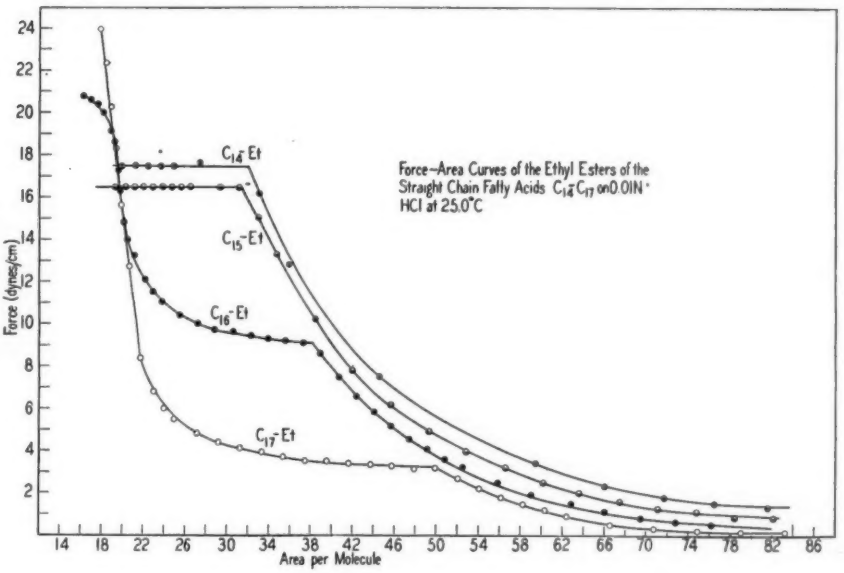

FIG. 9. Pressure-area relations of ethyl esters of the n-long chain paraffin acids. At the larger areas given these esters, except with very long chains, are in the vapor state, but the curves have the general form characteristic of the liquid expanded (L_1) state.

kcal. per mole (K).

$$K = 1.45 \times 10^{-3} \int_{\sigma_1}^{\sigma_2} h_s d\sigma.$$

In this equation q_s, s_s, h_e, q_e, or s_e, may be substituted for h_s.

A better conception of the extent of the area covered by one mole of film may be obtained if it is remembered that 1.5 times the area per molecule in A^2 gives the area in acres per mole. Since the lowest area covered by a mole of an organic substance which contains a hydrocarbon chain is 20A^2, the lowest area per mole is 30 acres.

The heat absorbed (Q_m) and the increase of heat content (ΔH_m) exhibit the following relations: (1) For the spreading process $Q_m \sim \Delta H_m$ for either phase. (2) For extension $Q_m < \Delta H_m$. (3) The value of Q_m and ΔH_m for spreading or extension, with increase of temperature: decrease rapidly in the *transition* region, and increase rapidly in the *liquid* expanded phase. (4) The values of ΔH_m and of Q_m for spreading from D to B, that is for the total intermediate and liquid expanded regions, seem to decrease with increasing temperature, while for extension there is also a decrease, but this is not so large.

8. Energy of Spreading of the Intermediate Film of an Ester, Which May be Formed by Transition on Compression from a Vapor Film

Highly compressed vapor films, designated by Adam as vapor expanded, may, on compression, undergo a change of phase to the intermediate state (Figs. 9 and 10). The ethyl esters of the n-long chain paraffin acids are known to exhibit this type of behavior, and it is found that the increase of heat content (h_s) for the spreading of the palmitate is 200 erg cm^{-2} at 20°. This is

TABLE VII. *Heat absorbed (Q_m) and increase of heat content (ΔH)$_m$ for the spreading (Sp) and extension (Ex) of a pentadecylic acid film in the intermediate phase (EC) and the liquid expanded phase (CB). (Energy in kcal. mole^{-1}, area (σ) in A^2 molecule^{-1}.) (Energy values calculated from those for h_s in Table VI.)*

Intermediate Phase			ΔH_m		Q_m		Liquid Expanded Phase		ΔH_m		Q_m	
σ_1	σ_2	$t°$	Sp.	Ex.	Sp.	Ex.	σ_1	σ_2	Sp.	Ex.	Sp.	Ex.
1	2	3	4	5	6	7	8	9	10	11	12	13
21.5	42.0	18.0	8.3	11.8	$\Delta H_m - 0.080$	9.6	42.0	43	Very small since $\Delta\sigma$ very small			
20.8	35.5	21.7	6.4	8.9	$\Delta H_m - 0.160$	7.4	35.5	44	0.7	2.1	$\Delta H_m - 0.025$	1.2
20.5	33.5	25.0	5.4	7.6	$\Delta H_m - 0.0190$	6.2	33.5	45	1.0	3.1	$\Delta H_m - 0.054$	1.8
20.5	31.5	27.5	4.6	6.5	$\Delta H_m - 0.0195$	4.9	31.5	46	1.3	3.7	$\Delta H_m - 0.097$	2.2

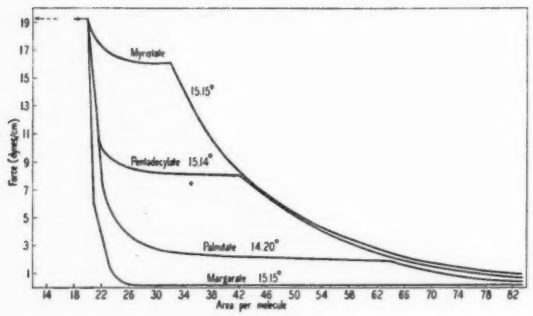

FIG. 10. Ethyl esters at a temperature ten degrees below that for Fig. 9.

about two-thirds of the value found for the corresponding, and other similar acids. This means that the energy of extension (h_e) is 316 erg cm^{-2}, the heat absorbed (q_s) in spreading 206 erg cm^{-2}, and in extension 236 erg cm^{-2}.

However, this does not show that Q_m, the integrated heat, between D and C (Fig. 1), i.e., the heat absorbed in the expansion of the film through the whole range of the intermediate state, is smaller for the esters, since the increase of area, which enters into the equation, is much larger for the esters. Thus the heat absorbed in this phase seems to be about the same for these two classes of compounds. To state that they are just the same would involve the question as to the proper condition for comparison of the two sets of compounds. The condition adopted here is that the two compounds are compared at such temperatures as cause the pressure π of the films to be the same at the point of transition from the intermediate phase into either the liquid expanded or the compressed vapor phase. Our data which exhibit the behavior of the esters is as yet scanty, so it is difficult to specify with any exactness the closeness in the equality of Q_m for the spreading of the two classes of compounds. The closeness of the two energy values suggests that with the two classes of compounds the expansion through the intermediate, or transition, state, involves the same type of change in the relations of the molecules to each other. For example, with a micelle theory it would indicate that the change from the micellular to the nonmicellular state involves the same energy per molecule for the esters as for the acids. This approximate equality in energy should be predicted from any other tenable theory. Thus it might be assumed that the general relations of the intermediate phase are in accord with an assumption of rapidly increasing molecular rotation as the phase expands, until, when this rotation becomes complete there is a (possibly second-order) transformation to the L_1 state. Neither this theory nor that which assumes micelles has been put on a quantitative basis in accord with the energy relations exhibited in this paper.

9. CONCLUSIONS

The two-dimensional phase change solid →liquid at E (Fig. 1) has been found in this work to exhibit a zero latent heat, so this seems to be a change of the second order.

It might be assumed that the phase change which, on *expansion* of the film, gives rise to the liquid phase (L_1) occurs at C. If this is the case, then this change of state has a very small latent heat, since $\Delta\sigma$ is small for the region in which the very rapid change of slope of the π, σ curve occurs. However, this region is preceded by the intermediate or transition phase in which there is a large change of area associated at every point on the almost horizontal portion of the isotherm with a large value of h_s (or h_e). Thus this whole region possesses the high latent heat which is characteristic of an ordinary change of the first order. However, no discontinuity in σ, the area, $[(\partial F/\partial\pi)_{p,\,T}=\sigma]$ occurs between the condensed liquid (L_1) and C, so this is not a *normal* change of the first order,[11] though it has the general characteristic classified by Mayer and Streeter[12] as a transition of a diffuse first order.

Since the isothermal changes of the films occur at constant pressure, and the change of volume in spreading or extension of the film is presumably small, it may be concluded that $\Delta E_m=\Delta H_m$. That is, the increase in the internal energy of the film is practically that given by the increase in the heat content.

The vaporization of the liquid expanded film (L_1) has not been investigated, but it is hoped that an apparatus sufficiently sensitive for this purpose can be developed. From what is known of the temperature coefficient in this region it seems probable that at 18° the latent heat of vaporization of the pentadecylic acid film is several thousand calories, but this decreases

[11] P. Ehrenfest, Proc. K. Akad. Amst. **36**, 115 (1933).
[12] J. E. Mayer and S. F. Streeter, J. Chem. Phys. **7**, 1017 (1939).

rapidly as the temperature rises, since $\sigma_{mA} - \sigma_{mB}$ (Fig. 1) decreases very rapidly.

The determination of the energy relations of gaseous films requires apparatus of high sensitivity and considerable accuracy. It is apparent from the equations that as the area of a gaseous film increases the increment of heat content (h) approaches zero for spreading, while for expansion it approaches h_w or about 116 erg cm^{-2} at ordinary temperatures, and q_e approaches q_w, or about 44 erg cm^{-2}. It is obvious that in this case $(\Delta H_m)_e$ and $(Q_m)_e$, which refer to one mole of the substance of the monolayer, lose their significance, but this is not true of h_e and q_e.

It is often forgotten that a film, such as that of an amphipathic (polar-nonpolar) organic substance on water, includes all of the region of the surface which contributes to the surface energy, that is all of the energy associated with the surface which is not accounted for by three-dimensional thermodynamic treatment which neglects the extent of the surface. The contribution of the first layer of water molecules to this energy is very important, whether it is covered by the organic layer completely or incompletely, and while the second and third, etc., layers rapidly become less important, it is obvious that the first layer of water molecules, though it contributes by far the greatest share of the surface energy due to the water in the surface region, is not the only one involved. Thus in the utilization of the results of this paper in connection with the problem of intermolecular attraction in the monolayer or the film, the energy of spreading and of extension are both of fundamental importance. It has been considered advisable to limit the present paper to the thermodynamics of films. Any applications to molecular theory has been deferred to later papers.

DECEMBER, 1940 JOURNAL OF CHEMICAL PHYSICS VOLUME 8

Effect of Gravitational Field on the Thermal Diffusion Separation Method

MILTON FARBER AND W. F. LIBBY
Department of Chemistry, University of California, Berkeley, California

(Received May 11, 1940)

A test of the effect of gravitational field on the operation of the Clusius-Dickel thermal diffusion method for gas separation has been made by use of a hollow disk with one hot surface, the whole disk spinning at various speeds. Linear increases in both the equilibrium separations and the rates of separation with increasing centrifugal force were obtained for speeds below a certain maximum value. Above this both the rate and equilibrium separations fell rapidly. He-CO_2 mixtures were used. The results indicate that the standard column would be improved if it were placed in a larger field up to ten times that caused by gravity. Theories for the action of the thermal diffusion column should show this. The apparatus cannot compete with the standard column type for isotopic separations but may have some application to industrial separation problems.

CLUSIUS and Dickel[1] have shown that the counter current flow obtained in the gas between two vertical concentric cylinders, the inner one of which is heated, operates to increase the effect of the thermal diffusion separation of gases.[2–4] The effects of pressure, dimensions of the apparatus, temperature gradient, and character of the gaseous components all have been investigated in some detail,[5–11] both theoretically

[1] K. Clusius and G. Dickel, Naturwiss. **26**, 546 (1938).
[2] S. Chapman, Proc. Roy. Soc. London **A93**, 1 (1917); Phil. Trans. Roy. Soc. London, **217**, 157 (1917); 181 (1918).
[3] D. Enskog, Physik. Zeits. **12**, 538 (1911); Zeits. f. Physik **2**, 538 (1911).
[4] T. L. Ibbs, Proc. Roy. Soc. London **A99**, 385 (1921); **107**, 470 (1925).
[5] A. K. Brewer and A. Bramley, Phys. Rev. **55**, 590 (1939).
[6] K. Clusius and G. Dickel, Zeits. f. physik. Chemie, **B44**, 397 (1939).
[7] A. O. Nier, Phys. Rev. **57**, 30 (1940).
[8] W. Furry, R. Jones and L. Onsager, Phys. Rev. **55**, 1083 (1939).
[9] L. Waldeman, Naturwiss. **27**, 230 (1939); Zeits. f. Physik **114**, 53 (1939).
[10] P. Debye, Ann. d. Physik **36**, 284 (1939).
[11] J. Bardeen, Phys. Rev. **57**, 35 (1940).

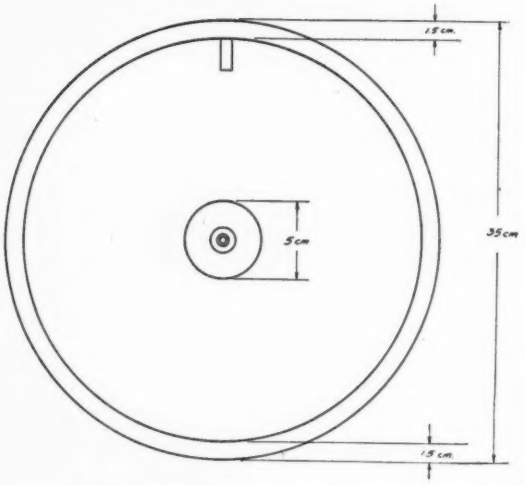

FIG. 1A. Side diagram of the centrifugal thermal diffusion apparatus (drawn to scale).

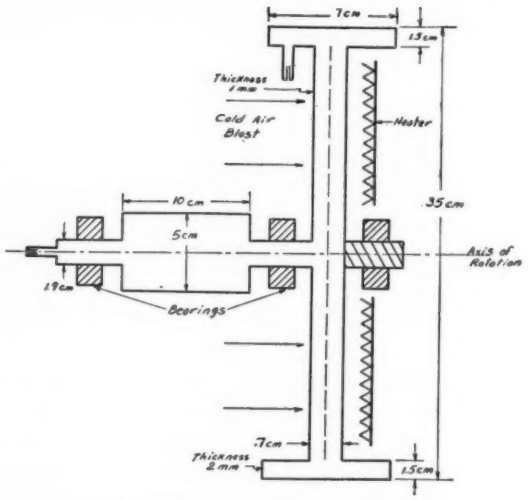

FIG. 1B. Cross-sectional diagram of apparatus (not drawn to scale).

and experimentally. The authors have attempted to investigate the effects of variation of the gravitational field by use of a rather drastically modified form of the apparatus.

APPARATUS

Since the use of centrifugal force is the only way of varying the gravitational field, the apparatus was designed so the necessary counter current would occur perpendicular to an axis of rotation. The standard tube arrangement was replaced by a rotating hollow disk one surface of which was heated and the other cooled. Reservoirs for the gas were provided at the rim and on the axis of rotation as shown in Figs. 1A and 1B. The whole apparatus consisted of brass approximately 1 mm thick. The hot plate was heated by radiation from a Nichrome wire heater wound on a transite sheet and mounted approximately 1 cm from the brass surface while the opposite face was cooled with an air blast from a large electric fan. The rim reservoir was in the shape of a hollow rectangular tire with a volume of 780 cc. A metal cock for sampling the rim gas was located on the inner surface of the rim as shown. A reservoir of 200 cc volume was located on the axis of rotation with a sampling cock attached. The wheel was rotated by a direct-current motor of variable speed by means of a belt running over a wooden pulley mounted around the cylindrical reservoir on the rotational axis. Three ball bearings were mounted in iron brackets on a sturdy platform for support of the wheel. The speeds of rotation were measured with a standard stroboscope to about one percent accuracy. The speed of rotation was constant to one or two percent at each speed, though a small amount of irregular vibration set in at the highest speeds of approximately 1000 r.p.m.

The surface temperatures were measured by placing Chromel-Alumel thermocouples in direct contact with the surfaces. Various segments of the heater coil were provided with separate leads so that the area of the heated surface might be varied in both magnitude and distance from the axis of rotation.

The inner surfaces of the plates were 7 mm apart and the volume of the interplate region was 600 cc.

The gas analyses were made on 10-cc samples taken by stopping the wheel and using the rim and axis cocks. It was shown by sampling on the axis during rotation and after stopping that stopping the wheel did not lead to appreciable mixing in the two or three minutes required to take the sample. For most of the work, in which CO_2 and He were being separated, the analysis was accomplished by freezing out the CO_2 in a liquid-air trap and reading the pressure change on a capillary manometer. By using capillary tubing throughout the system and taking reasonable care to make the correction accurately for

the decrease in pressure of the He caused by the cooling, it was possible to reproduce the analyses to within one percent.

The $He-CO_2$ gas used was mixed in a pressure cylinder at several atmospheres pressure and introduced into the apparatus at atmospheric pressure. The air was removed by flushing with excess of the gas. It was not possible to evacuate the wheel because the walls were too thin to support atmospheric pressure.

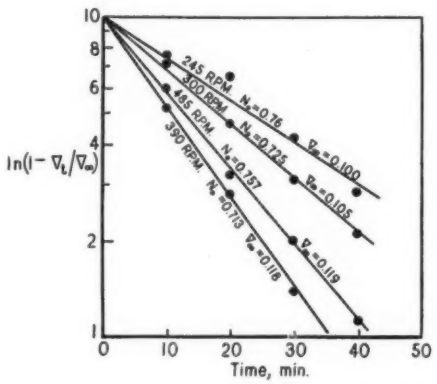

FIG. 2. Separation *vs.* time at various speeds of rotation. $\Delta T = 290°C$, heater area = 278 cm².

RESULTS

Separation *vs.* time

Figure 2 presents data obtained with the hot plate at 340°C and the cold plate at 50°C, the wheel rotating at various speeds and the initial composition of the gas having various values. The ordinates are logarithms of one minus the ratio of the separation at any given time to that for the equilibrium state. The separations, Δ_t, were calculated as the difference between the mole fraction, N, of He at the rim or the axis and the initial mole fraction, N_0. A typical set of data is given in Table I. The data seem to justify approximately the exponential expression

$$\Delta_t = \Delta_\infty (1 - e^{-\lambda t}) \qquad (1)$$

TABLE I. *Separation vs. time. 485 r.p.m.,* $\Delta T = 290°$, Δ_∞*(center)* $= 0.119$, $N_0 = 0.757$.

TIME (MIN.)	0	10	20	30	40
$1-\frac{\Delta_t}{\Delta_\infty}$	1	0.60	0.32	0.20	0.11

for the dependence of the separation on the time, Δ_t being the separation at any given time t, Δ_∞ the equilibrium separation, and λ a constant measuring the rate of separation. Figure 3 presents the data for the effect of variation of the temperature gradient on the rate of separation, λ. Figure 4 shows the variation of the rate, λ, with r.p.m. A rather sudden break occurs at about 400 r.p.m. The main point about these data is the approximately linear rise in the rate with the square of the speed of rotation, ω^2, until the break occurs.

Figure 5 shows a similar set of data for the variation of the equilibrium separation, Δ_∞ (center) with ω^2. Here also, an approximately linear rise occurs till ω becomes approximately 400 r.p.m. Figure 6 presents the data for the variation of Δ_∞ (center) with the temperature difference. Figure 7 shows the Δ_∞ (center) *vs.* ω^2 for two heaters the larger having an area of 435 cm² and the smaller having 278 cm² proving that the heater area had no serious effect on the speed at which the linear rise in Δ_∞ (center)

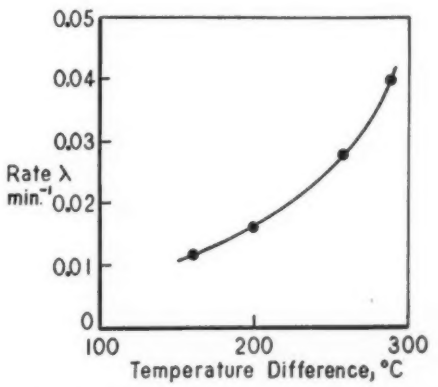

FIG. 3. Rate of separation *vs.* temperature difference.

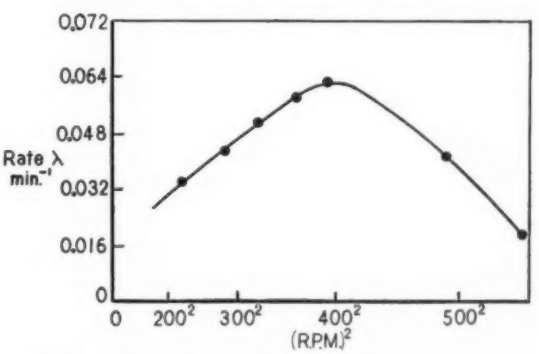

FIG. 4. Rate of separation *vs.* speed of rotation.

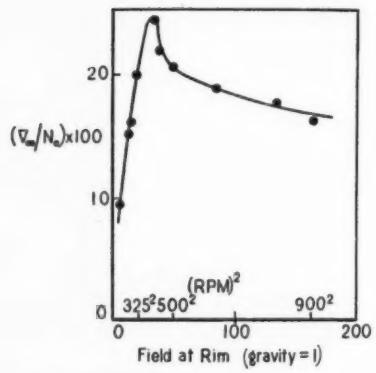

FIG. 5. Equilibrium separation *vs.* speed of rotation. $\Delta T = 290°C$, $N_0 = 0.65$, heater area = 278 cm². Time for each run, 2 hr.

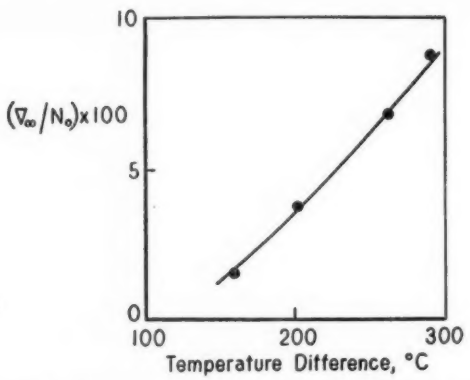

FIG. 6. Equilibrium separation *vs.* temperature difference.

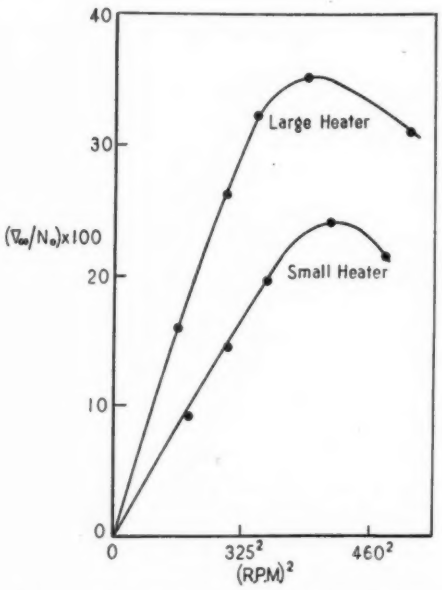

FIG. 7. Effect of heater area on equilibrium separation. For large heater, $\Delta T = 290°C$ heater area = 435 cm², $N_0 = 0.62$. For small heater, $\Delta T = 290°C$ heater area = 278 cm², $N_0 = 0.65$.

breaks. Figure 8 gives the dependence of Δ_∞ (center) on the heater area, the open circles referring to variations obtained by changing the radius of the inner edge of the heated region, while the solid circles belong to data obtained by varying the radius of the outer edge. Apparently there is no large difference between these two sets of data.

DISCUSSION

The gas flow which occurs is a combination of a general movement of the gas near the hot surface inward toward the axis with a transfer flow of part of this hot gas across to the outward moving cold stream as illustrated in Fig. 9. The hot gas flows across to the cold stream at a rate which is constant for each unit of area of plate surface. The truth of this statement is apparent if one notices that both the force acting to push the gas toward the rim and the area across which it moves in flowing toward the rim increase directly with the distance, a, from the axis of rotation. To maintain approximately constant pressure throughout the gas it is necessary that, instead of compression occurring as the hot gas stream moves inward, a partial movement across to the cold stream must occur to compensate for the decrease in volume available. This also keeps the outward moving stream from suffering a pressure decrease. For a given movement inward from a to $a-da$ the decrease in total rate of flow is proportional to ada because the area across which the flow occurs is proportional to a and the decrease in the force causing the flow is proportional to da. This decrease must be equal to the flow to the cold stream. The area of the plane parallel to the wheel surfaces across which this flow occurs obviously is proportional to ada also, so the ratio, the flow from hot to cold stream per unit area of wheel surface, is constant over the whole wheel.

Using the dimensions of the apparatus, the viscosity of the gas, and approximate values for the temperature gradient the velocity of flow is calculated to be about 150 cm/sec. at the inner edge of the heater and 500 cm/sec. at the rim at 375 r.p.m. The hot to cold stream flow is about 25 cm/sec. under these conditions. At other

speeds the values should be higher or lower in proportion to ω^2.

The data show that in the neighborhood of 400 r.p.m. the increases of both the rate and equilibrium separation with increasing ω^2 break rather sharply into decreases. Both the suddenness of the breaks and the gas velocities at which they occur indicate that turbulence sets in under these conditions.

The Chapman-Enskog thermal diffusion process, which concentrates the light constituent near the hot side, must be established rapidly with respect to the rates of flow below those for 380 r.p.m. or the linear rises shown in Figs. 4 and 5 for λ and Δ_∞ (center) *vs.* ω^2 probably would not exist. In order that the counter current action should increase directly with the rate of flow, equilibrium must be nearly completely established for the whole range of speeds. It is conceivable that the breaks in Figs. 4 and 5 are caused by failure to establish equilibrium rather than by turbulence. The chief argument against this interpretation is the sharpness with which the breaks occur.

The linear increase of Δ_∞ and λ with the area of the heated surface indicates strongly that the most important part of the current flow is the transfer of the hot gas to the outward moving cold stream which has been shown above to occur at a constant rate per unit area of heated surface, independently of the distance from the axis of rotation. It seems reasonable that this

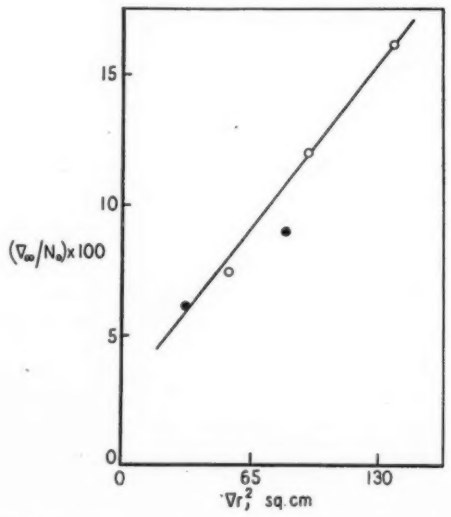

FIG. 8. Equilibrium separation *vs.* heater area ($\omega = 340$ r.p.m., $\Delta T = 290°C$).

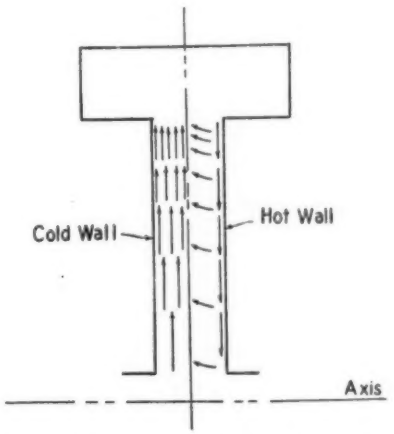

FIG. 9. Type of flow taking place while apparatus is in operation.

should be the case. The gas moving to the cold stream carries an excess of the heavy component with it leaving the inward moving hot stream somewhat purified.

It seems certain also that turbulence should set in for this type of flow at somewhat lower velocities than for those existing in the standard cylindrical thermal diffusion apparatus. On the other hand, it may be true that the condition that equilibrium be established rapidly with respect to the counter current velocity may be less easily violated in the wheel apparatus because of the intimate nature of the contact between the inward moving hot gas and that part of it which is just leaving to join the cold stream. However, since the rises were observed to continue till the main part of the gas was subjected to a field approximately 20 times that due to gravity, it is relatively certain that the ordinary Clusius-Dickel, Brewer-Bramley column would be much improved if it were possible to increase the gravitational field to some ten times the normal value. We should expect all theories for the actions of the columns to show this possibility.

The wheel method seems to offer little promise as a competitor with the columnar type of apparatus. Our apparatus was about equivalent in action to an average column five or six feet long. It is possible, however, that the use of wheels of much larger radii with surfaces heated by flames or superheated steam instead of electricity would afford a less expensive method of separating certain gases of industrial importance.

The Low Temperature Gaseous Heat Capacities of Certain C_3 Hydrocarbons

G. B. KISTIAKOWSKY, J. R. LACHER* AND W. W. RANSOM†
Mallinckrodt Laboratory, Harvard University, Cambridge, Massachusetts

(Received August 15, 1940)

The low pressure thermal conductivities of allene, propylene, propane, methyl acetylene and cyclopropane have been measured over the temperature range 150 to 340°K. The heat capacities derived from these measurements are compared with those from other sources. Data are presented in support of the bracketing method for deriving heat capacities from heat conductances. Heats of certain hydrogenation reactions, when calculated to 0°K and to the nonvibrating state, are found to exhibit the same regularities as the experimental values determined at 335°K.

THE work reported here is a continuation of that discussed in two previous papers.[1,2] The apparatus, technique and the method of calculation of the heat capacities from the heat conductances were substantially as developed before, with the exception of the innovations described in the following.

In addition to the two pipettes used before, a third one of larger volume was used in experiments above 273°K. It admitted 1.5×10^{-2} mm pressure of gas, which resulted in more accurate determinations of heat conductance in this temperature range.

Although in the work on ethane previously described the metal pipettes gave very satisfactory service, it was found that variable quantities of three-carbon hydrocarbons were adsorbed in the pipettes. The occurrence of this adsorption vitiated a basic assumption of the experiments: that the compared gases are at the same pressure, or at least that their pressure ratio is known. After several trials a procedure was developed which has provided this information. It consisted of admission of gases from an all-glass pipette under conditions minimizing adsorption there and then varying the temperature of the 12-liter flask to determine the extent of adsorption on its surface.

A 12-liter flask was placed in a furnace and was connected through a 2-mm capillary to two Pirani gages placed in ice. Since it was found that the presence of stopcocks lubricated with Apiezon grease did not affect the results, the flask was connected to the pump through a large stopcock and the pipette was formed by a length of tubing between two stopcocks. On the opposite side, the pipette communicated with a flask filled to *ca.* 10 mm pressure, measured to an accuracy of about 0.1 percent with a manometric system soon to be described and patterned after the one described by Kistiakowsky and Rice.[3] The large Pyrex flask was new and was washed only with organic solvents and water before use. It was baked out under vacuum and no air was admitted to it from the beginning to the end of the whole series of measurements on all gases.

The procedure with each gas was to admit a known quantity (*ca.* 3×10^{-3} mm) while the twelve-liter flask was at 200°C, then cool the flask to room temperature and finally heat it again to 200°. The two Pirani readings at 200° were combined to establish the "rate of leak" (about 3×10^{-7} mm per minute). This was used to correct the observed ratio between Pirani readings with the flask at 200° and at 30°. After evacuation a second quantity of gas was admitted, the cycle repeated, etc. The readings at each temperature agreed to better than 0.3 percent with the exception of the first admission of each gas.

Assuming the validity of the limiting low pressure thermal transpiration law and knowing the heated and unheated volumes in the system,

* Present address: Department of Chemistry, Brown University, Providence, Rhode Island.
† Present address: E. I. duPont de Nemours and Company, Station B, Buffalo, New York.

[1] G. B. Kistiakowsky and F. Nazmi, J. Chem. Phys. **6**, 18 (1938).

[2] G. B. Kistiakowsky, J. R. Lacher and Fred Stitt, J. Chem. Phys. **7**, 289 (1939).

[3] G. B. Kistiakowsky and W. W. Rice, J. Chem. Phys. **7**, 281 (1939).

it is easy to calculate the theoretical ratio of Pirani readings at 30° and 200°. To compare it with experiment one must know whether the heat conductance in the gages is linear with pressure. This was tested with ethylene over a range from 4 to 20×10^{-3} mm by adding successive pipettes of gas without intermediate evacuation. The heat conductance values fell within 0.1 percent of a straight line through the origin. For all gases discussed later and also acetylene and cyanogen, but not dimethyl ether, the measured Pirani values at 200° were found to be 6.6 ($\pm$0.6) percent higher than those calculated. For dimethyl ether the experimental value was 12.8 percent higher than that calculated. Observations were made on ethylene at several intermediate temperatures and percentage differences between calculated and observed values were found to be linearly dependent on the temperature of the 12-liter flask. These facts suggest very strongly that with all gases tried excepting dimethyl ether the reversible adsorption on glass at 30° is negligibly small and that the deviations of calculated from observed values are due to inapplicability of the limiting thermal transpiration law.

The possible occurrence of very strong ("irreversible") adsorption which persists even at 200° should have no effect on these measurements since gases so adsorbed could not be removed during the relatively brief evacuations between successive admissions from the pipette. It was therefore assumed that for any pair of gases, excluding dimethyl ether, the ratios of Pirani gage readings from this system were ratios of heat conductances at identical gas pressures. These ratios, denoted in the following as true Pirani ratios, were averaged over all readings and are certain to 0.5 percent.

Several Pirani gages were used in the course of the work on the heat capacities of gases here discussed because of occasional mechanical failures. These gages were prepared from the same spool of wire and all were annealed at 500° for 18 to 24 hours. Neither of the gages made for the described calibration system was actually used at the time the heat capacity determinations were made but one of them was prepared in exactly the same manner as the previous ones. The second gage, however, was annealed for 48 hours and it gave true Pirani ratios which differed by as much as 2 percent from those of the other gage for gases very dissimilar kineti-

TABLE I. *Allene. Platinized wires.*

(a)

Mean Temperature °K	$Y+R/2$	$\frac{\alpha_{ALLENE}}{\alpha_{ETHYLENE}}$ Exp.	Interp.
342.1	16.30	1.056	1.056
333.5	16.00	1.053	1.053
332.9	*15.79*	*1.040*	*1.040*
325.3	*15.54*	*1.041*	*1.038*
314.1	15.29	1.049	1.048
313.9	*15.09*	*1.035*	*1.036*
313.9	*15.09*	*1.035*	*1.036*
294.5	*14.40*	*1.030*	*1.032*
292.1	14.40	1.040	1.042
291.1	*14.19*	*1.026*	*1.031*

(b)

Mean Temperature °K	$\frac{\alpha_{ALLENE}}{\alpha_{ETHYLENE}}$ Interp.	$C_p°$ Exp.	Stat.
258.4	*1.024*	12.83	12.82
256.4	1.032	12.76	12.75
223.4	*1.016*	11.75	11.76
218.1	*1.015*	11.61	11.61
212.3	1.018	11.39	11.43
157.6	*1.002*	9.89	9.95
157.6	*1.002*	9.92	9.95
148.1	*1.000*	9.71	9.72

TABLE II. *Allene. Bare wires.*

(a)

Mean Temperature °K	$Y+R/2$	$\frac{\alpha_{ALLENE}}{\alpha_{ETHYLENE}}$ Exp.	Interp.
344.3	17.70	1.146	1.138
335.7	17.28	1.138	1.131
332.6	*16.95*	*1.122*	*1.115*
324.9	*16.51*	*1.111*	*1.110*
316.7	*16.11*	*1.103*	*1.105*
316.7	*16.11*	*1.103*	*1.105*
316.4	16.23	1.112	1.118
295.6	*15.20*	*1.091*	*1.092*
294.2	15.17	1.093	1.102
291.6	*14.99*	*1.087*	*1.090*

(b)

Mean Temperature °K	$\frac{\alpha_{ALLENE}}{\alpha_{ETHYLENE}}$ Interp.	$C_p°$ Exp.	Stat.
259.0	*1.069*	12.74	12.84
258.3	1.077	12.64	12.82
223.9	*1.047*	11.68	11.77
218.6	*1.043*	11.48	11.62
213.9	1.046	11.33	11.47
158.0	*1.005*	9.92	9.96
158.0	*1.005*	9.94	9.96
148.3	*1.000*	9.71	9.73

TABLE III. *Propylene.*

(a)

MEAN TEMPERATURE, °K	$Y+R/2$ WIRE No. 1	$Y+R/2$ WIRE No. 2	$\alpha_{PROPYLENE}/\alpha_{ALLENE}$ WIRE No. 1	$\alpha_{PROPYLENE}/\alpha_{ALLENE}$ WIRE No. 2
335.7	16.82		1.000	
333.5		16.81		1.004
316.7	*16.16*		*1.002*	
316.7	*16.16*		*1.002*	
313.9		*15.99*		*0.998*
313.9		*15.97*		*0.997*
294.2	15.31		1.004	
292.1		15.24		1.004
291.6	*15.21*		*1.003*	
291.1		*15.16*		*1.001*

(b)

MEAN TEMPERATURE, °K	$C_p°$ WIRE No. 1	$C_p°$ WIRE No. 2	C_{ir}	C_{ir} CALC; $V=2100$ CAL./MOLE
291.1		*15.16*	2.20	2.12
259.0	*14.04*			
258.4		*13.98*		
258.3	13.97			
256.4		13.90	2.19	2.17
223.9	*12.83*			
223.4		*12.82*		
220.2		*12.70*	2.17	2.17
219.9	*12.68*			
213.9	12.50			
212.3		12.46	2.16	2.16
158.0	*10.87*			
157.6		*10.86*	1.88	1.91
157.3		10.86		
148.3	*10.64*			
148.1		*10.63*	1.83	1.84

TABLE IV. *Propane.*

(a)

MEAN TEMPERATURE, °K	$Y+R/2$ WIRE No. 1	$Y+R/2$ WIRE No. 2	$\alpha_{PROPANE}/\alpha_{ALLENE}$ WIRE No. 1	$\alpha_{PROPANE}/\alpha_{ALLENE}$ WIRE No. 2
344.3	19.71		0.998	
342.1		19.55		0.995
316.4	18.48		1.005	
314.1		18.30		1.001
291.6	*17.36*		*1.013*	
291.1		*17.19*		*1.004*

(b)

MEAN TEMPERATURE, °K	$C_p°$ WIRE No. 1	$C_p°$ WIRE No. 2	C_{ir}	C_{ir} CALC; $V=3300$ CAL./MOLE
259.0	*15.89*			
258.4		*15.73*	4.03	3.96
258.3	15.75			
256.4		15.64	3.90	3.96
220.2		*14.18*	3.73	3.60
219.9	*14.22*			
218.6	*14.18*			
218.1		*14.11*	3.72	3.60
213.9	14.03			
212.3		13.96	3.58	3.54
158.0	*12.05*			
157.6		*12.03*	2.96	2.76
148.3	*11.70*			
148.1		*11.68*	2.84	2.66

TABLE V. *Methyl acetylene.*

MEAN TEMPERATURE, °K	$Y_E+R/2$ WIRE No. 1	$Y_E+R/2$ WIRE No. 2	$C_p°$ K. AND R. AND STATISTICAL	$Y_A+R/2$ WIRE No. 2	$Y_A+R/2$ WIRE No. 1
339.6	17.13				15.28
339.6	17.17				15.31
338.9		16.24	15.71	15.56	
338.9		16.24	15.71	15.56	
329.4		15.99	15.45	15.37	
328.5	16.82				15.13
306.2		15.15	14.79	14.67	
306.0	15.90				14.55
294.5	15.38				14.19
294.3		14.71	14.43	14.31	
259.0	13.94				13.19
258.4		13.53	*13.36*	13.23	
218.6	12.39				12.07
218.1		12.24	*12.15*	12.07	
158.0	10.35				10.32
157.6		10.29	*10.30*	10.32	

cally. The differences were in a direction to indicate that additional annealing reduced accommodation coefficients the more the smaller they were to begin with.

Hot wire conductance ratios found in earlier experiments were corrected to equal pressures of compared gases by means of the true Pirani ratios of the 24-hour annealed gage under the assumption of linear dependence of conductance on pressure. Thus corrected hot-wire ratios were then substituted into equations of the type of (3) of the preceding paper[2] for the calculation of the heat capacities given in Tables I to VIII.

At cryostat temperatures below 250°K the results were found to depend slightly on the pressure in the system when three-carbon molecules were compared with ethylene, indicating differential effects of thermal transpiration.* The conductance ratios were plotted against pressure and were extrapolated to zero pressure. The limiting values differed not more than 1 percent from the last experimental point at the lowest temperatures.

To apply the bracketing procedure, two gases of known heat capacity are needed for compari-

* These differential effects were larger than in the calibration system because the connecting tubing between the hot wire gages and the 12-liter flask was of 4-mm bore rather than of 2-mm bore as with the Pirani gages in the calibration experiments.

son, one with smaller, the other with larger accommodation coefficient. Such gases were found for methyl acetylene and cyclopropane, but for other compounds we were obliged to use the much cruder treatment which is based on the assumption that at low temperatures the accommodation coefficient ratios approach unity.[1,2]

Results

Allene

The heat conductance of allene was compared with that of ethylene but no suitable gas could be found to complete the bracketing procedure. The sample of ethylene used in this research has been described.[1] The sample of allene used was part of the material employed in the measurements of the heats of hydrogenation by Kistiakowsky and co-workers.[4] It was subjected to repeated dry ice to liquid-air distillations to remove water and to successive bulb to bulb distillations in vacuum to remove air.

The heat conductances of allene and ethylene were measured with two sets of bare and platinized wires. The results are presented in Tables I and II. The italicized and nonitalicized values in the columns of Tables I to VI represent the use of different wires. The second columns of the (a) sections of the tables give values of $Y+R/2$ calculated from the true heat conductance ratios.[2] For the purpose of this calculation the heat capacity of ethylene was evaluated statistically with the aid of an unpublished vibrational assignment of Linnett.[5]

The third columns of the (a) sections of Tables I and II give accommodation coefficient ratios calculated from the Y's in conjunction with the heat capacities of allene found by graphical interpolation of the experimental data of Kistiakowsky and Rice.[6] Columns four of the (a) sections and columns two of the (b) sections give accommodation coefficient ratios found by interpolation in the best straight line drawn through the experimental values and the value unity at 150°K.

Table VI. *Cyclopropane.*

Mean Temperature, °K	$Y_E+R/2$ Wire No. 1	$Y_E+R/2$ Wire No. 2	C_p° K. and R. and statistical	$Y_A+R/2$ Wire No. 2	$Y_A+R/2$ Wire No. 1
339.6					15.08
339.6					15.16
338.9			15.34	15.35	
338.9				15.37	
332.9		15.66	15.07	15.02	
332.6	16.40				14.70
325.3		15.20	14.69	14.66	
324.9	15.95				14.45
316.7	15.51				14.15
316.7	15.51				14.18
313.9		14.64	14.13	14.17	
313.9		14.64	14.13	14.17	
295.6	14.26				13.15
295.4		13.64	13.20	13.26	
291.6	14.05				13.01
291.1		13.40	13.03	13.12	
259.0	12.24				11.62
258.4		11.86	*11.50*	11.65	
223.9	10.49				10.17
223.4		10.30	*10.08*	10.17	
220.2		10.23	*9.96*	10.09	
219.9	10.36				10.06
158.0	8.49				8.47
157.6		8.44	*8.36*	8.44	

The difference in accommodation coefficient ratios from the two sets of wires noticeable in Tables I and II vanishes when heat conductances of allene are compared with those of gases having more nearly the same accommodation coefficients, i.e., the three-carbon molecules (cf. the following). It is gratifying to note that the heat capacities of allene calculated from comparisons with ethylene are identical for the two sets of wires.

Of course the assumption that the accommodation coefficient ratio becomes unity below 150°K is completely *ad hoc* but it cannot be tested in the absence of bracketing data. Actually, such an extrapolation represents well the change with temperature of the experimental accommodation coefficients on platinized wires as shown in Section (a) of Table I. Further, the total extrapolation amounts to less than 3 percent and hence knowledge of the precise dependence of the ratios on temperature is immaterial so long as heat capacities are to be determined to a few tenths of a percent only. Within this limit of error the experimental values are seen to be in excellent agreement with

[4] G. B. Kistiakowsky, J. R. Ruhoff, H. A. Smith and W. E. Vaughan, J. Am. Chem. Soc. **58**, 146 (1936).

[5] In the range 178.6 to 293.6°K Linnett's values are within 0.1 percent of the experimental values of Eucken and Parts (A. Eucken and A. Parts, Zeits. f. physik. Chemie **B20**, 184 (1933)). At 368.2°K, however, Linnett's value is 0.6 percent higher than the experimental.

[6] G. B. Kistiakowsky and W. W. Rice, J. Chem Phys. **8**, 610 (1940).

statistical values calculated from the same vibrational assignment as used by Kistiakowsky and Rice. Thus the present measurements may be regarded as a further confirmation of the correctness of the vibrational assignment given by Linnett and Avery.[7]

The accommodation coefficient ratios on the bare wires are very much larger and a linear extrapolation does not represent well the temperature dependence of the experimental values. It is therefore not surprising that here the calculated heat capacities do not agree so well with the statistical data.

Propylene

Propylene was part of the sample used for the heat of bromination determinations.[8] It was subjected to the same further treatment as was allene.

As the preceding section has shown, the statistical heat capacities of allene are completely trustworthy and therefore the heat conductances of propylene were compared with those of allene. The values of the accommodation coefficients given in Section (a) of Table III were obtained from the Y values using interpolations of the experimental heat capacities of propylene given by Kistiakowsky and Rice.[6] It will be seen that within experimental error all the accommodation coefficient ratios on the two bare (No. 1) and the two platinized (No. 2) wires are equal to unity. It was therefore assumed that the experimental values of $Y+R/2$ at the lower temperatures also represent directly the heat capacities and these are given in columns two and three of Section (b) of Table III.

The fourth column of Section (b) gives the residual heat capacities obtained on deducting $4R$ and the statistical vibrational heat capacity from the experimental values. The vibrational assignment of Wilson and Wells[9] was used. The residual values are due to internal rotation and they are in good agreement with statistical values calculated on the assumption that the restricting potential is 2100 cal./mole as discussed by Crawford, Kistiakowsky, Rice, Wells and Wilson.[9] The experimental values in the present communication are slightly higher than those previously reported because of the use here of the true Pirani ratios correcting heat conductance to equal pressures which were not available at the time of the preliminary publication.

The heat capacities here reported do not agree well with the assumption of a restricting potential of less than 800 cal./mole, whether the Wilson-Wells or the Pitzer vibrational assignment is chosen. We believe, therefore, that the higher value of the restricting potential is much more probable.

Propane

Through an error propane used in this work was taken from a cylinder containing impure material. This propane was scrubbed with bromine, sulphuric acid and sodium hydroxide solutions and was dried and vacuum distilled, but was found to contain up to 5 mole percent of lower and higher saturated hydrocarbons. This determination was made by Mr. Edwin E. Roper, to whom we are indebted for the information. Unfortunately, the discovery of the use of an impure material came too late to repeat the measurements and the following data are given with some reservations.

The heat conductances of propane were compared with those of allene and the results are given in Table IV. The accommodation coefficient ratios of Section (a) were computed using interpolated values of the heat capacity of propane measured by Kistiakowsky and Rice.[6] Although these ratios are very nearly unity, they do show a trend with temperature which is contrary to all other observations on such ratios. We are inclined to interpret the drift as due to the impurities in the material and the heat capacities at lower temperatures, calculated in Section (b) under the assumption that the accommodation coefficient ratios are unity, cannot be regarded as very accurate.

In the fourth column of Section (b) are given residual heat capacities after $4R$ and the vibrational contribution have been deducted from the experimental values. The vibrational assignment used here is that given by Kistiakowsky and Rice.[6] The last column gives statistical internal

[7] J. W. Linnett and W. H. Avery, J. Chem. Phys. **6**, 686 (1938).
[8] J. B. Conn, G. B. Kistiakowsky and E. A. Smith, J. Am. Chem. Soc. **60**, 2764 (1938).
[9] B. L. Crawford, Jr., G. B. Kistiakowsky, W. W. Rice, A. J. Wells and E. B. Wilson, Jr., J. Am. Chem. Soc. **61**, 2980 (1939).

TABLE VII. *Heats of hydrogenation in various states (kcal./mole).*

REACTION	ΔH_{298}	DIFF.	ΔH_0	DIFF.	ΔH_s	DIFF.
$C_2H_2+H_2$	−42.24	2.65	−39.38	2.61	−47.5	2.2
$C_3H_4+H_2$	−39.59		−36.78		−45.3	
$C_2H_4+H_2$	−32.82	2.71	−30.96	2.78	−39.1	2.5
$C_3H_6+H_2$	−30.11		−28.18		−36.6	

rotation heat capacity contributions calculated for a restricting potential of 3300 cal./mole from Pitzer's tables.[10] The agreement of these two sets of values is satisfactory in view of all the uncertainties of the experimental data.

Methyl acetylene

A sample was available from the work on its heat of hydrogenation[11] and was used after a bulb to bulb distillation in vacuum.

The heat capacity of this compound was determined, to within limits of a few hundredths calorie, by the bracketing procedure, for which ethylene and allene were used. The feasibility of this procedure is apparent from inspection of Table V, which shows that Y_E calculated from comparison with ethylene is smaller on the platinized wire (No. 2) than on the bare one (No. 1), while Y_A shows the reverse behavior. The actual heat capacity of methyl acetylene should lie, therefore, between the Y_E and Y_A values, but nearer to the latter. This follows because the accommodation coefficients between any three-carbon molecules have been generally found to be closer to unity than between such molecules and ethylene and also because Y_A values on the bare and platinized wires are closer together than are the Y_E's.

These conclusions are borne out in practice as shown by column four in which the italicized values of the heat capacity have been obtained statistically from the vibrational assignment of Crawford,[12] while the data at higher temperatures were interpolated from the measurements of Kistiakowsky and Rice.[6]

[10] K. S. Pitzer, J. Chem. Phys. **5**, 469 (1937).
[11] J. B. Conn, G. B. Kistiakowsky and E. A. Smith, J. Am. Chem. Soc. **61**, 1868 (1939).
[12] B. L. Crawford, Jr., J. Chem. Phys. **7**, 140 (1939).

Cyclopropane

The cyclopropane sample was taken from a Mallinckrodt cylinder of anaesthetic grade. It was distilled from dry ice in vacuum and the middle portion only was used for measurements. The impurities were found to be less than 0.5 mole percent using the differential vapor pressure method.

Cyclopropane is also bracketed by ethylene and allene in much the same manner as methyl acetylene. This is shown by the Y_E and Y_A values of Table VI. The true heat capacities of cyclopropane should lie again between the Y_E's and Y_A's, nearer to the latter. At lower temperatures, where Y_A's on the bare and platinized wires are practically identical, one would expect the heat capacity to be equal to Y_A. Column four gives the interpolated heat capacities of Kistiakowsky and Rice[6] and, in italics, statistically calculated heat capacities at lower temperatures. The vibrational assignment of Linnett[13] as modified by Kistiakowsky and Rice has been used for these calculations.

The data of column four do not fully agree with the Y values, being too low by about 1 percent at the lower temperatures and too near the Y_A values (i.e., again too low by about 1 percent) at the higher ones. A perfect fit of the two sets of data could be obtained either by reducing all Y values by one percent or by raising all heat capacities by a similar amount. The latter is very difficult to justify and one is forced to the conclusion that the true Pirani ratios for cyclopropane are wrong by about one percent. On the other hand, the ratios of Pirani gage readings in the calibration system at 30 and 200°C were identical for allene and cyclopropane and both Pirani gages used in this determination gave the same true Pirani ratios. The matter, therefore, cannot be definitely decided at present.

ON SOME HEATS OF GASEOUS REACTIONS AT 0°K

Experimental measurements of heat capacities of lower gaseous hydrocarbons, published recently from this laboratory, have agreed on the whole extremely well with statistical calculations based on the vibrational analyses developed

[13] J. W. Linnett, J. Chem. Phys. **6**, 692 (1938).

mainly by Wilson and his collaborators. In view of this, the calculations of the heat contents of lower hydrocarbons above absolute zero and of the zero point energies of these compounds may now be performed with reasonable accuracy. Hence it becomes possible to convert some of the heats of hydrogenation determined in this laboratory at 355°K to absolute zero and to the nonvibrating state of the molecules.

For this purpose the vibrational frequencies of ethylene were taken from Conn and Sutherland[14] except that the value for the torsional frequency was chosen as 820 cm^{-1} rather than 700 cm^{-1}. The former affords a better fit with the experimental heat capacity and has been suggested from overtone considerations.[15] The frequencies of ethane were taken from Stitt,[16] as were those of acetylene.[17] Assignments for methyl acetylene, propylene and propane have already been referred to. Contributions from internal rotation were taken from the tables of Pitzer,[10] with $V=3300$ cal./mole for propane, $V=2700$ for ethane and $V=2100$ for propylene. For hydrogen, data of Davis and Johnston[18] were used and its vibrational frequency taken as 4276 cm^{-1}.

In Table VII are reproduced the heats of hydrogenation of lower hydrocarbons as given by Conn, Kistiakowsky and Smith[11] for 355°K, together with the values for ΔH_0, the heats of gaseous reaction at absolute zero, and ΔH_s, the heats of reaction in the nonvibrating states. As was to be expected, the absolute values for the several reactions considered change greatly with the change of state of the molecules involved, but the differences of the reaction heats within each homologous series remain the same as closely as can be calculated.

TABLE VIII. *Ratio of heat capacities of the two butenes-2.*

AUTHOR	K. AND R.			NAZMI			
T, °K	371.2	332.9	298.6	303	253	223	193
C_p (*trans*) / C_p (*cis*)	1.062	1.076	1.082	1.09	1.09	1.09	1.10

[14] G. K. T. Conn and G. B. B. M. Sutherland, Proc. Roy. Soc. **A172**, 172 (1939).
[15] Eyster, private communication.
[16] F. Stitt, J. Chem. Phys. **7**, 297 (1939).
[17] F. Stitt, J. Chem. Phys. **8**, 56 (1940).
[18] Davis and Johnston, J. Am. Chem. Soc. **56**, 1045 (1934).

It is thus evident that the dependence of the heat change in a given reaction upon the adjacent groups in the molecule, a subject treated at length in recent years in thermochemical publications from this and other laboratories, is not something "superficial," due to an accidental choice of a particular state of the molecule for thermochemical measurement. Instead, it must be assigned to a fundamental alteration of the bonding strength within a molecule by adjacent substituents, a conclusion in general agreement with that reached by Conn, Kistiakowsky and Smith.

Before ending this paper we should like to comment on the energy difference between *cis*- and *trans*-butenes-2. Several years ago Dr. Falih Nazmi determined the heat conductances of these two gases by the hot wire method and found them different by about 10 percent.[19] At the time the results appeared so improbable that they were withheld from publication but recently Kistiakowsky and Rice[20] published measurements of the heat capacities of these compounds by the adiabatic method, finding similar differences. Table VIII gives the ratios of the two heat capacities (correcting heat conductance ratios from C_v to C_p) at several temperatures. Allowing for the inaccuracies of the then not fully developed "hot-wire" technique, the two sets of measurements are in excellent agreement and show that the percentage difference in the heat capacities observed at higher temperatures persists at least down to 190°K. Allowing for a decrease of the heat capacities with temperature it would seem that the difference remains substantially constant over this temperature interval. Hence the heat of isomerization of the *cis*- to the *trans*-compounds, which is equal to about 950 cal./mole at 355°K, increases with decreasing temperature and is equal to some 1200 cal./mole at absolute zero according to a rough extrapolation of the data given above.

Note added in proof.—Recently Kistiakowsky and Rice[3] have determined the heat capacities of the gases cyclopropane, ethylene oxide and di-methyl ether. As these gases were commercial

[19] F. Nazmi, Thesis, Harvard University, 1933.
[20] G. B. Kistiakowsky and W. W. Rice, J. Chem. Phys. **8**, 618 (1940).

samples it was thought advisable to secure accurate estimates of the amounts of impurities present.

The change in vapor pressure accompanying isothermal distillation of 95 percent of a sample identical with that used in heat capacity measurements was determined by Mr. W. W. Rice. The results at an average total pressure of 450 mm are as follows. Cyclopropane: 4.4 mm; ethylene oxide: 12.4 mm; di-methyl ether: 4.9 mm. These measurements indicate that the amount of impurity present in these samples is within the experimental error given for the heat capacity determinations.

DECEMBER, 1940 JOURNAL OF CHEMICAL PHYSICS VOLUME 8

Statistical Theory of Duplex Films

LAWRENCE S. K. FENG AND WILLIAM BAND
Physics Department, Yenching University, Peiping, China

(Received July 6, 1940)

The dissociation treatment of condensing systems is applied to duplex films. Complete agreement with the data on the saturated state of the films of myristic acid published by Adam and by Harkins is obtained on the following assumptions: (i) the momentum of each entire molecule contributes to the monolayer gas pressure; (ii) the interaction potential between the "liquid ends" of the molecules is equivalent to an "intrinsic pressure" which has the effect of increasing the surface tension at the interface between parent liquid and monolayer; (iii) this intrinsic pressure is derivable from a Lennard-Jones type of interaction potential depending on mean molecular area: $W=W_0+\alpha/A^{4.5}-\beta/A^3$; (iv) the tails of the molecules can form clusters, thus forming micelles in the duplex film, in which there are six bonds per molecule, each with interaction energy $\epsilon=-8.8\times10^{-14}$ erg per molecule. The field constants α, β seem to depend slightly on the nature of the parent liquid, but the energy ϵ is independent of this. The duplex film therefore appears to have its liquid layer in contact with the parent liquid, the free tails forming the gas layer. More data on different parent liquids are needed before a definite decision on this point can be made.

INTRODUCTION

IN previous work[1] the phase change of expanded mobile monolayers of fatty acids has been described in terms of the dissociation treatment of condensing systems. The equations for the saturated state of the expanded film were obtained in the form

$$FA=kT(1+\nu)/(1+\sigma), \qquad (1)$$

where ν and σ were sums depending on the value of ϵ/kT, ϵ being the mean energy per bond per molecule in the condensed phase; A was the area per molecule. Fair agreement with the data of Adam and Jessop[2] was obtained with a value $\epsilon=-3.7\times10^{-14}$ erg, assumed constant throughout the range of temperatures covered.

According to Langmuir's theory,[3] the condensed phase is duplex; the tails are responsible for the interaction energy W, and behave as a liquid layer, while the soluble heads behave as a gas layer. Langmuir studied the behavior of duplex films down through the second phase change where the tails condense into an assembly of micelles. In this study, the duplex film was supposed to behave essentially as a perfect gas, the pressure being reduced by a constant because of the attraction between the tails. Available area was also reduced by an amount which should be roughly the same as the area in the condensed film. The equation derived on these ideas was

$$(F-F_1)(A-A_0)=kT, \qquad (2)$$

[1] (a) "Statistical mechanics of condensation phenomena in mobile monolayers," J. Chem. Phys. **8**, 116–119 (1940). (b) "Adsorption isotherms for mobile monolayers," J. Chem. Phys. **8**, 178–180 (1940).

[2] Adam and Jessop, Proc. Roy. Soc. **A112**, 362 (1926).

[3] Langmuir, J. Chem. Phys. **1**, 756 (1933).

where F_1 was the pressure (actually negative) due to the tails, and A_0 the area correction per molecule. Langmuir obtained good agreement with the actual isotherms by using a constant value for F_1 and a value of A_0 which increased linearly with temperature, but was always much less than the area in the condensed phase.

Two weaknesses were recognized by Langmuir in this; first the required value of A_0 was too small, and secondly the value of F_1 had to be decreased considerably at the higher temperatures in order to fit the data. It has since been suggested by Harkins[4] that this may be due to some of the adsorbed molecules dissolving into the parent liquid at the higher temperatures.

It is proposed in the present paper to examine Langmuir's theory by means of the dissociation treatment of condensing systems.

Equation of State for Duplex Film

The equation of state for gaseous monolayers has already been given,[5] and to obtain that for duplex films at least an approximate equation of state is required for the liquid layer. It is obvious that Langmuir's assumption that the liquid tension is independent of area is the simplest, but a somewhat nearer approximation will be suggested here. In fact, it is clear that the liquid film should be regarded as generally in a greatly extended condition; just after the condensation from the true gas state, the liquid layer has a total area more than ten times that to which it collapses before the gas layer of the duplex film begins to condense. It is maintained in this extended condition simply by the pressure of the gas layer. The assumption of a constant attraction during an area change from 500 to 50A² per molecule seems highly questionable.

As a definitely better approximation the liquid layer will instead be pictured as an imperfect gas trapped in an intrinsic pressure—the two-dimensional analog of Laplace's liquid intrinsic pressure. In developing the statistical mechanics of a gas, the mass of the molecule is used; if there are two independent layers, each behaving as a gas, how much of the molecular mass operates in each layer? This question can hardly be answered so long as the duplex picture is retained. But if both layers behave as gases, there seems no real reason for considering them separately. Instead the film behaves essentially as a single monolayer, the entire molecule being operative in producing the pressure; the attractions between their "liquid ends" have no other effect than that of producing an intrinsic pressure acting on the assembly.

Write the partition function for a molecule in the form

$$f(T)=f_0(T)\exp(-W/kT), \tag{3}$$

where W is to be interpreted as the mean internal free energy per molecule at their liquid ends. The pressure exerted by the assembly will then be

$$F=kT\partial/\partial A(\ln f(T)) = kT\partial/\partial A(\ln f_0(T))-\partial W/\partial A, \tag{4}$$

where A is the area per molecule. The first part of this expression is the gas pressure, F_g say, from which all terms due to mutual attractions between the liquid ends of the molecules have been eliminated; the second part of the expression is the negative intrinsic pressure due to these attractions. The first term leads to the same result as formerly, see (24)I:

$$F_g=[kT/(A-A_0)](1+\nu)/(1+\sigma), \tag{5}$$

where A_0 is an area which depends only on the collision cross section of the molecules, and will be temperature dependent. The resultant pressure is therefore

$$F=F_g+F_1, \tag{6}$$

where

$$-F_1=\partial W/\partial A \tag{7}$$

is the intrinsic pressure due to the attraction between the liquid ends of the molecules. Although the whole molecule is now considered operative in producing F_g, it is still convenient to speak of the plane containing the free ends of the molecules as the "gas layer," and the plane containing the liquid ends as the "liquid layer."

Saturated State of Duplex Films

The conditions for saturation of the gas layer are presumably not altered by the presence of the liquid layer. The relative number of clusters, or

[4] Harkins and Nutting, J. Am. Chem. Soc. **61**, 2041 (1939).

[5] Reference 1, Eq. (24): such equations will be indicated hereafter by (24) I.

micelles, of type s in the gas layer is still given by (21)I, which with (20)I becomes:

$$\mu_s=(A/\rho)(1-\beta_s)s^2\exp(\phi_s-\phi_1)/kT. \quad (8)$$

From (15)I this gives

$$F_g=(kT/\rho)\sum_{s=2} s^2\exp(\phi_s-\phi_1)/kT \quad (9)$$

or

$$F_g=(kT/\rho)(1+\nu), \quad (10)$$

for the pressure of the gas in its saturated state. From the definition of ρ, (19)I, we now find that

$$6\epsilon/kT=\ln F_g-\ln(1+\nu)-(5/2)\ln kT -\tfrac{1}{2}\ln A_0-\ln(4\pi^2m^1/h^3). \quad (11)$$

Here the number of bonds per molecule has been assumed to be six, ϵ is the energy per bond per molecule in the micelle, and m is the mass of the entire molecule; A_0 should be almost identical with the A_0 in (5).

It is found in fact that ϵ/kT is between minus two and three, while ν and σ are very small compared with unity. Because of these circumstances, the expansions for ν and σ, Eq. (28)I, are practically equal to their first terms. These reduce to:

$$\nu=4\exp(0.3378\times 6\epsilon/kT),\qquad \sigma=8\exp(0.3378\times 6\epsilon/kT). \quad (12)$$

In (11) the term in $(1+\nu)$ is, therefore, entirely negligible, so this equation gives

$$\epsilon/kT=0.3838[\log F_g-\tfrac{1}{2}\log A_0 -(5/2)\log T-8.352]. \quad (13)$$

Again because $(1+\nu)/(1+\sigma)$ differs but slightly from unity, our Eqs. (5) and (6) together almost coincide with (2); then, since Langmuir found good agreement between (2) and the isothermals by using constant F_1, we may assume that (5) and (6) give a good approximation to the isothermals near saturation with nearly constant F_1 for any one isothermal. With this approximation the slope of the isothermals near saturation can thus be determined by differentiating (6), using (5):

$$dF/dA=-(F_g^2/kT)(1+\sigma)/(1+\nu). \quad (14)$$

Using (12) and (13), and assuming, as will be shortly verified, that A_0 is roughly 15A², this can be written

$$dF/dA=-(F_g^2/kT)\frac{0.5190T^{0.8445}+2(F_g)^{0.3378}}{0.5190T^{0.8445}+(F_g)^{0.3378}}. \quad (15)$$

The experimental data on dF/dA for isothermals close to the saturation point then determine F_g from (15) as a function of T. The values of F_1 at once follow from (6). Equation (13) also permits a direct evaluation of ϵ/kT, and this in turn, through (12) gives ν and σ. Equation (5) now gives

$$A_0=A-(kT/F_g)(1+\nu)/(1+\sigma), \quad (16)$$

which determines A_0 from quantities already found.

Table I gives the results of this method of analyzing the data given by Adam[2] for myristic acid on 0.01N HCl; Table II refers to the data given by Harkins[4] for myristic acid on 0.01N H_2SO_4.

TABLE I.* *Analysis of Adam's data.*

T	dF/dA	F	A	F_1	A_0	$\frac{(1+\nu)}{(1+\sigma)}$	$\epsilon\times10^{14}$
280.3	−0.37	1.2	43.0	10.6	11.6	0.963	−8.83
282.2	−0.50	2.7	40.9	11.0	13.7	0.962	−8.80
285.2	−0.75	5.6	36.9	11.2	14.5	0.960	−8.79
287.2	−0.97	7.8	35.0	11.4	15.3	0.959	−8.77
291.2	−1.57	12.8	32.2	11.8	16.6	0.958	−8.75
295.4	−2.12	17.4	30.6	11.3	17.1	0.957	−8.79
299.3	−2.28	21.7	29.1	8.2	16.0	0.956	−8.90

* Units: F in dynes/cm, A in angstroms², ϵ in ergs. Mean value of $\epsilon=-8.8\times10^{-14}$ erg.

TABLE II.* *Analysis of Harkins' data.*

T	dF/dA	F	A	F_1	A_0	$\frac{(1+\nu)}{(1+\sigma)}$	$\epsilon\times10^{14}$
279.8	−0.28	0.6	41.2	9.4	4.1	0.966	−8.92
282.6	−0.60	2.7	36.9	12.3	12.0	0.962	−8.76
285.6	−0.94	6.2	32.8	12.6	12.8	0.960	−8.72
287.9	−1.20	8.0	31.5	13.4	13.8	0.958	−8.72
289.7	−1.40	10.4	30.4	12.7	13.9	0.958	−8.73
294.8	−1.99	18.1	27.6	9.6	13.7	0.956	−8.80
298.1	−1.83	20.9	25.9	5.9	11.7	0.956	−8.93

* Units: F in dynes/cm, A in angstroms², ϵ in ergs. Mean value of $\epsilon=-8.8\times10^{-14}$ erg.

DISCUSSION

It is specially to be remarked that on the present interpretation, A_0 refers to the collision cross section in the gas layer, not in the liquid layer, and is roughly the area per molecule in the micelle at its narrow end. The values obtained lie fairly close to the straight line used by Langmuir.

The values of F_1 are not well represented by Langmuir's constant. As is obvious from the figures, there is a marked falling off of F_1 between

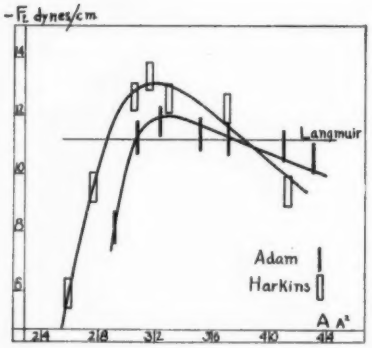

FIG. 1. Intrinsic pressure due to liquid layer shown as a function of molecular area.

20°C and 25°C, and the form of the curves suggests that there may be a true dependence of F_1 upon molecular area in the film. The values refer to the saturated state, and therefore the curves can at once be translated into curves of F_1 against A. Equation (7) then gives $\partial W/\partial A$ as a function of A, as shown in Fig. 1.

Now it is interesting to speculate that perhaps the area-dependent part of the internal energy W depends upon mean molecular distance in the general Lennard-Jones manner, thus:

$$W=W_0+\alpha_0/r^9-\beta_0/r^6,$$

or, translating into areas with appropriate adjustment of the constants:

$$W=W_0+\alpha/A^{4.5}-\beta/A^3. \tag{17}$$

If this were so, it would follow that

$$\partial W/\partial A=-4.5\alpha/A^{5.5}+3\beta/A^4, \tag{18}$$

and therefore that a plot of $(\partial W/\partial A)A^4/3$ against $(\frac{3}{2})A^{-1}$ should be a straight line, with $-\alpha$ as the gradient, and β as the intercept. These plots are shown in Fig. 2 and are seen actually to lie very nicely on straight lines, specially in the case of Harkins' data. There is no trouble with the points corresponding to higher temperature, and no need to suppose special dissolving of the film there. The values of α and β for the two sets of data are, expressed in c.g.s. units:

$$\begin{aligned}\text{Adam's data}\quad &\alpha=2.0\times10^{-79},\\ &\beta=2.1\times10^{-57},\\ \text{Harkins' data}\quad &\alpha=1.4\times10^{-79},\\ &\beta=1.7\times10^{-57}.\end{aligned}$$

On this hypothesis it is evident that the nature of the parent liquid seems to have some slight effect on the tension in the liquid layer of the duplex film. On the other hand it is also evident that there is practically no difference between the values of ϵ in the two cases. These facts could be nicely accounted for by supposing that the heads of the molecules, adsorbed to the parent liquid, are the first to condense to form the duplex film, their energy W depending on the nature of the parent liquid. The tails are not in contact with the parent liquid, and their interaction

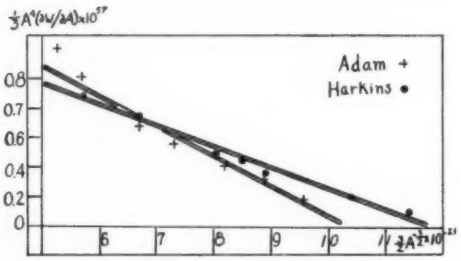

FIG. 2. Straight lines to determine the Lennard-Jones constants from the intrinsic pressure as a function of molecular area.

energy ϵ, upon condensing into micelles, is independent of the nature of this liquid. This picture of the duplex film is essentially in agreement with that originally proposed by Adam,[6] but opposite to that presented more convincingly by Langmuir[3] and later accepted also by Adam.[7] The present picture also explains the anomalously small values of A_0 compared with the area per molecule in the condensed film; for the tails of the molecules determine A_0, and these are smaller than the heads which determine the area of the condensed film.

However, if the two points corresponding to lowest T in Adam's data are ignored, the constants can be made almost the same as those for Harkins' data. At these lower temperatures the gradients of the isothermals are very small and the saturation point cannot be determined with high precision. Too much stress should therefore not be put upon the differences between the two sets of constants. It would be very interesting to have more extensive data on the isotherms of myristic acid duplex films formed on different parent liquids and to analyze such data from the present point of view.

[6] N. K. Adam, *The Physics and Chemistry of Surfaces*, 1st edition (Oxford University Press, New York, 1930).
[7] *The Physics and Chemistry of Surfaces*, 2nd edition (Oxford University Press, New York, 1938).

The Gaseous Heat Capacity and Restricted Internal Rotation of Diborane

FRED STITT*
Mallinckrodt Chemical Laboratory, Harvard University, Cambridge, Massachusetts,
and
Department of Chemistry, Indiana University, Bloomington, Indiana

(Received September 30, 1940)

The heat capacity of gaseous diborane has been measured from 95° to 324°K with the low pressure thermal conductivity apparatus described earlier. The bracketing method was applied over most of this temperature range, with acetylene and ethylene as comparison gases. At 95°K, ethylene and ethane were used as comparison gases and the accommodation coefficient ratios were assumed to be unity. The heat capacity at low temperatures indicates that internal rotation in the diborane molecule is restricted by a potential barrier whose height is probably between 4000 and 6000 cal./mole if the barrier is assumed to be a sinusoidal function of the internal rotational angle.

THE low temperature gaseous heat capacity of ethane[1–3] furnishes probably the most direct evidence that internal rotation in this molecule is hindered by a moderately high potential barrier. Similar evidence reported here indicates that internal rotation in diborane is hindered by a potential barrier probably somewhat higher than that of the ethane molecule.

The heat capacity of gaseous diborane from 94° to 324°K has been determined from low pressure thermal conductivity measurements. Over most of this temperature range the heat conductances of diborane, ethylene, and acetylene gases were compared under similar conditions; the heat capacity of diborane was calculated from these data by application of the bracketing method described earlier.[2]

Experimental Details

I am indebted to Dr. A. B. Burg for very kindly furnishing a sample of pure diborane for these measurements. The material, sent by air mail, was kept at dry ice temperature to prevent its slow thermal decomposition. Immediately before each sample was taken, the material was pumped off at liquid-air temperature to remove any hydrogen which might have formed. The sample was then taken from the first portion of the liquid to vaporize, as decomposition products other than hydrogen are nonvolatile compared to diborane. There was no evidence of appreciable decomposition at any time.

Ethylene and acetylene were used as comparison gases at all temperatures except in the neighborhood of 95°K, where ethylene and ethane were used. The ethylene and ethane were from the same samples used in earlier work.[2] The acetylene was Prest-o-lite material purified by passage through saturated $NaHSO_3$ solution, 10 percent NaOH solution, $0.2N$ I_2 in KI solution, $0.3N$ $Na_2S_2O_3$ solution, water, calcium chloride, and dehydrite.

The gaseous thermal conductivity apparatus previously described[2,4] was used also in this study with essentially the same experimental procedure. Three conductivity cells were used as before: the Pirani gauge (maintained at 0°C), cell No. 1 with bare platinum wire, and cell No. 2 with platinized platinum wire. At each bath temperature the thermal conductivities of the gases were compared at more than one pressure with a difference of approximately 15° between the temperatures of the cell wire and the cryostat.

Experimental Results

The method of calculating the heat capacity from the thermal conductivity data has already

* National Research Fellow in Chemistry, 1937–39. Present address: Department of Chemistry, Indiana University, Bloomington, Indiana.

[1] (a) G. B. Kistiakowsky, J. R. Lacher, and F. Stitt, J. Chem. Phys. **6**, 407 (1938). (b) E. B. Wilson, Jr., J. Chem. Phys. **7**, 408 (1938).

[2] G. B. Kistiakowsky, J. R. Lacher, and F. Stitt, J. Chem. Phys. **7**, 289 (1939).

[3] K. Schäfer, Zeits. f. physik. Chemie **B40**, 357 (1938).

[4] G. B. Kistiakowsky and F. Nazmi, J. Chem. Phys. **6**, 18 (1938).

TABLE I. *Values of Y_x of Eq. (1).*

Run No.	Bath Temp. °K	No. Pipets*	Cell No. 1 Mean Temp. °K	Cell No. 1 $Y_{C_2H_2}$	Cell No. 1 $Y_{C_2H_4}$	C_v C_2H_2	C_v C_2H_4	Cell No. 2 Mean Temp. °K	Cell No. 2 $Y_{C_2H_2}$	Cell No. 2 $Y_{C_2H_4}$
40	317.13	1	324.0	13.67	12.78	9.01	8.92	324.0	13.53	13.35
		2		13.65	12.75				13.51	13.35
39	280.88	1	288.2	12.53	11.75	8.38	8.13	288.0	12.33	12.19
		2		12.51	11.72				12.29	12.17
43	242.76	1	250.3	11.24	10.75	7.64	7.36	250.3	10.90	10.85
		2		11.16	10.67				10.84	10.81
42	211.81	1	219.8	10.11	9.76	6.96	6.82	219.7	9.89	9.86
		2		10.01	9.73				9.86	9.85
45	178.28	1	185.4	9.01	8.82	6.22	6.38	185.2	8.91	8.86
		2		8.95	8.82				8.87	8.87
44	145.46	1	152.8	8.16	8.07	5.60	6.12	152.6	8.18	8.12
		2		8.20	8.07				8.20	8.10
		3		8.21	8.10				8.22	8.15

* For all except run 44, each pipet corresponded to a pressure of about 0.014 mm at room temperature. For run 44, each pipet corresponded to a pressure of about 0.0024 mm at room temperature.

been presented.[2] The values of Y calculated from the heat conductance ratios as shown below in Eq. (1), are recorded in Table I for all measurements except those at the lowest temperature of the cryostat. The mean temperatures recorded in the table refer to the mean of the wire and the bath temperatures. Y is defined by the equation

$$Y_x=(C_v+R/2)_{B_2H_6}\frac{\alpha_{B_2H_6}}{\alpha_x}$$

$$=\frac{Q_{B_2H_6}}{Q_x}(C_v+R/2)_x\left(\frac{M_{B_2H_6}}{M_x}\right)^{\frac{1}{2}}, \quad (1)$$

where x refers to the comparison gas, Q refers to the heat conducted, and M refers to the molecular weight. The values of the molal heat capacity taken as correct for the comparison gases[5] are also included in Table I. Note that $Y_{C_2H_2}$ is greater for cell No. 1 than for cell No. 2, whereas the reverse is true of $Y_{C_2H_4}$. This indicates that the accommodation coefficients for these gases bear the following relationship to each other:

$$\alpha_{C_2H_4}>\alpha_{B_2H_6}>\alpha_{C_2H_2}.$$

This conclusion assumes that the hypotheses underlying the bracketing method[2] hold for this case, namely, that both the accommodation coefficient for each gas and the accommodation coefficient ratio for any two of the gases are more nearly unity for the platinized than for the bare platinum wire. The fact that the Y values at a given temperature differ less for cell No. 2 than for cell No. 1 is in agreement with these hypotheses. Note also that all of the Y values become more nearly the same at lower temperatures, in agreement with the general rule that all the accommodation coefficients approach unity as the temperature is lowered.

Differential adsorption was tested and corrected for by means of the Pirani gauge in the same manner as in the earlier work.[2] No evidence of adsorption was found in any of the measurements relating to Table I except for run 44, for which the bath temperature was 145.46°K. In this case the correction was small, being about 1 percent and 1.5 percent for ethylene and acetylene, respectively, as comparison gases, acetylene being the most adsorbed and diborane the least.

Because of thermal transpiration[6] the gaseous pressure is not the same throughout the apparatus, the pressure being somewhat lower in the colder portions. The magnitude of these so-called thermomolecular pressure differences depends on the size of the tubing connecting the portions at different temperatures, the temperature differences, and the mean free path of the gas mole-

[5] The heat capacity of ethylene was found as in reference 2. That of acetylene was calculated from the experimental fundamental vibration frequencies given in Table II of F. Stitt, J. Chem. Phys. **8**, 56 (1940) using the rigid rotator-harmonic oscillator approximation. These values are in satisfactory agreement with the few experimental values available for acetylene.

[6] O. Reynolds, Phil. Trans. Roy. Soc. London **170**, 727 (1879); M. Knudsen, Ann. d. Physik **31**, 205 (1910).

cules present. If the kinetically effective molecular diameters of the gases compared are not approximately the same, the thermomolecular pressure differences will be different for the various gases, and the experimental heat conductance ratios must be corrected for this effect. Thus when the cryostat temperature is below that of the 12-l reservoir (300°K), the same gas pressure in the reservoir corresponds to a greater pressure in the cryostat cells for diborane than for the comparison gas due to the larger molecular diameter of the former; consequently, use of the experimental heat conductance ratio in Eq. (1) would lead to too high a value of the heat capacity of diborane. The Y values of Table I have not been corrected for this effect. Weber[7] has recently studied thermomolecular pressure differences both theoretically and experimentally, testing various equations for the calculation of these differences. Although the kinetic data necessary for a precise calculation of this effect in the case of diborane are not available, its magnitude can be readily estimated. Fortunately the differential effect in comparing two gases is small enough so that the uncertainty in this correction does not contribute much to the uncertainty of the final heat capacity values. This correction has been estimated by using the following equation[8] to calculate the thermomolecular pressure difference for each gas:

$$\frac{p_2}{p_1}=\left(\frac{T_2}{T_1}\right)^{\frac{1}{2}\{1/(1+2R/\lambda)\}} \qquad (2)$$

where $R=1.5$ mm is the radius of the cylindrical tubing connecting the portions of the apparatus at the temperatures T_1 and T_2, and λ is an average value of the mean free path of the molecules.[9] The values of the effective molecular diameter employed were 5.0, 5.3, 4.7, and 5.8A for ethylene, ethane, acetylene, and diborane, respectively.[10] Although Eq. (2) is not adequate for an accurate calculation of the thermomolecular pressure differences, its use for calculating differential effects leads to results differing less from those calculated with the more accurate Eqs. IV and VII of Weber[7(c)] than the uncertainty due to the absence of a reliable value of the effective collision diameter of diborane. The values of the heat capacity of diborane calculated from the Y values of Table I for cell No. 2 by correcting for the thermal transpiration effect and by assuming the accommodation coefficient ratio of Eq. (1) to be unity are shown in Table II. The correction factors applied for the thermal transpiration effect are included in the table. The values thus calculated from $Y_{C_2H_2}$ and $Y_{C_2H_4}$ should form upper and lower limits, respectively, to the correct values of the heat capacity of diborane. It is seen that, except for the highest two temperatures, these two values are the same within experimental error. The small variations in the Y values of Table I with pressure, although of the same order of magnitude as experimental error, are seen to be in rough agreement with those expected due to thermal transpiration. In this connection it is interesting to note that the heat conductance ratio may either increase or

TABLE II. *Heat capacity of diborane.*

No. Pipets*	Temp. °K	Transpiration Factor (C_2H_2)	C_v of B_2H_6 in cal./deg.-mole $\alpha_{B_2H_6}=\alpha_{C_2H_2}$	$\alpha_{B_2H_6}=\alpha_{C_2H_4}$	Transpiration Factor (C_2H_4)
1	324.0	1.003	12.57	12.38	1.002
2		1.002	12.54	12.37	1.001
1	288.0	0.996	11.29	11.16	0.997
2		0.997	11.27	11.16	0.998
1	250.3	0.991	9.81	9.79	0.994
2		0.993	9.77	9.77	0.995
1	219.7	0.983	8.73	8.75	0.988
2		0.987	8.74	8.77	0.991
1	185.2	0.976	7.71	7.72	0.983
2		0.983	7.73	7.77	0.988
1	152.6	0.970	6.95	6.96	0.979
2		0.960	6.88	6.88	0.972
3		0.960	6.90	6.92	0.971

* See footnote to Table I.

[7] (a) S. Weber, Leiden Communications, Supplement 71b, (1932); No. 246*b* (1937), (b) S. Weber, W. H. Keesom, and G. Schmidt, *ibid.* No. 246*a* (1937); (c) S. Weber and G. Schmidt, *ibid.* No. 246*c* (1937).

[8] This approximate integrated equation was used by Knudsen, Ann. d. Physik **31**, 633 (1910).

[9] In Eq. (2), λ was taken as the arithmetic mean of the mean free paths calculated from the molecular diameter and molecular concentration for the two regions of different temperature.

[10] Kennard, *Kinetic Theory of Gases* (McGraw-Hill, New York, 1938), p. 149, lists values for ethane and ethylene. Those for acetylene and diborane are assumed.

TABLE III. *Heat capacity of diborane at 95°K.*

Run No.	No. Pipets*	Mean Temp. °K	Adsorption Factor	Transpiration Factor	$Q_{B_2H_6}/Q_s$		C_v of B_2H_6 cal./deg.-mole		Comparison Gas
					Cell No. 1	Cell No. 2	Cell No. 1	Cell No. 2	
46	1	98	0.972	0.993	1.127	1.116	6.54	6.46	C_2H_4
46	1	98	1.205	1.002	0.876	0.874	6.72	6.70	C_2H_6
41	1	98	1.129	0.995	0.969	0.995	6.54	6.75	C_2H_4
46	2[a]	98	0.990	0.983	1.102	1.110	6.43	6.48	C_2H_4
46	2[b]	98	0.963	0.978	1.110	1.122	6.26	6.33	C_2H_4
46	2[a]	98	1.074	0.996	0.966	0.977	6.54	6.62	C_2H_6
46	2[b]	98	1.046	0.991	0.973	0.989	6.36	6.47	C_2H_6
41	2	98	1.090	0.985	1.006	1.030	6.49	6.67	C_2H_4
46	3[a]	98	0.990	0.972	1.090	1.103	6.27	6.36	C_2H_4
46	3[b]	98	0.970	0.972	1.093	1.103	6.15	6.22	C_2H_4
46	3[a]	98	1.040	0.972	0.993	1.009	6.32	6.44	C_2H_6
46	3[b]	98	1.021	0.971	0.996	1.009	6.21	6.29	C_2H_6
41	1†	98	1.012	0.969	1.055	1.068	6.17	6.26	C_2H_4
46	1	94	0.972	0.993	1.126	1.150	6.53	6.68	C_2H_4
41	1	94	1.129	0.995	0.963	1.010	6.50	6.86	C_2H_4
46	2	94	0.990	0.983	1.096	1.121	6.39	6.55	C_2H_4
41	2	94	1.090	0.985	1.015	1.029	6.56	6.66	C_2H_4
46	3	94	0.990	0.972	1.087	1.110	6.24	6.40	C_2H_4
41	1†	94	1.012	0.969	1.048	1.057	6.12	6.18	C_2H_4

* Each pipet corresponds to a pressure of 0.00067 mm at room temperature.
† One pipet corresponds to a pressure of 0.0024 mm at room temperature.
[a,b] These series compare measurements on two different diborane samples with those on a single sample of comparison gas.

decrease with increasing pressure as a result of thermal transpiration, depending on the pressure range involved.

The vapor pressure of diborane at 90°K was found to be considerably lower than that of ethane. Because of this fact it was necessary to work at very low pressures at this lowest temperature of the cryostat. At a pressure of 0.0017 mm in the cryostat cells, heat conductance measurements showed the pressure to be definite with no tendency to drift, whereas at a pressure corresponding to 0.0032 mm in the cryostat cells, the steady drop in pressure indicated that condensation was taking place. The vapor pressure of diborane at 89.5°K is, accordingly, between 0.0017 and 0.0032 mm. Similarly, in the earlier work the vapor pressure of ethane was found to be between 0.0055 and 0.0076 mm at this same temperature.

Two series of measurements were made with the cryostat at 90°K. Ethylene was used as the comparison gas in the first; in the second, both ethylene and ethane were used. Acetylene could not be used because its vapor pressure is too low at this temperature. Heat conductances were measured with two different wire temperatures in most cases, corresponding to differences of approximately 9° and 17° in the temperatures of the wire and the cryostat. The results of the measurements are shown in Table III, which contains the experimental heat conductance ratios and the factors by which these ratios were corrected for differential adsorption and thermal transpiration effects. In calculating the heat capacity values of Table III it was assumed that the accommodation coefficient ratios were unity on both the bare and the platinized platinum wires. This assumption probably leads to no error, for Tables I and II indicate that the accommodation coefficients of diborane and ethylene are effectively the same at 150°K on both wires, and earlier work[4] has shown the same to be true with regard to ethylene and ethane. Values of 5.97 and 6.60 calories per degree-mole were used for C_v of ethylene and ethane respectively. The correction for adsorption was determined as before. The thermal transpiration correction was calculated as described above; the values in Table III take into account the fact that because of adsorption the pressures of the gases compared are different in the 12-liter reservoir as well as in the cryostat cells. Because of the low pressures which had to be used, experimental errors in the heat conductance ratios of Table III are considerably larger than at higher temperatures, or than for the similar low temperature

measurements on ethane.[2] At the lowest pressures the heat loss from the wire by radiation was almost as great as that lost by conduction through the gas. Also, at these very low pressures the short arm of the conductivity cell affords inadequate compensation for the heat lost by conduction through the ends of the wire, leading to incorrect radiation corrections. These errors should be relatively smaller at higher pressures. On the other hand the thermal transpiration correction is larger and more uncertain for the higher pressures of Table III, but despite this, the higher pressure data are probably somewhat more reliable. In general the heat capacity values of Table III are the same for both comparison gases and for both cells. In most of the measurements on the same gas sample, the heat conductance ratio was slightly larger for cell No. 2 than for No. 1. This effect is probably not due to a difference in the accommodation coefficient ratios on the two wires, for in that case it would correspond to a larger ratio on the bare wire, which seems unreasonable in view of the higher temperature results. It may be due to slightly poorer compensation for end losses in cell No. 2 than No. 1. From the data of Table III it is concluded that diborane has $C_v = 6.35 \pm 0.20$ cal. per mole-degree at 95°K.

The values of the heat capacity of ethane calculated from the data of run 46 were 6.41, 6.50, 6.56 and 6.36, 6.46, 6.53 for one, two, and three pipets in cells Nos. 1 and 2, respectively, in satisfactory agreement with the earlier work. The values in Tables II and III of the heat capacity of diborane in the ideal gaseous state are shown graphically in Fig. 1.

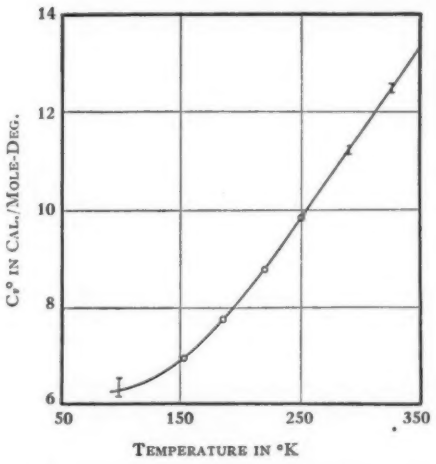

FIG. 1. The gaseous heat capacity of diborane as a function of the temperature.

DISCUSSION

The interatomic distances in the diborane molecule are considerably larger than the analogous ones in the similarly shaped ethane molecule.[11] Internal rotation of the methyl groups relative to each other about the carbon-carbon single bond has been shown to be restricted by a potential barrier of the order of 3000 calories per mole in ethane,[12] whereas in dimethlyacetylene free internal rotation of the methyl groups is found.[13] The origin of the restricting potential in ethane is not definitely known at present. If the magnitude of the potential is primarily dependent on the distance between the two methyl groups, it would be expected that internal rotation would be less restricted in diborane than in ethane, provided that other factors involved are not greatly different for the two cases. It is found, however, that the potential barrier is higher in diborane than in ethane.

At 95°K and above, translation and over-all rotation contribute $3R = 5.96$ calories to the molal heat capacity of diborane. Since the measured heat capacity at 95° is 6.35 ± 0.2 cal., there remains only 0.4 ± 0.2 cal. due to other degrees of freedom. If internal rotation were free, this remainder would be at least $R/2 = 0.99$ cal. If the potential barrier is assumed to be a sinusoidal function of the angle of internal rotation, the height of the barrier corresponding to an internal rotational contribution to the molal heat capacity of 0.4 ± 0.2 cal. at 95° is calculated[14] to be between 3300 and 6000 cal. per mole. The heat capacity at 142°K shows that the barrier must be greater than 4000 cal. since any lower barrier (except a very low one) results in a contribution of more than 1.10 cal. at 150°K from this librational degree of freedom. It is,

[11] S. H. Bauer, J. Am. Chem. Soc. 59, 1096 (1937).
[12] See reference 1(a) and papers referred to there.
[13] B. L. Crawford, Jr., and W. W. Rice, J. Chem. Phys. 7, 437 (1939); D. W. Osborne, C. S. Garner, and D. M. Yost, J. Chem. Phys. 8, 131 (1940).
[14] See K. S. Pitzer, J. Chem. Phys. 5, 649 (1937). The molecular dimensions found in reference 11 were used in calculating the moment of inertia.

accordingly, concluded that the potential barrier restricting internal rotation in the diborane molecule is probably between 4000 and 6000 cal. per mole.[15]

[15] Should the vibrational (or electronic) contribution to C_v at these low temperatures be appreciable, the barrier would be still higher.

The heat capacity at higher temperatures serves as a check on the analysis of the vibrational spectrum of diborane, which will be discussed in another paper.

In conclusion, I wish to thank Professor Kistiakowsky and Dr. W. W. Ransom for facilitating the pursuit of this investigation.

DECEMBER, 1940 JOURNAL OF CHEMICAL PHYSICS VOLUME 8

A Theoretical and Experimental Analysis of the Capillary Rise Method for Measuring the Surface Tension of Solutions of Electrolytes

GRINNELL JONES AND LAURENCE D. FRIZZELL
Mallinckrodt Chemical Laboratory, Harvard University, Cambridge, Massachusetts

(Received August 24, 1940)

Jones and Ray made measurements of the capillary rise of solutions of electrolytes which they interpreted as showing that there is a minimum in the surface tension-concentration curve at low concentration (about 0.001N). Langmuir has suggested that the liquid film above the meniscus may be several hundred angstroms thick and may be sufficiently different for water and for solutions of electrolytes to account for the observed capillary rises without drawing the conclusion that there is a minimum in the surface tension. Langmuir's theory is analyzed in detail and one of its premises is shown to be inconsistent with experimental evidence of several kinds which indicates that a solution-air interface is electrically charged. Langmuir's theory gives the thickness of the wetting film as an explicit function of the concentration and temperature of the solution; and of the capillary rise (which depends on the radius of the tube and on the surface tension of the liquid); and of the zeta-potential. But unfortunately zeta-potentials are not known with sufficient precision to permit reliable calculations of the thickness of the wetting film. Some of the consequences of the theory are tested experimentally.

IN an earlier paper Grinnell Jones and Wendell A. Ray[1] described a modification of the capillary rise method of measuring surface tension which makes it a more precise differential method and have reported measurements on aqueous solutions of three salts and of sucrose covering a wide range of concentration. The most striking feature of these results was that the capillary rise for dilute solutions of the three salts was less than for water, which was interpreted as showing that the surface tension of these dilute solutions was less than that of water and that the surface tension-concentration curve has a minimum at about 0.001N and then rises and becomes greater than for water at about 0.006N.

The fundamental equation for the calculation of the surface tension from capillary rise is

$$\sigma = h(D-\beta)gr/2, \tag{1}$$

postulating that the contact angle is zero, which for relative measurements becomes

$$\sigma_c/\sigma_0 = h_c(D_c-\beta)r_c/h_0(D_0-\beta)r_0. \tag{2}$$

In our modification of the capillary rise method the necessity of measuring the radius of the capillary is avoided by bringing the upper meniscus for both solution and water to the same marked position on the capillary so that the exact value of the radius does not need to be known for the calculation of the relative surface tension provided the difference between the thickness of the wetting film for the solution and for water is negligible in comparison with the radius, as was assumed. The experimental diffi-

[1] Grinnell Jones and Wendell A. Ray, J. Am. Chem. Soc. 59, 187 (1937).

culty of making a precise measurement of the height of the meniscus in the wide tube by a cathetometer is avoided by using an indirect method based on weighing the apparatus, which permits a more precise value for the relative capillary rise to be calculated.

Bikermann and Dole[2] have developed theories which account for the minimum in the surface tension as due primarily to a surface electric charge (commonly negative) which is caused by separation of ions in the surface layer under the influence of the dipoles in water.

Irving Langmuir[3] has suggested a different interpretation of our experimental data which would not lead to the conclusion that there is a minimum in the surface tension at low concentrations. He has applied the Debye theory of electrolytes to some problems in colloids and to the phenomena of liquid films in contact with solid surfaces, which has led him to the conclusion that the wetting films of liquids on solid surfaces, which have been drained as completely as possible, are not merely a few molecules thick as has been commonly assumed in the past, but are really much thicker and that the thickness of the wetting film is greatly influenced by the concentration of the ions. According to this theory the wetting film left after drainage is thicker for pure water than it is for solutions of electrolytes. Let r represent the real radius of the dry capillary, Δr_c the thickness for a solution of concentration c, and Δr_0 the thickness for water then Eq. (2) should read

$$\frac{\sigma_c}{\sigma_0}=\frac{h_c}{h_0}\left(\frac{D_c-\beta}{D_0-\beta}\right)\left(\frac{r-\Delta r_c}{r-\Delta r_0}\right). \tag{2a}$$

This reduces to Eq. (2) if $\Delta r_0=\Delta r_c$ or if both are negligible in comparison with r. On the other hand, if Δr_0 is greater than Δr_c this would give a correcting factor greater than 1. If it can be shown that Δr_0 is greater than Δr_c by an amount of about 250 angstroms our experimental results could be accounted for without interpreting them as showing that σ_c/σ_0 is less than unity, for any concentration.

[2] J. J. Bikermann, Trans. Faraday Soc. **34**, 1268 (1938); M. Dole, J. Am. Chem. Soc. **60**, 904 (1938).
[3] Irving Langmuir, Science **88**, 430 (1938); J. Chem. Phys. **6**, 873 (1938).

Langmuir suggested that his interpretation might be a better explanation than ours of our observation that the capillary rise for a dilute solution of an electrolyte is less than the rise for water. He gives the theory in generalized form only and suggests the mathematical treatment without working it out in full detail as applied to the capillary rise method of measuring surface tension, and in the calculations which he gives to test the theory as applied to our data he uses some mathematical approximations. We have repeated the calculations by the use of the rigid forms of his equations. In the following paragraphs we have applied his general theory specifically to the problem of capillary rise without making approximations purely for the purpose of simplifying the mathematics if such approximations could be avoided, except that we have restricted the analysis to the special case of a solution containing a uni-univalent salt.

According to the fundamental equations of the Debye theory, in any solution at a point having a potential, ψ, the number of positive ions per cm^3 is

$$n_+=n_0e^{-\epsilon\psi/kT} \tag{3}$$

and the number of negative ions

$$n_-=n_0e^{+\epsilon\psi/kT}. \tag{4}$$

The charge density is

$$\rho=n_0\epsilon(e^{-\epsilon\psi/kT}-e^{\epsilon\psi/kT}). \tag{5}$$

Here ψ, n and ρ are the average values over a sufficiently long time.

Introducing this into the Poisson equation,

$$\nabla\psi=-\frac{4\pi\rho}{D}, \tag{6}$$

gives the fundamental equation of the Debye theory

$$\nabla\psi=\frac{4\pi n_0\epsilon}{D}(e^{\epsilon\psi/kT}-e^{-\epsilon\psi/kT}). \tag{7}$$

Debye integrates this equation using the simplifying approximation that $\epsilon\psi\ll kT$ which gives a good approximation for many problems, but Langmuir avoids this approximation because he wishes to apply the results to problems where $\epsilon\psi$ may be greater than kT.

It should be pointed out that the Poisson-Boltzmann equation rests on a theoretical foundation[3a] which assumes $\epsilon\psi \ll kT$. However Gronwall's work makes it seem probable that the equation can be used successfully at higher values of $\epsilon\psi$.

Consider a plate of solid dielectric material (specifically glass or vitreous silica), immersed in an aqueous solution of an uni-univalent electrolyte. There is much experimental evidence that the plate will acquire an electric charge. This charge gives rise to a corresponding electric potential, which in the literature of the subject is commonly called the zeta potential (ζ). Although from a strictly mathematical point of view the source or origin of this charge is immaterial it seems probable that it is due either to ionization of the solid (loss of sodium ions from the glass leaving the glass negative) or to a selective adsorption of ions (usually anions) from the solution. The sign and magnitude of the charge on the solid may depend on the chemical nature of the solid (glass or silica) and of the solvent, and on the concentration, valence type, and individuality of the electrolyte. Ions once adsorbed may not be easily removed by a simple washing, so that the sign and magnitude of the zeta-potential may depend on the previous history of the specimen. In his mathematical treatment Langmuir adopts the convention that the charge on the solid is positive. Although the literature on zeta-potentials makes it probable that glass and silica will have a negative charge in most solutions, considerations of symmetry make the sign immaterial except when we are interested in comparing the effect of anions with that of cations. In the formal development of the theory we follow Langmuir in assuming that the solid has a positive charge. Negative ions will then be attracted to the plate and positive ions repelled to form a double layer of a more diffuse character than was assumed by Helmholtz. If this electric double layer were really perfect and complete with every positive charge on the plate matched by a nearby negative ion in the solution it would screen the potential completely so that at a short distance out in the solution the potential would be zero. However, owing to the heat motion such a double layer is diffuse and there will be a potential distribution decreasing outward with the distance from the plate. The potential will approach zero asymptotically at infinite distance (for this purpose one micron can be safely regarded as infinity). This then reduces to a one-dimensional case of the fundamental equation.

$$\frac{\partial^2\psi}{\partial x^2} = \frac{4\pi n_0 \epsilon}{D}(e^{\epsilon\psi/kT} - e^{-\epsilon\psi/kT}). \tag{8}$$

For the sake of convenience Langmuir then introduces two new variables which are functions of the original variables. Let

$$\eta = \epsilon\psi/kT \tag{9}$$

and

$$\theta = \kappa x, \tag{10}$$

where

$$\kappa = (8\pi\epsilon^2 n_0/DkT)^{\frac{1}{2}} \tag{11}$$

by definition, in accordance with the conventional notation of the Debye theory. Langmuir introduces another symbol, $\lambda = 1/\kappa$, but we prefer to use κ instead of λ, merely because it is more familiar. This amounts to changing the horizontal scale so that distances are measured not in absolute units but in units of the so-called thickness of the ionic atmosphere of the Debye theory. This scale will of course vary with the concentration. η is the ratio of the electric energy to the kinetic energy and at 25°C will have a value of unity when the potential is 0.025707 volt. The fundamental equation then reduces to the simple form

$$2\partial^2\eta/\partial\theta^2 = e^{\eta} - e^{-\eta}. \tag{12}$$

Now consider the case of the capillary tube of the surface tension apparatus. A is a point in the surface of the wetting film above the meniscus where the wetting film is essentially cylindrical (Fig. 1). The thickness of the film at this level is called Δr. The problem is to compute Δr as a function of the value of r and h and the concentration and temperature of the solution. It is convenient to measure horizontal distances from a point on the air-water interface instead of from the walls of the capillary, but this does not change the form of the differential equation. The potential at the walls is the so-called zeta-

[3a] T. H. Gronwall, V. K. La Mer and K. Sandved, Physik. Zeits. **29**, 358 (1928).

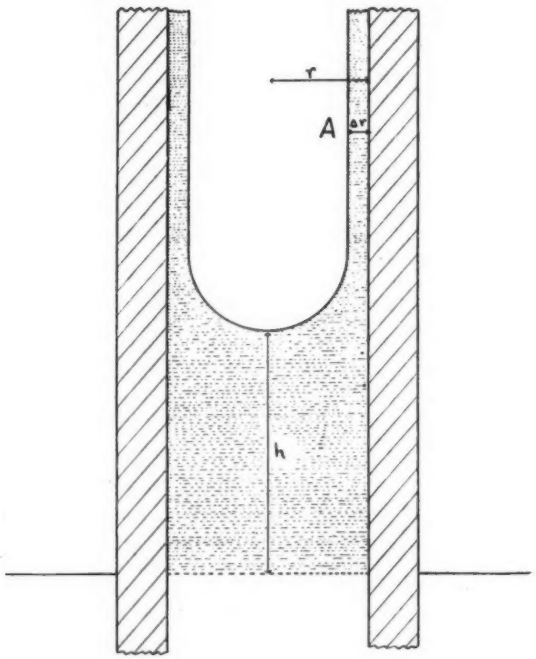

FIG. 1. Diagrammatic representation of capillary showing wetting film, drawn much out of scale. $h=10.86$ cm, $r=0.0136$ cm, and $\Delta r=200$A more or less.

potential, ζ, and is assumed to be the greatest value of ψ, and therefore the greatest value of η will be $\epsilon\zeta/kT$ where $\theta=\kappa\Delta r$. According to Langmuir,[4] at the air-water interface where $\theta=0$, the potential, ψ, and therefore, η, will have a minimum value, m, which is not zero, given by

$$m=\epsilon\psi_M/kT, \tag{12a}$$

Equation (12) strictly applies to a plane surface, whereas we wish to apply it to the inside of a cylindrical tube, but the radius of the tube (0.0136 cm) is so great in comparison with the thickness of the wetting film (Δr will at the most be only a few hundred angstroms) that this is probably permissible without a significant error).

Integrating Eq. (12) once gives

$$(\partial\eta/\partial\theta)^2=e^{\eta}+e^{-\eta}+C. \tag{13}$$

Langmuir determines the integration constant,[5] C, by saying that when $\theta=0$, $\eta=m$, its value at the air-water interface, and also that $\partial\eta/\partial\theta=0$ and hence $C=-e^{m}-e^{-m}$. Langmuir asserts this without proving it or explaining it, except by an analogy with the case of two parallel plane plates each having the same potential at the surface. In such a case the value of $\partial\psi/\partial x$ at the midpoint must be zero from the symmetry of the case. Langmuir then assumes that if one plate and one-half of the solution be removed and replaced by air there will be no change in the distribution of the ions and in the potential in the other half so that it will be true that $\partial\psi/\partial x=0$.

However, there is one consequence of this assumption which Langmuir does not discuss. There is a law of electrostatics[6] that for a charged surface between two phases (air-solution)

$$(D_s\partial\psi_s/\partial x+D_a\partial\psi_a/\partial x=-4\pi\rho_s$$

where ρ_s is the electric charge per unit of surface, D_s and D_a are the dielectric constants in the solution and air, respectively, and $\partial/\partial x$ denotes differentiation with respect to the normal drawn away from the surface into the solution or air. In the air inside the capillary tube the potential must be uniform and therefore $\partial\psi_a/\partial x=0$. Therefore the assumption that $\partial\psi_s/\partial x=0$ in the solution requires that $\rho_s=0$ at the interface and means that the concentration of the positive ions must equal the concentration of negative ions in the surface layer. On the other hand, there are in the literature experimental observations of several kinds which have been interpreted by the experimenters as showing that for most but not all solutions the surface of the solution at an air-solution interface is negatively charged, with a positive layer a short distance inside the solution. This negative layer at the surface is interpreted as due to a greater adsorption of negative ions than positive ions at the surface. This evidence is of several kinds: (1) Bubbles of air or other gases immersed in a solution move in an electric field like colloidal solid particles.[7] (2) Small drops

[4] Langmuir uses the symbol η_M for the value of η at the air-solution interface. To simplify the printing and reading we use m with the same meaning.

[5] The integration of this equation can be found in a paper by Horowitz (J. Chem. Ed. **16**, 519 (1939)) who evaluates the integration constant from the boundary condition $\partial\psi/\partial x=0$ and $\psi=0$ at $x=\infty$, but this boundary condition is not applicable to the special case in which we are interested.

[6] J. H. Jeans, *The Mathematical Theory of Electricity and Magnetism*, 5 Ed. (The University Press, Cambridge, England, 1927), p. 125.

[7] H. A. McTaggart, Phil. Mag. (5) **27**, 297 (1914); N. Bach and A. Gilman, Acta Physiochemica U. R. S. S. **9**, 1 (1938).

of water or solution dispersed in air (spray or mist) commonly are negatively charged and the charge depends on the nature and concentration of the solution.[8] (3) Direct measurements show a potential on the air-solution interface which is dependent on the nature and concentration of the solution.[9]

However, in order to follow Langmuir's argument, we introduce his value of the integration constant. A simple transformation of Eq. (13) gives

$$d\theta=\frac{d\eta}{(e^{\eta}+e^{-\eta}-e^{m}-e^{-m})^{\frac{1}{2}}}, \tag{14}$$

which must be integrated again. Write

$$K=e^{-m} \tag{15}$$

and

$$\sin\phi=e^{(-\eta+m)/2}. \tag{16}$$

Then a rigid transformation gives the equivalent equation

$$d\theta=-\frac{2K^{\frac{1}{2}}d\phi}{(1-K^2\sin^2\phi)^{\frac{1}{2}}}. \tag{17}$$

This equation has now been transformed into the form of an elliptic integral which must be integrated between the limits at the air-solution interface and the solution-quartz interface. At the air-solution interface $\theta=0$ and $\eta=m$, therefore $\sin\phi=e^0=1$; or $\phi=\pi/2$. At the solution-quartz interface $\theta=\kappa\Delta r$ and $\eta=\eta_1=\epsilon\zeta/kT$.

$$\sin\phi_1=\exp\left(\frac{-\eta_1+m}{2}\right)$$

$$=\exp\left(-\frac{\epsilon\zeta}{2kT}+\frac{m}{2}\right), \tag{18}$$

$$\Delta r=\frac{2K^{\frac{1}{2}}}{\kappa}\left[\int_0^{\pi/2}\frac{d\phi}{(1-K^2\sin^2\phi)^{\frac{1}{2}}}-\int_0^{\phi_1}\frac{d\phi}{(1-K^2\sin^2\varphi)^{\frac{1}{2}}}\right]. \tag{19}$$

[8] P. Lenard, Ann. d. Physik (4) **47**, 463 (1915); W. Obolensky, *ibid.* (4) **39**, 961 (1912); W. Busse, *ibid.* (4) **76**, 493 (1925); A. Bühl, *ibid.* (4) **83**, 1207 (1927); (4) **84**, 211 (1928); (4) **87**, 877 (1928); Kolloid Zeits. **59**, 346 (1932).

[9] F. B. Kenrick, Zeits. f. physik. Chemie **19**, 625 (1896); A. Frumkin, Zeits. f. physik. Chemie **109**, 34 (1924); **111**, 190 (1924); **116**, 485 (1925). See also H. Freundlich, *Kapillarchemie*, 4 Ed. (Leipzig, 1930), Vol. 1, pp. 388–399, which gives many additional references.

Now if the temperature and concentration of the solution are known and if the numerical values of the zeta-potential at the solution-quartz interface and of the potential at the air-solution interface are known and if it is true that the electric field vanishes at the air-solution interface, then the value of Δr can be computed.

In order to compute the value of the potential at the air-solution interface Langmuir postulates three kinds of forces which are in equilibrium. Consider a point, A (Fig. 1), on the surface of the wetting film a short distance above the meniscus. Here we have:

(1) Gravity pulling downward and tending to make the film thinner. This will exert a force per cm^2 or a pressure of $p=(D-\beta)hg$, where D is the density of the solution, and β the density of air.

(2) The surface tension of the cylindrical film inside the tube will tend to contract the cylinder and thus make the film thicker. This will exert a pressure of $p=\sigma/r=(D-\beta)hg/2$.

(3) The zeta-potential will produce a pressure. At any point within the solution between the point A and the quartz wall there will be a pressure having both an electric component and an osmotic component. The sum of these two components must be uniform across the tube because the system is in equilibrium. If in accordance with the assumption discussed above the potential gradient, $\partial\psi/\partial x$, becomes zero at the air-solution interface then the total pressure may be placed equal to the osmotic pressure at the air-interface which according to Van't Hoff's simple law would be

$$p=(n_+ + n_-)kT=n_0(e^{-\epsilon\psi/kT}+e^{\epsilon\psi/kT})kT$$

$$=n_0(e^{-m}+e^{m})kT=2n_0kT\cosh m. \tag{20}$$

Van't Hoff's law gives the osmotic pressure referred to pure water, that is, it measures the hydrostatic pressure which would be required to prevent water from passing through a membrane into the solution. However, for the present purpose we are not interested in the passage of water into the wetting film from a source of pure water but from the solution in the wide part of the apparatus where the osmotic pressure according to the Van't Hoff law is $2n_0kT$. Therefore the effective osmotic pressure which must be bal-

anced by hydrostatic pressure to prevent water entering the wetting film is

$$p=2n_0kT\cosh m-2n_0kT=2n_0kT(\cosh m-1).$$

This computation of the osmotic pressure by means of the simple Van't Hoff law neglects the effect of the interionic electric forces on the osmotic pressure.

The gravitational pull tends to make the film thinner and the surface tension and the osmotic pressure due to the zeta-potential tends to make the film thicker and at equilibrium these pressures must balance; therefore we may write

$$(D-\beta)hg=(D-\beta)hg/2+2n_0kT(\cosh m-1), \quad (21)$$

$$\cosh m=1+(D-\beta)hg/4n_0kT, \quad (22)$$

but $n_0=Nc\times10^{-3}$ and $Nk=R$

$$\cosh m=1+250(D-\beta)hg/RTc. \quad (23)$$

For any particular case in which the values of the capillary rise, density, temperature and ionic concentration are known, the value of the potential at the air-interface can be computed from this equation of Langmuir's. This equation contains the assumption that the potential gradient vanishes at the air-solution interface. According to this equation the potential at the air-solution interface is independent of the zeta-potential. This means that the thickness of the film adjusts itself so as to make the potential at the interface the value which will give a pressure just sufficient to balance the hydrostatic and surface tension components in the surface layer. The potential adjusts itself to such a value as to attract an excess of ions whose osmotic pressure will just balance the difference caused by the fact that the surface at the bottom of the meniscus is doubly curved whereas the cylindrical surface above the meniscus is singly curved. The thickness required will, however, depend on the zeta-potential in accordance with Eq. (19).

Therefore if zeta-potentials can be determined by an independent experimental method it should be possible to compute the thickness of the wetting film from Eqs. (19) and (23). There are in the literature a considerable number of measurements of zeta-potentials on glass surfaces and a few on vitreous silica surfaces for various salts at various concentrations. In most cases the temperature was not controlled but was a somewhat indefinite laboratory temperature which is not stated. The most reliable of these measurements appear to have been made by the streaming potential method. In this method a solution is forced through a capillary tube by means of a measured pressure and the electromotive force generated by the mobile part of the electrostatic double layer is measured by a pair of electrodes at the ends of the capillary tube. The results have been computed by the equation $\zeta=4\pi\eta\kappa E/DP$ where η=viscosity, κ=specific conductivity; P=pressure, E=electromotive force generated, D=dielectric constant. This equation has some theoretical weaknesses.[10] It assumes a Helmholtz double layer instead of a diffuse double layer. However, Adam[11] argues that the error introduced by this assumption is not great. Another weakness is that the value of the dielectric constant used in the calculations is that for water and the value for the solutions may be appreciably different.

In Table I are shown values of the zeta-potential obtained by various authors for potassium chloride solutions by the streaming potential method. The third column gives the results of Kruyt and van der Willigen[12] on vitreous silica capillaries and the next two columns give similar results by the same authors on Jena 59III glass and on a glass described as "gewöhnliches," respectively. It is interesting to note that these experimenters find that the values for vitreous silica are intermediate between the two varieties of glass, and that the

TABLE I. *Summary of zeta-potentials in millivolts for* KCl *solutions.*

		KRUYT							
c	ψ_m	QUARTZ	JENA 59III	ORDINARY GLASS	FURUTANI PYREX	FREUNDLICH JENA 16III	LACHS JENA 16III	DUBOIS GLASS	RUTGERS JENA 16III
10^{-7}	197				46.7	35	101		
10^{-6}	139				55	38	96.2		
10^{-5}	81	91	107	73	33.5	22	95.5		200
2.5×10^{-5}	60	91	112	72					180
5×10^{-5}	46	91	109	70	28.4		105		177
10^{-4}	35	92	110	67	27.7	4	120	45	165
2.5×10^{-4}	23	88	96	62					153
5×10^{-4}	16.5	83	89	58	17.6			44	
10^{-3}	11.8	75	81	52	13.1		125	40	

[10] J. W. McBain, J. Phys. Chem. **28**, 706 (1924).

[11] N. K. Adam, *The Physics and Chemistry of Surfaces*, second edition (Oxford, The Clarendon Press, 1938), p. 354.

[12] H. R. Kruyt and van der Willigen, Kolloid Zeits. **45**, 307 (1928).

zeta-potential is independent of the concentration within the range 10^{-5} to 10^{-4} but shows a marked decrease within the range 10^{-4} to 10^{-3}. Furutani, Kurokochi and Asoda[13] report similar measurements on Pyrex and "hard Japanese glass" but the results are substantially lower than those of Kruyt and van der Willigen. Freundlich and Ettisch[14] using Jena 16III glass report much lower values than anyone else but Lachs and Biczyk[15] with the same glass get very different results which are in approximate agreement with Kruyt and van der Willigen's results with Jena 59III glass except at $10^{-3}N$. DuBois and Roberts[16] have made measurements using a slit of precisely known dimensions in glass of an undescribed variety. They also made measurements by the electrosmosis method using the same slit. For conductivity water the zeta-potentials computed from their electrosmotic measurements are approximately twice those given by the streaming potential method; for potassium chloride solutions, on the other hand, the zeta-potentials are about 20 percent greater than by the electrosmotic method; and for barium chloride solutions the two methods are in substantial agreement.

Recently Rutgers[17] has criticized all previous measurements on the ground that the variation of the specific conductivities near the surface has been ignored. He attempts to eliminate this source of error by using three different capillaries of Jena 16III glass which varied in diameter. This enabled him to make allowance for the surface conductivities in his computation of the zeta-potentials. His results are much higher than those obtained by any other experimenter as shown in the last column of Table I. The values of Δr computed from his zeta-potentials are correspondingly higher, about 600 angstroms for water.

It is apparent from this table that no confidence can be placed in the reliability of any estimate of zeta-potentials that can be obtained from the literature. All of the experimenters agree as to the negative sign of the charge on the glass but evidently all of the factors which influence the phenomena were not known and controlled in their experiments.

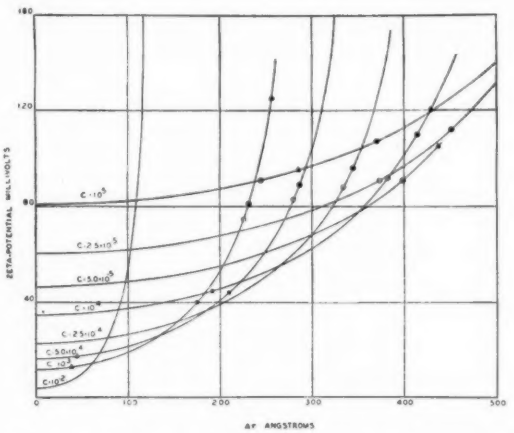

FIG. 2. ○ Kruyt and van der Willigen for vitreous silica. ● Kruyt and van der Willigen for Jena 59III glass. △ Furutani, Kurokochi and Asoda for Pyrex. ▲ Lachs and Biczyk for Jena 16III. ■ DuBois and Roberts for glass.

The second column gives the minimum value of the potential in millivolts at the air-solution interface in our capillary as computed by Langmuir's equation (No. (23) and (12a) above).

As will be seen many of the recorded measurements of the zeta-potential at the glass-solution interface are less than the computed minimum for the air-solution interface. This discrepancy must mean either (1) the experimental measurements of the zeta-potential are unreliable, (2) measurements on glass are not applicable to vitreous silica surfaces, or (3) Langmuir's equation for the potential at the air-solution interface needs modification.

The next step was to attempt to ascertain how accurately the zeta-values need to be known for the calculations of Δr. These calculations have been carried out for a series of solutions ranging in concentration from $c=10^{-6}$ to $c=10^{-2}$. For our particular instrument the capillary rise for water and for dilute solutions at 25°C is $h=10.83$ cm. Substituting this value, together with $g=980.3$, $R=8.31\times10^{7}$, $T=298.18$ reduces Eq. (23) to

$$\cosh m=1+\frac{1.07243(D-\beta)\times10^{-4}}{c}.$$

[13] Furutani, Kurokochi and Asoda, Jap. J. Gastroent. **2**, 148 (1930).
[14] H. Freundlich and G. Ettisch, Zeits. f. physik. Chemie **116**, 401 (1925).
[15] H. Lachs and J. Biczyk, Zeits. f. physik. Chemie **A148**, 441 (1930).
[16] R. DuBois and A. H. Roberts, J. Phys. Chem. **40**, 543 (1936).
[17] A. J. Rutgers, Trans. Faraday Soc. **36**, 69 (1940); A. J. Rutgers, Ed. Verlende, and MaMoorkens, Proc. K. Ned. Akad. Wet. (Amsterdam) **41**, 763 (1938).

Then a succession of arbitrary values of zeta are assumed and the corresponding values of Δr computed by the use of Eq. (11), (15), (18), and (19) and the results plotted on a large scale as shown on a much reduced scale in Fig. 2. It is evident from these curves that for solutions which are $0.01N$ and stronger the corrections will be small and the zeta-potential does not need to be known with great precision.

Here the points designated show the values for the zeta-potentials computed from the measurements of streaming potentials and the corresponding values for Δr based on the experimental data given in Table I. However, many of the data shown in Table I are not shown on the figure because they are below the computed minimum including all of Freundlich's measurements and all Furutani's except for the two most concentrated solutions.

It is evident that the data on zeta-potentials available in the literature are not sufficiently consistent to permit reliable corrections to be calculated by the Langmuir theory. New measurements of zeta-potentials have been undertaken in this laboratory in the hope that substantial improvements in the technique can be devised which will give results of sufficient precision and reliability to settle the question. Although hopeful progress has been made, much more remains to be done before the results are ready for publication.

The present paper reports the results of two other methods of testing the Langmuir theory:

(1) Langmuir says, "The addition of thorium nitrate in concentration of 10^{-6} M brings the potential of glass to about zero. This should eliminate the Jones-Ray effect." This was tested experimentally.

(2) Since according to the Langmuir theory the thickness of the wetting film is dependent on the concentration of ions there should be a correlation between the purity of the water as measured by its conductivity and the capillary rise which is influenced by the thickness of the wetting film.

Experimental

The first 36 experiments were preliminary runs in which practice in the use of the apparatus was acquired and some modifications of procedure tried.

Additional precautions against the contamination of the surface of the water or apparatus during the cleaning and drying were tried. The air admitted to the apparatus was further purified by various filters, scrubbing through washing liquids and finally by passing over red hot copper oxide. However, these additional precautions did not cause any essential difference in the results and led to the conclusion that the earlier procedure used by Dr. Ray was adequate. Also greater care was taken in the actual measurement of the capillary rise by means of the cathetometer in the hope that these measurements could be made as precise as, or even more precise than, the indirect measurements based on the weight of the instrument. As a result the "probable error" of the results obtained with the cathetometer were approximately but not quite as low as the "probable error" by the weight method when comparisons of very dilute solutions with water were being made. Since the readings of the height of the lower meniscus are influenced by the adjustment of the illuminating device it seems possible that there may be constant errors which would not be manifested in the "probable error." Therefore, when working with more concentrated solutions having a capillary rise sufficiently different so that adjustments of the device for illuminating the lower meniscus are required, the weight method should have an advantage. The general conclusion of this work was that the cathetometer confirmed the results obtained by the balance but did not provide a more precise technique and therefore could not supersede the older method.

Then ten runs with water (No. 37–42, 47, 51–53) interspersed with 6 runs with 0.001 N KCl gave $w_0=84.0801\pm0.00276$; $W_c=84.1082\pm0.00309$; $h_0=10.8631\pm0.00017$, $D_c=0.997119$; $D_0=0.997074$ and hence $\dot{\sigma}_c/\sigma_0[(r-\Delta r_0)/(r-\Delta r_c)]$ $0.999,888\pm0.000,027$ calculated from the weights by Jones and Ray Eq. (11) or $0.999,862\pm0.000,014$ calculated directly from the cathetometer readings.[18] This is comparable with Dr. Ray's result of 0.999,82. The apparent decrease in surface tension due to the addition

[18] See Jones and Ray, reference 1, for explanation of the symbols and computations.

of 0.001 N KCl as compared to water is thus confirmed by another independent series of measurements, although the magnitude of the decrease is slightly less than was found by Dr. Ray.*

The next step was to determine the effect of thorium ion at low concentrations which Langmuir predicts would eliminate the minimum in the surface tension. Thorium chloride was chosen in preference to the nitrate because it is easier to obtain it free from other salts. Solutions made from the available C.P. thorium chloride were turbid and gave an opalescent blue color and were obviously colloidal due to hydrolysis. The double salt with ammonium chloride was prepared by mixing concentrated solutions of thorium chloride and ammonium chloride and the double salt purified by recrystallizing twice from water with centrifugal drainage. The salt was ignited and then mixed with pure sugar charcoal and placed in a silica boat inside a silica tube. Dry chlorine was then passed over the boat which was heated in an electric furnace thereby forming anhydrous thorium chloride ($ThCl_4$) which sublimed and condensed in the cold end of the tube. When sufficient thorium chloride had been collected a few cm^3 of water were added which readily formed a clear solution. This solution was transferred to a volumetric flask and diluted to the mark and an aliquot portion analyzed by precipitation of thorium oxalate and ignition to the oxide. The analytical data served as a basis for the preparation of a stock 0.001 M $ThCl_4$ solution by quantitative dilution. This solution was clear and is still clear more than a year after it was prepared. The more dilute solutions used in the experiments were prepared from this stock solution by dilution. The zeta-potential of Jena glass against solutions of thorium nitrate have been computed by Freundlich and Ettisch[19] from measurements of streaming potentials; and by Bach and Gilman[20] from the cataphoretic mobility of suspensions of Jena glass powder in solutions of thorium chloride. A comparison of their data is given in Table II. Although the quantitative agreement between these results is poor they at least agree that the zeta-potential goes through zero between the concentration of 10^{-7} and 10^{-6} M. Abramson[21] says "the isoelectric point of a glass particle in a solution of Th^{++++} may be at 1×10^{-6} M." We therefore adopted 10^{-6} M $ThCl_4$ solution as another reference liquid in addition to water.

A long series of runs (No. 55–175) were made with solutions of $ThCl_4$ of various concentrations (10^{-9} to 5×10^{-5} M) and with solutions of potassium chloride of various concentrations (10^{-6} to 10^{-2} M) containing also 10^{-6} M $ThCl_4$; and with water and with 10^{-6} M $ThCl_4$ interspersed.

TABLE II. *Zeta-potentials in millivolts of Jena glass in thorium nitrate or chloride solutions.*

Conc.	Freundlich and Ettisch	Bach and Gilman
10^{-7}	− 3	
2.5×10^{-7}		− 90
7.5×10^{-7}		+ 29
10^{-6}	+21	
1.25×10^{-6}		+ 34
2.5×10^{-6}		+ 43
10^{-5}	+16	
1.25×10^{-5}		+ 95
2.5×10^{-5}		+113
10^{-4}	+ 4	
1.25×10^{-4}		+110
2.5×10^{-4}		+840
2.5×10^{-3}		+ 84

TABLE III. *Summary of experimental data.*

Run Numbers	Solution	W	D
37–42, 47, 51–53	water	84.0801±0.00276	0.997074
43–46, 48–50	0.001 M KCl	84.1082±0.00309	0.997123
54	10^{-6} M $ThCl_4$	84.0668	0.997074
55, 56, 58, 59, 64–71, 143, 144, 148, 150, 153, 154, 158, 159, 162	10^{-6} M $ThCl_4$	84.1186±0.00270	0.997074
60–63	0.001 KCl in 10^{-6} $ThCl_4$	84.1043±0.00085	0.997123
72–77, 79, 80	2×10^{-6} $ThCl_4$	84.1191±0.00132	0.997074
81–84	water	84.0976±0.00204	0.997074
85–94	3×10^{-6} $ThCl_4$	84.1105±0.00271	0.997074
95–102	5×10^{-6} $ThCl_4$	84.1238±0.00221	0.997074
103–108	10^{-5} $ThCl_4$	84.1318±0.00177	0.997083
109–112	5×10^{-5} $ThCl_4$	84.1350±0.00374	0.997090
113–117	10^{-6} $ThCl_4$	84.1199±0.00469	0.997074
118–121	10^{-7} $ThCl_4$	84.1166±0.00167	0.997074
122–124	10^{-9} $ThCl_4$	84.1163±0.01090	0.997074
125–142	water	84.1118±0.00172	0.997074
145–147	0.001 KCl 10^{-6} $ThCl_4$	84.1516±0.00178	0.997126
151, 152	0.002 KCl 10^{-6} $ThCl_4$	84.1580±0.00375	0.997177
155, 156, 157	0.005 KCl 10^{-6} $ThCl_4$	84.1694±0.00430	0.997317
160, 161	0.01 KCl 10^{-6} $ThCl_4$	84.1997±0.00050	0.997557
163, 164, 169, 170	water	84.1200±0.00457	0.997074
162, 165–168, 171	10^{-6} KCl	84.1298±0.00190	0.997074

* In this particular case the "probable error" by the cathetometer method happens to be less than the "probable error" by the weight method, but that is not usually the case. We are, of course, aware that "probable errors" calculated according to the conventional formula do not include systematic or constant errors.

[19] F. Freundlich and G. Ettisch, Zeits. f. pkysik. Chemie **116**, 408 (1925).

[20] N. Bach and A. Gilman, Acta Physicochimica U. R. S. S. **9**, 22 (1938).

[21] H. A. Abramson, *Electrokinetic Phenomena* (Chemical Catalog Co., N. Y., 1934), p. 186.

TABLE IV. *Apparent relative surface tension of* $ThCl_4$ *solutions.*

C	REFERRED TO WATER	REFERRED TO 10^{-6} M $ThCl_4$
10^{-9}	0.999,97±0.000,07	1.000,01±0.000,07
10^{-8}	0.999,94±0.000,03	0.999,99±0.000,03
10^{-7}	0.999,96±0.000,02	1.000,01±0.000,02
10^{-6}	0.999,95±0.000,01	(1.000,00)
2×10^{-6}	0.999,95±0.000,01	1.000,00±0.000,02
3×10^{-6}	1.000,00±0.000,02	1.000,05±0.000,02
5×10^{-6}	0.999,92±0.000,02	0.999,97±0.000,03
10^{-5}	0.999,88±0.000,02	0.999,92±0.000,02
5×10^{-5}	0.999,87±0.000,03	0.999,90±0.000,03

These results (Table III) can only be published in summarized form in order to save space in printing. The "probable error" is given as a measure of the variability of the data. In calculating the averages and "probable errors" a very few obviously grossly erratic results were eliminated. The data are shown in the table in approximately the order of the experiments except for the data on water and on 10^{-6} M $ThCl_4$ which were the two competing standards of reference. These measurements were interspersed with the others and are brought together for averaging. 10^{-6} M $ThCl_4$ solution was placed in our apparatus for the first time in run No. 54.

The equation used to compute the relative surface tension in our earlier work (Jones and Ray paper, Eq. (11)) is based on the assumption that the radius of the capillary is identical for the solution and for water and could be canceled out. However, if in view of the Langmuir theory this assumption is avoided, the equation should be changed to

$$\frac{\sigma_c r_0}{\sigma_0 r_c}=\frac{\sigma_c}{\sigma_0}\left(\frac{r-\Delta r_0}{r-\Delta r_c}\right)=\left\{\frac{D_c-\beta_c}{D_c-\beta_0}\right\}\times\left\{1+\frac{1}{\pi R^2 h_0(1-r/R)}\left(\frac{W_0}{D_0}-\frac{W_c}{D_c}\right)\right\}.$$

The right-hand part of the equation gives an "apparent relative surface tension" which may be converted into a real "relative surface tension" by multiplying by the factor $(r-\Delta r_c)/(r-\Delta r_0)$. This factor should become unity if the zeta-potential is low enough to make the wetting film negligible.

In Table IV are given the apparent relative surface tension for solutions of $ThCl_4$ referred to water as reference liquid ($W_0=84.1109\pm0.00161$ from the average of 26 runs No. 81–84, 125–142, 163, 164, 169, 170) and also referred to 10^{-6} M $ThCl_4$ as reference liquid ($W_0=84.1186\pm0.00270$ from runs 64–71, 143, 144, 148, 150, 153, 154, 158, 159, 162).

This table shows that the solutions of thorium chloride are identical in their behavior within the "probable error" of the observations between the limits of concentration of 10^{-9} and 5×10^{-6} M $ThCl_4$. This conclusion is somewhat surprising in view of numerous statements in the literature of a maximum in the $\zeta-C$ curves at low concentrations.[22] There seems to be two possible interpretations of this table.

(1) A concentration of 10^{-6} M $ThCl_4$ or even 5×10^{-6} M $ThCl_4$ does not reduce the zeta-potential sufficiently to make the Δr negligible but a concentration of 10^{-5} M $ThCl_4$ or more is required for this purpose.

(2) In any solution of $ThCl_4$ the zeta-potential is low enough to make Δr negligible and the drop in apparent surface tension for the 10^{-5} and 5×10^{-5} M $ThCl_4$ solution is due to a real decrease in surface tension.

Direct measurements of zeta-potentials for these thorium chloride solutions seems to be needed to settle this question but such measurements are not available.

In Table V are given the apparent relative surface tension of solutions of potassium chloride varying in concentration from 0.001 to 0.01 N which were made up by the use of a 10^{-6} M $ThCl_4$ solution instead of water, referred to the 10^{-6} M $ThCl_4$ solution as standard. In all of these measurements the thorium ions were present and it was therefore expected that the zeta-potentials would be low enough to make the wetting films negligible.

TABLE V. *Apparent relative surface tension of* KCl *solutions containing added* 10^{-6} M $ThCl_4$.

C	CONTAINING ADDED 10^{-6} M $ThCl_4$ FRIZZELL	WITH NO ADDED $ThCl_4$	
		RAY	FRIZZELL
0.001	0.999,93±0.000,02	0.999,82	
0.001	0.999,87±0.000,02	0.999,82	0.999,86
0.002	0.999,91±0.000,03	0.999,88	
0.005	1.000,05±0.000,03	0.999,98	
0.01	1.000,22±0.000,02	1.000,13	

[22] Reference 21, pp. 202–204.

Two different results are given for 0.001 M KCl, the first based on runs 60–63 and the second on runs 145, 146 and 147 which were made four months later. The first series was immediately preceded by five runs using 10^{-6} M $ThCl_4$, and no stronger solution of $ThCl_4$ had ever been present in the tube. Between the first and second series solutions of $ThCl_4$ containing as much as 5×10^{-5} M $ThCl_4$ had been in the tube, although immediately before this second series, two runs using 10^{-6} M $ThCl_4$ had been used, with 18 runs with water preceding these.

Contrary to the prediction of Langmuir the addition of 10^{-6} M $ThCl_4$ did not eliminate the apparent decrease in surface tension. It is possible that a higher concentration of $ThCl_4$ would have the effect which he expected. Direct measurements of zeta-potential of these solutions seem to be needed to aid a definite interpretation.

In the earlier work the water used as a standard of reference was good quality "conductivity water" but it had not been protected from the carbon dioxide present in the normal air of the laboratory and therefore it must have contained sufficient carbon dioxide to produce a concentration of hydrogen and bicarbonate ions of about 3×10^{-6} N. According to the Langmuir theory the thickness of the wetting film should be a function of the concentration of the ions and accordingly some correlation between the capillary rise and the specific conductivity should be expected. In order to test this hypothesis we therefore developed an elaborate apparatus for cleaning and drying the capillarimeter and filling it with purified water to the reference mark in such a way as to prevent any contamination by carbon dioxide or other impurities present in ordinary laboratory air, and then measuring the capillary rise and the specific conductivity of the water used. A detailed description of the complicated closed equipment is omitted for the sake of brevity. With this apparatus the capillarimeter could be cleaned by boiling nitric acid, rinsed by live steam and water. All of the air which came in contact with the inside of the apparatus or with the water had been passed over red-hot copper oxide to ensure the absence of organic matter and scrubbed to remove any carbon dioxide or ammonia. The water used was distilled from alkaline permanganate, rejecting a large first fraction then from very dilute sulfuric acid and finally alone. It was mostly condensed directly in the silica capillarimeter, and partly in an auxiliary reservoir using a silica condenser, from which it could be added drop by drop to the capillarimeter to bring the upper meniscus to the reference mark. A sample was withdrawn into a closed cell and its specific conductivity measured. With this apparatus the indirect determination of the capillary rise from the weight of the water was not feasible but the direct determination of the capillary rise by the cathetometer had to be relied on. However, as is explained above, direct measurement had been improved so that the results are substantially as precise as can be obtained indirectly. For the sake of comparison several runs were made with the apparatus open to air as usual and without using the elaborate air purifying or water purifying system but all other details as nearly as possible unchanged.

TABLE VI. *Capillary rise for water of varying ionic concentration.*

NUMBER OF RUNS	SPEC. COND. $\times10^6$	CAPILLARY RISE	CONC. $c\times10^6$	m	MINIMUM POTENTIAL AT AIR-SOL. INTERFACE MILLIVOLTS
4 open	1.67	10.8622 ±0.00025	4.2	3.973	102
1 closed	0.93	10.8622	2.3	4.55	117
1 open	0.8	10.8622	2.0	4.69	121
1 open	0.7	10.8622	1.75	4.82	124
4 closed	0.37	10.8619 ±0.00032	0.925	5.45	140

The results are shown in Table VI arranged in order of decreasing conductivity or increasing purity of the water used. These results show no variation in capillary rise in spite of a fourfold variation in specific conductivity and hence in ionic concentration. The ionic concentration given in column four is estimated on the assumption that the equivalent conductance of the mixture of ions (H^+, HCO^-_3, OH^-) present is 400. The corresponding values for m computed from Eq. (23) and for the potential at the air-solution interface, ψ_M, are given in the last two columns.

Figure 3 gives a plot of the $\psi-\Delta r$ curves for the best and for the poorest water used in the experiments recorded in Table VI. However, since the value of the zeta-potential on vitreous silica in water of this purity is not known it is impossible to compute the value for Δr. Lachs

and Biczyk[15] give a summary of zeta-potential measurements of glass in conductivity water by five different groups of observers. These values vary from 14 to 102 millivolts. Then they give measurements of their own using Jena 16III glass at 18°C. The results vary from 55 millivolts for water of $\kappa=3.0\times10^{-6}$ at 18°; to 146 mv for water of $\kappa=0.72\times10^{-6}$. They estimate by extrapolation that water of $\kappa=0.5\times10^{-6}$ would give 180 mv. Rutgers[17] estimates the zeta-potential for water on this same variety of glass to be 230 millivolts.

For the general theory to be applicable at all the zeta-potential at the silica-water interface would have to be above the values given in the last column of Table VI. However, at these low ionic concentrations values of the zeta-potential only a few millivolts above those at the air-solution interface are required to give appreciable values of Δr. Thus, for example, for the best water (spec. cond. 0.37×10^{-6}) a zeta-potential of 150 millivolts would correspond to a Δr of 250A; and for the poorest water (spec. cond. 1.67×10^{-6}) a zeta-potential of 112.5 millivolts would give the same value of Δr. This is, of course, a consequence of Langmuir's assumption that the $\partial\psi/\partial x$ approaches zero at the air-solution interface. These two curves have vertical asymptotes at $\Delta r=651$A for the best water and at $\Delta r=642$A for the poorest water. These two curves cross at $\psi=300$ millivolts and $\Delta r=633$A. If the zeta-potentials are 300 millivolts or more within this range of quality of water, then the values of Δr would be practically independent of the purity but high (633–650A). However, as far as we know there is no independent evidence that zeta-potentials as high as this occur, and the measurements of Lachs and Biczyk make it very improbable. In order to reconcile our experimental evidence that the capillary rise is independent of the quality of the water within the range of $\kappa=0.37\times10^{-6}$ and 1.67×10^{-6}, with the theory it would be necessary to show either (1) that the zeta-potential on vitreous silica is about 300 millivolts or above, which would give a value of Δr of about 630 angstroms regardless of the purity of the water; or (2) that the zeta-potential varies with the ionic concentrations in such a way that the Δr becomes independent of the purity of the water. Since neither of the hypotheses seems probable, although perhaps not definitely excluded by the available experimental evidence, we conclude that the constancy of the capillary rise in spite of a fourfold variation in the ionic concentration does not support the theory.

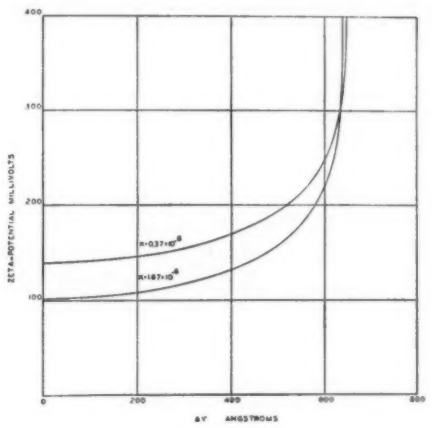

FIG. 3.

The striking constancy of the capillary rise in spite of a fourfold variation in the specific conductivity is gratifying because it shows that it is not necessary to protect the reference water against carbon dioxide present in the air, nor is it necessary to measure the specific conductivity of each sample of reference water in order to compute a correction to the capillary rise which would be variable for each sample.

While this paper was in proof, a paper by Dole and Swartout[23] has been published which confirms the existence of a minimum in the surface tension curve for potassium chloride at 0.001 *M*, which is the same concentration as the minimum found by Jones and Ray. Dole and Swartout have measured the difference between the forces required to pull a double ring of platinum-iridium wire out of a solution and out of water. They have modified the technique of this much used method of measuring surface tension so as to improve greatly its precision and to make it a differential method. Dole and Swartout conclude that the Langmuir film theory cannot be applied to their method.

We wish to express to Albert Sprague Coolidge our thanks for his helpful interest and suggestions, especially on the theoretical parts of this paper.

[23] Malcolm Dole and J. A. Swartout, J. Am. Chem. Soc. **62**, 3039 (1940).

LETTERS TO THE EDITOR

This section will accept reports of new work, provided these are terse and contain few figures, and especially few halftone cuts. The Editorial Board will not hold itself responsible for opinions expressed by the correspondents. Contributions to this section should not exceed 600 words in length and must reach the office of the Managing Editor not later than the 15th of the month preceding that of the issue in which the letter is to appear. No proof will be sent to the authors. The usual publication charge ($3.00 per page) will not be made and no reprints will be furnished free.

Note on the Chain Photolysis of Acetaldehyde in Intermittent Light

When acetaldehyde is decomposed by a chain mechanism at elevated temperatures it is believed that the chain is propagated through the steps

$$CH_3+CH_3CHO\rightarrow CH_4+CH_3CO \quad (1)$$

$$CH_3CO\rightarrow CH_3+CO. \quad (2)$$

It was suggested to one of us by Dr. D. V. Sickman that use of a rotating sector to illuminate the acetaldehyde by intermittent light might be of value in studying the mechanism in this case.

Experiments of this sort have now been performed. Because the rate of photolysis of acetaldehyde depends upon the square root of the light intensity, the quantum yield is greater for a rapidly moving sector than for a slowly moving one. With acetaldehyde at 20 cm pressure and 200°C, with an illuminated volume of 15.2 cc, and with a light intensity such that 73 cu.mm of CO were formed in 120 sec. when the sector was not moving, we found that with the moving sector the change in quantum yield occurred at a rotation speed of about 2 rotations per second. By comparison of our data with those of Grahame and Rollefson,[1] we find that our quantum yield under these conditions is about 48, corresponding to a chain length of 24 if two chains are started by each quantum (actually, of course, some of the absorbed light may not produce chains, but a small factor is not important for our calculation). The experiments with the moving sector indicate that the chain lasts about $\frac{1}{2}$ sec.

Now unless the reaction (2) has an activation energy of 20–25 kcal., or more, which is much more than is usually assumed,[2] this reaction will occur so rapidly that the length of time that the chain carrier is in the form CH_3CO will be negligible. If this is the case, a comparison of the number of collisions made by a methyl radical in $\frac{1}{2}$ sec. with the chain length, will give an indication of the probability that a collision results in reaction. Assuming an effective collision radius of 3.5A we find that a methyl radical makes about 7×10^8 collisions in $\frac{1}{2}$ sec., so that one collision in about 3×10^7 results in reaction. This corresponds to an Arrhenius factor, $e^{-E/RT}$, with $E=16$ kcal. per mole, and this should give the order of magnitude of the activation energy for reaction (1). The value is certainly very reasonable.

Actually, it must be noted that 16 is to be considered an upper limit, since, in obtaining it, it was assumed that no mutual orientation of the methyl radical and the acetaldehyde molecule was necessary for reaction to occur. The true value can be obtained by experiments at various temperatures, and such experiments are now under way.

W. L. Haden, Jr.
E. P. H. Meibohm
O. K. Rice

University of North Carolina,
Chapel Hill, North Carolina,
November 14, 1940.

[1] D. C. Grahame and G. K. Rollefson, J. Chem. Phys. **8**, 98 (1940). We are indebted to Dr. Grahame for some correspondence concerning this paper.
[2] M. Burton, J. Chem. Phys. **7**, 1072 (1939) assumes 4 kcal.

Erratum: High Velocity Atomic Beams

(J. Chem. Phys. **8**, 7 (1940))

On page 10 of this paper, the caption under Fig. 3 contains the expressions: $7.608\times10^{-18}\log_{10} IP_2/IP_1$ *versus* $(P_1/T_1-P_2/T_2)$ and $7.608\times10^{-18}\log_{10} IP_2/IP_1=$(collision cross section) $(P_1/T_1-P_2/T_2)$.

In both cases $(P_1/T_1-P_2/T_2)$ should read

$$273\ (P_1/T_1-P_2/T_2).$$

I. Amdur
H. Pearlman

Research Laboratory of Physical Chemistry,
Massachusetts Institute of Technology,
Cambridge, Massachusetts,
November 12, 1940.

THE JOURNAL OF CHEMICAL PHYSICS

VOLUME 8 NUMBER 12

DECEMBER, 1940

Published by the

AMERICAN INSTITUTE OF PHYSICS

Incorporated

LANCASTER, PA., AND NEW YORK, N. Y.

THE JOURNAL OF CHEMICAL PHYSICS

ADVISORY EDITORIAL BOARD

R. T. BIRGE — JAMES FRANCK
A. H. COMPTON — IRVING LANGMUIR
JOHN T. TATE

BOARD OF EDITORS

HAROLD C. UREY, *Managing Editor*
JOSEPH E. MAYER, *Assistant Editor*

Associate Editors

Term ending December 31, 1940	*Term ending December 31, 1941*	*Term ending December 31, 1942*
DONALD ANDREWS	R. H. CRIST	ANDREW R. GORDON
R. BOWLING BARNES	G. E. KIMBALL	EDWARD A. GUGGENHEIM
KARL HERZFELD	G. B. KISTIAKOWSKY	RICHARD C. LORD
F. H. SPEDDING	G. K. ROLLEFSON	LINUS PAULING
B. E. WARREN	H. S. TAYLOR	HERTHA SPONER
	O. R. WULF	EDWARD TELLER

THE JOURNAL OF CHEMICAL PHYSICS is published monthly by the American Institute of Physics. Its purpose is to bridge a gap between journals of physics and journals of chemistry. The artificial boundary between physics and chemistry has now been in actual fact completely eliminated, and a large and active group is engaged in research which is as much the one as the other. It is to this group that the Journal is rendering its principal service and makes its greatest appeal, both as a prompt and efficient medium for publication of research and as a convenient and carefully edited assemblage of pertinent information.

Manuscripts for publication should be submitted to Joseph E. Mayer, Havemeyer Hall, Columbia University, New York, New York.

Proof and all correspondence concerning papers in the process of publication should be addressed to the Publications Manager, American Institute of Physics, 175 Fifth Avenue, New York, New York. Subscriptions and orders for single copies should be addressed to Prince and Lemon Sts., Lancaster, Pa., or American Institute of Physics, 175 Fifth Avenue, New York, New York.

Subscription price: United States and Possessions, Canada and Mexico, $10.00 per year; Foreign, $11.00.

The Journal of Chemical Physics is published monthly at Prince and Lemon Streets, Lancaster, Pennsylvania.

Entered as second-class matter December 30, 1932, at the Post Office at Lancaster, Pa., under the Act of August 24, 1912. Acceptance for mailing at special rate of postage, provided for in the Act of February 28, 1925, embodied in paragraph 4, Section 538, P. L. & R.: authorized February 3, 1933.

THE AMERICAN INSTITUTE OF PHYSICS

INCORPORATED

ADMINISTRATIVE STAFF

HENRY A. BARTON, *Director*

MADELINE M. MITCHELL, *Publications Manager*

JOHN T. TATE, *Adviser on Publications*

Office: 175 Fifth Avenue, New York, New York

JOURNALS

THE PHYSICAL REVIEW
REVIEWS OF MODERN PHYSICS
JOHN T. TATE, *Editor*
J. W. BUCHTA, *Assistant Editor*

THE JOURNAL OF THE OPTICAL SOCIETY OF AMERICA
GEORGE R. HARRISON, *Editor*

JOURNAL OF THE ACOUSTICAL SOCIETY OF AMERICA
FLOYD A. FIRESTONE, *Editor*

AMERICAN JOURNAL OF PHYSICS
(Formerly THE AMERICAN PHYSICS TEACHER)
DUANE ROLLER, *Editor*

THE REVIEW OF SCIENTIFIC INSTRUMENTS
GAYLORD P. HARNWELL, *Editor*

THE JOURNAL OF CHEMICAL PHYSICS
HAROLD C. UREY, *Editor*
JOSEPH E. MAYER, *Assistant Editor*

JOURNAL OF APPLIED PHYSICS
ELMER HUTCHISSON, *Editor*

GOVERNING BOARD

PAUL E. KLOPSTEG, *Chairman*
Central Scientific Company

GEORGE B. PEGRAM, *Secretary*
Columbia University

For the American Physical Society:

KARL T. COMPTON
Massachusetts Institute of Technology

GEORGE B. PEGRAM
Columbia University

JOHN T. TATE
University of Minnesota

For the Optical Society:

R. C. GIBBS
Cornell University

A. C. HARDY
Massachusetts Institute of Technology

W. B. RAYTON
Bausch & Lomb Optical Company

For the Acoustical Society of America:

FLOYD A. FIRESTONE
University of Michigan

HARVEY FLETCHER
Bell Telephone Laboratories

WALLACE WATERFALL
The Celotex Corporation

For the Society of Rheology:

WHEELER P. DAVEY
Pennsylvania State College

A. STUART HUNTER
E. I. duPont de Nemours & Company

H. R. LILLIE
Corning Glass Works

For the American Association of Physics Teachers:

GEORGE R. HARRISON
Massachusetts Institute of Technology

PAUL E. KLOPSTEG
Central Scientific Company

FREDERIC PALMER, JR.
Haverford College

The American Institute of Physics is a membership corporation of which five societies are the founding members. These five societies are the principal national societies devoted to pure and applied physics in America. Their names, and those of their representatives who form the Governing Board of the Institute, are given above. The principal work of the Institute is the publication of journals sponsored by the societies or by itself. The names and the editors of the journals are also listed above.

The broad purpose of the Institute is to represent, in all matters of wide or common interest, the five thousand or more members and subscribers associated with the Founder Societies and the journals. It aims to advance the science and profession of physics, and to promote cooperation between pure research, the applied sciences and the industries. To achieve these aims, it is greatly in need of an endowment and is empowered by law to administer grants and funds of any kind.

CONTENTS

J. CHEM. PHYS. 8 (1940) DECEMBER

Ozone in Silent Electric Discharge . . . . . WILLIAM H. OTTO AND WILLARD H. BENNETT 899

Further Concentration of S^{32} . . . . . DAVID W. STEWART AND KARL COHEN 904

Absorption Spectra of Europium Ion in Some Hydrated Salts . . . . . F. H. SPEDDING, C. C. MOSS AND R. C. WALKER 908

Normal Vibrations of Molecules of the Tetramethylmethane Type . . . . . SAMUEL SILVER 919

Entropy of Dilution of Strong Electrolytes in Aqueous Solutions . . . . . H. S. FRANK AND A. L. ROBINSON 933

Diamagnetic Anisotropy and Electronic Structure of Aromatic Molecules . . HARVEY BROOKS 939

Separation by Thermal Diffusion of Mixtures of Gases Having the Same Molecular Weight . . . . . F. T. WALL AND C. E. HOLLEY, JR. 949

Thermodynamics of Films: Energy and Entropy of Extension and Spreading of Insoluble Monolayers . . . . . WILLIAM D. HARKINS, T. FRASER YOUNG AND EDWARD BOYD 954

Effect of Gravitational Field on the Thermal Diffusion Separation Method . . . . . MILTON FARBER AND W. F. LIBBY 965

Low Temperature Gaseous Heat Capacities of Certain C_5 Hydrocarbons . . . . . G. B. KISTIAKOWSKY, J. R. LACHER AND W. W. RANSOM 970

Statistical Theory of Duplex Films . . . . . LAWRENCE S. K. FENG AND WILLIAM BAND 977

Gaseous Heat Capacity and Restricted Internal Rotation of Diborane . . . . . FRED STITT 981

Theoretical and Experimental Analysis of the Capillary Rise Method for Measuring the Surface Tension of Solutions of Electrolytes . . . . . GRINNELL JONES AND LAURENCE D. FRIZZELL 986

Letters to the Editor:

Note on the Chain Photolysis of Acetaldehyde in Intermittent Light . . . . . W. L. HARDEN, JR., E. P. H. MELBOURN AND O. K. RICE 998

Erratum: High Velocity Atomic Beams . . . . . I. AMDUR AND H. PEARLMAN 998

Author Index to Volume 8 999

Analytic Subject Index to Volume 8 1004

Volume Table of Contents iii

LANCASTER PRESS, INC., LANCASTER, PA.